RADIOTRACER STUDIES OF THE FLUORINE BOND LABILITY OF SOME BINARY FLUORIDES.

Thesis submitted to the University of Glasgow in fulfilment of the requirement of the degree of Doctor of Philosophy.

by

MOHAMMED FOUZI GHORAB M.Sc.

Department of Chemistry
University of Glasgow
September, 1988.

To my mother and father.

ACKNOWLEDGEMENTS.

I would like to thank my supervisor Dr. J.M. Winfield for all his help and guidance during the course of this work.

I would also like to thank my colleagues of the Fluorine Chemistry Group for their helpful discussions, Messrs. R.R. Spence and L. McGhee for their technical assistance, Messrs. W. McCormack and R. Wilson of the glass blowing workshop and Mrs. F. Lawrie and Mr. G. McCulloch of the infrared service for their cooperation. Many thanks are due to Mrs. L. Hughes for her efficient typing of this thesis.

The nuclear facilities provided by Dr. J.E. Whitley and his colleagues at the Scottish Universities Research and Reactor Centre, East Kilbride, without which the present work would have been a much more difficult task, are gratefully acknowledged.

My very special thanks go to my parents for their support and encouragement and my friends for their good company.

Finally, I would like to acknowledge the financial support granted to me by the Ministry of Higher Education (M.E.S), Algeria.

CONTENTS page

ACKNOWLEDGEMENTS

SUMMARY (i)

CHAPTER 1. INTRODUCTION 1

1.1 Preparation and Physical Properties of the Hexafluorides of Molybdenum, Tungsten and Uranium. 4

1.2 Chemical Reactivity of the Hexafluorides of Molybdenum Tungsten and Uranium. 5

1.3 Preparation of the Hepta-and Octa-fluoroanions of Molybenum, Tungsten and Uranium. 7

1.4 Structures of the Hepta- and Octa-fluoroanions of Molybdenum, Tungsten and Uranium. 9

1.5 Fluorine Bond Lability of the Hexafluorides of Molybdenum, Tungsten, Uranium and their Derivatives. 11

1.6 Chemistry of Boron Trifluoride and the Penta-Fluorides of Phosphorus and Arsenic. 14

1.7 Chemistry of Antimony Pentafluoride 17

1.8 Chemistry of the Pentafluorides of Niobium and Tantalum 19

1.9 Lewis Acidity Order of Binary Fluorides 20

1.9.1 General Definitions 20

1.9.2 Lewis Acid-Base Definition 21

1.9.3 Lewis Acidity Order 22

CHAPTER 2 EXPERIMENTAL

2.1	Equipment	25
2.1.1	Vacuum Line	25
2.1.2	Inert Atmosphere	25
2.1.3	Vibrational Spectroscopy	25
2.2	Preparation and Purification of Reagents	26
2.2.1	Purification of Acetonitrile	26
2.2.2	Purification of Diethylether	27
2.2.3	Preparation and Purification of Molybdenum Hexafluoride	27
2.2.4	Preparation and Purification of Dinitrogen Tetroxide	28
2.2.5	Preparation of Nitrosyl Fluoride	29
2.2.6	Preparation of Tris(dimethylamine)sulphonium Difluorotrimethylsilicate	30
2.2.7	Preparation of Trimethylfluorosilane	31
2.2.8	Purification of the Pentafluorides of Niobium and Tantalum	31
2.2.9	Preparation of Arsenic Pentafluoride-Acetonitrile Adduct.	32
2.2.10	Preparation of Antimony Pentafluoride-Acetonitrile Adduct	33
2.2.11	Preparation of Acetonitrile Adduct of the Pentafluorides of Niobium and Tantalum	34
2.2.12	Preparation of Lithium Tetrafluoroborate, Lithium Hexafluorophosphate and Lithium Hexafluoroarsenate	35

2.2.13	Preparation of Nitrosonium Hexafluoro-phosphate and Nitrosonium Hexafluoroarsenate	36
2.2.14	Preparation of Lithium Hexafluoroantimonate	36
2.2.15	Preparation of Lithium Hexafluoroniobate Lithium Hexafluorotantalate and Copper(II) Hexafluoroniobate Pentakis Acetonitrile	37
2.2.16	Preparation of Copper(II) Heptafluoro-tungstate(VI) Pentakis Acetonitrile	39
2.2.17	Preparation of Thallium(I) Heptafluoro-tungstate(VI)	39
2.2.18	Preparation of Nitrosonium Heptafluoro-tungstate(VI)	40
2.2.19	Preparation of Caesium Heptafluorotungstate(VI) and Caesium Heptafluoromolybdate(VI)	41
2.3	Activation of Caesium Fluoride	42
2.4	Radiochemical Techniques	43
2.5	Isotopic Exchange Reactions	44
2.6	[^{18}F]-Fluorine as Radiotracer	47
2.7	Counting Apparatus	49
2.8	Radioactive Decay	50
2.9	Background	51
2.10	Statistical Errors	51
2.11	Radiochemical Balance	53
2.12	[^{18}F]-Fluorine Reaction Vessels	55
2.12.1	Single-Limb Vessel	55
2.12.2	Double-Limb Vessel	56
2.13	Preparation of Radiolabelled Compounds	57

2.13.1 Preparation of [^{18}F]-Fluorine Labelled Caesium Fluoride 57

2.13.2 Preparation of [^{18}F]-Fluorine Labelled Hexafluorides of Molybdenum, Tungsten and Uranium 58

2.13.3 Preparation of [^{18}F]-Fluorine Labelled Boron Trifluoride Phosphorus Pentafluoride, Arsenic Pentafluoride and Trimethylfluorosilane 59

2.13.4 Preparation of [^{18}F]-Fluorine Labelled Lithium Hexafluorophosphate and Lithium Hexafluoro-arsenate 60

2.13.5 Preparation of [^{18}F]-Fluorine Labelled Nitrosyl Fluoride 61

CHAPTER 3 REACTIONS OF THE HEPTAFLUOROTUNGSTATE(VI) AND HEPTAFLUOROMOLYBDATE(VI) ANIONS WITH [^{18}F]-FLUORINE LABELLED HEXAFLUORIDES OF MOLYBDENUM AND TUNGSTEN.

3.1 Introduction 63

3.2 Experimental 64

3.3 Reaction Between Thallium(I) Heptafluoro-tungstate(VI) and [^{18}F]-Fluorine Labelled Tungsten Hexafluoride in Acetonitrile 64

3.4 Reaction Between Copper(II) Heptafluoro-tungstate(VI) Pentakis Acetonitrile and [^{18}F]-Fluorine Labelled Tungsten Hexafluoride in Acetonitrile 65

3.5	Reaction Between [^{18}F]-Fluorine Labelled Nitrosonium Heptafluorotungstate(VI) and Tungsten Hexafluoride in Acetonitrile	66
3.6	Reaction Between Nitrosonium Heptafluorotungstate(VI) and [^{18}F]-Fluorine Labelled Molybdenum Hexafluoride in Acetonitrile	68
3.7	Reaction Between Caesium Heptafluorotungstate(VI) and [^{18}F]-Fluorine Labelled Molybdenum Hexafluoride in Acetonitrile	69
3.8	Evidence For the Formation of Caesium Heptafluoromolybdate and Caesium Heptafluorotungstate	69
3.9	Reaction Between Caesium Heptafluoromolybdate(VI) and [^{18}F]-Fluorine Labelled Tungsten Hexafluoride in Acetonitrile	73
3.10	Reaction Between Thallium(I) Heptafluorotungstate(VI) and [^{18}F]-Fluorine Labelled Tungsten Hexafluoride Under Heterogeneous Conditions.	75
3.11	Reaction Between Copper(II) Heptafluorotungstate(VI) Pentakis Acetonitrile and [^{18}F]-Fluorine Labelled Tungsten Hexafluoride Under Heterogeneous Conditions	76
3.12	Reaction Between Nitrosonium Heptafluorotungstate(VI) and [^{18}F]-Fluorine Labelled Tungsten Hexafluoride Under Heterogeneous Conditions	77

3.13 Reaction Between [^{18}F]-Fluorine Labelled Nitrosonium Heptafluorotungstate(VI) and Tungsten Hexafluoride Under Heterogeneous Conditions. 78

3.14 Reaction Between Nitrosonium Heptafluorotungstate(VI) and [^{18}F]-Fluorine Labelled Molybdenum Hexafluoride Under Heterogeneous Conditions 79

3.15 Reaction Between Caesium Heptafluoromolybdate(VI) and [^{18}F]-Fluorine Labelled Tungsten Hexafluoride Under Heterogeneous Conditions. 79

3.16 Reaction Between Nitrosonium Heptafluorotungstate(VI), Thallium(I) Heptafluorotungstate(VI) and [^{18}F]-Fluorine Labelled Uranium Hexafluoride Under Heterogeneous Conditions 80

CHAPTER 4 HETEROGENEOUS REACTIONS BETWEEN ACTIVATED CAESIUM FLUORIDE, COPPER DIFLUORIDE, THALLIUM FLUORIDE AND [^{18}F]-FLUORINE-LABELLED GASEOUS HEXAFLUORIDES OF MOLYBDENUM TUNGSTEN AND URANIUM.

4.1 Introduction 82

4.2 Experimental 83

4.3 Reaction Between Activated Caesium Fluoride and [^{18}F]-Fluorine Labelled Tungsten Hexafluoride Under Heterogeneous Conditions 84

4.4 Reaction Between Activated Caesium Fluoride and [^{18}F]-Fluorine Labelled Molybdenum Hexafluoride Under Heterogeneous Conditions 88

4.5 Reaction Between Activated Caesium Fluoride and [^{18}F]-Fluorine Labelled Uranium Hexafluoride Under Heterogeneous Conditions 91

4.6 Reaction Between Copper Difluoride and [^{18}F]-Fluorine Labelled Hexafluorides of Molybdenum Tungsten and Uranium Under Heterogeneous Conditions. 93

4.7 Reaction Between Thallium Fluoride and [^{18}F]-Fluorine Labelled Hexafluorides of Molybdenum Tungsten and Uranium Under Heterogeneous Conditions. 95

CHAPTER 5 REACTIONS BETWEEN THE FLUOROANIONS OF BORON, PHOSPHORUS, ARSENIC, ANTIMONY, NIOBIUM AND TANTALUM AND [^{18}F]-FLUORINE LABELLED HEXAFLUORIDES OF MOLYBDENUM, TUNGSTEN AND URANIUM IN ACETONITRILE

5.1 Introduction 97

5.2 Experimental 99

5.3 Reaction Between Lithium Tetrafluoroborate and [^{18}F]-Fluorine Labelled Hexafluorides of Molybdenum, Tungsten and Uranium in Acetonitrile. 100

5.4 Reaction Between Lithium Hexafluorophosphate and [^{18}F]-Fluorine Labelled Hexafluorides of Molybdenum, Tungsten and Uranium in Acetonitrile. 102

5.5 Reaction Between Lithium Hexafluoroarsenate and [^{18}F]-Fluorine Labelled Hexafluorides of Molybdenum, Tungsten and Uranium in Acetonitrile. 104

5.6 Reaction Between Lithium Hexafluoroantimonate and [^{18}F]-Fluorine Labelled Hexafluorides of Molybdenum, Tungsten and Uranium in Acetonitrile. 106

5.7 Reaction Between Lithium Hexafluorotantalate and Copper(II) Hexafluoroniobate Pentakis (Acetonitrile) and [^{18}F]-Fluorine Labelled Tungsten Hexafluoride in Acetonitrile. 108

5.8 Reaction Between Acetonitrile Adducts of Antimony, Arsenic and Niobium Pentafluorides and [^{18}F]-Fluorine Labelled Tungsten Hexafluoride in Acetonitrile. 109

CHAPTER 6 REACTIONS BETWEEN TRIS(DIMETHYLAMINO)-SULPHONIUM DIFLUOROTRIMETHYLSILICATE AND THE HEXAFLUORIDES OF MOLYBDENUM AND TUNGSTEN, BORON TRIFLUORIDE, PHOSPHORUS PENTAFLUORIDE AND [^{18}F]-FLUORINE LABELLED TRIMETHYLFLUOROSILANE IN ACETONITRILE

6.1 Introduction 110

6.2 Experimental 111

6.3 Reaction Between Tris(dimethylamino)sulphonium Difluorotrimethylsilicate and the Hexafluorides of Molybdenum and Tungsten in Acetonitrile 111

6.4 Reaction Between Tris(dimethylamino) sulphonium Difluorotrimethylsilicate and Boron Trifluoride and Phosphorus Penta-Fluoride in Acetonitrile. 112

6.5 Reaction Between Tris(dimethylamino) sulphonium Difluorotrimethylsilicate and [^{18}F]-Fluorine Labelled Trimethylfluoro-silane in Acetonitrile. 114

CHAPTER 7 DISCUSSION

7.1 Fluorine Bond Lability of the Fluoroanions of Boron, Phosphorus, Arsenic, Antimony, Niobium and Tantalum. 115

7.2 Fluorine Bond Lability of the Heptafluoro-anions of Molybdenum and Tungsten. 128

7.3 Reaction of Activated Caesium Fluoride, Thallium Fluoride and Copper Difluoride with [^{18}F]-Fluorine Labelled Hexafluorides of Molybdenum, Tungsten and Uranium. 126

7.4 The Chemical Reactivity of Tris(dimethyl-amino)sulphonium Difluorotrimethylsilicate 135

7.5 Concluding Remarks 137

REFERENCES 141

SUMMARY

Fluorine bond lability with respect to exchange is an important chemical property of binary fluorides. This can be useful in predicting new synthetic routes for derivatives of fluorine compounds or elucidating the mechanisms of processes taking place at fluorinated surfaces.

In the present study fluorine bond lability with respect to exchange of some fluoroanions namely, boron, phosphorus, arsenic, antimony, niobium and tantalum has been investigated during their interaction with [^{18}F]-labelled hexafluorides of molybdenum, tungsten and uranium in acetonitrile. Two distinct types of exchange behaviour are identified among the fluoroanions. It is firmly established that the M-F bond (M = B,P, Nb and Ta) in BF_4^-, PF_6^-, NbF_6^- and TaF_6^- is labile with respect to exchange whereas the As-F and Sb-F bonds in AsF_6^- and SbF_6^- are inert although AsF_6^- is found to exchange in the presence of UF_5 ^{18}F under the same conditions. The latter result is consistent with the higher fluoride ion affinity of UF_6 as compared with that of MoF_6 or WF_6. An associative mechanism is used to account for the fluorine exchange of BF_4^-, PF_6^-, NbF_6^-, TaF_6^- and AsF_6^- although a dissociative mechanism can not be ruled out. The difference in the fluoride bond lability among the fluoroanions under investigation is consistent with the difference in the Lewis acidity order of their parent fluorides.

Evidence for the existence of the heptafluoromolybdate(VI) ion in solution has been obtained for the first time in this study by reaction between CsF and $MoF_5{}^{18}F$ in MeCN. The existence of the heptafluorotungstate(VI) ion in solution is confirmed by reaction between CsF and $WF_5{}^{18}F$ in MeCN. Both ions are assigned in the D_{5h} symmetry. The fluorine bond lability with respect to exchange of MoF_7^- and WF_7^- has been investigated both under homogeneous (MeCN) and heterogeneous (gas plus solid) conditions in the presence of $MF_5{}^{18}F$ (M = Mo, W or U). The WF_7^- ion has been used as its copper(II), thallium(I), nitrosonium and caesium salts whereas MoF_7^- ion has been used as its caesium salt only. All systems are found to undergo rapid and complete [^{18}F]-fluorine exchange with $MF_5{}^{18}F$ (M = Mo or W) in MeCN at room temperature and below (253K). The nature of the cation does not have any effect on the exchange behaviour of the systems. However under heterogeneous conditions the same systems undergo partial exchange in the presence of $MF_5{}^{18}F$ (M = Mo, W or U). In MeCN the experimental observations are consistent with, but do not prove, a displacement mechanism for the exchange and an associative mechanism can not be ruled out. Under heterogeneous conditions fluorine exchange is best accounted for by an associative mechanism. The partial exchange of [^{18}F]-fluorine is ascribed to the anion-cation interaction.

The reaction between activated caesium fluoride and $MF_5{}^{18}F$ (M = Mo, W and U) results in the formation of more than

one species, MoF_7^-, WF_7^- and UF_8^{2-} being the major ones. The formation of more than one species is ascribed to the lack of uniformity of the surface reactions. The amount of hexafluoroacetone used during the activation of CsF is found to have a direct effect on its reactivity and most probably its surface area. [^{18}F]-Fluorine exchange is observed only when uptakes of MF_6 are considerable. The exchange is shown to take place between the adsorbed species and free hexafluorides. An associative mechanism similar to that between MF_7^- (M = Mo or W) and $MF_5{}^{18}F$ (M= Mo,W or U)under heterogeneous conditions is used to account for the exchange between adsorbed species and free $MF_5{}^{18}F$ (M = Mo, W).

The interaction of $MF_5{}^{18}F$ (M = Mo, W and U) with CuF_2 and TlF under heterogeneous conditions results in a smaller uptake and [^{18}F]-fluorine exchange in the case of CuF_2 as compared with TlF. In neither case has it been possible to determine the nature of the adsorbed species. The difference in affinity for the hexafluorides between TlF and CuF_2 is consistent with the difference in the Lewis acidity of Tl^+ and Cu^{2+}.

The reaction between tris(dimethylamino)sulphonium difluorotrimethylsilicate, TAS^+F^-, and MF_6 (M = Mo and W) in MeCN yields a brown viscous liquid thought to be due to either the formation of MF_7^- or MF_5NMe_2 (M = Mo and W) species. It is shown that the reaction between TAS^+F^- and BF_3 or PF_5 results in the formation of colourless crystalline $TAS^+BF_4^-$

or $TAS^+PF_6^-$ salts respectively. Complete $[^{18}F]$-fluorine exchange between TAS^+F^- and $[^{18}F]$-labelled Me_3SiF is found to take place in MeCN most probably via an associative mechanism.

CHAPTER ONE

INTRODUCTION

1. Introduction.

The chemistry of the high oxidation binary fluorides of the second and third transition metal series has been dominated over the past years by the study of their oxidising properties. It has been established [1] that the oxidising power of the hexafluorides increases with increase in the atomic number and decrease in the molecular volume in any series both in solution [2], and in the gas phase [3]. For instance it has been shown [3] that molybdenum hexafluoride oxidises nitric oxide whereas tungsten hexafluoride does not.

However knowledge about the fluorine bond lability as well as its mechanism with respect to fluorine-for-fluorine exchange of the same binary fluorides is scarce. This chemical property can be useful in predicting new synthetic routes or elucidating mechanisms of catalytic processes taking place at fluorinated surfaces. In this respect more information is needed. Furthermore, although the hepta- and octa-fluoroanions of some of these transition metals have long been synthesised and characterised [4] little is known about their chemical behaviour.

It is with the hope of filling this gap that this project was undertaken. The hexafluorides under investigation were those of molybdenum, tungsten and uranium in the presence of various chemical environments such as solid thallium fluoride, copper difluoride and activated caesium fluoride under heterogeneous conditions. The behaviour of the same

hexafluorides was examined both under homogeneous (in acetonitrile) and heterogeneous (gas plus solid) conditions in the presence of heptafluorotungstate(VI) ion using different counter-cations namely copper(II), thallium(I), nitrosonium(NO^+) and caesium(Cs^+). The reaction between tungsten hexafluoride and caesium heptafluoromolybdate(VI) was investigated in MeCN and under heterogeneous conditions.

It has been shown [5] using radiotracer techniques that no observable [^{18}F]-fluorine exchange takes place between caesium hexafluoroarsenate and [^{18}F]-labelled arsenic pentafluoride or between caesium tetrafluoroborate and [^{18}F]-labelled boron trifluoride under heterogeneous conditions at room temperature. However the same study has shown that partial exchange of [^{18}F]-fluorine takes place between $CsBF_4$ and [^{18}F]-BF_3 in acetonitrile. Fluoroanions of the main group are widely used as inert counter-anions in synthetic and electrochemical studies, and in view of the findings mentioned above it was of interest to investigate the behaviour of the hexafluorides of molybdenum, tungsten and uranium in the presence of fluoroanions such as tetrafluoroborate, hexafluorophosphate, hexafluoroarsenate and hexafluoroantimonate ions as well as the transition metal ions hexafluoroniobate and hexafluorotantalate in acetonitrile. This allows comparison to be made with studies in which relative Lewis acidities have been determined as will be shown later in this thesis. The ordering of Lewis acid fluorides still lacks uniformity [6].

Tris(dimethylamino)sulphoniumtrimethyl difluorosilicate (TAS^+F^-) is used as a source of soluble fluoride ion donor. It has been used for example to stabilise the trifluoromethoxide anion, F_3CO^-, the crystal structure of which has been determined [7]. Part of this project was devoted to the examination of the behaviour of TAS^+F^- as fluoride ion donor in the presence of the hexafluorides of molybdenum and tungsten, boron trifluoride, phosphorus pentafluoride and trimethylfluorosilane in acetonitrile.

In this project the radiotracer technique with [^{18}F]-fluorine as the radiotracer was the method of investigation used. ^{19}F N.m.r. has been used as an alternative method in solution studies [8]. One of the advantages of radiotracer techniques is their sensitivity in detecting the radioisotope during reactions. On the other hand these techniques do not enable direct identification of chemical species to be made, and therefore analogies with more conventionally characterised chemical species must be used to interpret the results.

In the forthcoming parts of this chapter some aspects of the chemistry of the hexafluorides and hepta- and octafluoroions of molybdenum, tungsten and uranium are reviewed (Sections 1.1 to 1.5). Sections 1.6 to 1.8 review some aspects of the chemistry of boron trifluoride and the pentafluorides of phosphorus, arsenic, antimony, niobium and tantalum. In the remaining part of this chapter

(Section 1.9) a brief discussion of the Lewis acidity of some binary fluorides is presented.

1.1 Preparation and Physical Properties of the Hexafluorides of Molybdenum, Tungsten and Uranium.

The hexafluorides of molybdenum, tungsten and uranium can be prepared by various methods [9,10]. However, the reaction between metals and elemental fluorine in flow systems at high temperature is the most convenient method. Uranium hexafluoride finds extensive use in the separation of ^{235}U from natural uranium on an industrial scale. Because of this it has been subject to extensive research as compared with MoF_6 or WF_6 and numerous methods for its synthesis have been developed [11]. Figures 1.1, 1.2 and 1.3 represent summaries of the preparative methods leading to MoF_6 WF_6 and UF_6 respectively. These hexafluorides have relatively high vapour pressures at room temperature. Their boiling points are 308K for MoF_6, 290 K for WF_6 and 329K for UF_6. This makes their manipulation in a vacuum system possible. These fluorides are monomeric having an octahedral arrangement of six fluorine atoms around the central metal atom. Their average metal-fluorine bond distances are 1.820Å (MoF_6) [1], 1.832Å (WF_6) [1] and 1.995Å (UF_6) [11]. They possess orthorhombic symmetry in the solid lattices. The results of neutron powder diffraction studies on MoF_6, WF_6 and UF_6 at low temperatures [12] have shown that the two former exist as more compact and spherically shaped molecules than the latter in the solid state.

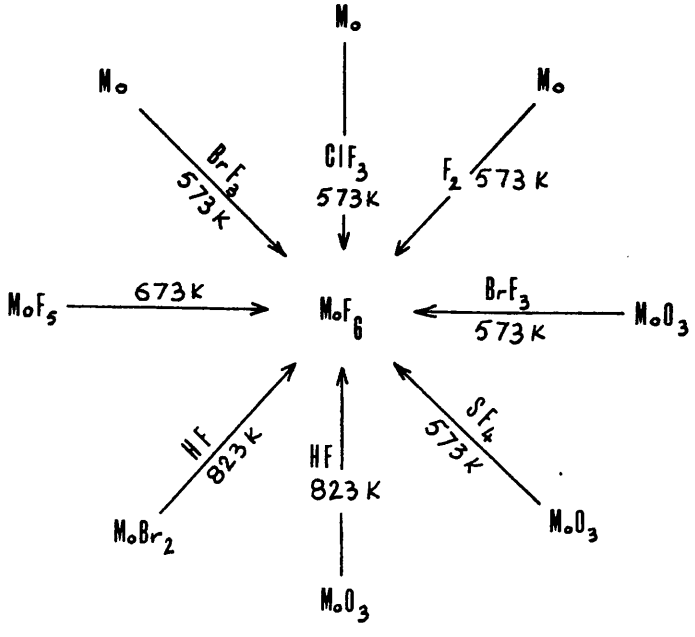

Figure 1.1 Preparation of Molybdenum Hexafluoride [9,10].

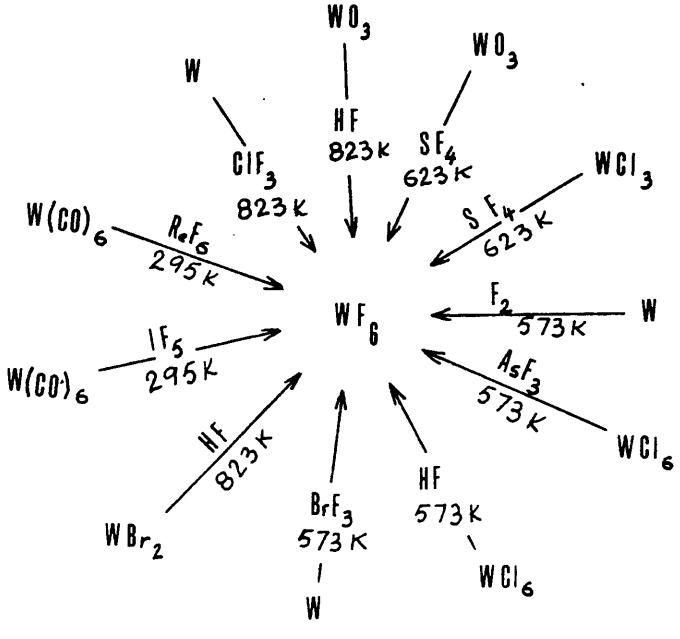

Figure 1.2 Preparation of Tungsten Hexafluoride [9,10].

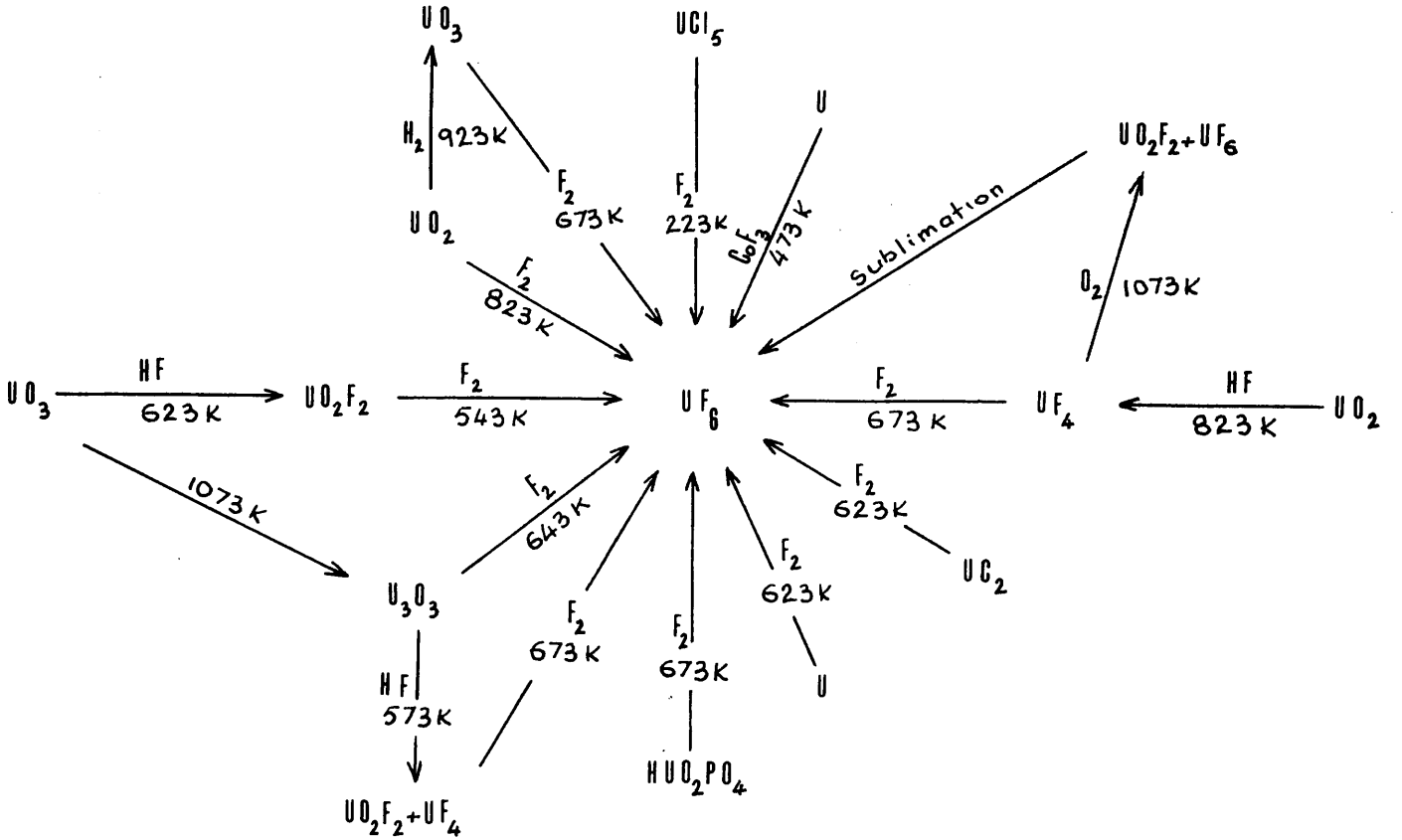

Figure 1.3 Preparation of Uranium Hexafluoride [11].

1.2 Chemical Reactivity of the Hexafluorides of Molybdenum, Tungsten and Uranium.

The oxidising properties of the hexafluorides of molybdenum, tungsten and uranium have been investigated both in the gas phase and in solution.

In the gas phase it has been shown that nitric oxide is oxidised by MoF_6 and UF_6 to give adducts which contain NO^+ cation and where the central atom is reduced to a pentavlent state [3, 13, 14]. However WF_6 shows no oxidising ability towards NO [3,13] even at 373K. O'Donnell and co-workers [15] have carried out systematic studies related to the relative reactivities of some high oxidation binary fluorides; those relevant to the present study, were MoF_6, WF_6 and UF_6. Their investigations carried out in the presence of phosphorus trifluoride have shown that UF_6 oxidises readily PF_3 to PF_5. Molybdenum has been found to oxidise PF_3 more slowly than UF_6 whereas WF_6 shows complete inertness towards it and hydrogen fluoride is needed to catalyse the reaction. From their results the authors concluded that the relative reactivity of the hexafluorides with respect to oxidation is in the order $UF_6 > MoF_6 > WF_6$.

It has also been recognised [16] that f- and d-block hexafluorides oxidise graphite with concomitant intercalation of the hexafluoroanions. Hexafluoride intercalated graphite has been shown to exhibit high conductivity [17]. The ability of these hexafluorides to oxidise and intercalate graphite has been related to their electron affinities [16].

Studies involving the third transition series hexafluorides have demonstrated [18] that a hexafluoride must have an electron affinity of at least 452 kJ mol^{-1} if it is to intercalate into graphite spontaneously and oxidatively. Hence due to its relatively low electron affinity, 338 kJ mol^{-1} [19], WF_6 does not oxidise graphite [16].

The oxidising behaviour of the hexafluorides of molybdenum, tungsten and uranium has been studied in various solvents. In acetonitrile a number of transition and post transition metals are oxidised by MF_6 (M = Mo, W, U) to give solvated cations of the corresponding MF_6^- anion [20,21]. In some cases the oxidation state of the metal depends on the hexafluoride used. This is illustrated by the example of thallium which is oxidised to Tl(III) by MoF_6 and UF_6 and to Tl(I) by WF_6 showing hence the relatively poor oxidising ability of the latter as compared with the two former [20].

The inferior oxidising ability of WF_6 as compared with MoF_6 or UF_6 towards iodine in MeCN has been demonstrated by Anderson et. al. [22], who have shown that molecular iodine is oxidised by MoF_6 and UF_6, but not by WF_6, to give solvated mononuclear I^+, isolated as $[I(NCMe)_2][MF_6]$ (M = Mo, U). However in iodine pentafluoride only UF_6 oxidises I_2 to I_2^+ [23]. The difference in behaviour between the hexafluorides emphasises the role played by MeCN in solvation. The role played by the solvent in the behaviour of the hexafluorides is illustrated further by the example

of sulphur dioxide in which MoF_6 and WF_6 have been shown [24] to oxidise alkali metal iodides to iodine and the corresponding hexafluorometallates (VI) equation (1.1)

$$2MF_6 + 2EI \rightarrow I_2 + 2EMF_6 \qquad (1.1)$$

(M = Mo, W; E = alkali metal except lithium)

The oxidation reaction between the hexafluorides of molybdenum and tungsten has been investigated by Bond et al. [24] in anhydrous hydrogen fluoride. These authors have shown that the electrochemistry of these systems involves a reversible one electron reduction step, equation (1.2).

By determining the half wave potentials $E_{\frac{1}{2}}$ of the couples MoF_6/MoF_6^- and WF_6/WF_6^- the authors have found that MoF_6 is stronger oxidiser than WF_6 by one volt. The same difference between MoF_6 and WF_6 has been found in MeCN [25].

$$MF_6 + e \rightleftharpoons MF_6^- \qquad (1.2)$$

(M = Mo, W)

1.3 Preparation of the Hepta- and Octafluoroions of Molybdenum, Tungsten and Uranium.

The hepta- and octa-fluorometallate(VI) anions of molybdenum and tungsten were first prepared and characterised by Hargreaves and Peacock [27] by reacting alkali fluorides, namely potassium, rubidium fluoride and caesium fluoride, with the corresponding hexafluoride in liquid

iodine pentafluoride at room temperature. In both cases the heptafluorometallate(VI) anions were obtained with rubidium and caesium as counter cations whereas the octafluorometallate(VI) anions were obtained with the smaller potassium cation. Beuter et. al. [28] did not succeed in reproducing the results of Hargreaves and Peacock instead they used alkali iodides to prepare the heptafluoroanions which upon heating yielded the octafluoroanions. The hepta- and octa-fluorocomplex anions of molybdenum, tungsten and uranium have also been prepared by various methods using different counter-cations. Sunder and co-workers [29] prepared MoF_7^-, WF_7^- and WF_8^{2-} by homogeneous gas reactions between nitrosyl fluoride and the corresponding metal hexafluoride according to equations (1.3) to (1.5)

$$MoF_6 + (NOF)_x \xrightarrow{273K,\ 66h} NOMoF_7 \qquad (1.3)$$

$$WF_6 + (NOF)_x \xrightarrow{323K,\ 17h} NOWF_7 \qquad (1.4)$$

$$NOWF_7 + (NOF)_x \xrightarrow{326K,\ 66h} (NO)_2WF_8 \qquad (1.5)$$

Bougon et. al. [30] prepared the heptafluorouranate(VI) by reaction between nitrosyl fluoride and uranium hexafluoride which in the presence of excess NOF yielded dinitrose-octafluorouranate(VI). The same workers prepared caesium heptafluorouranate(VI) by reaction between CsF and liquid UF_6 at 338K. Upon heating $CsUF_7$ yielded caesium octafluorouranate(VI).

Prescott et. al. [31] prepared WF_7^- using Cu^{2+} and Tl^+ as counter-cations by reaction between copper difluoride or thallium fluoride and WF_6 in acetonitrile.

1.4 Structures of the Hepta- and Octa-fluoroanion of Molybdenum, Tungsten and Uranium.

Seven and eight coordinated fluorocomplexes are limited to the left of the transition metal series and have usually been described in terms of two different structures. Hoard [32] described, on the basis of his x-ray study, dipotassium heptafluoroniobate and heptafluorotantalate as having a slightly distorted monocapped trigonal prism C_{2v}. The same structure was used by Brown and Walker [33] to interpret their neutron diffraction spectrum of K_2NbF_7. However, using vibrational spectroscopy Beuter et. al. [28] attributed a pentagonal bipyramid structure to K_2TaF_7. The discrepancy between these two results can be explained by the ease with which interconversion between the two structures can occur. The energy barrier between the two structures was found to be quite small [34]. But more recently English et. al. [35] were not able to interpret the infrared, Raman and ^{19}F n.m.r. spectra of K_2TaF_7 in terms of any structure and concluded from their study that this fluorocomplex could only be visualised as a non rigid molecule at room temperature.

Similarly the structures of the heptafluoroanions of molybdenum, tungsten and uranium are expected to be pentagonal bipyramid or monocapped trigonal prism, Figure 1.4. In

principle, it is possible to distinguish between these two structures from their vibrational spectra as their respective selection rules are dissimilar. For a D_{5h} structure 10 active vibrations are expected, 5 in the Raman and 5 in the infrared, following the rule of mutual exclusion. For a C_{2v} structure, 18 Raman and 15 infrared bands are expected. All infrared bands should coincide with the Raman lines, one Raman vibration being inactive. The structures of MF_7^- (M = Mo, W, U) ions have usually been described in the D_{5h} structure from their room temperature vibrational spectra although it has been shown that the symmetry of UF_7^- is no higher than C_{2v} at 77K [30,36,37]. The D_{5h} structure has been arrived at by different workers using nitrosonium (NO^+) or alkali metals as counter-cations [28-30,36,37], however, this does not rule out the possibility that the MF_7^- (M = Mo,W,U) anions do not adopt the C_{2v} structure at room temperature. This may probably be due to the short life time of the latter structure as compared with the former on the time scale of the vibrational spectroscopic techniques.

The vibrational spectra of the octa-fluoroanions of molybdenum and tungsten have been assigned in the square antiprism symmetry (D_{4d}) [28,29] Figure 1.5b. Those of the octa-fluorouranate(VI) anion have been assigned in the cubic symmetry (O_h) [30,36], Figure 1.5a, although its low temperature spectra have been interpreted in terms of dodecahydral symmetry (D_{2d}) [36], Figure 1.5c. In principle, it is possible to distinguish between the three structures. For a D_{4h} structure, 7 Raman and 5 infrared active vibrations

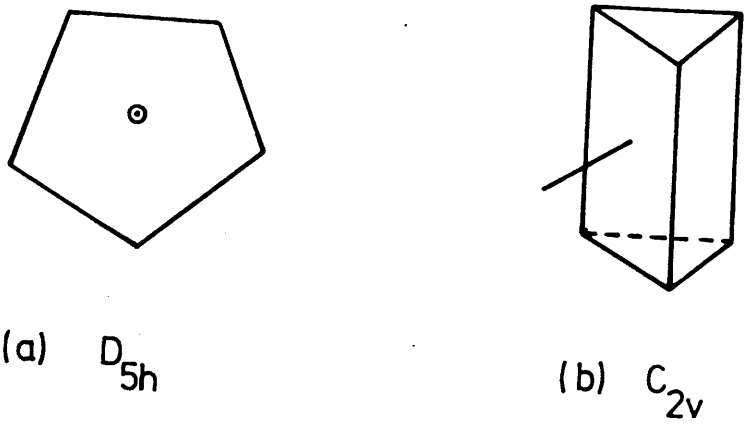

Figure 1.4 The Structure of the Heptafluoroanions.

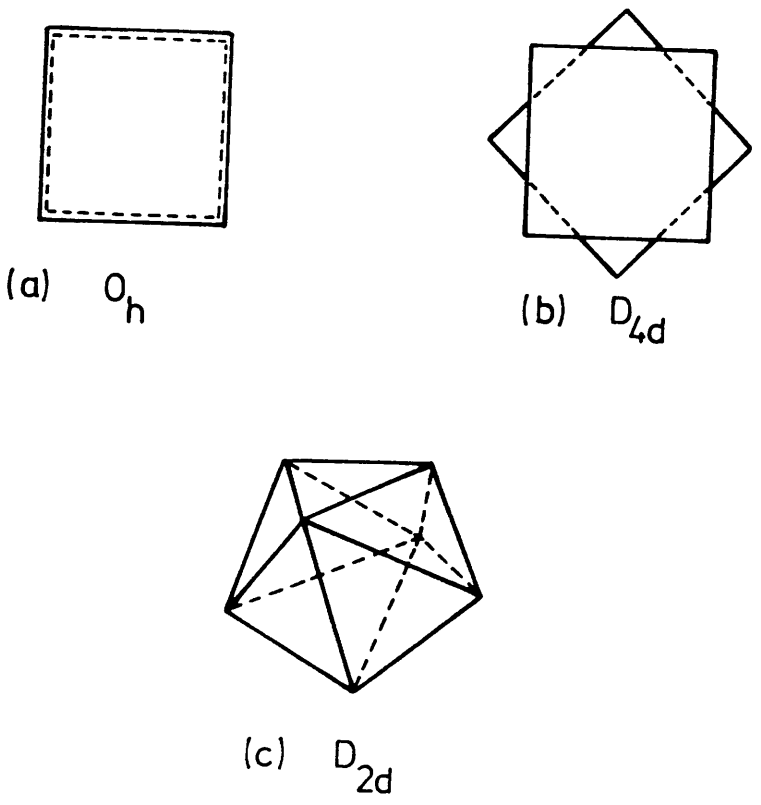

Figure 1.5. The Structure of the Octafluoroanions.

are expected following the rule of mutual exclusion. For a D_{2d} structure, 15 Raman and 9 infrared active vibrations are expected following the rule of mutual exclusion. For an O_h symmetry, 4 Raman and 2 infrared active vibrations are expected following the rule of mutual exclusions. As in the case of MF_7^- (M = Mo,W,U), although the assignment of the octa-fluoroanions have been made in the D_{4d} symmetry for MoF_8^{2-} and WF_8^{2-} and in the O_h symmetry for UF_8^{2-} this does not rule out the possibility that the structures do not coexist at room temperature. The D_{4d} and D_{2d} structures are approximately of equal stability and spatial rearrangement between them is facile [38]. It can be argued that the life time of the D_{2d} structure at room temperature is small compared with that of D_{4d} or O_h on the time scale of the vibrational spectroscopic techniques.

1.5 Fluorine Bond Lability of the Hexafluorides of Molybdenum, Tungsten, Uranium and their Derivatives.

Using [^{18}F]-fluorine as a radiotracer and hexafluorobenzene as a solvent Fraser et al. [39] have investigated the lability of tungsten(VI)-fluorine bonds of some tungsten hexafluoride derivatives in the presence of [^{18}F]-labelled trimethylfluorosilane. Their results have shown that [^{18}F]-fluorine exchange depends on the identity and number of substituents. Hence methoxytungsten(VI) pentafluoride, $WF_5(OMe)$, dimethoxytungsten(VI) tetrafluoride, $WF_4(OMe)_2$ and diethylaminotungsten(VI) pentafluoride, $WF_5(NEt_2)$ all undergo considerable ^{18}F exchange and further substitution of fluorine occurs readily. However, less [^{18}F]-fluorine exchange and a slow substitution

have been observed between $Me_3Si^{18}F$ and phenoxytungsten(VI) pentafluoride, WF_5OPh or pentafluorophenoxytungsten(VI) pentafluoride, $WF_5OC_6F_5$. No [^{18}F]-fluorine exchange has been observed between $Me_3Si^{18}F$ and cis-tetramethoxytungsten(VI) difluoride, cis-$WF_2(OMe)_4$ and further substitution of fluorine using trimethylmethoxysilicate has required elevated temperature. Even so complete conversion to $WF(OMe)_5$ has not been complete. Similarly, no measureable [^{18}F]-fluorine exchange has been found to occur between tetramethoxymolybdenum(VI) difluoride, $MoF_2(OMe)_4$, or pentamethoxymolybdenum(VI) fluoride and $Me_3Si^{18}F$ [40]. From their results the authors [40] have concluded that the qualitative similarity between [^{18}F]-fluorine exchange and substitution behaviour suggests that both processes may occur by similar mechanisms. These must be similar to that described by Sommer et. al. [41] for reactions between covalent halides and organosilicon ethers or amines which involve either S_{Ni}-Si or S_N2-Si pathways. This mechanism which involves a species containing Si-F-W bridge as an intermediate stresses both donor and acceptor properties of W(VI).

The behaviour of fluorine exchange in the series of fluoride methoxides of tungsten(VI) has been examined in more detail by Poole and Winfield [40]. Using the same radiotracer technique the authors have found that a complete [^{18}F]-fluorine exchange occurs between $WF_5(OMe)$ and $BF_2{}^{18}F$, $Me_3Si^{18}F$; $Me_2Si^{18}FF$ or $WF_5{}^{18}F$. From the linear McKay plots these authors argued that, although $WF_5(OMe)$ is monomeric in C_6F_6 and thus contains structurally non equivalent fluoride

ligands all these fluoride ligands exchange at similar rates. [^{18}F]-Fluorine exchange between $WF_5(OMe)$ and $Me_3Si^{18}F$ is thought to take place via an associative mechanism involving a transition state containing seven coordinate tungsten which acts both as donor and as an acceptor. This property has also been emphasised by Prescott et al. [31] who have shown that complete [^{18}F]-fluorine exchange takes place between thallium(I) heptafluorotungstate(VI) and $WF_5{}^{18}F$ in acetonitrile at room temperature.

Another study involving the exchange behaviour of high oxidation state transition metal fluorides is that due to Glavincevski and Brownstein [8,42] who have examined the fluorine exchange behaviour between azidohexafluorotungstate(VI) ion, $[WF_6(N_3)]^-$, and WF_6 in sulphur dioxide and between cyanohexafluorotungstate(VI) ion, $[WF_6(CN)]^-$ and WF_6 in dichloromethane. Using ^{19}F n.m.r. techniques, it has been found that in either case exchange takes place between the reactants and involves a mechanism of low activation energy. From their results the authors have suggested that the exchange takes place via a displacement mechanism (Equations 1.6 and 1.7).

$$[W^*F_6(N_3)]^- + WF_6 \longrightarrow [WF_6(N_3)]^- + W^*F_6 \qquad (1.6)$$

$$[W^*F_6(CN)]^- + WF_6 \longrightarrow [WF_6(CN)]^- + W^*F_6 \qquad (1.7)$$

in which complexed W^*F_6 is displaced by free WF_6.

Berry et al. [21] in their study of the oxidising and fluoride ion acceptor properties of uranium hexafluoride

have shown that complete [^{18}F]-fluorine exchange occurs between UF_7^- and $UF_5{}^{18}F$ in MeCN. More recently [^{18}F]-fluorine has been used to examine the exchange reaction between UF_6 and $BF_2{}^{18}F$ and $Me_3Si{}^{18}F$ [43]. The results of this study have shown that in either case substantial [^{18}F]-fluorine exchange occurs. The authors have argued that this is the result both of the effective Lewis acid centre, U(VI), and the donor properties of fluorine bound to U(VI). By comparison with previous studies involving MoF_6, WF_6 and UF_6 the same authors have obtained a qualitative order of MF_6 (M = Mo,W,U) bond lability towards $R_3Si{}^{18}F$ (R = Me,Et). This order is $UF_6 \sim MoF_6 > WF_6$.

1.6 Chemistry of Boron Trifluoride and the Pentafluorides of Phosphorus and Arsenic.

Boron trifluoride, phosphorus pentafluoride and arsenic pentafluoride are all gases at room temperature. They are strong Lewis acids and the order of their Lewis acidity has been determined by a variety of methods (Table 1.1). In most cases this order is $AsF_5 > PF_5 > BF_3$. Boron trifluoride forms stable non-ionic four coordinate complexes with organic donors such as ethers and amides [44], and, of relevance to the present work, acetonitrile. It has been shown in the latter case [45] that the C≡N force constant increases significantly upon complexation resulting in an increase in the C≡N stretching frequency. The crystal structure of this adduct has been determined [46] and shows that the boron

Table 1.1 Lewis Acidity Order of Some Binary Fluorides.

Order	Fluoride donor	Method	Reference
$BF_3 > TaF_5 > NbF_5 > TiF_4 > PF_5 > WF_6 >> SiF_4 \sim CoF_6$	HF - xylene	Solvent extraction of $ArH^+ MF^-_{n+1}$	97
$AsF_5 \sim BF_3 > PF_5 \sim WF_6 > NbF_5 \sim TaF_5 > SiF_4 \sim SbF_3 \sim CoF_3$	MF and/or HF	Solubility of MF or Lewis acid	98
$SbF_5 > AsF_5 > BF_3 > PF_5$	CF_3SF_3	Decomposition pressure	58
$AsF_5 > PF_5 > BF_3$	MI_{n+1} in CH_2Cl_2	Displacement reaction	99
$SbF_5 > AsF_5 > PF_5 \sim BF_3$	HF	Cryoscopy, conductivity	100
$AsF_3 > BF_3 > SiF_4 > AsF_5 > PF_5 > PF_3$	SF_6^-	Rate of F^- transfer	101
$AsF_5 > BCl_3 > PF_5 > BF_3 > SiF_4 > AsF_3, HCl > SO_2 > SF_4, SF_5$.	SF_6	Ion cyclotron resonance	6

atom has a pseudotetrahedral geometry. In the same way PF_5 and AsF_5 form stable non-ionic six-coordinate complexes with organic donor molecules such as ethers, sulphoxides, amides, esters [47] and in particular MeCN. The vibrational spectra of AsF_5.NCMe have been studied in detail [48] and have shown that the arsenic atom is in an octahedral environment. In the case of PF_5, although it has not been possible to isolate its MeCN adduct at room temperature [49], ^{19}F [49,50] and ^{31}P [49,51] n.m.r. spectroscopic studies have shown that rapid exchange takes place between free and complexed PF_5. The crystal structure of PF_5.py (py = pyridine) [52] and $PF_5.NH_3$ [53] have shown that in either case the phosphorus atom is in an octahedral environment.

With fluoride ion donors such as selenium tetrafluoride [54], sulphur tetrafluoride or tellurium tetrafluoride [55], BF_3, PF_5 and AsF_5 form adducts in which the cations SeF_3^+, SF_3^+ or TeF_3^+ and the corresponding anion are linked by fluorine bridges. Azeem et. al [56] have studied the structure of the adducts formed between SF_4 and BF_3, PF_5 and AsF_5 by investigation of the $[^{18}F]$-fluorine exchange between $[^{18}F]$-labelled SF_4 and BF_3 and between SF_4 and $[^{18}F]$-labelled BF_3. Furthermore, they have studied these adducts by examination of their vibrational spectra. Using ^{19}F n.m.r and conductivity techniques the same authors have also investigated the reaction between SF_4 and the $SF_4.BF_3$ adduct. Their experimental results have been best accounted for in terms of an ionic structure $SF_3^+MF_n^-$ with a relatively strong fluorine bridging between the ions. Later Bartlett and

co-workers [57] have solved the crystal structure of $SF_3^+BF_4^-$ and $SF_3^+AsF_6^-$ in which BF_4^- and AsF_6^- occupy a lattice site of symmetry lower than T_d and O_h respectively.

Fluorine bridged species are often used to account for the fluorine exchange behaviour of fluorides. Brownstein [58] has studied the reactions of BF_3, PF_5 and AsF_5 with their fluoroanions in dichloromethane. Using ^{19}F n.m.r. techniques he has shown for example that a rapid fluoride exchange takes place between BF_3 and PF_6^- via a bimolecular mechanism and postulated that a fluorine bridged species is the most likely intermediate in the exchange process.

The fluoroanions derived from BF_3, PF_5 and AsF_5 are widely used as counter-anions supporting electrolytes in electrochemical studies [59]. Supporting electrolytes decrease the electrical resistance of the solution by acting as a current carrier and thus ensure the movement of the electron active species by diffusion rather than by electrical migration in the voltage field across the electrochemical cell. The hexafluoroanions of phosphorus and arsenic as their lithium salts have been used to increase the efficiency of the charging/discharging process of polypyrrole films in lithium-polypyrrole batteries [60].

The oxidising properties of PF_5 and AsF_5 have been demonstrated in many ways.

In sulphur dioxide AsF_5 has been used to oxidise copper and nickel metals to give $CuAsF_6$ and

$Ni(AsF_6)_2.2SO_2$ [61] respectively. In MeCN copper metal is also oxidised by PF_5 although slowly to give solvated copper(I) hexafluorophosphate but AsF_5 shows no oxidising ability towards Cu under the same conditions [49]. This has been explained in terms of thermodynamic and kinetic factors as the AsF_5.NCMe adduct is more inert. In this respect the AsF_5 is a less oxidising agent than the hexafluorides MF_6 (M = Mo,W,Re and U) towards the same metal in MeCN [49]. However, in liquid iodine pentafluoride both PF_5 and AsF_5 show stronger oxidising ability towards iodine than MoF_6 or WF_6 [62].

In the presence of fluorine PF_5 and AsF_5 have been shown to intercalate oxidatively in graphite [63] to give C_8MF_6 (M = P or As) salts. When M = As the salt exhibits a conductivity comparable to that of aluminium metal [64].

1.7 Chemistry of Antimony Pentafluoride.

Antimony pentafluoride is a colourless and a very viscous liquid at room temperature. It is hygroscopic and fumes in moist air. The pure liquid can be handled and distilled in glass if moisture is excluded. Liquid SbF_5 has a polymeric structure as established by ^{19}F n.m.r. spectroscopy. This has been shown to have a cis-fluorine bridged structure in which each antimony atom is surrounded by six fluorine atoms in a octahedral arrangement (Figure 1.6). Vapour density measurements [66] and mass spectroscopic studies [67] suggest that the polymerisation of SbF_5 persists into the vapour state. Due to the recognition of its

"superacid" properties which are useful in stabilising carbocations [68], the solution chemistry of SbF_5 has prompted a wide interest since the late sixties. It is firmly established that SbF_5 is a very strong Lewis acid. Gillespie and Moss [65b] have used ^{19}F n.m.r. spectroscopy to study the HF/SbF_5 system and have shown that in very dilute SbF_5 solutions SbF_6^- is present and that polymeric anions, $[Sb_nF_{5n+1}]^-$, form with increasing SbF_5 concentration. This has also been confirmed by cryoscopic measurements [69] where it has been shown that SbF_5 behaves as a strong binary electrolyte in dilute solution. SbF_5 reacts with a variety of binary fluorides to give SbF_6^- or $Sb_2F_{11}^-$ anions, e.g, $BrF_2^+ SbF_6^-$ [70], $ClF_2^+ SbF_6^-$ [71], $NbF_4^+ Sb_2F_{11}^-$ [72], $XeF^+ Sb_2F_{11}^-$ [73] and $Li^+SbF_6^-$ [74]. With acetonitrile SbF_5 forms an adduct [115] for which a detailed vibrational spectroscopic study has been carried out [75]. This shows that the antimony atom is in an octahedral environment. In an ^{19}F n.m.r. study [58] it has been shown that rapid fluorine exchange takes place between SbF_6^- and PF_5 or AsF_5 in dichloromethane at room temperature. The fluorine exchange has been explained in terms of mechanism involving a fluorine bridged intermediate, $PSbF_{11}^-$ and $AsSbF_{11}^-$ for which ^{19}F n.m.r. evidence has been found. Antimony pentafluoride has been shown to oxidise molecular iodine in sulphur dioxide to give blue crystals of $I_2^+SbF_{11}^-$ [76] in which antimony is in a distorted octahedral arrangement.

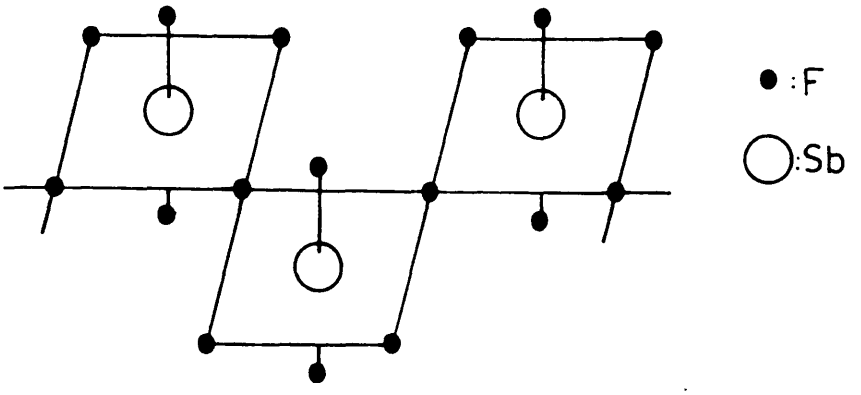

Figure 1.6 The Polymeric Structure of Liquid Antimony Pentafluoride.

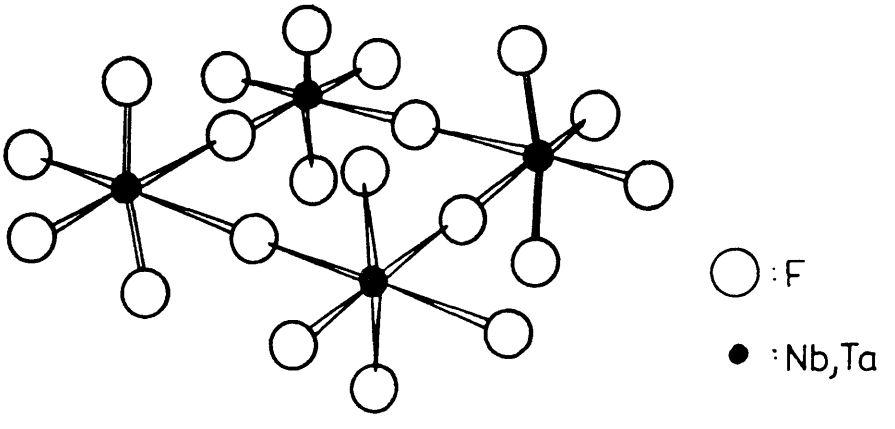

Figure 1.7 The Tetrameric Unit of Niobium and Tantalum Pentafluoride Structure.

1.8 Chemistry of the Pentafluorides of Niobium and Tantalum.

The close similarity of the atomic and ionic radii of niobium and tantalum is reflected in the similar properties of niobium and tantalum pentafluorides. These are thermally stable, form snowy-white crystalline solids, colourless liquids and colourless vapours. Both pentafluorides may be prepared by direct fluorination of the corresponding metals [77] or by reacting the metal pentachloride with hydrogen fluoride [78]. Their vapour pressures at 323K are relatively high which allows purification by vacuum sublimation to be effected. Both pentafluorides adopt the molybdenum pentafluoride structure. This consists of tetrameric units containing four metal atoms with four coplanar bridging fluorine atoms as shown in Figure 1.7 [79]. The vibrational spectra of their solid and liquid phases have been investigated and interpreted in terms of cis-fluorine bridging [80]. On the basis of electron diffraction [81], and vapour density [66] studies it has been concluded that both pentafluorides are trimeric in the vapour.

Niobium and tantalum pentafluorides are both strong Lewis acids complexing a wide variety of donors such as ethers [82], sulphides [82] and amines [83-85]. They both react with fluoride ions to form anions of the type MF_{5+n}^{n-} (M = Nb,Ta) [86]. Their hexafluoroanions have been shown to form bridging complexes in solution in the presence of their parent fluorides as well as in the presence of the pentafluorides of antimony and arsenic [86]. The structure of these bridging complexes have been derived from their

^{19}F n.m.r. spectra and consists of two octahedra joined by a fluorine bridge through the corners. The structure for $Nb_2F_{11}^-$ and $Ta_2F_{11}^-$ has been determined in the solid state by x-ray diffraction [87].

1.9 Lewis Acidity Order of Binary Fluorides.

1.9.1 General Definitions.

There have been many definitions offered for the terms acid and base. Since very early work in this area involved investigations in aqueous solution, the definition of Arrhenius [88] restricted acids and bases to this medium. Acids were defined as substances which on reaction with water increase the hydronium ion concentration of the solution. Bases were defined as substances that on reaction with water increase the hydroxide ion concentration of the solution. This definition was extended by Brønsted and Lowry [89,90] to include reactions taking place in solvents other than water. They defined an acid as a molecule or ion capable of losing a proton and a base as a molecule capable of adding a proton. The reaction of gaseous ammonia and hydrogen chloride (Equation 1.8) to produce ammonium chloride is a representative example.

$$NH_3 + HCl \rightarrow NH_4^+Cl^- \qquad (1.8)$$

Another definition worth mentioning was originally due to the ideas of Franklin [91] known also as the solvent system definition. Following this concept an acid is

defined as any substance that yields, either by direct dissociation or by interaction with solvent, the cation characteristic of that solvent. A base is defined as any substance that yields by direct dissociation or by interaction with the solvent, the anion characteristic of the solvent. Within this definition a donor acid is a substance that can split off solvent cations or can unite with solvent molecules to form cations. An acceptor acid is a substance that can combine with solvent anions. A base donor is a substance that can split off solvent anions or can unite with solvent molecules to form anions. An acceptor base is a substance that can combine with solvent cations.

1.9.2 Lewis Acid-Base Definition.

A more conceptually wider definition of acid-base was due to G.W. Lewis [92]. He originally defined an acid as any molecule radical or ion in which an atom, because of the presence of incomplete electronic group, can accept one or more electron pairs (i.e. as an electron-pair acceptor). Correspondingly a base is defined as a species that has within its molecular structure an atom(s) that is(are) capable of donating an electron pair (i.e. as an electron-pair donor). A typical Lewis acid-base reaction is presented by the reaction between trimethylamine and boron trifluoride (Equation 1.9)

$$Me_3N + BF_3 \rightarrow Me_3NBF_3 \qquad (1.9)$$

In modern use a Lewis base is any substance which has electron density that can be shared with another substance in a chemical reaction, and an acid is any substance capable of accepting electron density from a Lewis base. When the product of the acid-base reaction is the non-ionised combination of the acid and the base it is referred to as an addition compound or an adduct.

1.9.3 Lewis Acidity Order

In order to have a complete understanding of any body of information it is necessary to put that information on a quantitative basis. In this case it is important to set up quantitative criteria for the strengths of acids and bases. Although the Lewis definition has wider applications it suffers from the absence of a generally applicable order of acid or base strengths.

From the above definition an estimation of the enthalpy change accompanying reactions for a series of acids and reference base should, in principle, allow a quantitative ordering of their strengths. In practice, acidity strengths have been inferred from a variety of indirectly related properties such as solubilities, sublimation temperatures etc. These types of investigation have usually been carried out in solution, occasionally with formation of an insoluble product or reactant or both. Unfortunately many discrepancies still persist as far as the order of Lewis acidity of binary

fluorides of the main group is concerned. This is due to differences in solvational energies of products and reactants or lattice energy effects or both which may obscure intrinsic differences in acidity. Furthermore, it has been shown that the order of acid strengths is dependent on the reference base chosen [93,94]. Table 1.1 summarises the results of some investigations using different fluoride ion donors in various solvents. There have been, nonetheless, many attempts establishing a universal acidity scale. Among which is that due to Gutmann [95] otherwise known as the donor number. This is defined as the negative enthalpy of reaction of a base with the Lewis acid antimony pentachloride $SbCl_5$. Drago and co-workers [96] have proposed a way of expressing enthalpies of reactions in terms of contributing parameters of acids and bases (Equation 1.10)

$$-\Delta H = e_A e_B + c_A c_B + t_A t_B \qquad (1.10)$$

where ΔH is the enthalpy of formation of the Lewis acid-base adduct, $e_A c_A$ are parameters characteristic of the acid, $e_B c_B$ are parameters characteristic of the base and the $t_A t_B$ adds the energy of the electron density transfer effect.

A more objective approach to this problem uses ion cyclotron resonance techniques which do not involve solvents and allows the measurement of the ion affinity. The gas phase ion affinity is defined as the negative enthalpy change for the reaction (Equation 1.11)

$$A(g) + X^-(g) \rightarrow AX^-(g) \qquad (1.11)$$

The results of a recent study [6] using ion cyclotron resonance techniques for a series of Lewis acids is presented in Table 1.1 (bottom line).

Although ion cyclotron resonance techniques give a Lewis acidity order independent of the solvent factors the Lewis acidity order on an absolute scale is still the centre of some controversy. The accuracy of the enthalpy changes will depend on the ancillary data used for the appropriate enthalpy cycle. This is illustrated by the example of the fluoride ion affinity of BF_3 where there have been originally two reports of the value of the enthalpy change. Altshuller [102] gives a value of -297 kJ mol^{-1} whereas Bills and Cotton [103] give a value of -381 kJ mol^{-1}. The latter value was confirmed by Bartlett and co-workers [104] who, using lattice energy calculations found a value of -385 ± 25 kJ mol^{-1}. These authors [104] give also values for the enthalpy changes of the fluoride ion affinity of PF_5 and AsF_5. These have been found as -422.7 ± 33.5 and -464.5 ± 16.7 kJ mol^{-1} respectively. According to these values the Lewis acidity order of these fluorides is $AsF_5 > PF_5 > BF_3$.

CHAPTER TWO

EXPERIMENTAL

2. Experimental

2.1 Equipment.

Due to the moisture sensitivity of the reagents used in this work all manipulations were carried out using vacuum lines or a glove box.

2.1.1 Vacuum Line

The vacuum lines were constructed from Pyrex glass and evacuated using a mercury diffusion pump in series with an Edwards rotary oil pump which achieved a vacuum of $<10^{-4}$ Torr. A mercury vacustat and a gauge, Heise (P±0.5 Torr) were used to check the vacuum and measure the pressure of gases respectively. Standard glass joints were greased with Apiezon N or Kel F. P.T.F.E. stop-cocks (J. Young Ltd). were used at the inlets of the vacuum lines.

2.1.2 Inert Atmosphere.

An oxygen-free-nitrogen atmosphere box (H_2O < 10 p.p.m) was used to handle and store hygroscopic solids. All glass vessels were flamed-out before being taken inside the glove box.

2.1.3 Vibrational Spectroscopy.

The characterisation of compounds was carried out mainly by vibrational spectroscopy. Infrared spectra, in the range 4000 - 180 cm^{-1} were recorded on Perkin Elmer 983 or 580 ir-spectrophotometers. The samples were analysed

as Nujol mulls between silica or AgCl discs. Gas samples were analysed in a gas cell made from Pyrex glass (cellpath 5cm) and equipped with AgCl windows sealed to the glass with Araldite.

Raman spectra were obtained using a Spex Ramalog Spectrometer, using an argon ion (488.0, 514.5nm) or krypton ion (647.1, 520.8, 568.2nm) laser source. The samples, solids or solutions were sealed in Pyrex glass capillaries.

2.2 Preparation and Purification of Reagents.

2.2.1 Purification of Acetonitrile.

Acetonitrile (Rathburn HPLC Grade S) was purified according to an extended method [105] of that described by Walker and Rameley [106] and consisted of a series of refluxes followed by rapid distillation over:

1. $AlCl_3$ for 1 h.
2. $KMnO_4$ and Li_2CO_3 for 0.25 h.
3. $KHSO_4$ for 1 h.
4. CaH_2 for 1 h.
5. P_2O_5 for 0.5 h (twice)

Acetonitrile was then degassed under vacuum and transferred onto thermally activated alumina (neutral, 60 mesh) and shaken thoroughly. It was then transferred onto activated 3A molecular sieves, degassed and allowed to stand for 24 h. Before use, MeCN was finely vacuum distilled onto freshly

activated 3A molecular sieves.

Acetonitrile thus purified had an absorbance in the range 0.05 - 0.15 at 200nm and a cut off at 185nm.

2.2.2 Purification of Diethylether.

Analar diethylether was purified by treatment with freshly cut sodium until no further reaction was observed. It was then degassed under vacuum, transferred onto thermally activated 3A molecular sieves and allowed to stand for 24 h. Before use Et_2O was transferred onto freshly activated 3A molecular sieves.

2.2.3 Preparation and Purification of Molybdenum Hexafluoride [107]

Molybdenum hexafluoride was prepared by reaction between molybdenum powder (B.D.H.) and elemental fluorine in a flow system at high temperature. The reactor consisted of two sections : a metal section and a glass section (Figure 2.1).

The metal section was made of a nickel reaction tube 47 cm long and 1.6 cm internal diameter, containing a nickel boat loaded with 2-4g molybdenum powder. The glass section comprised a series of traps made of Pyrex glass. The end ground glass of the traps were joined to the reaction tube by Swagelok and Teflon ferrules. Traps A,B and E were cooled with a dry ice-dichloromethane bath (195K). These were used respectively, to dry the fluorine gas, collect MoF_6 and retain moisture.

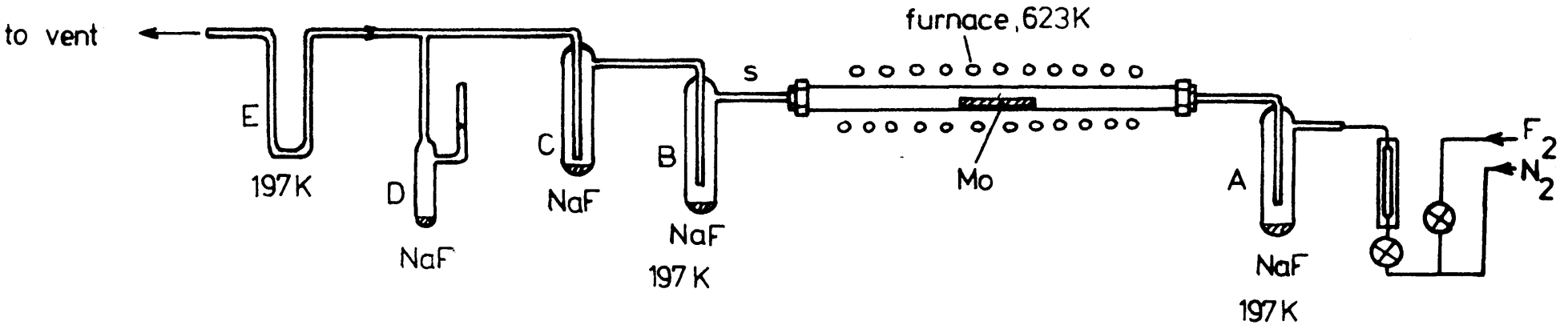

Figure 2.1 Preparation of Molybdenum Hexafluoride.

Before reaction the NaF contained in all the traps was activated with a hot flame and the whole glass section flamed-out under vacuum then flushed with nitrogen gas overnight. The reaction tube was heated to 623K and a mixture of fluorine and nitrogen (F_2:N_2 1:3) admitted to the tube until the reaction was completed.

Once the fluorination was completed the glass section was sealed off at point S and attached to a standard vacuum line (<10^{-4} Torr), trap B being kept at 77K. The MoF_6 was purified by trap-to-trap distillation over activated NaF and finally transferred into the breakseal ampoule D where it was stored over NaF at 77K until required.

2.2.4 Preparation and Purification of Dinitrogen Tetroxide [108].

Dinitrogen tetroxide was prepared by thermal decomposition of lead nitrate (Riedel-De Huen A.G) using a Pyrex glass reactor, figure (2.2.)

9g of $Pb(NO_3)_2$ were loaded in the reaction tube and dried under vacuum at 293K for 2h, then heated gently with a gas torch. Trap A was loaded with P_2O_5 and cooled with a liquid nitrogen-carbon tetrachloride slush bath (253K) to retain moisture or nitric acid from the decomposition of $Pb(NO_3)_2$. Trap 2 containing P_2O_5 was cooled with a dry ice dichloromethane bath (195K) in which N_2O_4 was collected. Once all the $Pb(NO_3)_2$ had decomposed the stop-cock was closed and N_2O_4 purified by trap-to-trap distillation over P_2O_5 and finally stored in a stainless steel pressure vessel until required.

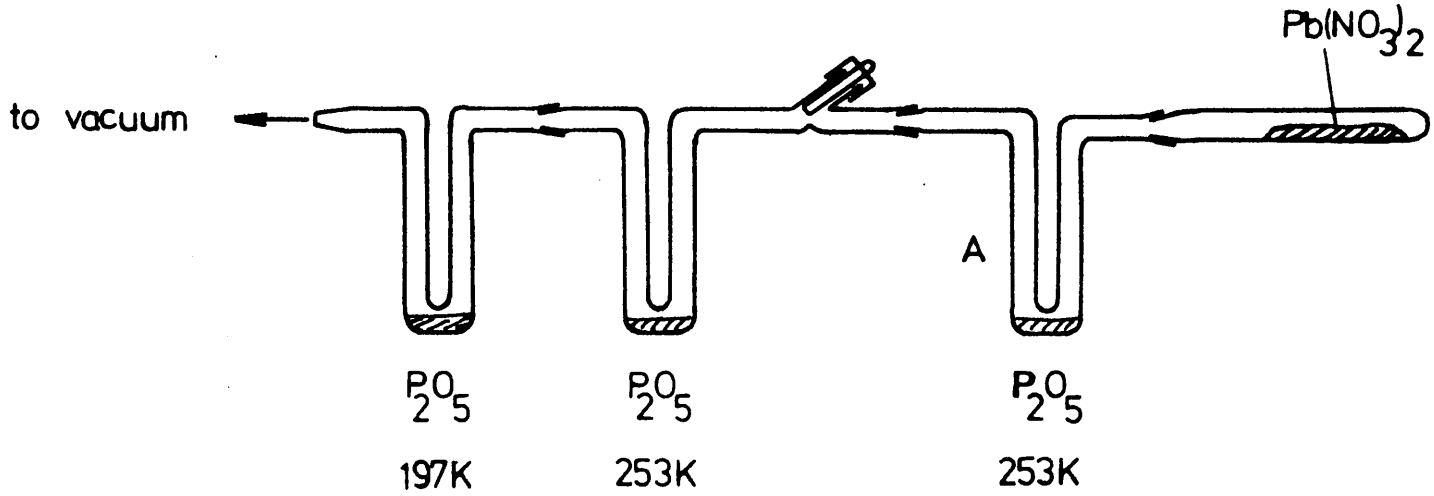

Figure 2.2 Preparation of Dinitrogen Tetroxide.

The infrared spectrum of N_2O_4 was recorded using a gas cell and is presented in Table 2.1. This reveals the presence of nitric oxide as shown by the bands at 1616 and 1322 cm^{-1} [109]. No trace of nitric acid was present.

2.2.5 Preparation of Nitrosyl Fluoride [110].

Nitrosyl fluoride was prepared by reaction of dinitrogen tetroxide with activated potassium fluoride (B.D.H).

4mmol of N_2O_4 were condensed in a Monel high pressure vessel (Hoke, $90cm^3$) containing excess KF which had been activated by reaction with $(CF_3)_2CO$ in MeCN and heated at 383K for 12 h. The bomb was warmed to room temperature and the reaction left to proceed for 0.5 h. The bomb was then cooled to 195K and NOF removed and immediately used. The yield of the reaction was 50%, based on the initial pressure of N_2O_4. However, the infrared spectrum of NOF (Table 2.2) revealed the presence of some nitric oxide as shown by the bands at 1616 cm^{-1} and 1322 cm^{-1} [109].

Table 2.1 Infrared Spectrum of Dinitrogen Tetroxide.

This work.	Literature [109]	Assignment
	3440 w	$\nu_5 + \nu_9$ comb.
	3111 m	$\nu_1 + \nu_9$ comb.
2920 w	2971 m	$\nu_5 + \nu_{11}$ comb.
	2747 w	$\nu_{11} + 2\nu_{12}$ comb.
2620 w	2630 m	$\nu_1 + \nu_{11}$ comb.
	2579 w	$\nu_8 + \nu_{11}$ comb.
	2124 w	$\nu_1 + \nu_{12}$ comb.
	1937 w	$\nu_{11} + \nu_8$ comb.
1750 s	1748 s	ν_9 NO str.
1616 s		NO
	1495 w	$\nu_9 - \nu_3$ comb.
1322 s		NO_2
1260 s	1262 s	ν_{11} NO str.
750 vs	750 vs	ν_{12} def.
	695 m	$\nu_3 + \nu_7$ comb.
	429 s	ν_7 NO_2 wag.
	381 m	ν_{10} NO_2 rock

vs = very strong; s = strong; m = medium; w = weak

Table 2.2 Infrared Spectrum of Nitrosyl Fluoride.

This work.	Literature [111]	Literature [112]	Assignment
2920 w			
	1887		N-O str. (NOF)
1860 s	1852		N-O str. (FNO)
1840 s		1844	NO str.
1830 s			
1750 m			
1616 s			NO_2
1322 m			NO_2
780			
765	751 vs	767	NOF bend
750	735		NOF bend (NOF)
520 s		521	N-F str.
	510		N-str (FNO)
	492		O-F str (NOF)

vs = very strong; s = strong; m = medium; w = weak

2.2.6 Preparation of Tris(dimethylamino)sulphonium Difluoro-trimethylsilicate.

Tris(dimethylamino)sulphonium difluorotrimethylsilicate, TAS^+F^-, was prepared by reaction between N,N-dimethyltrimethylsilylamine and sulphur tetrafluoride in dry diethylether (Equation 2.1) in a double limb vessel, Figure(2.3) using a modified version of the established method [113].

$$3Me_2NSiMe_3 + SF_4 \xrightarrow[298K]{Et_2O} (Me_2N)_3SMe_3SiF_2 + 2Me_3SiF \qquad (2.1)$$

24 mmol of Me_2NSiMe_3 (Aldrich Chemical Company, Inc) which had been degassed several times under vacuum and stored over activated 4A molecular sieves, were condensed in one limb of the reaction vessel containing dry Et_2O ($4cm^3$). 8 mmol of SF_4 (Matheson) were condensed into the other limb and werewarmed slowly to allow SF_4 to distil into the cooled reaction limb. The vessel was then warmed slowly to room temperature. At this stage white crystals started to precipitate immediately. The mixture was then shaken for two days to allow reaction to proceed to completion. After carefully removing the volatile material a white crystalline solid was isolated and stored in sealed ampoules at 273K until required. Infrared analysis of the volatile material showed bands attributable only to Et_2O and Me_3SiF.

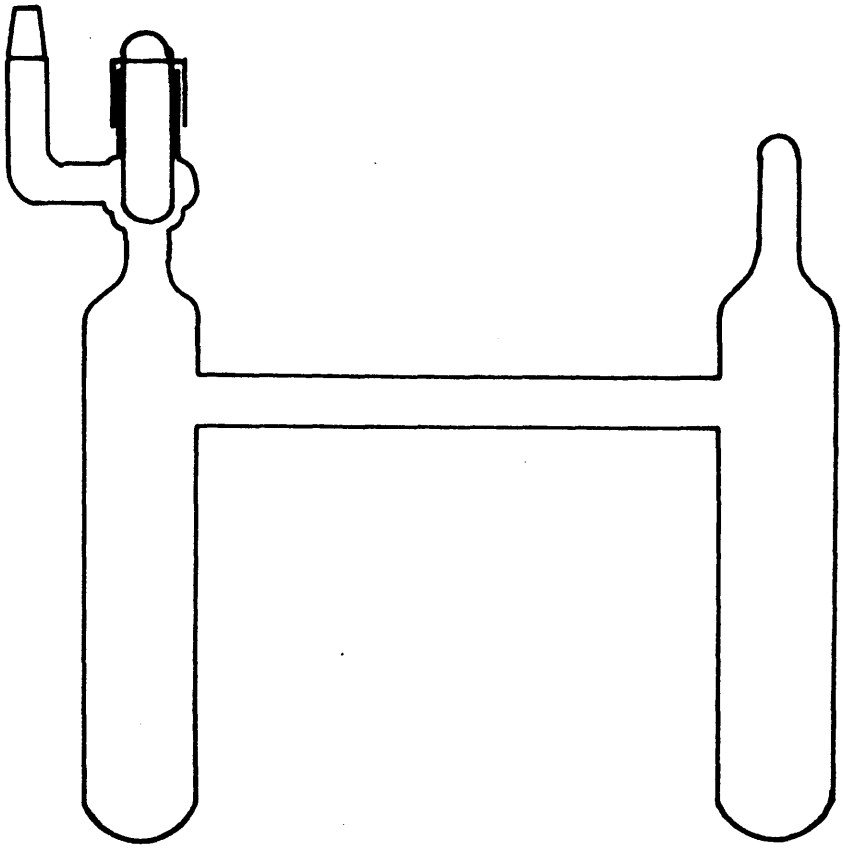

Figure 2.3 Double-limb Reaction Vessel

2.2.7 Preparation of Trimethylfluorosilane [39].

Trimethylsilylfluoride was prepared by reaction between tungsten hexafluoride and N,N-diethyltrimethylsilylamine (Equation 2.2) in a glass vessel.

$$WF_6 + 4Me_3SiNEt_2 \xrightarrow{233K} WF_2(NEt_2)_4 + 4Me_3SiF \qquad (2.2)$$

The vessel was cooled to 77K and WF_6 (16.0 mmol, Ozark Mahoning) admitted under vacuum. Excess Me_3SiNEt_2 (63.3 mmol, Aldrich Chemical Company, Inc) was then transferred. The mixture was kept at 233K overnight until the exothermic reaction subsided then the vessel was warmed slowly to room temperature and left for a further 6 h. The mixture was cooled to 197K and Me_3SiF removed and stored in vacuo over activated 4A molecular sieves. The yield was 80% on the basis of Me_3SiNEt_2 used. The infrared spectrum (Table 2.3) of Me_3SiF showed no impurities and was consistent with the literature [114]. Its molecular weight determined 90.3 ± 2.9 was in good agreement with the 92 theoretical value.

2.2.8 Purification of the Pentafluorides of Niobium and Tantalum.

The pentafluorides of niobium and tantalum were purified by sublimation using an all-glass manifold (Figure 2.4). NbF_5 or TaF_5 (5g, Fluorochem Ltd) were loaded into a previously evacuated and flamed breakseal vessel in the glove box. The vessel was re-evacuated

Table 2.3 Infrared Spectrum of Trimethylfluorosilane.

This work	Literature [114]	Assignment
2974 st	2968 v.st	ν_{as} CH_3
2922 m	2910 w	ν_s CH_3
1452 vw	1450 w	
1429 vw	1425 w 1415 w	ν_{as} CH_3
1310 vw	1312 w.	
1263 v.st	1262 st.	ν_s CH_3
920 v.st	912 v.st	ν_s Si-F
852 v.st	858 v.st	ν_{as} CH_3
767 st.	760 st	ν_s CH_2
	712 w	ν_{as} C_3Si
627 vw	619 vw	ν_s C_3Si

vs = very strong; s = strong; m= medium;

w = weak; vw = very weak

and sealed off at point A before being joined to the manifold. This was flamed out under vacuum, tap C closed and the seal broken open using a glass sealed metal bar. The pentafluorides were sublimed using an oil bath and collected at 77K in the u-shaped tube which was then sealed at points B_1 and B_2 and stored at 77K until required.

2.2.9 Preparation of Arsenic Pentafluoride-Acetonitrile Adduct [48].

Arsenic pentafluoride was handled easily as its acetonitrile adduct. The adduct was prepared by reaction between AsF_5 and MeCN in a double limb vessel.

The reaction vessel was evacuated, flamed-out and cooled to 77K. Acetonitrile (10 cm^3) was admitted by vacuum distillation, followed by AsF_5 (10 mmol Matheson). The mixture was warmed slowly to room temperature until the exothermic reaction subsided, the vessel was then shaken for a few hours and the colourless solution was decanted into the empty limb. After removal of excess MeCN a white solid was isolated, sealed in an ampoule and stored at 273K until required. The infrared spectrum of the solid contained bands due to coordinated MeCN (Table 2.4). The bands at ν_{max} 738 (ν_{18}), 720 (ν_5) and 670 (ν_6) cm^{-1} were due to As-F stretching modes in an octahedral environment.

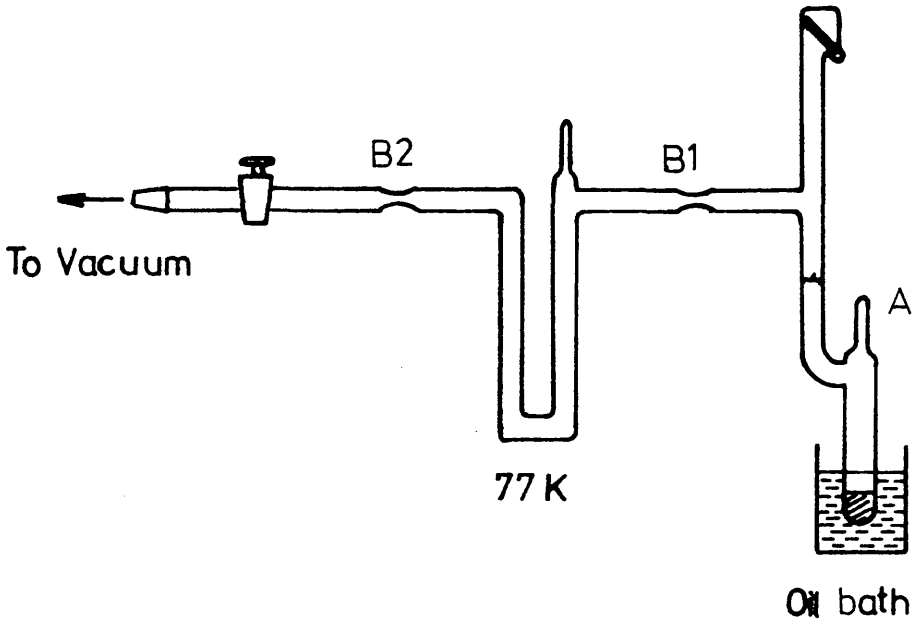

Figure 2.4 Sublimation Manifold

Table 2.4 Infrared Spectrum of AsF_5.NCMe

This work	Literature [48]	Assignment
3020 w	3023 mw	ν_{13} CH_3 str.
	2950 mw	ν_1 CH_3 str.
2340 s	2350 s	ν_2 CN str.
2310 ms	2315 ms	$\nu_3+\nu_4$ comb.
	1410 mw, br	ν_{14} CH_3 def.
1365 m	1364 mw	ν_3 CH_3 def.
1030 m	1030 mw	ν_{15} CH_3 rock
960 m	962 mw	ν_4 CC str.
738 vs	735 vs	ν_{16} AsF-el
720 vs	718 vs	ν_5 As-F axial str.
670 ms	671 ms	ν_6 As-F eq. str.
510 m		
435 m	435 m	ν_{17} CCN def
	390 sh,w	?

m: medium, m.s: medium strong, s: strong,
vs : very strong, mw: medium weak, w: weak,
sh : sharp

2.2.10 Preparation of Antimony Pentafluoride Acetonitrile Adduct [115].

Acetonitrile was the solvent used throughout the work; it was therefore more convenient to use SbF_5 as its MeCN adduct.

Pure SbF_5 (ca. 3g, 13.8mmol) which had been purified by low temperature trap-to-trap distillation was transferred under vacuum into a flamed-out double limb vessel containing MeCN (10 cm^3). The vessel was then warmed to room temperature, shaken for a few hours and the colourless solution decanted into the other limb. After removal of excess MeCN a white solid was isolated sealed in an ampoule and stored at 273K until required. The infrared spectrum of the solid (Table 2.5) contained bands due to coordinated MeCN. The bands at ν_{max} 1200 (ν_{10}), 962 ($\nu_8+\nu_{16}$), 640 (ν_5) and 680 (ν_6) were due to the stretching modes of Sb-F in an octahedral environment.

Table 2.5 Infrared Spectrum of SbF_5.NCMe

This work	Literature [75]	Assignment
3020 mw	3021 mw	ν_{13} CH_3 str.
	2948 mw	ν_1 CH_3 str.
2336 ms	2342 ms	ν_2 CN str.
2305 m	2312 m	$\nu_3+\nu_4$ comb.
2260 w	2276 w	$\nu_1-\nu_{16}$ comb.
	1448 w	$\nu_{15}+\nu_{19}$ comb.
	1404 mw	ν_{14} CH_3 def.
1362 mw	1358 mw	ν_3 CH_3 def.
1200 w	1198 w	$2\nu_{10}$ SbF_4 eq.str.
1150 vw	1153 vw	?
1127 w	1127 w	?
1028 w	1027	ν_{15} CH_3 rock
962 sh	974 sh	$\nu_8+\nu_{16}$ comb.
	965 mw	ν_4 CC str.
	714 m	$2\nu_{12}+\nu_{19}$ comb.
640 sh	617 w	ν_5 SbF axial str.
680 vs	663 vs	ν_6 SbF_4 eq.str.
413 sh	412 mw	ν_{17} CCN def.

m: medium, Ms: medium strong, mw : medium weak,

s: strong, vs: very strong w: weak,

vw: very weak, sh:sharp

2.2.11 Preparation of Acetonitrile Adduct of the Pentafluorides of Niobium and Tantalum [83,84,116].

The pentafluorides of niobium and tantalum were handled more conveniently as their acetonitrile adducts since the solvent used throughout the work was acetonitrile. The adducts were prepared by reaction between MeCN and the corresponding binary fluoride using a double limb vessel (Figure 2.3) and a sublimation manifold (Figure 2.4).

A breakseal vessel containing pure NbF_5 or TaF_5 (5g, Fluorochem Ltd) was joined to the sublimation manifold to which the double limb vessel was attached, flamed-out, then cooled to 77K. Acetonitrile (7 cm^3, section 2.3.1) was admitted by vacuum distillation and NbF_5 or TaF_5 sublimed. The vessel was allowed to reach room temperature and the mixture shaken overnight. The yellow solution was decanted into the empty limb and excess MeCN removed under vacuum to give a yellow solid in either case. These were stored in breakseal ampoules at 273K until required. The infrared spectrum of NbF_5.NCMe contained bands at ν_{max} 2335 (comb.), 2300 (CN), 1030 (CH_3 rock), 950 (CC) cm^{-1} due to coordinated MeCN and bands at 720 and 620 cm^{-1} assigned to Nb-F vibrations [83]. The infrared spectrum of TaF_5.NCMe contained bands at 720 and 590 cm^{-1} assigned to Ta-F vibrations [84,116].

2.2.12 Preparation of Lithium Tetrafluoroborate, Lithium Hexafluorophosphate and Lithium Hexafluoroarsenate.

The salts $LiBF_4$, $LiPF_6$ and $LiAsF_6$ were prepared by reactions between lithium fluoride and boron trifluoride, phosphorus pentafluoride or arsenic pentafluoride in acetonitrile using a double limb vessel. The experimental method was essentially identical in all cases.

Anhydrous LiF (0.2g, 7.7 mmol, B.D.H.) was loaded in the previously evacuated and flamed-out vessel in the glove box, transferred to the vacuum line and re-evacuated . Boron trifluoride (4.5mmol, Ozark Mahoning), PF_5 (4.5mmol, Matheson) or AsF_5 (4.5mmol, Matheson) were admitted at 77K followed by MeCN (5 cm^3). The mixtures were allowed to reach room temperature and shaken for 0.5 h. The colourless solutions were then decanted into the empty limb. After removal of the volatile material white solids were isolated, sealed in ampoules and stored at 273K until required. The infrared spectra of solids $LiBF_4$, $LiPF_6$ and $LiAsF_6$ (Nujol Mull) are presented in Tables 2.6 to 2.8 respectively. No satisfactory Raman spectra were obtained as the samples burned in the laser beam.

Table 2.6 Infrared Spectrum of Nitrosonium Tetrafluoroborate and Lithium Tetrafluoroborate.

$NOBF_4$	$LiBF_4$	KBF_4	Assignment
This work		[117]	
2340 m			ν NO
1100-1020 vs,br	1090-1040 vs,br	1035-1090 vs,br	ν_3 (F2)
770 m		773 m	ν_1 (A1)
530 s	530 s	536 vs	ν_4 (F2)
520 s		525 vs	
		370 w	ν_2 (E)
		357 w	

m: medium, w: weak, s:strong, vs: very strong, br: broad

Table 2.7 Infrared Spectrum of Nitrosium Hexafluorophosphate and Lithium Hexafluorophosphate.

$NOPF_6$	$LiPF_6$	KPF_6	Assignment
This work		[74]	
2340			ν NO [29]
840 (vs)	840 (vs)	830 (s)	ν_3 (F_{1u})
560 (m)	560 (m,sh)	560 (m)	ν_4 (F_{1u})

m : medium, s : strong, vs : very strong, sh : sharp

Table 2.8 Infrared Spectrum of Nitrosonium Hexafluoroarsenate and Lithium Hexafluoroarsenate.

This work		Literature		Assignment
$NOAsF_6$	$LiAsF_6$	$CsAsF_6$ [74]	$KAsF_6$ [118]	
2330 (sh)				$\nu\ NO^+$ [29]
705 (vs)	705 (s)	699 (s)	702 (s)	ν_3 (F_{1u})
	505 (m) ?			
	398 (m)	392 (m)	368 (s)	ν_4 (F_{1u})

m : medium, s : strong, vs : very strong sh : sharp

2.2.13 Preparation of Nitrosonium Hexafluorophosphate and Nitrosonium Hexafluoroarsenate.

Nitrosonium hexafluorophosphate and nitrosonium hexafluoroarsenate were prepared by homogeneous gas reactions between nitrosyl fluoride and phosphorus pentafluoride or arsenic pentafluoride respectively in a standard vacuum glass vessel.

4mmol of FNO (Section 2.3.5) was vacuum distilled into the evacuated and preflamed vessel followed by PF_5 or AsF_5 (6mmol, Matheson). The mixture was warmed very slowly to room temperature by which time the reaction was complete and a white solid was obtained. After removal of excess reactants the solids were transferred to the glove box and stored in ampoules under vacuum until required. The infrared spectrum of $NOPF_6$ (Table 2.7) contained a band at 2330 cm^{-1} attributed to νNO^+ and bands at 850 cm^{-1} and 560 cm^{-1} assigned to ν_3 and ν_4 mode of PF_6^- in the octahedral symmetry (O_h) respectively. The infrared spectrum of $NOAsF_6$ contained bands at 2330 cm^{-1} assigned to νNO^+ and 705 cm^{-1} assigned to the ν_3 mode of AsF_6^- in the octahedral symmetry (O_h). No satisfactory Raman spectra were obtained for both salts as the samples decomposed in the laser beam.

2.2.14 Preparation of Lithium Hexafluoroantimonate.

Lithium hexafluoroantimonate was prepared by reaction between lithium fluoride and antimony pentafluoride as its acetonitrile adduct in acetonitrile using a double

limb vessel (Figure 2.3).

0.2g, 7.7mmol of LiF (B.D.H) and SbF_5.NCMe (1g, 3.8mmol) were loaded in the flamed-out reaction vessel in the glove box. The vessel was transferred to the vacuum line, evacuated and MeCN ($5cm^3$, Section 2.3.1) distilled at 77K. The vessel was then warmed to room temperature and the mixture shaken for 0.5h. The colourless solution was decanted into the empty limb and after removal of volatile material a white solid was isolated. Both infrared and Raman spectra of the solid (Table 2.9) contained bands at 670 cm^{-1} assigned to the ν_3 (F_{1u}) and ν_1(A_{1g}) modes of vibration of SbF_6^- [74] respectively. No bands due to coordinated acetonitrile were present.

2.2.15 Preparation of Lithium Hexafluoroniobate, Lithium Hexafluorotantalate and Copper(II) Hexafluoroniobate Pentakis(Acetonitrile).

The salts $LiNbF_6$, $LiTaF_6$ and $[Cu(NCMe)_5][NbF_6]_2$ were prepared by reactions between lithium fluoride or copper difluoride and the corresponding acetontrile-adduct of niobium or tantalum pentafluorides in acetonitrile using a double limb vessel.

The flamed-out reaction vessel was loaded with LiF (0.5g, 5.8mmol, B.D.H) or CuF_2 (0.6g, 5.9mmol, Ozark Mahoning) followed by NbF_5.NCMe (0.9g, 4mmol, Section 2.3.1) or TaF_5.NCMe (1.3g, 4mmol, section 2.3.1). The vessel

Table 2.9 Infrared and Raman Spectra of Lithium Hexafluoroantimonate.

Infrared			Raman		
This work	Literature [74]	Assignment	This work	Literature [74]	Assignment
670 vs	669	ν_3 (F_{1u})	670	668	ν_1 (A_{1g})
				558	ν_2 (E_g)
	350	ν_4 (F_{1u})			
				294	ν_5 (F_{2g})
280 m					

m : medium, vs : very strong

was re-evacuated, cooled to 77K and MeCN (5 cm^3) vacuum distilled. The vessel was warmed to room temperature and the mixtures shaken overnight. The liquid phases were decanted into the empty limb and excess volatile material removed under vacuum to give white solids in the case of LiF and a blue solid in the case of CuF_2. All solids were soluble in MeCN without apparent decomposition.

The infrared spectrum of solid $LiNbF_6$ (Nujol Mull) contained bands at ν_{max} 685 (m), 625(vs) and 530 (m) cm^{-1}. The infrared spectrum of $KNbF_6$ [119] reveals only one band at 580 cm^{-1} assigned to the ν_3 vibration mode of NbF_6^- in the octahedral symmetry (Oh). In view of the additional bands present in the infrared spectrum of $LiNbF_6$ it is reasonable to argue that it is due to lowering of site symmetry in NbF_6^- considering the small size of Li^+ cation. The solid infrared spectrum of $LiTaF_6$ had bands at ν_{max} 655 (m), 595 (vs), 540 (w) and 225 (m) cm^{-1}. The infrared spectrum of $[Cu(NCMe)_5][TaF_6]_2$ [54] in the same regions contains bands at ν_{max} 590 ν_3 (F_{1u}) and 286 ν_5(F_{2g}) cm^{-1}. Using the same argument as for $LiNbF_6$ it is reasonable to consider that a lowering of the symmetry in TaF_6^- had taken place. The infrared spectrum of solid $[Cu(NCMe)_5]$-$[NbF_6]_2$ (Nujol Mull) contained bands due to coordinated MeCN, 2338 (comb.), 2300 ν(CN), 1035 p(CH_3), 950 ν(CC) cm^{-1}, and bands at 615 ν_3 (F_{1u}) and 540 ν_4 (F_{1u}) cm^{-1} in an octahedral environment (Oh). Its solid Raman spectrum contained a band at ν_{max} 684 ν_1 (A_{1g}) cm^{-1} [120].

2.2.16 Preparation of Copper(II) Heptafluorotungstate(VI) Pentakis(Acetonitrile) [31]

The solid $[Cu(NCMe)_5][WF_7]_2$ was prepared by reaction between copper difluoride and tungsten hexafluoride in acetonitrile using a double limb glass vessel (Figure 2.3)

Anhydrous CuF_2 (0.60g, 6mmol, Ozark Mahoning) was loaded into the flamed-out reaction vessel, transferred to the vacuum line and evacuated. Acetonitrile (5 cm^3, Section 2.3.1) was added by vacuum distillation followed by WF_6 (1.2g, 4mmol, Ozark Mahoning). The mixture was allowed to warm slowly to room temperature and shaken for several hours to give a blue solution. This was decanted into the empty limb and after removal of volatile material a blue solid was isolated. The infrared spectrum of the solid (Nujol Mull) contained bands due to coordinated MeCN, 2338 (comb.), 2300 ν(CN), 1035 p(CH_3), 950 ν(CC) [121] and a strong band at 620 cm^{-1} assigned to the ν_3 vibration mode of WF_7^- in the pentagonal bipyramid symmetry (D_{5h}) [28]. Its Raman spectrum contained a band at 704 cm^{-1} assigned to the ν_1 vibration mode of WF_7 in the D_{5h} symmetry.

2.2.17 Preparation of Thallium(I) Heptafluorotungstate(VI)[31].

Thallium(I) heptafluorotungstate(VI) was prepared by reaction between thallium fluoride and tungsten hexafluoride in acetonitrile using a double limb glass vessel (Figure 2.3).

Anhydrous TlF (1.35g, 6.6mmol, K and K Laboratories) was thoroughly ground and loaded in the previously evacuated and flamed-out reaction vessel in the glove box, transferred to the vacuum line and re-evacuated. The vessel was cooled to 77K and MeCN (5 cm^3, Section 2.3.1) vacuum distilled followed by WF_6 (1.2g, 4mmol, Ozark Mahoning). The mixture was allowed to reach slowly ambient temperature and shaken for a few hours. The colourless solution was then decanted into the empty limb and after removal of volatile material a white solid was isolated. The infrared and Raman spectra of the solid contained bands at ν_{max} 620 and 710 cm^{-1} assigned respectively to the ν_3 and ν_1 mode of vibration of WF_7^- in the pentagonal bipyramid symmetry (D_{5h}) [28]. Bands due to coordinated MeCN were absent.

2.2.18 Preparation of Nitrosonium Heptafluorotungstate(VI)

Nitrosonium heptafluorotungstate(VI) was prepared by homogeneous gas reaction between nitrosyl fluoride and tungsten heptafluoride in a standard vacuum glass vessel. Excess WF_6 (8mmol, Ozark Mahoning) was vacuum distilled into the evacuated and preflamed vessel followed by NOF (4mmol, section 2.2.5). The mixture was warmed very slowly to room temperature by which time the reaction was complete and a white solid was obtained. After removal of excess reactants the solid was transferred to the glove box and stored in an ampoule under vacuum until required. Its infrared spectrum contained bands at 2330 cm^{-1} and 620 cm^{-1}

assigned to the vibration of NO^+ and ν_3 vibration mode of WF_7^- in the pentagonal bipyramid symmetry (D_{5h}) [29], respectively. Its Raman spectrum contained bands at 2330 cm^{-1} and 714 cm^{-1} assigned to the vibration of NO^+ and ν_1 vibration mode of WF_7^- in the pentagonal bipyramid symmetry (D_{5h}) [29] respectively.

2.2.19 Preparation of Caesium Heptafluorotungstate(VI) and Caesium Heptafluoromolybdate(VI).

Caesium heptafluorotungstate(VI) and caesium heptafluoromolybdate(VI) were prepared by reaction between caesium fluoride and the corresponding hexafluoride in acetonitrile in a double limb glass vessel (Figure 2.3).

Caesium fluoride (0.76g, 5mmol, B.D.H, Optran grade) was thoroughly ground and loaded in the previously evacuated and flamed-out reaction vessel, transferred to the vacuum line and re-evacuated. The reaction limb was cooled to 77K and MeCN (5 cm^3, Section 2.2.1) transferred followed by WF_6 (1.2g, 4mmol Ozark Mahoning) or MoF_6 (0.85g, 4mmol, Section 2.2.3). The mixture was allowed to warm slowly to room temperature and shaken for a few hours. The colourless solutions were then decanted into the empty limb and after removal of volatile material white solids were isolated. The infrared and Raman spectra of $CsWF_7$ contained bands at 620 cm^{-1} assigned to ν_3 vibration mode of WF_7^- in the pentagonal bipyramid symmetry (D_{5h}) [28] and 714 cm^{-1} assigned to ν_1 vibration mode of

WF_7^- in the pentagonal bipyramid symmetry (D_{5h}) [28] respectively. Bands due to coordinated acetonitrile were absent in both cases. The infrared spectrum of $CsMoF_7$ contained a band at ν_{max} 630 cm^{-1} attributed to ν_3 vibration mode of MoF_7^- in the pentagonal bipyramid symmetry (D_{5h}) [28,29] and its Raman spectrum contained a band at ν_{max} 683 cm^{-1} attributed to ν_1 vibration mode of MoF_7^- in the pentagonal bipyramid symmetry (D_{5h}) [28,29].

2.3 Activation of Caesium Fluoride.

Caesium fluoride was activated by reaction with hexafluoroacetone in acetonitrile and thermal decomposition of its 1:1 hexafluoroacetone adduct [122]. This method has been shown to increase significantly its surface area [122,123] and enhance its reactivity [124].

Caesium fluoride (3g,20mmol,B.D.H Optran Grade) was thoroughly ground using an agate pestle and mortar in the glove box and loaded in a stainless steel pressure vessel (Hoke Inc.) containing four stainless steel ball-bearings. The vessel was transferred to a vacuum line and evacuated. Acetonitrile (5 cm^3) and $(CF_3)_2CO$ (33mmol, 7 atmosphere autogeneous pressure, Fluorochem Ltd.) were added by vacuum distillation and the mixture shaken overnight. After removal of MeCN and excess $(CF_3)_2CO$ the vessel was heated at 393K for sixteen hours. The CsF hence activated was off-white in colour. The solid was transferred to the glove box,

ground and stored until required. The infrared spectrum recorded after activation contained bands due to a small quantity of $(CF_3)_2CO$ being retained as heptafluoroisopropoxide ion [125].

2.4 Radiochemical Techniques

Radioactive isotopes have wide applications in research. Neutron activation, isotope dilution, radiometric titration and last but not least radioisotopic exchange are only some of the methods of investigation. In some cases they make experiments possible which could not be carried out in any other way. In others they offer a more convenient and a simpler procedure than conventional methods.

The basic assumption in all tracer work is that the radioactive isotope behaves chemically in an identical manner to a non-radioactive isotope. This assumption is valid in the great majority of cases although hydrogen and some of the lighter elements are exceptions. Owing to large differences in relative atomic mass, isotopes of lighter elements have different velocities which would make considerable difference in kinetic studies.

Before 1934 the application of radioactive isotopes was limited to the use of naturally occurring isotopes but at the beginning of that year artificial radioactivity was discovered by Curie and Joliot [126]. They found

that aluminium foil which had been bombarded with α particles gave off radiation after the bombardment had ceased (Equation 2.3)

$$^{27}_{13}Al + {}^{4}_{2}He \longrightarrow {}^{30}_{15}P + {}^{1}_{0}N \qquad (2.3)$$

This finding along with the successful operation of nuclear reactors and the development of particle accelerators since 1945 led to the production of artificial radioactive isotopes of nearly all the elements with half lives ranging from microseconds to many millions of years.

2.5 Isotopic Exchange Reactions.

Radioactive isotopes were used in exchange reactions as early as 1920 when Heresey [127] showed that exchange occurred between lead ions in precipitated lead chloride and lead in solution.

An isotopic exchange reaction can be defined by equation (2.4)

$$AX + BX^{*} \rightleftharpoons AX^{*} + BX \qquad (2.4)$$

where * represents the radioactive isotope which is interchanging between the chemical form BX and another chemical form AX. The rate of disappearance of the isotopic species from an initially labelled reactant (BX) or the

rate of appearance in an initially unlabelled reactant (AX) is described by a first order rate law [128]. Where isotopic exchange takes place, and provided the reaction is conducted in a stable homogeneous phase the overall concentrations of AX and BX do not change. The rate R at which X atoms interchange between AX and BX is given by The McKay equation (2.5)

$$R = -\frac{2.303}{t} \times \frac{ab}{a+b} \times \log (1-F) \qquad (2.5)$$

where a and b are the total concentrations ($AX+AX^*$) and ($BX+BX^*$) respectively. If AX or BX contain n equivalent exchangeable atoms or groups, the effective concentrations will be n times the ordinary ones. F is the fraction of isotope exchanged at time t and defined by equation (2.6).

$$f = \frac{\text{fraction of activity in the initially unlabelled compound}}{\text{fraction of isotope (mg atom) in the initially unlabelled compound}} \qquad (2.6)$$

In the present work f was determined experimentally using equations (2.7) and (2.8)

$$f = \frac{S_o - S_t}{S_o - S_\infty} \qquad (2.7)$$

$$f = \frac{A_1}{A_1+A_2} \left(\frac{xm_1}{xm_1 + ym_2} \right)^{-1} \qquad (2.8)$$

where S_o, count min^{-1} $mmol^{-1}$, is the specific count rate of the initially labelled compound, S_t, count min^{-1} $mmol^{-1}$, is the specific count rate of the same compound at time t. S_∞, count min^{-1} $mmol^{-1}$, is the specific count rate corresponding to complete exchange. A_1 and A_2, count min^{-1}, are the count rates after exchange between m_1 and m_2 mmol reactants (1 being inactive initially) containing respectively x and y F atoms.

In practice three main situations arise:

1. The situation where only F exchange takes place and where there is no retention of labelled compound by the initially unlabelled compound. In this case equations (2.7) and (2.8) yield the same value provided the radiochemical balance >95% (section 2.12) and f ranges between 0, corresponding to the absence of exchange, and 1, corresponding to random distribution of activity.

2. The situation where both retention and exchange take place in which case equation (2.8) yields f values >1. Equation (2.7) must therefore be used. This situation was encountered in the heterogeneous systems involving activated CsF and MF_5 ^{18}F (M = Mo, W, U).

3. The situation where there is uptake but no exchange in which case equation (2.7) yields f values = 0 and equation (2.8) yields f values >1.

2.6 [^{18}F]-Fluorine as Radiotracer.

Naturally occurring fluorine is monoisotopic with a spin number $I = \frac{1}{2}$. This makes it useful in n.m.r. studies. The element has five artificially produced radioisotopes (^{17}F, ^{18}F, ^{20}F, ^{21}F and ^{22}F) of which [^{18}F]-fluorine has the longest half life. The most recently determined value for its half life is 109.72±0.06 min [129].

During the process of decay of [^{18}F]-fluorine to [^{18}O]-oxygen an emission of a positron β^+, that is a positively charged electron takes place. This results in the decrease of the atomic number by one but leaves the mass number of the isotope unchanged. The kinetic energy of the emitted positron is reduced through interactions with surrounding particles and collides with an electron resulting in a mutual annhilation and an emission of 0.511 MeV γ-photons.

[^{18}F]-Fluorine is an attractive radiotracer as its γ-radiation is easily detected. Since its discovery in 1937 [130], [^{18}F]-fluorine has been used in inorganic chemistry [131] and due to the strong C-F bond (477k J mol^{-1}) it has been probably more extensively used in biological and medical studies [132].

Due to its short half life [^{18}F]-labelled compounds are not commercially available. Hence they must be produced and used during one working day. After six half lives only 1-2% of the starting activity is left and therefore correction for radioactive decay is required.

Figure 2.5. Kinetic Relationship between Incorporation and decay of [^{18}F]-Fluorine

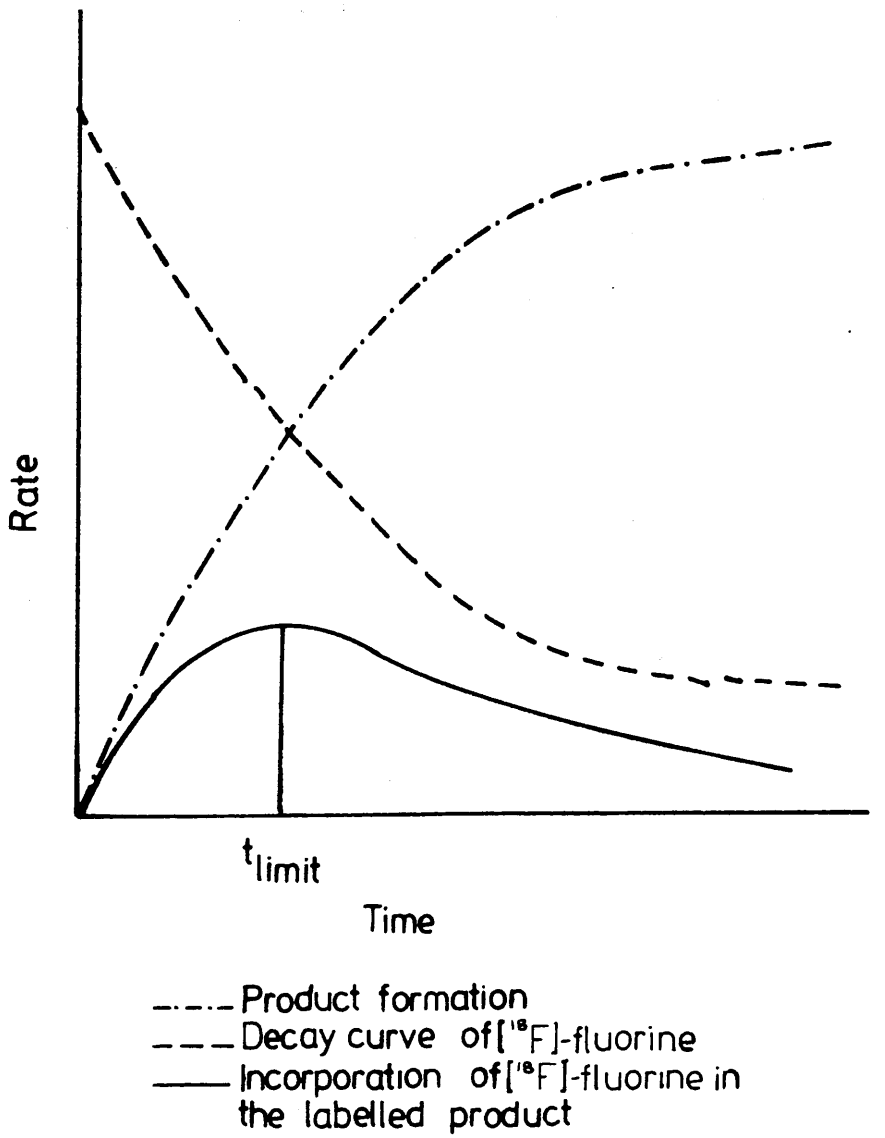

Depending on the access to suitable facilities [^{18}F]-fluorine can be produced by different methods but in general an accelerator, a cyclotron or a nuclear reactor is required. Table 2.10 gives some examples of cyclotron produced [^{18}F]-fluorine.

Table 2.10 Cyclotron Production of [^{18}F]-Fluorine

Reaction	Target Material	Energy Range of Particles (MeV)	Ref.
$^{16}O\ (\alpha,d)\ ^{18}F$	SiO_2; H_2O	20 ⟶ 0	133
$^{20}Ne(d,\alpha)\ ^{18}F$	Ne/H_2 gas	30 ⟶ 0	133, 134
$^{19}F(P, Pn)\ ^{18}F$	F_2 gas	31 ⟶ 7	135
$^{19}F(P,2n)\ ^{18}Ne$			
$^{18}Ne \xrightarrow[1.5\ s]{\beta^+} {}^{18}F$	F_2 gas	31 ⟶ 7	135

The incorporation of [^{18}F]-fluorine in the desired compound competes with its radioactive decay. Figure 2.5 represents the relationship between the incorporation, time and radioactive decay of [^{18}F]-fluorine. For a better radiochemical yield the incorporation time must not be longer than t_{limit}. The purity of radiotracers is of considerable importance. Two principle types of impurity exist:

1. Radionuclidic impurity where radioactive nuclides other than those desired are present.

2. Radiochemical impurity where the nuclide of interest is also present in a chemical form differing from the one specially needed.

The former can be checked by determining the half life and, where possible, the energy of the emitted particle by the radionuclide of interest. The latter can be checked by conventional methods, e.g., vibrational spectroscopy.

2.7 Counting Apparatus.

The γ-rays emitted during the annihilation process of the β^+ of [^{18}F]-fluorine were counted using a NaI well scintillation counter (Ekco Enterprises Ltd., N700A) equipped with a photo-multiplier, well dimensions 1.56 x 0.78 in. diameter, and a scaler ratemeter (Nuclear Enterprises, SR7).

The γ-rays emitted by the source are photoelectrically absorbed by the NaI crystal. The light photons produced interact with the photocathode and release photoelectrons, the number being proportional to the energy. The photoelectrons produced are accelerated by a potential to the first dynode of the photomultiplier, where each produces typically four more electrons. The electrons released are further accelerated to the following dynode and so on. With ten dynodes the total multiplication factor is 4^{10}. The resulting pulse is further amplified and recorded on the scaler.

Before use the scaler was calibrated using a [^{137}Cs]-caesium and a [^{22}Na]-sodium γ-ray sources, the γ-rays of the

latter being of identical energy to those emitted by [^{18}F]-fluorine. The γ-photopeak of [^{18}F]-fluorine was regularly checked using [^{18}F]-labelled CsF as source. The voltage corresponding to the maximum count rate from Cs^{18}F was used during all measurements

2.8 Radioactive Decay.

In view of the relatively short half life of [^{18}F]-fluorine as compared with the time required to carry out one experiment (1-2 h), considerable [^{18}F]-fluorine activity was lost through its decay. To account for this, correction for decay was used.

The decay of a radionuclide follows the exponential rate law which is given by equation(2.9.)

$$A = Aoe^{\lambda t} \qquad (2.9)$$

or $$\ell n\, A = \ell n Ao - \lambda t$$

where A_o = activity (count rate) at some initial time

A = activity (count rate) after elapsed time t.

λ = characteristic decay constant (s^{-1}) = $\frac{\ell n 2}{t_{\frac{1}{2}}}$

$t_{\frac{1}{2}}$ = half life of isotope

Before being analysed all count rates were corrected to the time of the last measurement rather than the first so as to avoid creating fictitious counts. The calculations were carried out by microcomputer [125].

2.9 Background.

In the absence of a radioactive source, counting devices such as a Geiger-Müller counter, proportional counter or scintillation counter will register some radioactive events. These are mainly due to the small amount of radioactive radon and its decay products in the atmosphere as well as to cosmic radiations and radiation from materials used in the construction of laboratories. This background radiation can be minimised by shielding the counting device. The scintillation counter used in this work for counting [^{18}F]-fluorine activity is encased in lead. In order to obtain the true value of a radiochemical measurement the average background count was subtracted from the observed measurement.

2.10 Statistical Errors.

The random nature of the decay of a radioisotope means that if a source of constant activity is measured, assuming all other errors in measurement are excluded, the number of disintegrations observed in successive periods of fixed duration will not be constant. The probability W(m) of obtaining m disintegrations in time t from No original radioactive atoms is given by the binominal expression [136] equation (2.10.)

$$W(m) = \frac{No!}{(No-m)!m!} pm(1-p)^{No-m} \qquad (2.10)$$

where p is the probability of a disintegration occurring within the time of observation. From this equation it can be shown [136] that the expected standard deviation for radioactive disintegration, δ is given by equation(2.11)

$$\delta = \sqrt{me^{-\lambda t}} \qquad (2.11)$$

In counting practice the observation time t is small compared to the half life, hence λt can be neglected and equation(2.11)becomes

$$\delta = \sqrt{m} \qquad (2.12)$$

The relative standard deviation, expressed in percent, is often used and is given by equation(2.13)

$$100\delta = \frac{100}{\sqrt{m}} \qquad (2.13)$$

This means for $\delta \leqslant 1\%$ m must be $\geqslant 10,000$.

The errors quoted on radiochemical measurements in this work are the combination of the radiochemical

errors and the uncertainty in the physical measurements such as weights of samples and pressures of gas.

2.11 Radiochemical Balance.

Expressed in percent, the radiochemical balance is a criterion used to show how good is the recovery of radiolabelled compounds after separation. It is defined by equation(2.14)

$$\frac{\text{Total counts after separation}}{\text{Total counts before separation}} \times 100\% \qquad (2.14)$$

Radiochemical balances >95% are required in order to minimise errors.

In some reactions involving [^{18}F]-labelled hexafluorides, MF_6 (M = Mo, W, U) in acetonitrile radiochemical balances were >100%. There are two possible reasons for this.

1. On occasions the initial specific activities produced in $MF_5{}^{18}F$ (M = Mo, W, U) were very high. This led to the situation where dead time contributions were very significant. Consequently some of the [^{18}F]-fluorine activity was not recorded. After reaction and separation of the reactants considerable radioactive decay had occurred and contribution from the dead time became less significant resulting in smaller losses of [^{18}F]-fluorine activity.

2. When $MF_5{}^{18}F$ (M = Mo, W, U) was added to solutions of fluorocomplexes the concentrations of the latter were such that the solubility of MF_6 (M = Mo, W, U) was reduced. Hence small amounts of MF_6 (M = Mo, W, U) were left in the gas phase in the dead volume of the counting vessel. As a result some of the [^{18}F]-fluorine activity was not recorded. However, after separation of the reactants the hexafluorides MF_6 (M = Mo, W, U) were counted on their own in MeCN where their solubility increased as compared to before separation leading to smaller losses of [^{18}F]-fluorine activity.

As a consequence of the reasons stated above and after correction for background and radioactive decay the total counts after separation were higher than those before separation.

Note: The dead time is an inherent property of the counting and recording devices. This refers to the time during which the device is no longer operational due to its saturation by the avalanche of particles being counted. It is defined by equation (2.15)

$$N_T = \frac{N_{obs}}{1 - \tau N_{obs}} \qquad (2.15)$$

where N_T = True counts

N_{obs} = Observed counts

τ = dead time, usually $10^{-6} < \tau < 10^{-4}$ s.

2.12 [^{18}F]-Fluorine Reaction Vessels.

All reaction vessels used were made from Pyrex glass and equipped with P.T.F.E. stop cocks (J. Young Ltd). The calibrated vessels were evacuated, flamed-out and weighed before loading compounds using an analytical balance (Oertling LA 164).

2.12.1 Single Limb Vessel.

The fraction of [^{18}F]-fluorine exchanged in solution was determined using a single limb counting vessel, Figure(2.7b) which fitted into the well scintillation counter. The loop was designed in order to prevent the solution from contaminating the manifold on distillation resulting in the loss of the solid compound.

The following experimental procedure was used. Solutions were made up by loading a known amount of a solid compound into the vessel in the glove box and adding 1 cm^3 of MeCN by vacuum distillation. The total weight of the solution was then recorded. [^{18}F]-Fluorine labelled hexafluoride (WF_6, MoF_6 or UF_6) whose weight had been determined using a similar vessel, was transferred by vacuum distillation in the reaction vessel. The mixture was quickly warmed to room temperature and the reaction allowed to proceed for 20 minutes, during which time the solution was counted for [^{18}F]-fluorine activity. After reaction both vessels were transferred to the vacuum line and the reactants were separated, weighed and counted for [^{18}F]-fluorine activity.

Figure 2.7 [^{18}F]-Fluorine Reaction Vessels (a)double-limb vessel (b) single-limb vessel

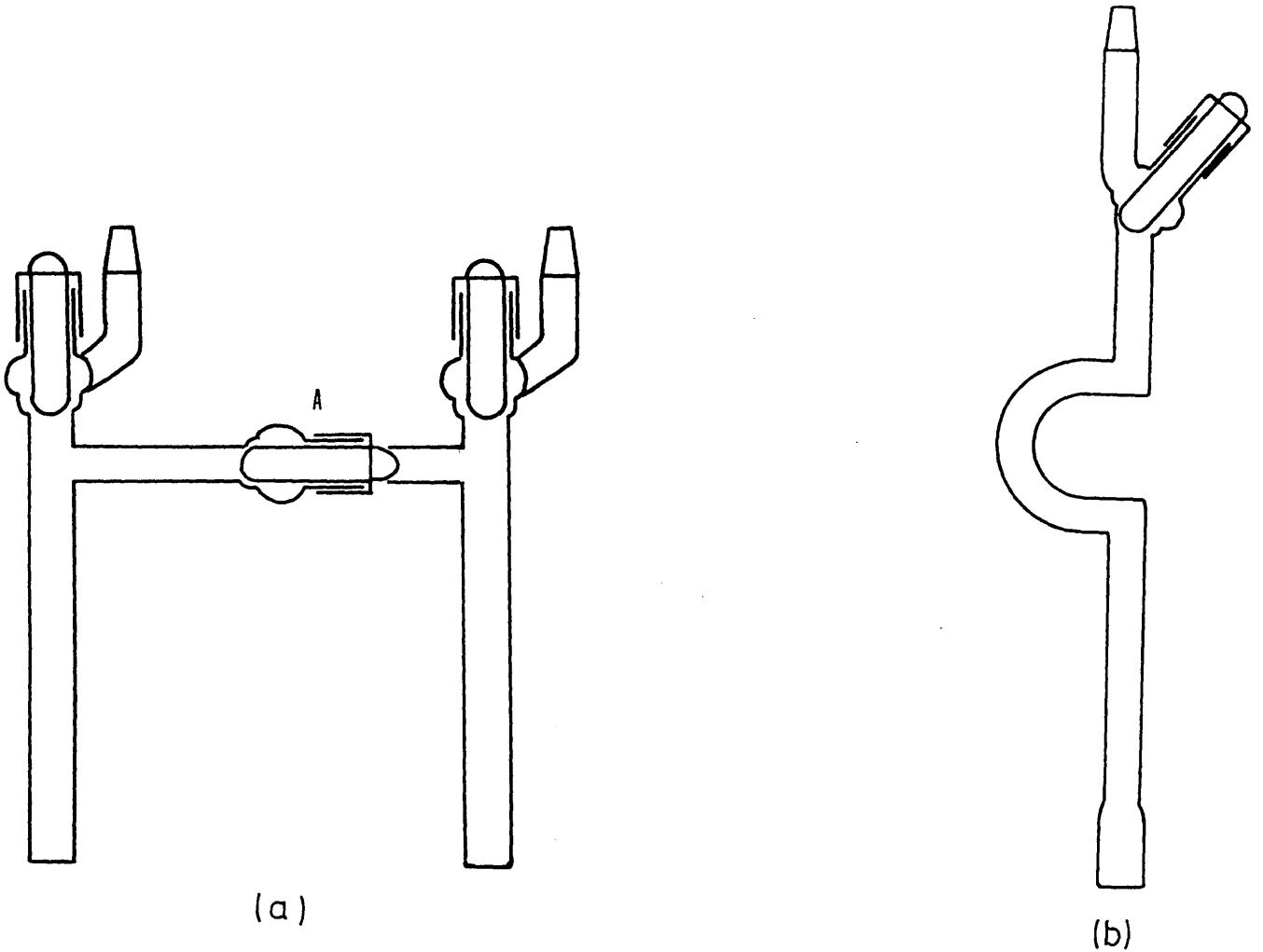

These data, corrected for [^{18}F]-fluorine decay and background, were used to calculate the fraction exchanged f by using equations (2.7) and (2.8).

2.12.2 Double Limb Vessel.

Reactions between [^{18}F]-labelled hexafluorides (WF_6, MoF_6 or UF_6) and solid fluorides and their complexes in solution or under heterogeneous conditions were followed with time using a double limb vessel, Figure (2.7a). Each limb fitted into the well of the scintillation counter. A known amount of solid compound was loaded in one limb in the glove box. The vessel was transferred to the vacuum line and evacuated. When required MeCN (1 cm^3) was added by vacuum distillation and its weight determined. [^{18}F]-Fluorine labelled hexafluoride (MoF_6, WF_6 or UF_6) whose weight had been determined using a single limb vessel (Figure 2.7b) was vacuum distilled into the other limb, stop cock A being closed. The reaction vessel was then allowed to reach ambient temperature and stop cock A opened. Reactants in each limb were counted for [^{18}F]-fluorine activity, alternately over 0.75-1h. Counts from the limb containing the solid or solution were due to [^{18}F]-fluorine incorporated in the solid or solution plus gaseous [^{18}F]-MF_6 only, while counts from the other limb were due to [^{18}F]-MF_6 only. Substraction of the latter from the former gave counts due to the solid or solution. These data, corrected for [^{18}F]-fluorine decay and background were used to obtain count rate vs. time relationships. After reaction [^{18}F]-MF_6 was removed by vacuum

distillation into a single limb vessel, weighed and its specific count rate determined. [^{18}F]-Fluorine labelled hexafluorides were counted in MeCN.

2.13 Preparation of Radiolabelled Compounds.

2.13.1 Preparation of [^{18}F]-Fluorine Labelled Caesium Fluoride [137].

[^{18}F]-Fluorine was prepared as [^{18}F]-labelled caesium fluoride in the Scottish Universities Research and Reactor Centre, East Kilbride, using the nuclear sequence $^{6}Li(n,\alpha)^{3}H$, $^{16}O(^{3}H,n)^{18}F$. In this scheme ^{6}Li and ^{16}O must be intimately mixed. This was achieved by using lithium carbonate as target material.

Two grams of Li_2CO_3 (B.D.H. Analar) were irradiated with a neutron flux of 3.6×10^{12} neutrons cm^{-2} s^{-1} for 0.5 h. The $Li^{18}F$ produced was allowed to cool for 0.5 h, then reacted with H_2SO_4 (50%). The $H^{18}F$ evolved was distilled into a solution of CsOH (Aldrich) at 273K. Neutralisation of the solution with aqueous HF followed by evaporation to dryness gave $Cs^{18}F$ as finely divided white powder. The activity of $Cs^{18}F$ thus prepared was in the range 1.85 - 3.33 MBq (50 - 90 μCi). [^{18}F]-labelled potassium fluoride can be used as a substitute to $Cs^{18}F$. It was prepared from KOH (B.D.H) using the same procedure described above and gave a satisfactory activity yield.

Prior to their use in labelling the gaseous fluorides $Cs^{18}F$ or $K^{18}F$ were reacted under vacuum with hexafluoroacetone at 295K for 0.5 h then dried at 393K for a further 0.5 h. This treatment has been shown [125] to facilitate the incorporation of [^{18}F]-fluorine into the compounds being labelled.

2.13.2 Preparation of [^{18}F]-Fluorine Labelled Hexafluorides of Molybdenum, Tungsten and Uranium.

[^{18}F]-Fluorine labelled molybdenum hexafluoride and tungsten hexafluoride were prepared by high temperature reaction with activated $Cs^{18}F$ (Section 2.13.1) in a stainless steel, high pressure vessel (Hoke, 70 cm^3).

Molybdenum hexafluoride (5-10mmol) or WF_6 (5-10mmol, Ozark Mahoning) were condensed at 77K onto activated $Cs^{18}F$. The pressure vessel was heated to 348K for 0.5 h then $MoF_5{}^{18}F$ or $WF_5{}^{18}F$ transferred to a glass vessel loaded with activated sodium fluoride to remove any hydrogen fluoride. The $MoF_5{}^{18}F$ was also prepared by reaction between MoF_6 and [^{18}F]-labelled boron trifluoride at room temperature for 0.5 h. Both $BF_2{}^{18}F$ (30mmol)and MoF_6 (5-10 mmol) were condensed in a Monel pressure vessel (Hoke, 90 cm^3). After exchange the vessel was cooled to 195K and $BF_2{}^{18}F$ removed. In both cases the specific count rate was $>10^4$ count min^{-1} $mmol^{-1}$.

The radiochemical purity of $MoF_5{}^{18}F$ and $WF_5{}^{18}F$ was checked by determining their γ-ray spectrum and the [^{18}F]-fluorine half life over at least two half lives. The latter was found

to be 97.6 and 108.3 min for $MoF_5{}^{18}F$ and $WF_5{}^{18}F$ respectively [129]. Typical γ-ray spectra for $MoF_5{}^{18}F$ and $WF_5{}^{18}F$ are shown in Figures 2.8 and 2.9.

[^{18}F]-Fluorine labelled uranium hexafluoride was prepared by reaction between $BF_2{}^{18}F$ and UF_6 at room temperature in a Monel pressure vessel (Hoke, 90 cm^3) [43]. Uranium hexafluoride (5-10 mmol) was condensed in the reaction vessel followed by excess $BF_2{}^{18}F$ (30 mmol). The mixture was warmed to room temperature and exchange allowed to proceed for 0.5 h. The reaction vessel was then cooled to 195K, $BF_2{}^{18}F$ removed and $UF_5{}^{18}F$ transferred into a glass vessel loaded with activated NaF. The radiochemical purity of $UF_5{}^{18}F$ was checked by determining its γ-ray spectrum and the [^{18}F]-fluorine half life over at least two half lives. This was found to be 105.0 min [129]. The γ-ray spectrum of $UF_5{}^{18}F$ is presented in Figure 2.10. The specific count rate of $UF_5{}^{18}F$ was $>10^4$ count min^{-1} $mmol^{-1}$.

2.13.3 Preparation of [^{18}F]-Fluorine Labelled Boron Trifluoride, Phosphorus Pentafluoride, Arsenic Pentafluoride and Trimethylfluorosilane.

[^{18}F]-Fluorine labelled boron trifluoride, phosphorus pentafluoride and arsenic pentafluoride were prepared by high temperature reaction with activated $Cs^{18}F$ (Section 2.13.1) in a stainless steel pressure vessel (Hoke, 70 cm^3).

Figure 2.8 γ - Ray Spectrum of [^{18}F]-MoF_6

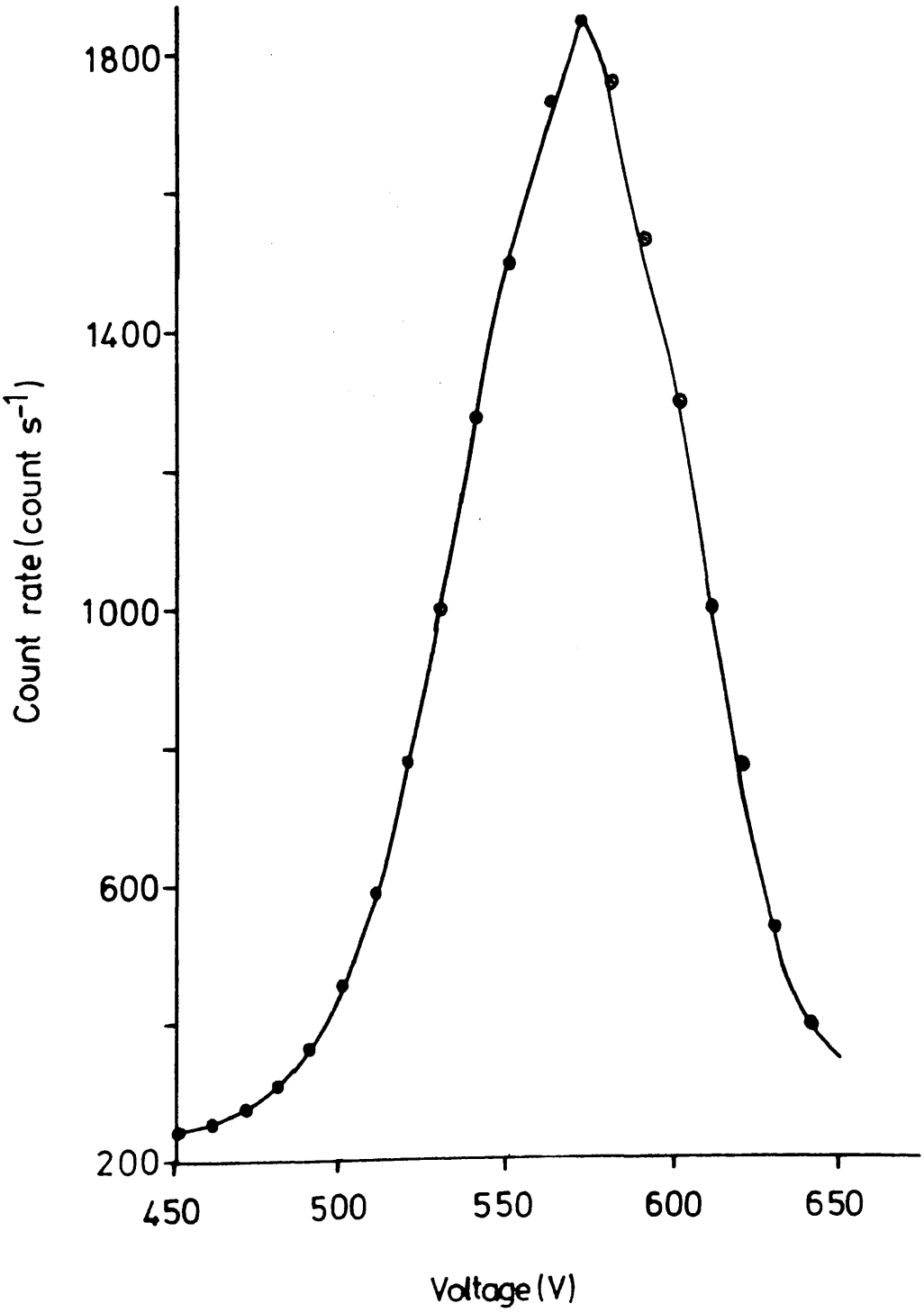

Figure 2.9 γ-Ray Spectrum of [^{18}F]-WF_6

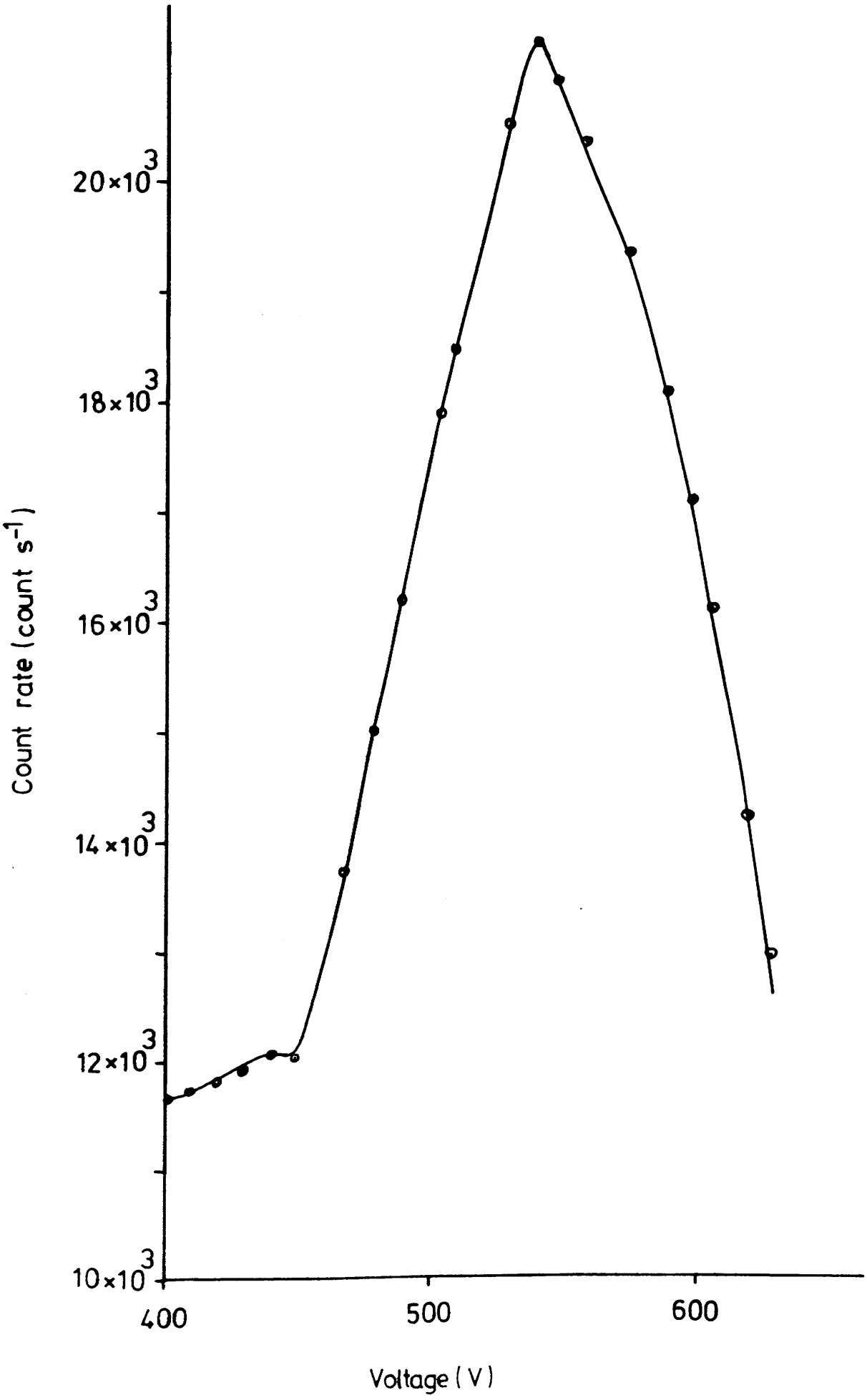

Figure 2.10 γ-Ray Spectrum of $[^{18}F]$-UF_6

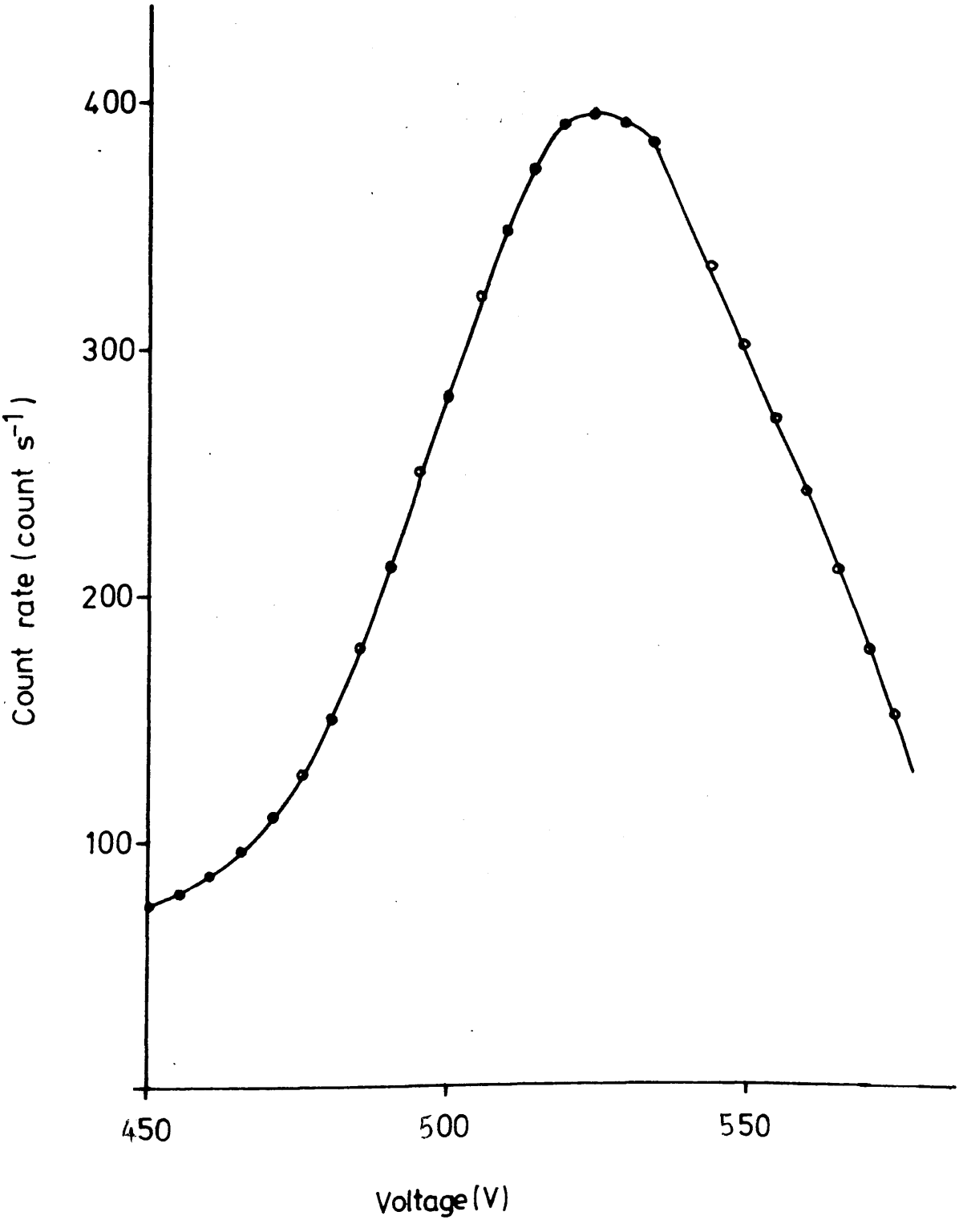

The pressure vessel containing activated $Cs^{18}F$ was cooled to 77K and BF_3 (30 mmol, Ozark Mahoning), PF_5 (30 mmol, Matheson) or AsF_5 (30 mmol, Matheson) were admitted then the reaction heated to 358K for 0.5 h. In all cases the specific count rate was $>10^4$ count min^{-1} $mmol^{-1}$. In the case of BF_3 and AsF_5 it is believed that the exchange takes place through two stages[125]. During the first the gaseous fluoride is adsorbed to form the corresponding fluoroanion followed by [^{18}F]-fluorine exchange between adsorbed fluoroanion and free fluoride. Equally it is reasonable to assume that the same exchange stages are involved in the case of PF_5.

[^{18}F]-Fluorine labelled trimethyl fluorosilane was prepared by reaction between Me_3SiF (7 mmol) and activated $Cs^{18}F$ in a stainless steel pressure vessel at 348K for 0.5 h. The specific count rate was $>10^4$ count min^{-1} $mmol^{-1}$.

2.13.4 Preparation of [^{18}F]-Fluorine Labelled Lithium Hexafluorophosphate and Lithium Hexafluoroarsenate.

[^{18}F]-Fluorine labelled lithium hexafluorophosphate and lithium hexafluoroarsenate were prepared *in situ* by reaction between lithium fluoride (B.D.H.) and [^{18}F]-labelled phosphorus pentafluoride (Matheson) or [^{18}F]-labelled arsenic pentafluoride (Matheson) using a specially designed Pyrex double limb vessel, Figure 2.11.

0.2g (7.7 mmol) of LiF were loaded into the flamed out vessel in the glove box. The vessel was then transferred to the vacuum line and evacuated. Acetonitrile (5 cm^3) was added by vacuum distillation. [^{18}F]-Fluorine labelled PF_5 or AsF_5 (1.8 mmol) were then condensed and the vessel warmed slowly to room temperature. The mixture was shaken for 0.5 h and left to settle. 1 cm^3 of the solution containing $LiAsF_6$ or $LiPF_6$ was decanted into the other limb which served as counting vessel and sealed at point A.

2.13.5 Preparation of [^{18}F]-Fluorine Labelled Nitrosyl Fluoride.

[^{18}F]-Fluorine labelled nitrosyl fluoride was prepared by reaction between N_2O_4 and activated $Cs^{18}F$ at room temperature in a stainless steel pressure vessel at room temperature.

Dinitrogen tetroxide (4 mmol) was condensed onto activated $Cs^{18}F$ at 77K, the vessel warmed to room temperature and the reaction allowed to proceed for 20 min. Once the reaction was completed the vessel was cooled to 195K and $NO^{18}F$ removed and counted for [^{18}F]-fluorine activity.

[^{18}F]-Fluorine labelled nitrosyl fluoride was also prepared by exchange reaction between NOF and activated $Cs^{18}F$ at room temperature for 20 min. In both cases the specific count rate was $>10^4$ count min^{-1} $mmol^{-1}$. Although the radiochemical yield was satisfactory $NO^{18}F$ was not of

Figure 2.11 Double-limbed Reaction Vessel.

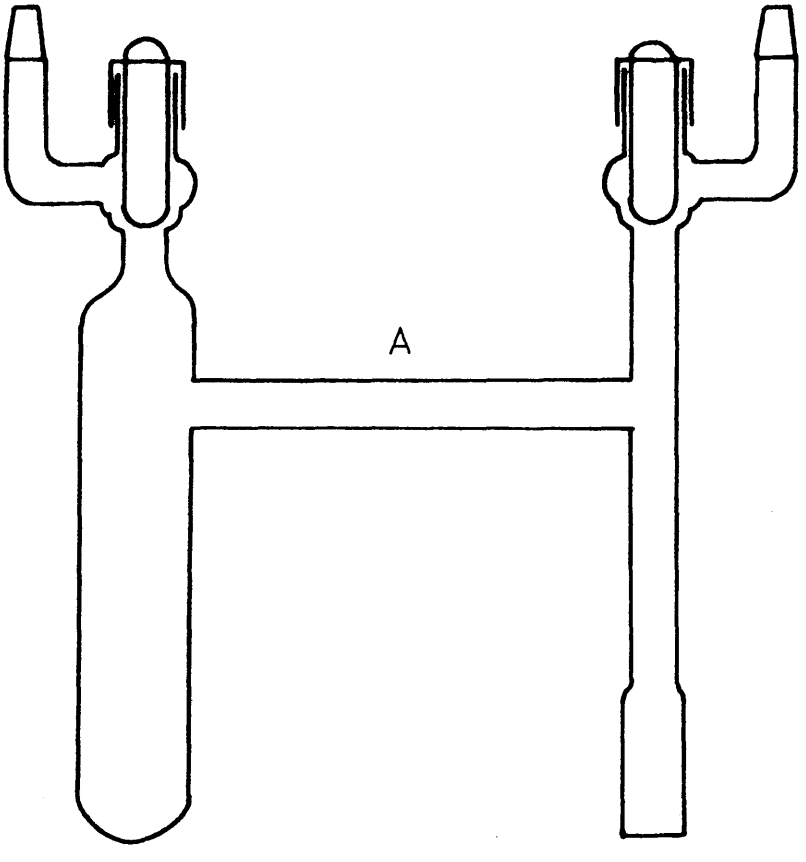

high chemical purity for radiotracer experiments to be carried out. Exposure of $NO^{18}F$ to glass apparatus resulted in its decomposition to NO_2 which is recognisable by its brown colour and probably hydrogen fluoride. Because of this no further work involving NOF was undertaken.

CHAPTER THREE

REACTIONS OF THE HEPTAFLUOROTUNGSTATE AND HEPTAFLUOROMOLYBDATE ANIONS WITH [^{18}F]-FLUORINE LABELLED HEXAFLUORIDES OF MOLYBDENUM AND TUNGSTEN.

3. Reactions of the Heptafluorotungstate and Heptafluoromolybdate anions with [^{18}F]-Fluorine Labelled Hexafluorides of Molybdenum and Tungsten.

3.1 Introduction

Prescott et al. [31] have shown that heterogeneous Lewis acid-base reactions between anhydrous copper difluoride or thallium fluoride and tungsten hexafluoride in acetonitrile generate soluble copper(II) heptafluorotungstate(VI) pentakis acetonitrile, $[Cu(NCMe)_5][WF_7]_2$ or thallium(I) heptafluorotungstate(VI), $TlWF_7$, respectively. Using [^{18}F]-fluorine as radiotracer the same authors have mentioned briefly that complete exchange of [^{18}F]-fluorine occurs between $TlWF_7$ and $WF_5{}^{18}F$ within one hour.

To find more about the fluorine bond lability with respect to exchange of the heptafluoroions the previous study [31] was extended to include the heptafluorotungstate and heptafluoromolybdate ions in the presence of the hexafluorides of molybdenum and tungsten. These systems were investigated both under homogeneous (acetonitrile) and heterogeneous (gas + solid) conditions. To determine whether counter cation has any effect on the fluorine exchange behaviour, WF_7^- ion was used with several cations namely nitrosonium, NO^+, thallium Tl^+, copper Cu^{2+} and caesium Cs^+. The MoF_7^- ion was used as its caesium salt only. Radiotracer technique using [^{18}F]-fluorine as the radiotracer was the main method of investigation used.

3.2 Experimental.

The reactions between the heptafluoroanions of molybdenum or tungsten and [^{18}F]-labelled hexafluorides of molybdenum or tungsten were carried out in acetonitrile or under heterogeneous conditions using a single or double-limb vessel respectively. The procedure used was described in Section 2.12. The solid heptafluoroanions were analysed by infrared spectroscopy before and after reactions. In the latter case bands at approximately 1000 cm^{-1} were present. This was probably due to some hydrolysis of the samples as these were kept in the reaction vessels attached to the vacuum line overnight to allow [^{18}F]-fluorine activity to decay before recording the spectra.

3.3 Reaction Between Thallium(I) Heptafluorotungstate(VI) and [^{18}F]-Fluorine Labelled Tungsten Hexafluoride in Acetonitrile.

The reaction between thallium(I) heptafluoro-tungstate(VI), $TlWF_7$, and [^{18}F]-labelled tungsten hexafluoride $WF_5{}^{18}F$ was studied in acetonitrile for four reaction times, 7, 14, 20 and 60 minutes and at two reaction temperatures, 252 and 293K. By varying the reaction time and temperature it was intended to determine the fraction exchanged (f) as function of these two parameters. The amount of $TlWF_7$ used was in the range 0.37 -0.39±0.01 mmol. All samples were dissolved in MeCN ($1cm^3$). During the preparation of solutions of $TlWF_7$ it was observed that a white solid, presumably TlF, precipitated but redissolved when WF_6 was

added. This observation was consistent with the slight decomposition of $TlWF_7$ according to equation (3.1)

$$TlF + WF_6 \rightleftharpoons Tl^+_{(solv.)} + WF^-_{7\ (solv.)} \qquad (3.1)$$

The amount of $WF_5{}^{18}F$ used was in the range 0.76-1.82±0.01 mmol. Table 3.1 summarises the results of these reactions. Comparison of the specific count rates of $WF_5{}^{18}F$ before and after reaction showed that these decreased in all cases indicating that an exchange of [^{18}F]-fluorine had occurred. Furthermore the masses of the reactants before and after reaction were equal within experimental error. No chemical reaction was observed as the infrared spectra of the solids recorded after reaction were identical to those recorded before reactions. Using equation (2.8) the fraction exchanged (f) was found to be close to unity in all cases corresponding to complete exchange of [^{18}F]-fluorine. Figure 3.1 represents the growth of [^{18}F]-fluorine activity in the solution of $TlWF_7$ which was obtained by using a double-limb vessel. The growth followed a rapid increase then reached an equilibrium after 10 min reflecting the complete mixing of reactants.

3.4 Reaction Between Copper(II) Heptafluorotungstate(VI) Pentakis Acetonitrile and [^{18}F]-Fluorine Labelled Tungsten Hexafluoride in Acetonitrile.

The reaction between copper(II) heptafluorotungstate(VI)pentakis acetonitrile, $[Cu(NCMe)_5][WF_7]_2$ and

Table 3.1 Reactions between $TlWF_7$ and $WF_5{}^{18}F$ in MeCN. Summary of results.

Reactants				Specific count rate of WF_6 (count $min^{-1}mmol^{-1}$)		Count rate of Reactants after reaction (count $min^{-1}mmol^{-1}$)		Temp.	Reaction Time	Radiochemical Balance	Fraction Exchange
$TlWF_7$ (mmol)		WF_6 (mmol)									
Initial	Final	Initial	Final	Initial	Final	WF_6	WF_7^-	(K)	(min)	(%)	
0.37 ±0.01	0.39 ±0.01	1.82 ±0.01	1.80 ±0.01	27301 ±209	23424 ±182	42163 ±205	10545 ±103	293	7	106	1.04 ±0.03
0.37 ±0.01	0.38 ±0.01	1.55 ±0.01	1.53 ±0.01	27301 ±209	22057 ±187	33808 ±184	9040 ±190	293	14	101	0.95 ±0.03
0.39 ±0.01	0.40 ±0.01	1.52 ±0.01	1.47 ±0.01	11832 ±79	8431 ±91	12393 ±111	3807 ±62	293	20	92	1.01 ±0.03
0.39 ±0.01	0.41 ±0.01	0.76 ±0.01	0.74 ±0.01	27301 ±209	18884 ±316	13974 ±118	8250 ±112	293	60	109	0.99 ±0.03
0.41 ±0.01	0.42 ±0.01	1.40 ±0.01	1.20 ±0.01	5920 ±114	4348 ±66	5218 ±72	1998 ±89	252	20	87	0.92 ±0.07

Figure 3.1 Reaction of $TlWF_7$ with WF_5 ^{18}F in MeCN vs Time.

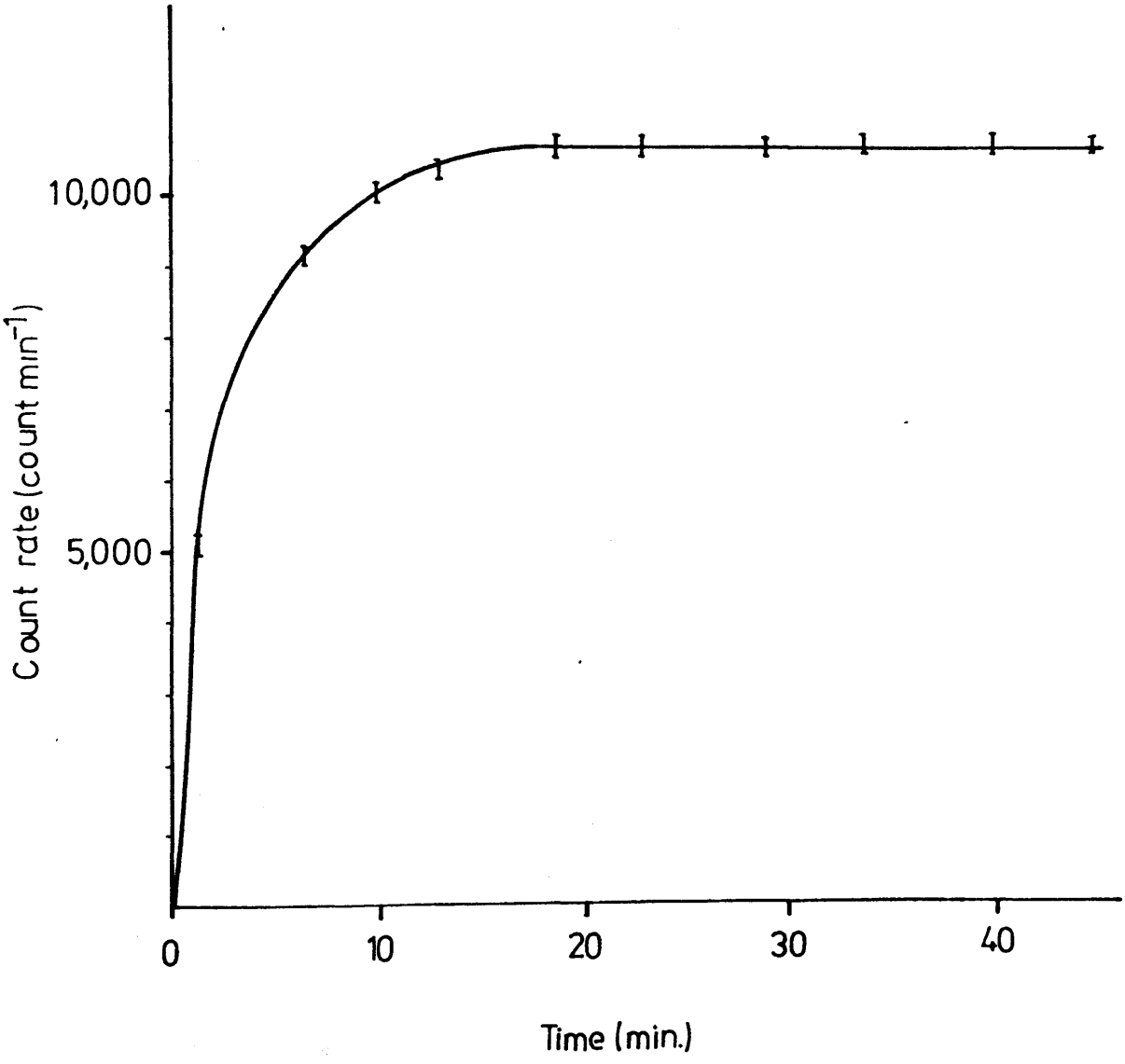

[^{18}F]-labelled tungsten hexafluoride, $WF_5{}^{18}F$, was studied in acetonitrile for two reaction times, 10 and 20 minutes and at two reaction temperatures, 252 and 293 K. The amount of $[Cu(NCMe)_5][WF_7]_2$ used was in the range 0.08-0.20±0.01 mmol dissolved in MeCN (1cm^3). However it was observed that $[Cu(NCMe)_5][WF_7]_2$ did not dissolve completely in MeCN at 252 K. The amount of $WF_5{}^{18}F$ ranged between 0.74-1.82±0.01 mmol. Table 3.2 summarises the results of these reactions. A transfer of [^{18}F]-fluorine activity to $[Cu(NCMe)_5][WF_7]_2$ together with decrease in the count rate of $WF_5{}^{18}F$ after reaction was observed in all cases. This was consistent with an exchange of [^{18}F]-fluorine. The masses of the reactants before and after reaction were equal within experimental error. No chemical reaction between the reactants was observed as their infrared spectra recorded before and after reactions were identical. [^{18}F]-Fluorine exchange was complete at room temperature and partial at 252 K. The latter result was due to the low solubility of the salt at this temperature as mentioned above. The growth of [^{18}F]-fluorine activity in the solution of $[Cu(NCMe)_5][WF_7]_2$ with time (Figure 3.2) was similar to that obtained in the case of $TlWF_7$ (Figure 3.1).

3.5 Reaction Between [^{18}F]-Fluorine Labelled Nitrosonium Heptafluorotungstate(VI) and Tungsten Hexafluoride in Acetonitrile.

The reaction between [^{18}F]-labelled nitrosonium heptafluorotungstate(VI), $NOWF_6{}^{18}F$, and tungsten hexa-

Table 3.2 Reactions between $[Cu(NCMe)_5][WF_7]_2$ and WF_5 ^{18}F in MeCN. Summary of Results.

Reactants				Specific count rate of WF_6 (count min^{-1} $mmol^{-1}$)		Count Rates of Reactants After Reaction (count min^{-1})		Temp. (K)	React. Time (min)	Radio chemical balance (%)	Fraction Exchanged
$[Cu(NCMe)_5][WF_7]_2$		WF_6 (mmol)									
Initial	Final	Initial	Final	Initial	Final	WF_6	WF_7^-				
0.20 ±0.01	0.21 ±0.01	0.73 ±0.01	0.72 ±0.01	11832 ±79	7053 ±137	5078 ±71	3367 ±58	293	20	98	1.01 ±0.03
0.17 ±0.01	0.17 ±0.01	1.32 ±0.01	1.28 ±0.01	2912 ±61	2508 ±48	3210 ±57	520 ±23	252	10	97	0.61 ±0.03
0.08 ±0.01	0.08 ±0.01	1.45 ±0.01	1.41 ±0.01	48494 ±560	43996 ±187	62035 ±249	4576 ±68	252	20	95	0.63 ±0.03

Figure 3.2 Reaction of $[Cu(NCMe)_5][WF_7]_2$ with $WF_5{}^{18}F$ in MeCN vs Time.

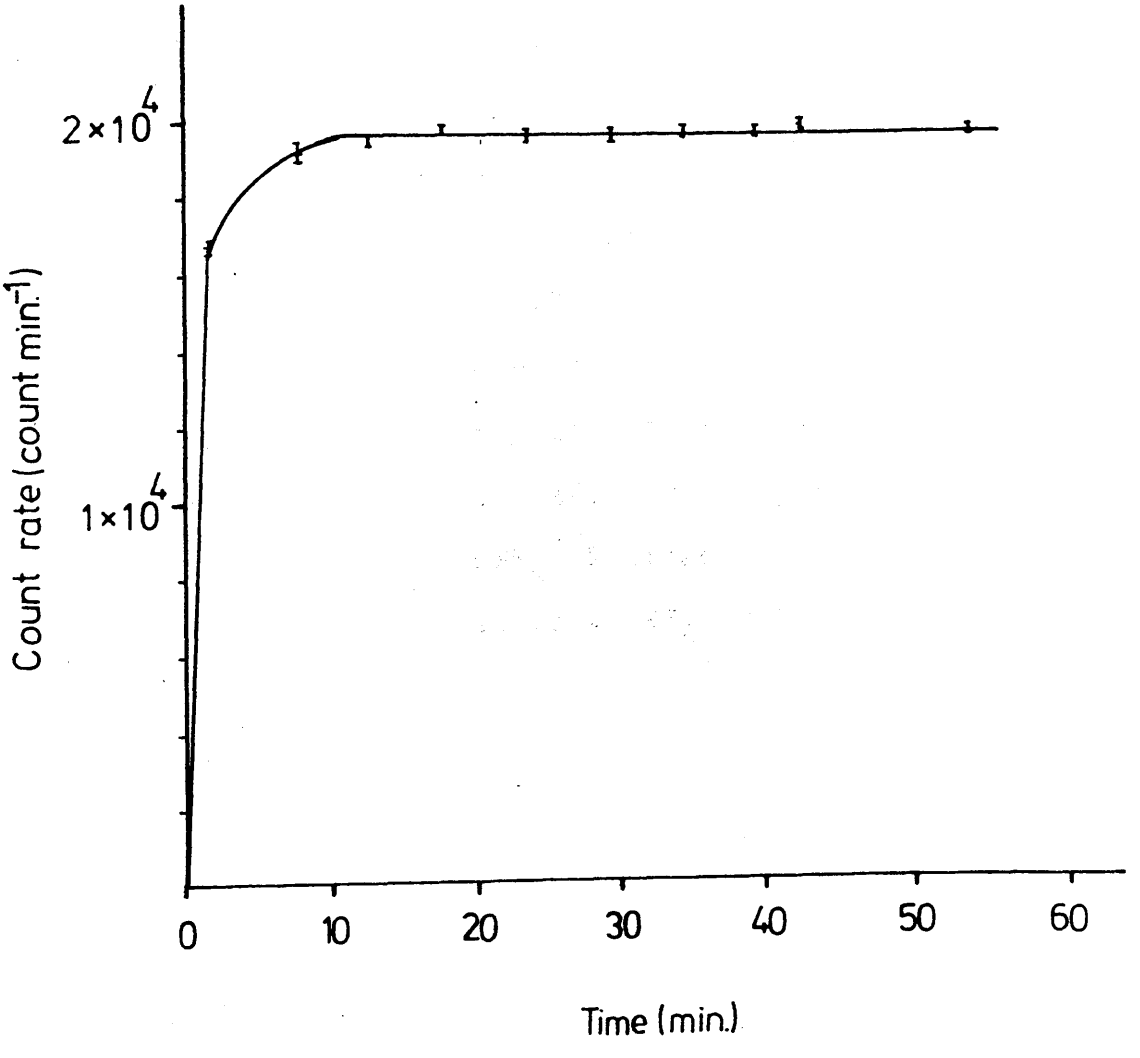

fluoride in acetonitrile was designed with the objective of determining whether back exchange of [^{18}F]-fluorine activity takes place between the heptafluoroanion WF_7^- and WF_6.

[^{18}F]-Fluorine labelled $NOWF_7$ was prepared *in situ* in a single-limb reaction vessel (Figure 2.11) by reaction between an equimolar mixture (*ca.* 2 mmol) of [^{18}F]-labelled tungsten hexafluoride (Section 2.13.2) and nitrosyl fluoride. The compounds $WF_5{}^{18}F$ and FNO were condensed in the reaction vessel at 77 K and the mixture was warmed to room temperature. After removal of excess reactants a colourless radioactive solid was obtained. This was considered to be $NOWF_6{}^{18}F$ (0.58±0.01 mmol). The small yield was due to the short time used during the preparation (*ca.*0.5h). Acetonitrile (1 cm^3) was added by vacuum distillation at 77 K. After warming the solution to room temperature $NOWF_6{}^{18}F$ dissolved without any apparent decomposition. Inactive WF_6 (2.59±0.01 mmol) was added to the solution of $NOWF_6{}^{18}F$ and the reaction allowed to proceed for 20 minutes. After separation of reactants the initially inactive WF_6 was found to contain [^{18}F]-fluorine activity. Tungsten hexafluoride (2.54±0.01 mmol) recovered after reaction had a [^{18}F]-fluorine count rate of 48280±220 count min^{-1}.

The results described in Sections 3.3 to 3.5 indicate that [^{18}F]-fluorine exchange between WF_7^- and WF_6 in MeCN involves an equilibrium between the two species,

equation 3.2

$$WF_7^- + WF_5{}^{18}F \rightleftharpoons WF_6{}^{18}F^- + WF_6 \qquad (3.2)$$

3.6 Reaction Between Nitrosonium Heptafluorotungstate(VI) and [^{18}F]-Fluorine Labelled Molybdenum Hexafluoride in Acetonitrile.

Two reactions between nitrosonium heptafluorotungstate(VI), $NOWF_7$, and [^{18}F]-labelled molybdenum hexafluoride $MoF_5{}^{18}F$ were carried out in acetonitrile at room temperature for 20 minutes. A summary of the results is presented in Table 3.3. A transfer of [^{18}F]-fluorine activity to $NOWF_7$ together with a decrease in the specific count rate of $MoF_5{}^{18}F$ after reaction were observed in each case. Radiochemical and mass balances were >95%. The infrared spectrum of $NOWF_7$ recorded after reaction contained no additional band as compared with that recorded before reaction. Using equation (2.8) the results showed that complete exchange of [^{18}F]-fluorine ($f = 1$) was observed in each case.

Taking into account these results the reaction of $NOWF_7$ with $MoF_5{}^{18}F$ can be written as follows, equation (3.3)

$$WF_7^- + MoF_5{}^{18}F \longrightarrow WF_6{}^{18}F^- + MoF_5{}^{18}F \qquad (3.3)$$

Table 3.3 Reactions Between $NOWF_7$ or $CsWF_7$ and $MoF_5{}^{18}F$ in MeCN. Summary of Results.

AWF_7	Reactants				Specific count rate of $WF_5{}^{18}F$ (count $min^{-1}mmol^{-1}$)		Final count rate of Reactants (count min^{-1})		Radio-chemical balance (%)	Fraction Exchanged
	AWF_7 (mmol)		MoF_6 (mmol)							
	Initial	Final	Initial	Final	Initial	Final	MoF_6	WF_7^-		
$NOWF_7$	0.18 ±0.01	0.18 ±0.01	1.07 ±0.02	1.01 ±0.02	81197 ±1588	61060 ±793	61671 ±248	14680 ±121	99	1.10 ±0.10
	0.18 ±0.01	0.19 ±0.01	1.10 ±0.02	1.04 ±0.02	81197 ±1588	61415 ±774	63782 ±253	13812 ±118	95	1.10 ±0.10
$CsWF_7$	0.34 ±0.01	0.35 ±0.01	1.46 ±0.02	1.42 ±0.02	14654 ±191	11537 ±210	16383 ±128	4903 ±70	96	0.93 ±0.08

3.7 Reaction Between Caesium Heptafluorotungstate(VI) and [^{18}F]-Fluorine Labelled Molybdenum Hexafluoride in Acetonitrile.

A reaction between caesium heptafluorotungstate(VI) $CsWF_7$ (0.34±0.01 mmol), and [^{18}F]-labelled molybdenum hexafluoride, $MoF_5{}^{18}F$ (1.46±0.01 mmol) was carried out in acetonitrile at room temperature for 20 minutes. This resulted in a transfer of [^{18}F]-fluorine activity to $CsWF_7$ as well as decrease in the specific count rate of $MoF_5{}^{18}F$ (Table 3.3). The decrease in the specific count rate of $MoF_5{}^{18}F$ was consistent with complete exchange of [^{18}F]-fluorine, f = 1. Examination of the Raman spectrum of $CsWF_7$ recorded after reaction (Figure 3.3(a)) showed bands at ν_{max} 713 (vs), 442 (m) and 683 (m) cm^{-1} which were assigned to $\nu_1(A_1')$ and $\nu_8(E'')$ modes of WF_7^- and $\nu_1(A_1')$ mode of MoF_7^- respectively. The Raman spectra of $CsMoF_7$ (Figure 3.3(b)) and $CsWF_7$ (Figure 3.3(c)) are presented for comparison. The Raman spectrum indicated that WF_6 had been displaced to a small extent by MoF_6 from $CsWF_7$ resulting in the formation of $CsMoF_7$.

3.8 Evidence for the Formation of Caesium Heptafluoromolybdate and Caesium Heptafluorotungstate.

Beuter et. al. [28] studied the vibrational spectra of the heptafluoroions of molybdenum and tungsten using various alkali metal cations. These salts were prepared by reactions between alkali metal iodides and the corresponding hexafluorides in liquid iodine pentafluoride, equation (3.4)

Figure 3.3 Raman Spectra of (a) $CsWF_7$ after reaction with MoF_6 in MeCN, (b) $CsMoF_7$ and (c) $CsWF_7$

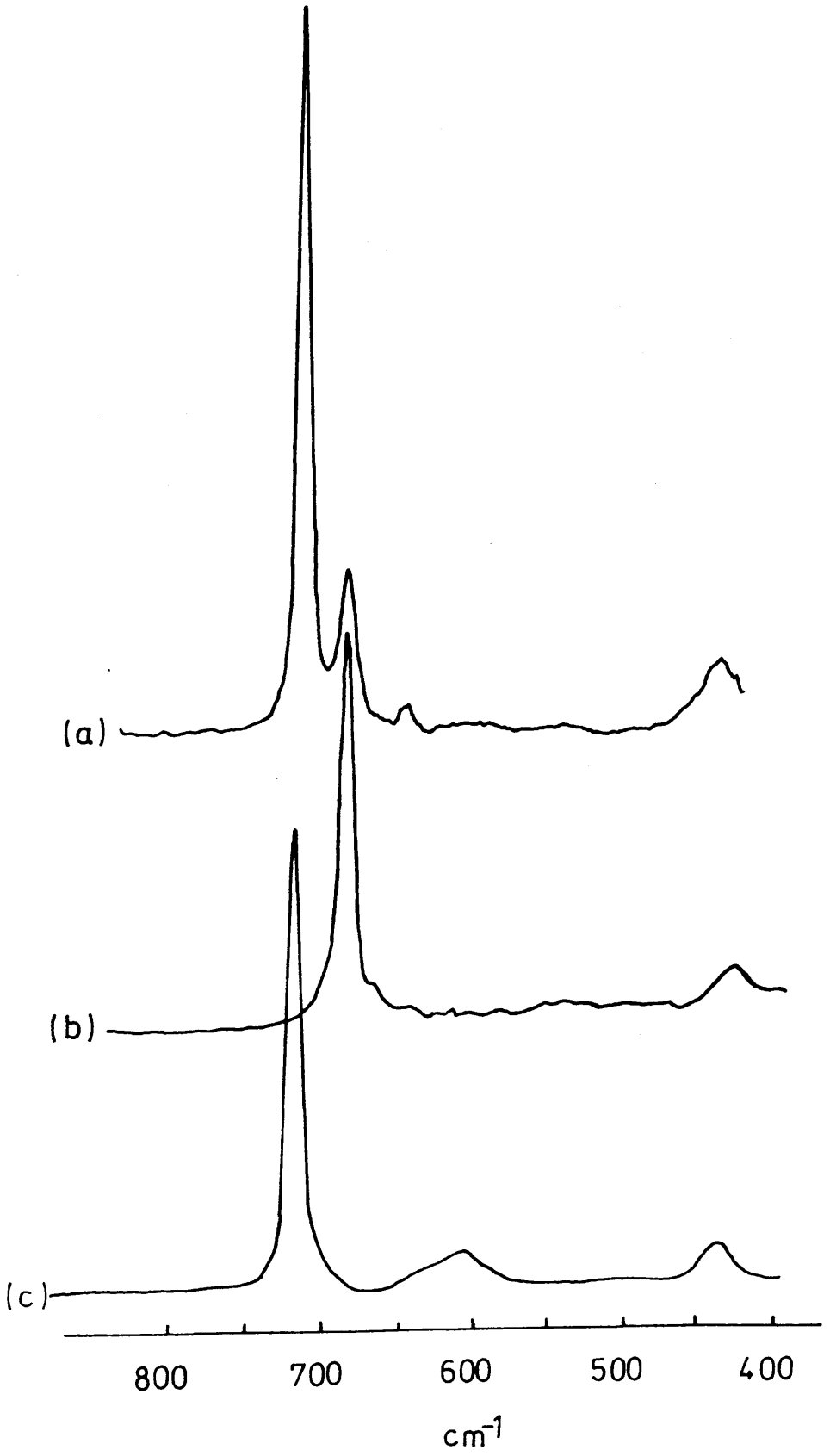

$$2AI + 2MF_6 + IF_5 \xrightarrow{IF_5} 2AMF_7 + IF_3 + I_2 \qquad (3.4)$$

(A = K,Rb, Cs ; M = Mo, W)

On the basis of their results the authors assigned the MoF_7^- and WF_7^- ions in the pentagonal bipyramid symmetry (D_{5h}) when Cs^+ was used and to a lower symmetry when the smaller Rb^+ and K^+ cations were used. In the latter case the assignment was based on the additional bands present in both Raman and infrared spectra.

In the present study $CsMoF_7$ and $CsWF_7$ were prepared by reactions of caesium fluoride and the corresponding hexafluorides in acetonitrile (Section 2.2.19) and their vibrational spectra recorded. These are presented in Table 3.4 together with those obtained by Beuter et. al. [28]. Comparison of the two sets of spectra shows that, with only minor differences, they are similar

Five Raman and ten infrared bands are expected for a pentagonal bipyramid symmetry. Although a full assignment was not possible the strong bands in the Raman at 683 and 714 cm^{-1} and in the infrared at 630 and 620 cm^{-1} for $CsMoF_7$ and $CsWF_7$ respectively, undoubtedly represent a totally symmetric stretching fundamental of the A_1' and A_2'' species (D_{5h}). Occasionally weak bands at around 1000 cm^{-1} were observed in both Raman and infrared spectra. These were probably due to some impurities.

Table 3.4 Vibrational Spectra of $CsMoF_7$ and $CsWF_7$

$CsMoF_7$				$CsWF_7$				Assignment
This work		Literature [28]		This work		Literature [28]		
IR	R	IR	R	IR	R	IR	R	
	683 vs		687 vs		714 vs		716 vs	$\nu_1(A_1')$
630 vs		635 vs		620 vs		618 vs		$\nu_3(A_2'')$
					608 w		617 vw	$\nu_2(A_1')$
490 w		500 w						?
	429 w		433 w		442 m		444 s	$\nu_8(E_1'')$
				330 m		335 s		$\nu_6(E_1')$
330 m		330 w		285 m		289 w		$\nu_4(A_2'')$

m = medium; s = strong; vs = very strong; w = weak; vw = very weak

It can therefore be concluded that reactions between CsF and MF_6 (M = Mo, W) in MeCN yield $CsMoF_7$ and $CsWF_7$ respectively in which the symmetry of the heptafluoro-ions is assigned in the D_{5h} point group. Further evidence for the formation of $CsMoF_7$ and $CsWF_7$ were obtained from mass balances and by using $MoF_5{}^{18}F$ and $WF_5{}^{18}F$. This evidence is presented here in detail for two reactions.

The reactions between CsF and $MF_5{}^{18}F$ (M = Mo,W) were carried out in a single-limb reaction vessel according to the procedure described in Section 2.2.11. The vessel and all reactants were weighed before and after reaction. These were also assayed for [^{18}F]-fluorine activity before and after separation. A summary of the results is presented in Table 3.5.

$CsF + MoF_6$

The decrease in the amount of MoF_6 (0.57±0.04 mmol) was, within experimental error, equivalent to that of CsF (0.58±0.02 mmol) indicating a 1:1 combining ratio. Furthermore the mass of the solid after reaction (0.2026± 0.0030 g) corresponded to 0.56±0.02 mmol $CsMoF_7$.

The amount of $CsMoF_7$ formed was also determined from the solid count rate. To do this it was necessary to calculate the theoretical specific count rate of $CsMoF_7$ formed by reaction of CsF and $MoF_5{}^{18}F$ the specific count rate of which had been determined separately. The following assumptions were made:

Table 3.5 Reactions Between CsF and $MF_5{}^{18}F$ (M=Mo,W) in MeCN. Summary of Results.

MF_6	Reactants				Initial Specific count rate of MF_6 count min^{-1}_{mmol}	Solid count rate count min^{-1}	Radio-chemical balance (%)	Amount of $CsMF_7$ (mmol) determined from:	
	CsF		MF_6 (M=Mo,W)					Mass balances	Solid count rate
	Initial	Final (g)	Initial	Final					
MoF_6	0.0873 ±0.0030 g 0.58 ±0.02 mmol	0.2026 ±0.0030 g	0.1151 ±0.0030 g 0.72 ±0.02 mmol	0.0323 ±0.0030 g 0.15 ±0.02 mmol	19493 ±303	10724 ±104	103	0.56 ±0.02	0.53 ±0.04
WF_6	0.1129 ±0.0030 g 0.74 ±0.01 mmol	0.3360 ±0.0030 g	0.4050 ±0.0030 g 1.36 ±0.01 mmol	0.1180 ±0.0030 g 0.40 ±0.01 mmol	13712 ±97	10969 ±105	88	0.75 ±0.02	0.75 ±0.04

1. All CsF had reacted with $MoF_5{}^{18}F$ to give $CsMoF_7$
2. Solid $CsMoF_7$ had undergone complete exchange of $[^{18}F]$-fluorine with excess $MoF_5{}^{18}F$

The specific count rate S_∞ corresponding to complete exchange was determined by using equation (3.5)

$$S_\infty = \frac{Ao}{n_1 m_1 + n_2 m_2} \qquad (3.5)$$

where S_∞, count min^{-1} (mg F atom)$^{-1}$, is the specific count rate per fluorine atom; Ao, count min^{-1}, is the starting count rate of $MF_5{}^{18}F$ (M = Mo,W); n_1, mmol, is the quantity of $CsMF_7$ (M = Mo,W) with m_1 exchangeable F atoms; n_1 is based on the number of mmol of CsF; n_2 mmol, is the quantity of MF_6 (M = Mo,W) with m_2 exchangeable F atoms.

After substitution of the experimental data S_∞ became 2864 ± 210 count min^{-1} (mg F atom)$^{-1}$. Therefore for $CsMoF_7$ containing seven fluorine atoms the specific count rate expressed in count min^{-1} $mmol^{-1}$ became 20048 ± 1470. The solid count rate of 10724 count min^{-1} corresponded to 0.53 ± 0.04 mmol $CsMoF_7$.

CsF + WF_6

The decrease in the amount of WF_6 (0.96 ± 0.02 mmol) was greater than the one corresponding to a 1:1 combining ratio with CsF. This was due to loss of some WF_6 during separation of the reactants as reflected by the radiochemical balance 88%. However the mass of the solid after reaction (0.3360 ± 0.0030 g) corresponded to 0.75 ± 0.02 mmol $CsWF_7$,

in good agreement with a 1:1 combining ratio between CsF and WF_6.

The amount of $CsWF_7$ formed was also determined from the solid count rate using the same assumptions and calculations as in the case of $CsMoF_7$. The theoretical specific count rate of $CsWF_7$ was 14665±329 count min^{-1} $mmol^{-1}$. Therefore the solid count rate of 10969 count min^{-1} was equivalent to 0.75±0.04 mmol $CsWF_7$.

The results obtained from mass balances and [^{18}F]-fluorine indicate the formation of $CsMF_7$ (M = Mo,W) by reaction between CsF and MF_6 (M = Mo,W) in MeCN.

3.9 Reaction Between Caesium Heptafluoromolybdate(VI) and [^{18}F]-Fluorine Labelled Tungsten Hexafluoride in Acetonitrile.

Two reactions between caesium heptafluoromolybdate(VI) $CsMoF_7$, and [^{18}F]-labelled tungsten hexafluoride, $WF_5{}^{18}F$, were carried out in acetonitrile at room temperature for 20 minutes. A summary of the results is presented in Table 3.6. The decrease in specific count rate of $WF_5{}^{18}F$ corresponded to a complete exchange of [^{18}F]-fluorine in each case. However there was an increase in the mass of the solid and decrease in that of the hexafluoride after reaction. The change in the mass of reactants was consistent with the total displacement of MoF_6 in $CsMoF_7$ by WF_6. This is shown in detail for Reaction 1 (Table 3.6). Assuming all MoF_6 had been displaced by WF_6 the mass of the solid after reaction was equivalent to 0.55±0.01 mmol $CsWF_7$. Equally the decrease in the mass

Table 3.6 Reactions Between $CsMoF_7$ and WF_5 ^{18}F in MeCN. Summary of Results.

Reaction No.	Reactants.				Specific count rate of WF_6 (count min^{-1} $mmol^{-1}$)		Count rate of Reactants after Reaction (count min^{-1})		Radio-chemical balance (%)	Fraction Exchanged
	$CsMoF_7$		WF_6							
	Initial	Final	Initial	Final	Initial	Final	WF_6	MoF_7^-		
1	0.2009 ±0.0030 g 0.56 ±0.01 mmol	0.2483 ±0.0030 g	0.5089 ±0.0030 g 1.71 ±0.01mmol	0.4564 ±0.0030 g	16946 ±162	12782 ±136	21858 ±148	8209 ±91	104	0.89±0.04
2	0.2575 ±0.0030 g 0.71 ±0.01 mmol	0.3158 ±0.0030 g	0.6018 ±0.0030 g 2.02 ±0.01mmol	0.5288 ±0.0030 g	16946 ±162	12311 ±275	24868 ±158	10272 ±101	103	0.94±0.04

of WF_6 was also consistent with the displacement of MoF_6. Assuming 0.56±0.02 mmol MoF_6 had been displaced the mass of the hexafluoride corresponded to a mixture of 0.56±0.02 mmol MoF_6 and 1.15±0.01 mmol WF_6, i.e., 0.4602±0.0060 g. This was in good agreement with the experimental result (0.4564± 0.0030 g).

Supporting evidence for the displacement of MoF_6 in $CsMoF_7$ by WF_6 was obtained from the Raman spectrum of the solid recorded after reaction (Figure 3.4a). This contained bands at ν_{max} 714 (vs), 442 (m) and 683 (w) cm^{-1} assigned to $\nu_1(A')$ and $\nu_8(E'')$ modes of WF_7^- and $\nu_1(A')$ mode of MoF_7 respectively. The Raman spectra of $CsMoF_7$ (Figure 3.4b) and $CsWF_7$ (Figure 3.4c) are presented for comparison. In view of the results presented above the reaction between $CsMoF_7$ and WF_6 can be written as the following equation (3.6)

$$CsMoF_7 + WF_6 \longrightarrow CsWF_7 + MoF_6 \qquad (3.6)$$

It is worth noticing the similarity between the spectrum obtained here and that obtained in the reaction between $CsWF_7$ and MoF_6 in MeCN (Figure 3.3a).

The results presented in Section 3.3 to 3.7 have shown that [^{18}F]-fluorine exchange was rapid and complete between the heptafluoroanions of molybdenum and tungsten and [^{18}F]-labelled hexafluorides of molybdenum or tungsten in acetonitrile. In view of this it was decided to investigate the same systems under heterogeneous (gas plus solid) conditions. The reactions between MF_7^- (M = Mo,W) and

Figure 3.4 Raman Spectra of (a) $CsMoF_7$ After Reaction with WF_6 in MeCN (b) $CsMoF_7$ and (c) $CsWF_7$

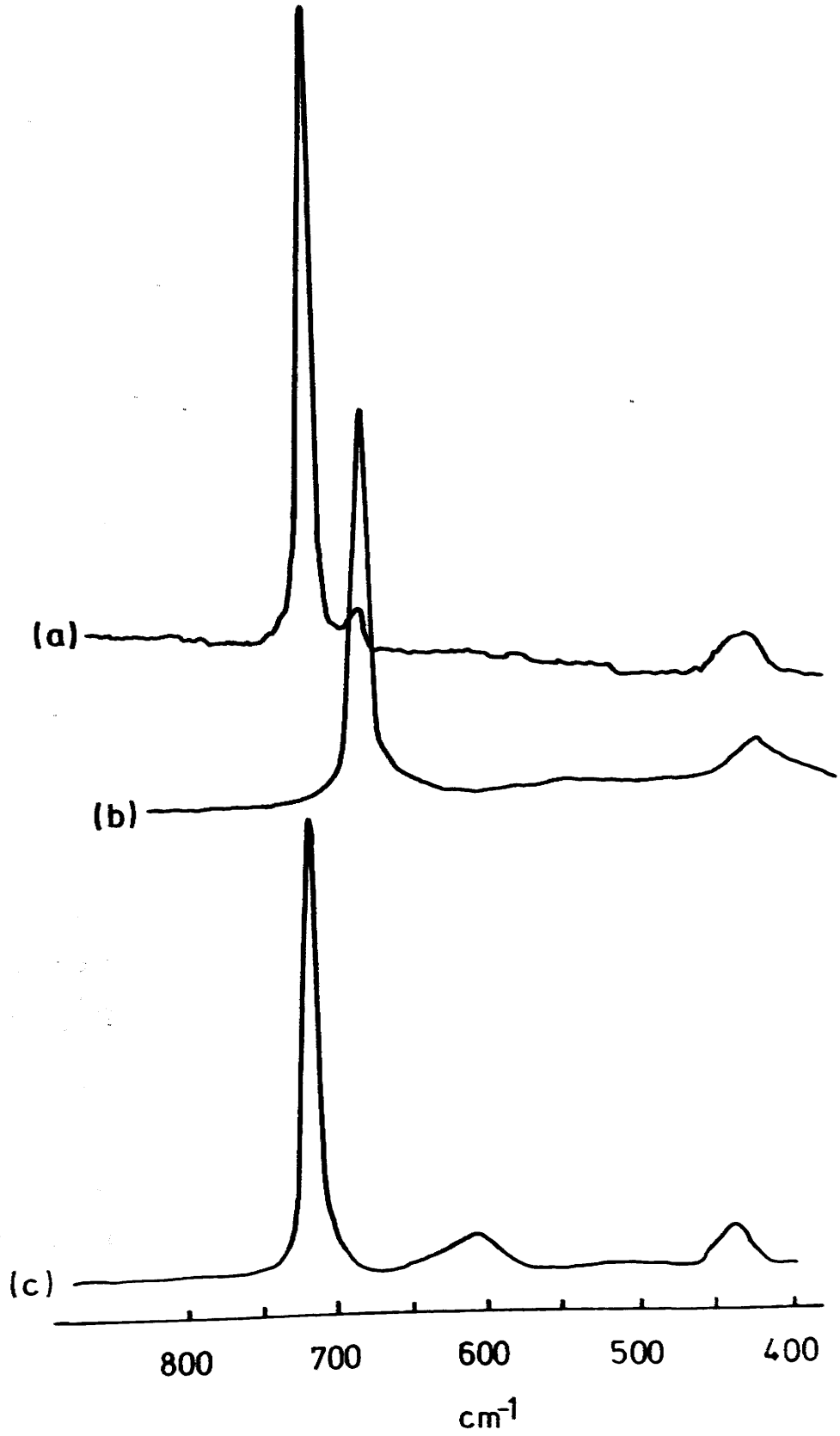

$MF_5{}^{18}F$ (M = Mo,W) were followed with time and their fraction of [^{18}F]-fluorine exchanged (f) was determined according to the procedure described in Section 2.12.1. In addition to $MoF_5{}^{18}F$ and $WF_5{}^{18}F$ the behaviour of the WF_7^- anion as its nitrosonium, NO^+, and thallium, Tl(I) salts was investigated in the presence of [^{18}F]-labelled uranium hexafluoride under the same conditions.

3.10 Reaction Between Thallium(I)Heptafluorotungstate(VI) and [^{18}F]-Fluorine Labelled Tungsten Hexafluoride Under Heterogeneous Conditions.

Two reactions between thallium(I)heptafluorotungstate(VI), $TlWF_7$ and [^{18}F]-labelled tungsten hexafluoride were carried out under heterogeneous conditions for approximately 1h. A summary of the results is presented in Table 3.7. The specific count rate of $WF_5{}^{18}F$ decreased after reaction in each case indicating that [^{18}F]-fluorine exchange had occurred. Using equation(2.7) this was found to be partial (f = 0.20, 0.24±0.03). An increase in the mass of $TlWF_7$ after reaction took place in both cases corresponding to an uptake of WF_6 by the solid. Although the extent of [^{18}F]-fluorine exchange was similar in both cases the uptake of WF_6 was somewhat different (0.13±0.05 and 0.02±0.05 WF_6:WF_7^- mole ratio). This may be explained in terms of the difference in the physical state of the surfaces of the samples. The infrared spectrum of the solid recorded after reaction (Figure 3.5) contained additional bands at ν_{max} 710 (m), 515 (wsh) and 425 (m) cm^{-1}.

Table 3.7 Reactions Between AWF_7 ($A = Tl^+, Cu^{2+}, NO^+$) and WF_5 ^{18}F under Heterogeneous Conditions. Summary of Results.

AWF_7	Reactants				Specific count rate of WF_6 (count $min^{-1} mmol^{-1}$)		Count rate of Reactants after Reaction (count min^{-1})		Radio-chemical balance (%)	Uptake mmol WF_6 / mmol WF_7^-	Fraction Exchanged
	AWF_7		WF_6 (mmol)								
	Initial	Final	Initial	Final	Initial	Final	WF_6	WF_7^-			
$TlWF_7$	0.4262 ±0.0030g 0.82 ±0.01mmol	0.4580 ±0.0030g	2.43 ±0.01	2.27 ±0.01	33578 ±168	31363 ±181	71194 ±267	2084 ±46	98	0.13 ±0.05	0.24 ±0.03
	0.2983 ±0.0030g 0.57 ±0.01mmol	0.3017 ±0.0030g	0.85 ±0.01	0.81 ±0.01	169894 ±5530	155100 ±1955	125631 ±354	5623 ±75	96	0.02 ±0.05	0.20 ±0.03
$[Cu(NCMe)_5]-[WF_7]_2$	0.6225 ±0.0030g 0.69 ±0.01mmol	0.6758 ±0.0030g	1.56 ±0.01	1.34 ±0.01	29138 ±315	26164 ±246	35060 ±187	5236 ±72	90	0.26 ±0.05	0.20 ±0.03
	0.1378 ±0.0030g 0.16 ±0.01mmol	0.1565 ±0.0030g	0.92 ±0.01	0.83 ±0.01	84150 ±230	81133 ±102	67506 ±260	1554 ±40	99	0.41 ±0.05	0.12 ±0.03
$NOWF_7$	0.0690 ±0.0030g 0.20 ±0.01mmol	0.0693 ±0.0030g	1.16 ±0.01	1.14 ±0.01	19960 ±238	19196 ±309	21884 ±349	1357 ±39	100	0	0.23 ±0.03

Figure 3.5 Infrared Spectra of (a) $TlWF_7$ (b) $[Cu(NCMe)_5][WF_7]_2$ After Reaction with WF_6 and (c) $[Cu(NCMe)_5][WF_7]_2$

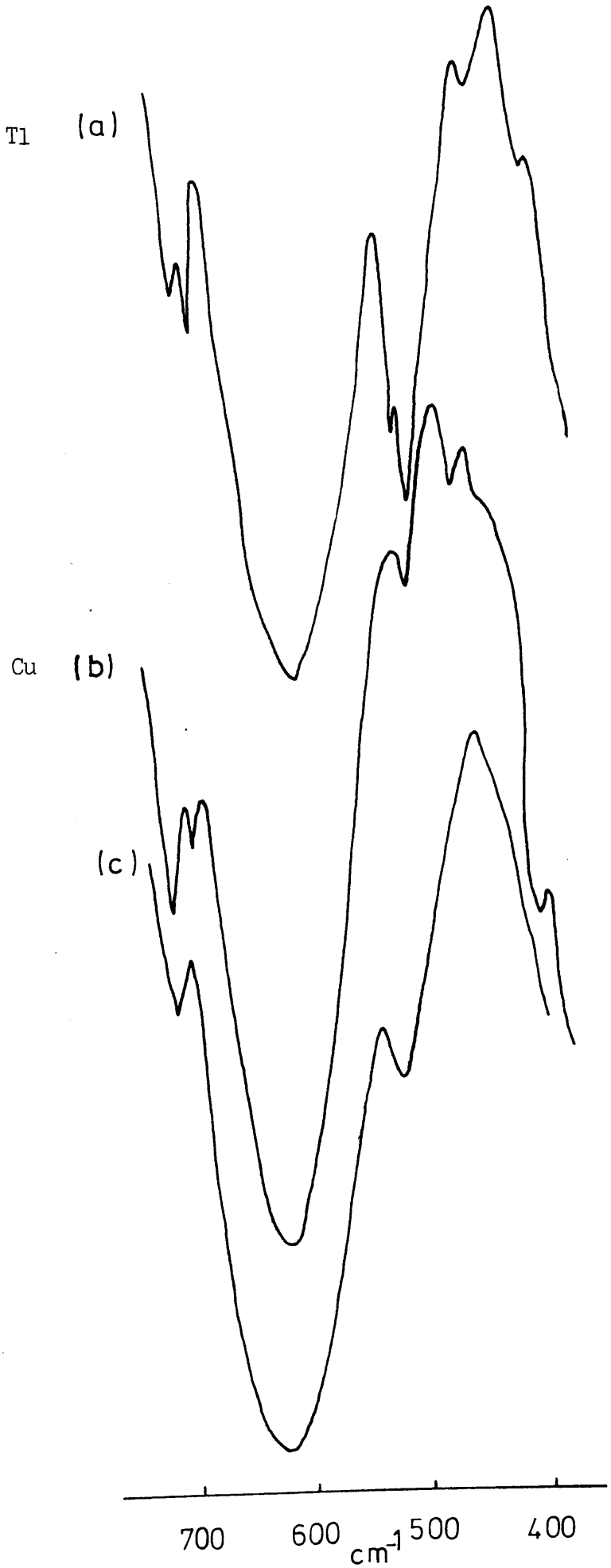

A possible explanation was the formation of fluorine bridged species between $TlWF_7$ and WF_6 [138]. Figure 3.6 shows the growth of [^{18}F]-fluorine activity in $TlWF_7$ with time. The shape of the curve can be explained in terms of a slow uptake of WF_6 and slow exchange of [^{18}F]-fluorine taking place simultaneously, the latter being more important.

3.11 Reaction Between Copper(II)Heptafluorotungstate(VI) Pentakis Acetonitrile and [^{18}F]-Fluorine Labelled Tungsten Hexafluoride Under Heterogeneous Conditions.

Admission of [^{18}F]-labelled tungsten hexafluoride $WF_5{}^{18}F$, to copper(II)heptafluorotungstate(VI) pentakis acetonitrile, $[Cu(NCMe)_5][WF_7]_2$ under heterogeneous conditions resulted after 1h in a decrease in the specific count rate of $WF_5{}^{18}F$ together with an increase in the mass of the solid. The results of two reactions are summarised in Table 3.7. The decrease in the specific count rate of $WF_5{}^{18}F$ corresponded to a partial exchange of [^{18}F]-fluorine (f = 0.20, 0.12±0.03). The increase in the mass of the solid after interaction was equivalent to an uptake of 0.26 and 0.41±0.05 WF_6:$[Cu(NCMe)_5]$-$[WF_7]_2$ mole ratio. The uptake of WF_6 by $TlWF_7$ (Section 3.10) was small as compared with the present case. This was probably due to the difference in the stoicheiometry of the two complexes. Additional bands at ν_{max} 710 (mw), 480 (mw) and 410 (mw) cm^{-1} were present in the infrared spectrum of the solid after reaction (Figure 3.5b). Figure 3.5c represents the infrared spectrum of $[Cu(NCMe)_5][WF_7]_2$ before reaction. The possibility of a fluorine-bridged species put forward in the case of $TlWF_7$ can be used to account for the

Figure 3.6 Reaction of $TlWF_7$ with WF_5 ^{18}F vs. Time
(Heterogeneous Conditions)

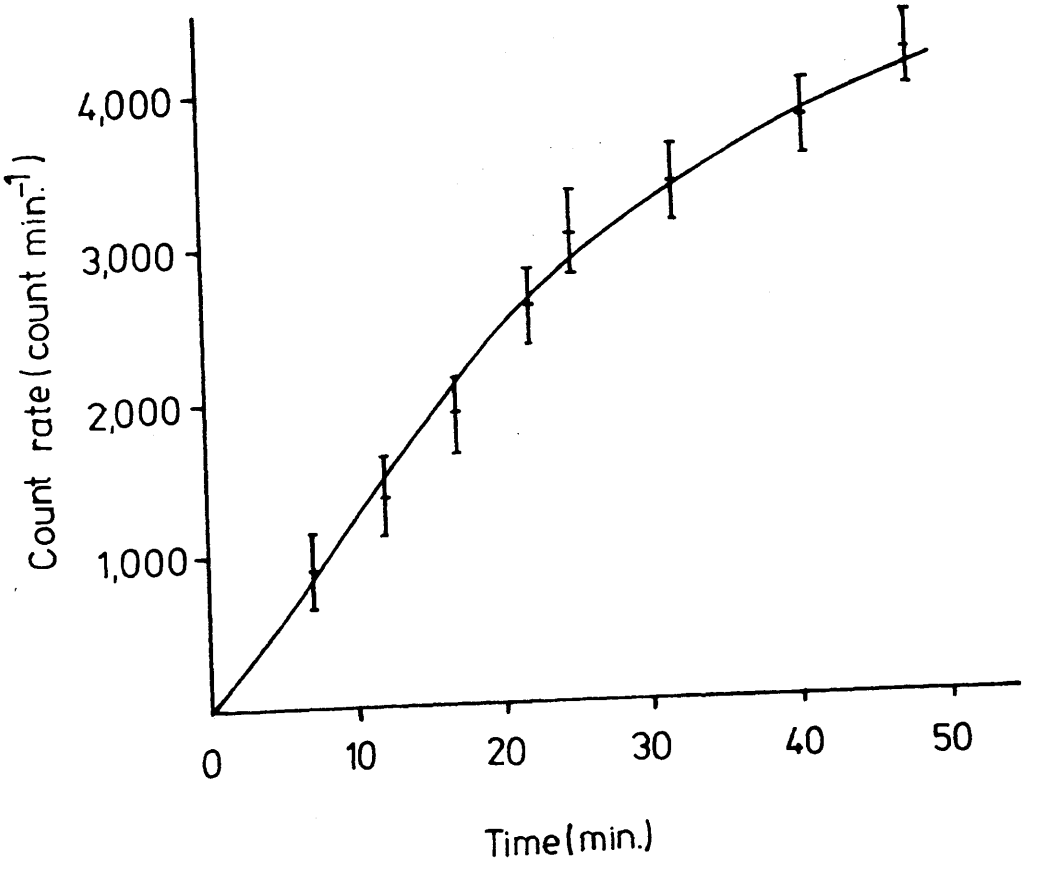

additional bands found in the present system. Figure 3.7 represents the growth of [^{18}F]-fluorine activity in $[Cu(NCMe)_5][WF_7]_2$ with time. The rapid growth of the curve can be explained in terms of a rapid uptake of $WF_5{}^{18}F$ followed by a slow exchange of [^{18}F]-fluorine.

3.12 Reaction Between Nitrosonium Heptafluorotungstate(VI) and [^{18}F]-Fluorine Labelled Tungsten Hexafluoride Under Heterogeneous Conditions.

A reaction between nitrosonium heptafluorotungstate(VI), $NOWF_7$, (0.20±0.01 mmol) and [^{18}F]-labelled tungsten hexafluoride, $WF_5{}^{18}F$, (1.16±0.01 mmol) resulted in a decrease in the specific count rate of $WF_5{}^{18}F$ after 1h of interaction (Table 3.7). Using equation (2.7) the decrease in the specific count rate of $WF_5{}^{18}F$ was equivalent to a partial exchange ($f = 0.23\pm0.03$). Unlike the two previous cases no evidence for uptake of WF_6 by $NOWF_7$ was obtained, as the masses of the solid before and after reaction were equal within experimental error. Therefore the solid count rate was due only to an exchange of [^{18}F]-fluorine. The growth of [^{18}F]-fluorine activity in $NOWF_7$ with time is presented in Figure 3.8. As there was no evidence for uptake of $WF_5{}^{18}F$ the shape of the curve can be explained in terms of a rapid exchange of [^{18}F]-fluorine during the first ten minutes, without being complete, followed by a slower process.

Figure 3.7 Reaction of $[Cu(NCMe)_5][WF_7]_2$ with WF_5 ^{18}F vs. Time (Heterogeneous Conditions)

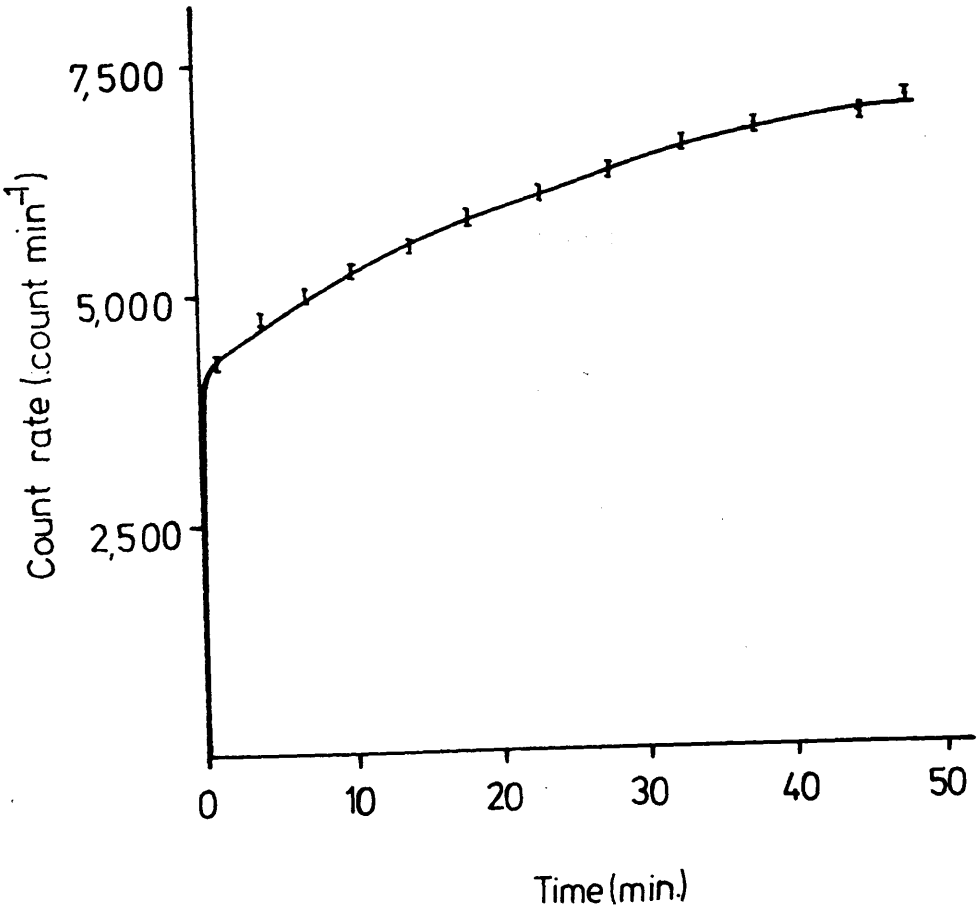

3.13 Reaction Between [^{18}F]-Fluorine Labelled Nitrosonium Heptafluorotungstate(VI) and Tungsten Hexafluoride Under Heterogeneous Conditions.

The reaction between [^{18}F]-labelled nitrosonium heptafluorotungstate(VI), $NOWF_6{}^{18}F$, and tungsten hexafluoride under heterogeneous conditions was designed with the objective of determining whether back exchange of [^{18}F]-fluorine activity takes place between the heptafluoroanion, WF_7^- and WF_6.

[^{18}F]-Fluorine labelled $NOWF_7$ (0.2406 ± 0.0030 g, 0.69 ± 0.01 mmol) was prepared *in situ* in a double limb vessel (Figure 2.7) as described in Section 3.5. Inactive WF_6 (2.09 ± 0.01 mmol) was transferred to the other limb and the reaction allowed to proceed for 1 h. After separation of reactants the initially inactive WF_6 was found to be radioactive indicating that an exchange of [^{18}F]-fluorine had occurred between the reactants. A slight increase in the mass of $NOWF_6{}^{18}F$ (0.2533 ± 0.0030 g) together with a decrease in the amount of WF_6 (1.94 ± 0.01 mmol) were observed after reaction. The increase in the mass of $NOWF_6{}^{18}F$ corresponded to an uptake of 0.04 ± 0.02 mmol WF_6.

In view of the results presented in Sections 3.12 and 3.13 [^{18}F]-fluorine exchange between WF_7^- and WF_6 under heterogeneous conditions can be accounted for by an equilibrium similar to that described by equation (3.2).

Figure 3.8 Reaction of $NOWF_7$ with WF_5 ^{18}F under Heterogeneous Conditions vs. Time.

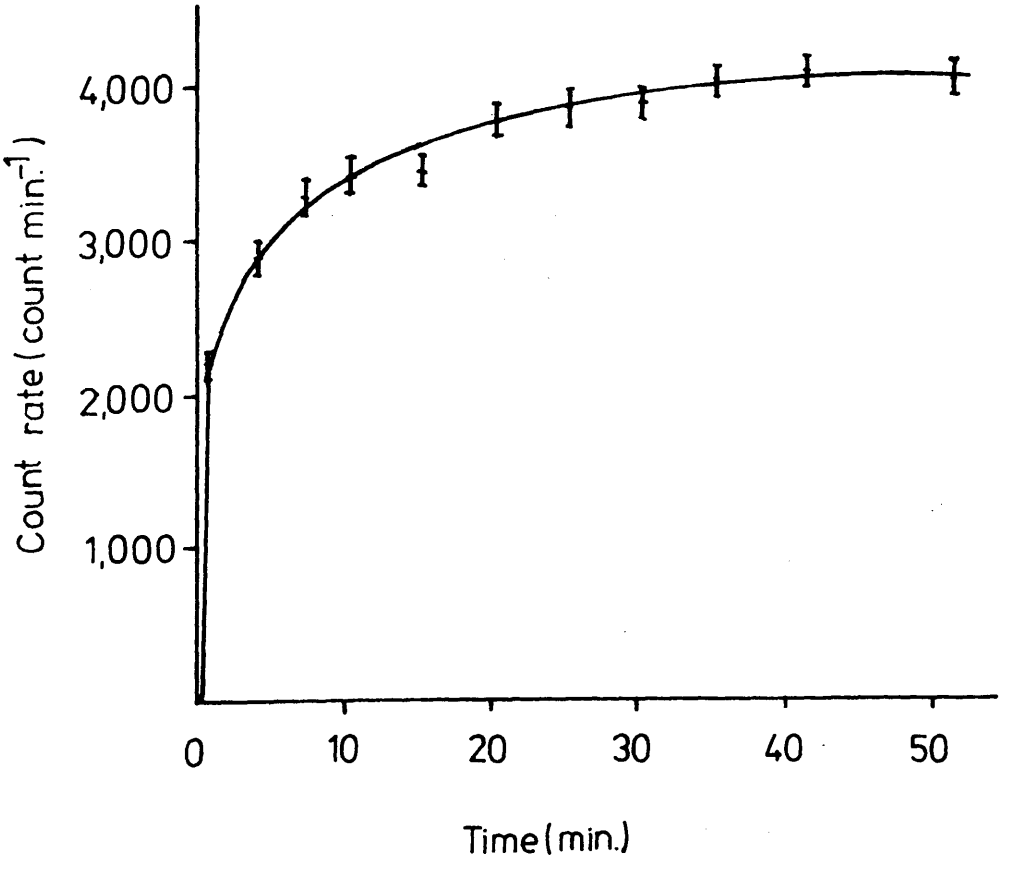

3.14 Reaction Between Nitrosonium Heptafluorotungstate(VI) and [^{18}F]-Fluorine Labelled Molybdenum Hexafluoride Under Heterogeneous Conditions.

Admission of [^{18}F]-labelled molybdenum hexafluoride, $MoF_5{}^{18}F$, (0.83±0.02 mmol) to nitrosonium heptafluorotungstate(VI), $NOWF_7$ (0.59±0.01 mmol) under heterogeneous conditions resulted in a decrease in the specific count rate of $MoF_5{}^{18}F$ together with a marginal increase in the mass of $NOWF_7$ after reaction (Table 3.8). Therefore the solid count rate was mainly due to an exchange of [^{18}F]-fluorine. The decrease in the specific count rate of $MoF_5{}^{18}F$ was equivalent to a partial exchange (f = 0.40±0.02). Figure 3.9 shows the growth of [^{18}F]-fluorine activity in $NOWF_7$ with time. There was a close similarity between the behaviour of $NOWF_7$ in the presence of $WF_5{}^{18}F$ and in the presence of $MoF_5{}^{18}F$. [^{18}F]-Fluorine activity followed a rapid growth during the first ten to twenty minutes then slowed considerably thereafter. In addition the uptake of $MoF_5{}^{18}F$ or $WF_5{}^{18}F$ by $NOWF_7$ was marginal in each case.

3.15 Reaction Between Caesium Heptafluoromolybdate(VI) and [^{18}F]-Fluorine Labelled Tungsten Hexafluoride Under Heterogeneous Conditions.

Two reactions between caesium heptafluoromolybdate(VI), $CsMoF_7$, and [^{18}F]-labelled tungsten hexafluoride $WF_5{}^{18}F$ were carried out under heterogeneous conditions for 1h. A summary of the results is presented in Table 3.9. The specific count rate of $WF_5{}^{18}F$ decreased

Table 3.8 Reaction Between $NOWF_7$ and MoF_5 ^{18}F Under Heterogeneous Conditions. Summary of Results.

Reactants				Specific count rate of MoF_6 (count min mmol^{-1})		Solid Count Rate (count min^{-1})	Radio-Chemical Balance (%)	Uptake mmol MoF_6 / mmol WF_7	Fraction Exchanged.
$NOWF_7$		MoF_6 (mmol)							
Initial	Final	Initial	Final	Initial	Final				
0.2043 ±0.0030g 0.59 ±0.01 mmol	0.2061 ±0.0030g	0.83±0.02	0.79±0.02	29751 ±408	24408 ±464	5272 ±73	100	0.02 ±0.03	0.40±0.02

Figure 3.9 Reaction of $NOWF_7$ with MoF_5 ^{18}F under Heterogeneous Conditions vs. Time.

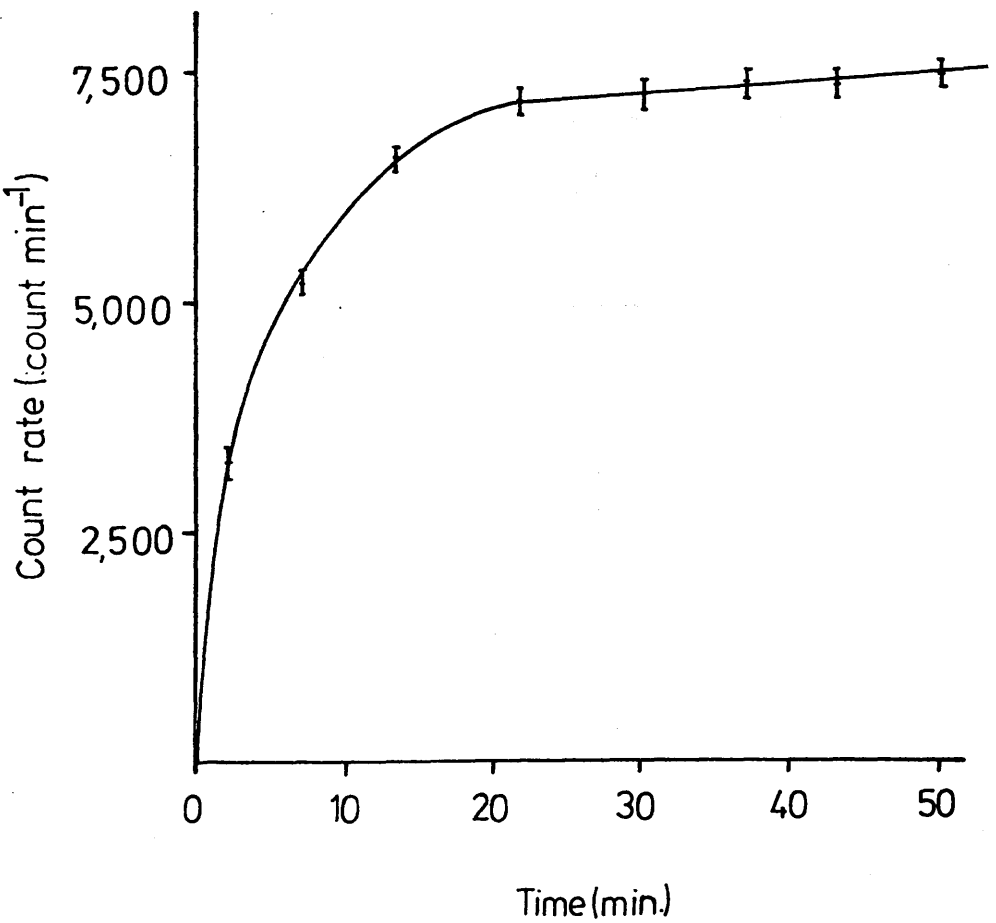

Table 3.9 Reactions between $CsMoF_7$ and WF_5 ^{18}F under Heterogeneous Conditions. Summary of Results.

Reaction No.	Reactants				Specific count rate of WF_6 (count min^{-1} $mmol^{-1}$)		Count rate of reactants after reaction (count min^{-1})		Radiochemical balance (%)	Uptake mmol WF_6 mmol $CsMoF_7$	Fraction Exchanged
	$CsMoF_7$		WF_6 (mmol)								
	Initial	Final	Initial	Final	Initial	Final	WF_6	$CsWF_7$			
1	0.1873 ±0.0030 g 0.52 ±0.01 mmol	0.2356 ±0.0030 g	2.70±0.01	2.50±0.01	18254 ±238	17738 ±133	44345 ±211	4931 ±70	100	0.31 ±0.03	0.15 ±0.03
2	0.2639 ±0.0030 g 0.73 ±0.01 mmol	0.2696 ±0.0030 g	1.98±0.01	1.97±0.01	16934 ±162	16249 ±123	32011 ±179	2626 ±51	103	0.03 ±0.03	0.13 ±0.03

in each case corresponding to partial exchange of [^{18}F]-fluorine (f = 0.13, 0.15±0.03). A substantial increase in the mass of the sample in Reaction 1 was observed. This was equivalent to an uptake of 0.31±0.03 WF_6:$CsMoF_7$ mole ratio. However in Reaction 2 the uptake was marginal (0.03±0.03 WF_6:$CsMoF_7$ mole ratio). The difference in behaviour between the two samples was probably due to the difference in the physical state of their surfaces. Figure 3.10 represents the growth of [^{18}F]-fluorine activity in $CsMoF_7$ with time in Reaction 1. The shape of the curve can be explained in terms of a simultaneous process of uptake and exchange of [^{18}F]-fluorine between $WF_5{}^{18}F$ and $CsMoF_7$.

3.16 Reaction Between Nitrosonium Heptafluorotungstate(VI), Thallium(I) Heptafluorotungstate(VI) and [^{18}F]-Fluorine Labelled Uranium Hexafluoride Under Heterogeneous Conditions.

The results of the reactions between nitrosonium heptafluorotungstate(VI), $NOWF_7$, thallium(I)heptafluorotungstate(VI), $TlWF_7$ and [^{18}F]-labelled uranium hexafluoride, $UF_5{}^{18}F$, under heterogeneous conditions are presented in Table 3.10. A decrease in the specific count rate of $UF_5{}^{18}F$ was observed in all cases resulting in a substantial but not complete exchange of [^{18}F]-fluorine. An increase in the mass of $NOWF_7$ after reaction was observed corresponding to an uptake of 0.11 and 0.13±0.03 UF_6:$NOWF_7$ mole ratio. However a negligeable uptake of UF_6 was observed in the case of $TlWF_7$ (0.03±0.03 UF_6:$TlWF_7$ mole ratio). The radiochemical balance was low in all cases. This was due to

Figure 3.10 Reaction of $CsMoF_7$ with WF_5 ^{18}F under Heterogeneous Conditions vs. Time.

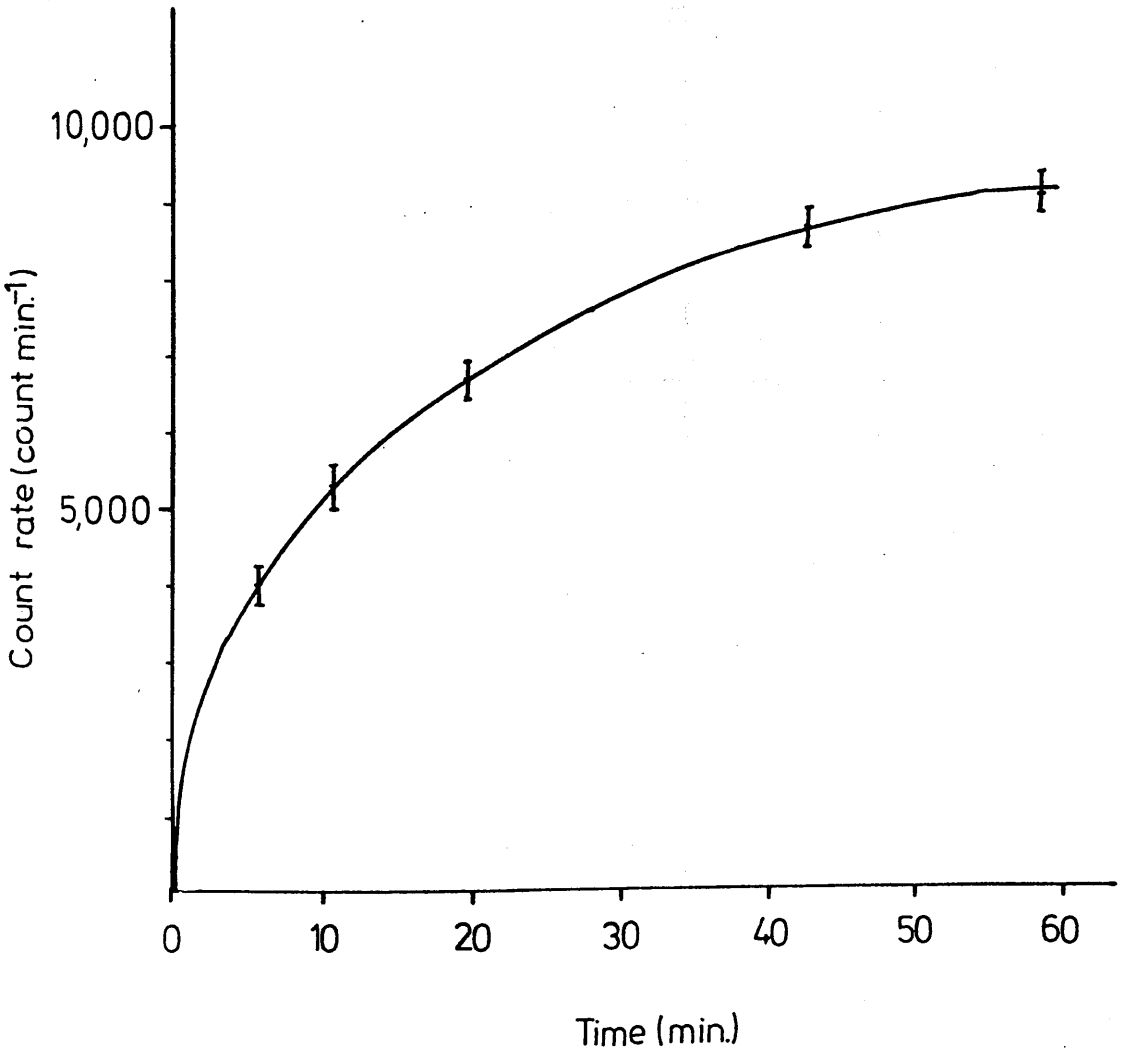

Table 3.10 Reactions between $NOWF_7$ or $TlWF_7$ and $UF_5{}^{18}F$ under Heterogeneous Conditions. Summary of Results.

AWF_7	Reactants				Specific count rate of $UF_5{}^{18}F$ (count $min^{-1} mmol^{-1}$)		Count Rate of Reactants after Reaction. (count min^{-1})		Radio-chemical balance (%)	Uptake mmol WF_6 mmol WF_7^-	Fraction Exchanged
	AWF_7		$UF_5{}^{18}F$ (mmol)								
	Initial	Final	Initial	Final	Initial	Final	UF_6	WF_7^-			
$NOWF_7$	0.0361 ±0.0030g 0.01 ±0.01mmol	0.0402 ±0.0030g	0.29±0.01	0.27±0.01	142690 ±3337	113993 ±1086	30778 ±175	4682 ±68	82	0.11 ±0.03	0.70 ±0.05
	0.0702 ±0.0030g 0.20 ±0.01mmol	0.0796 ±0.0030g	0.66±0.01	0.61±0.01	24290 ±344	20539 ±385	12529 ±112	1515 ±39	88	0.13 ±0.03	0.51 ±0.03
$TlWF_7$	0.4811 ±0.0030g 0.92 ±0.01mmol	0.4911 ±0.0030g	1.14±0.01	1.11±0.01	24290 ±344	20641 ±234	22912 ±151	734 ±27	85	0.03 ±0.3	0.31 ±0.03

the difficulty associated with the distillation of UF_6 which resulted in loss of some of the samples. Figures 3.11 and 3.12 represent the growth of [^{18}F]-fluorine activity in $NOWF_7$ and $TlWF_7$ with time respectively. In each case the growth of the curve can be accounted for by a slow exchange of [^{18}F]-fluorine together with an uptake of $UF_5{}^{18}F$.

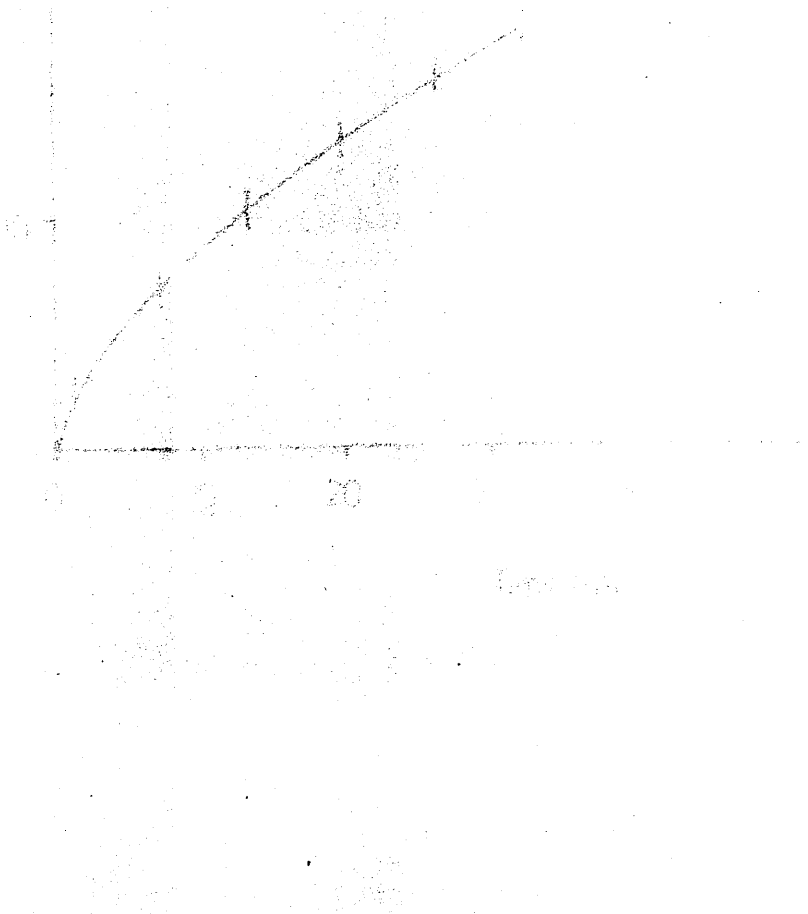

Figure 3.11 Reaction of $NOWF_7$ with UF_5 ^{18}F under Heterogeneous Conditions vs. Time.

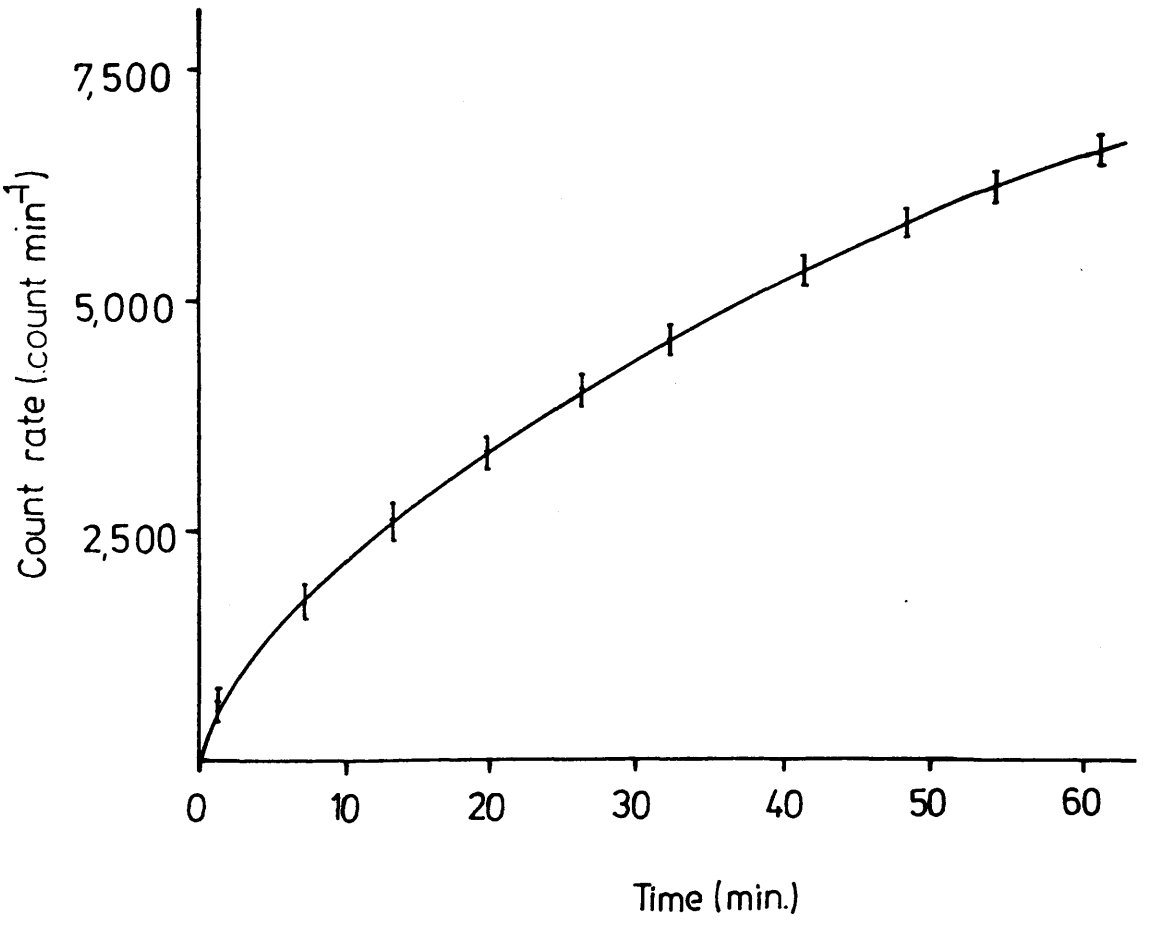

Figure 3.12 Reaction of $TlWF_7$ with UF_5 ^{18}F under Heterogeneous Conditions vs. Time.

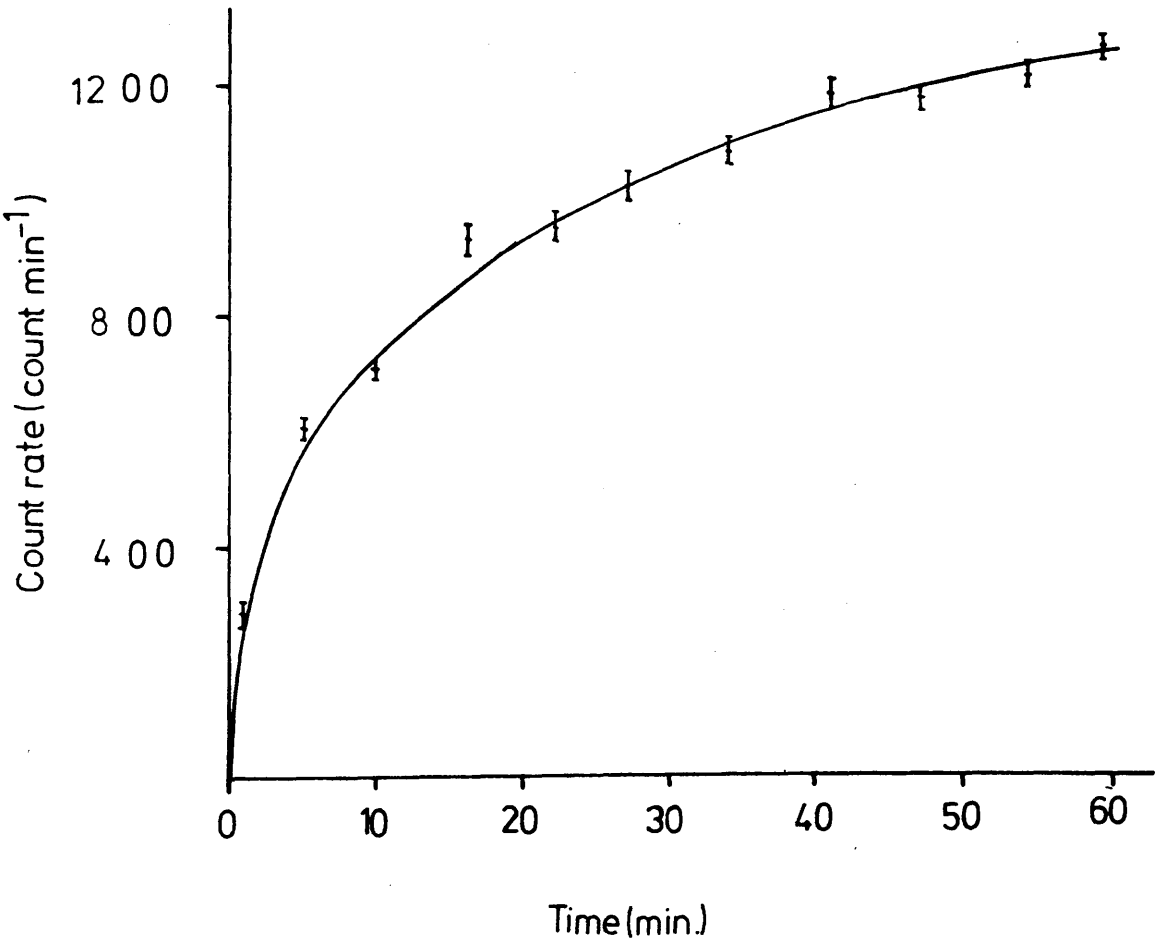

CHAPTER FOUR

HETEROGENEOUS REACTIONS BETWEEN ACTIVATED CAESIUM FLUORIDE, COPPER DIFLUORIDE, THALLIUM FLUORIDE AND [^{18}F]-FLUORINE LABELLED GASEOUS HEXAFLUORIDES OF MOLYBDENUM, TUNGSTEN AND URANIUM.

4. Heterogeneous Reactions Between Activated Caesium Fluoride, Copper Difluoride, Thallium Fluoride and [^{18}F]-Fluorine Labelled Gaseous Hexafluorides of Molybdenum Tungsten and Uranium.

4.1 Introduction

Cox et. al. [139] claimed to have prepared the octaflurometallate(VI) anions of molybdenum and tungsten by reactions between alkali fluorides namely potassium fluoride, rubidium fluoride and caesium fluoride and gaseous hexafluorides of molybdenum and tungsten. Their results were based only on chemical analysis of the complexes. Sheft et. al. [140] used [^{18}F]-fluorine as radiotracer to show that reaction between sodium fluoride and gaseous uranium hexafluoride at high temperature lead to the formation of a complex corresponding to UF_6.2NaF. Later in two separate papers Katz [141] reported the results of his studies involving heterogeneous reactions between high-surface area sodium fluoride and the hexafluorides of molybdenum, tungsten and uranium at elevated temperature. High-surface area NaF was obtained by treatment of NaF with hydrogen fluoride or UF_6 followed by thermal decomposition of the adducts formed. The interaction between NaF and UF_6 at 383 K resulted in a fast and almost complete reaction yielding a complex of the form UF_6.2NaF. Similar results were obtained with MoF_6 and WF_6 although in this case the reactions were slower and incomplete. These results were

arrived at by chemical analysis and measurement of the dissociation pressure of the complexes.

In this chapter the results of the reactions between activated caesium fluoride, copper difluoride and thallium fluoride and [^{18}F]-labelled hexafluorides of molybdenum, tungsten and uranium under heterogeneous conditions at room temperature are presented. Caesium fluoride was activated by formation followed by thermal decomposition of its hexafluoroacetone adduct (Section 2.3). Copper difluoride and thallium fluoride were used without any treatment.

4.2 Experimental.

The reactions between activated CsF, CuF_2, TlF and $MF_5{}^{18}F$ (M = Mo, W or U) were investigated following the procedure described in Section 2.12.2. [^{18}F]-Fluorine labelled MF_6 (M = Mo, W or U) were prepared as described in Section 2.13.2. Four different batches of activated CsF were used. These were activated according to the procedure described in Section 2.3. Table 4.1 shows the conditions of activation of the batches of CsF used. Each batch was reacted with $MF_5{}^{18}F$ (M = Mo, W or U).

Table 4.1 Preparation of Activated CsF.

Batch No.	1	2	3	4
CsF (mmol)	20	20	20	20
$(CF_3)_2CO$ (mmol)	33	13	-	33
MeCN (cm^3)	5	5	5	5

4.3 Reaction Between Activated Caesium Fluoride and [^{18}F]-Fluorine Labelled Tungsten Hexafluoride Under Heterogeneous Conditions.

A total of eight reactions between activated caesium fluoride and [^{18}F]-labelled tungsten hexafluoride were carried out under heterogeneous conditions at room temperature for 1h. The results of these reactions are presented in Tables 4.2 and 4.3. An increase in the mass of the solid together with a decrease in the amount of $WF_5{}^{18}F$ after reactions were observed in all cases indicating that uptake of WF_6 by CsF had occurred. The mole ratio WF_6:CsF calculated from the uptake was in the range 1:1 to 0.1:1. Table 4.3 shows that where the uptake was substantial a decrease in the specific count rate of $WF_5{}^{18}F$ was observed

Table 4.2 Mass Balances of the Reactions Between Activated CsF and WF_5 ^{18}F Under Heterogeneous Conditions.

Exp. No.	Batch. No.	CsF Initial (g) (mmol)	CsF Final (g)	Mass Increase of CsF (g)	Number of mmol. WF_6 corresponding to Mass Increase (mmol)	WF_6 (g) (mmol) Initial	WF_6 (g) (mmol) Final	Decrease of WF_6 (mmol)	Uptake mmol WF_6 / mmol CsF
1	1	0.2235 ±0.0030 1.47 ±0.02	0.6580 ±0.0030	0.4345 ±0.0030	1.46 ±0.010	0.9831 ±0.0030 3.30 ±0.01	0.4367 ±0.0030 1.47 ±0.01	1.83 ±0.02	0.99 ±0.03
2	1	0.2167 ±0.0030 1.43 ±0.02	0.6665 ±0.0030	0.4498 ±0.0030	1.51 ±0.01	1.0537 ±0.0030 3.54 ±0.01	0.4296 ±0.0030 1.44 ±0.01	2.10 ±0.02	1.06 ±0.03
3	2	0.1700 ±0.0030 1.12 ±0.02	0.2309 ±0.0030	0.0609 ±0.0030	0.20 ±0.01	0.8740 ±0.0030 2.93 ±0.01	0.8043 ±0.0030 2.70 ±0.01	0.23 ±0.02	0.18 ±0.03
4	2	0.1365 ±0.0030 0.90 ±0.02	0.1902 ±0.0030	0.0537 ±0.0030	0.18 ±0.01	0.5708 ±0.0030 1.92 ±0.01	0.5085 ±0.0030 1.71 ±0.01	0.21 ±0.02	0.20 ±0.03
5	3	0.3789 ±0.0030 2.49 ±0.02	0.4583 ±0.0030	0.0794 ±0.0030	0.27 ±0.01	0.6899 ±0.0030 2.32 ±0.01	0.5869 ±0.0030 1.97 ±0.01	0.35 ±0.02	0.11 ±0.03

contd..

Table 4.2 Mass Balances of the Reaction Between Activated CsF and WF_5 ^{18}F Under Heterogeneous Conditions.

Exp. No.	Batch. No.	CsF Initial (g) (mmol)	CsF Final (g)	Mass Increase of CsF (g)	Number of mmol. WF_6 corresponding to Mass Increase (mmol)	WF_6 (g) (mmol) Initial	WF_6 (g) (mmol) Final	Decrease of WF_6 (mmol)	Uptake mmol WF_6 / mmol CsF
6	3	0.2463 ±0.0030 1.62 ±0.02	0.3073 ±0.0030	0.0610 ±0.0030	0.21 ±0.01	1.3808 ±0.0030 4.64 ±0.01	1.3125 ±0.0030 4.41 ±0.01	0.23 ±0.02	0.13 ±0.03
7	4	0.2422 ±0.0030 1.59 ±0.02	0.5680 ±0.0030	0.3258 ±0.0030	1.09 ±0.01	0.9759 ±0.0030 3.28 ±0.01	0.6426 ±0.0030 2.16 ±0.01	1.12 ±0.02	0.69 ±0.03
8	4	0.3071 ±0.0030 2.02 ±0.02	0.6913 ±0.0030	0.3842 ±0.0030	1.29 ±0.01	0.8252 ±0.0030 2.77 ±0.01	0.4162 ±0.0030 1.40 ±0.01	1.37 ±0.02	0.64 ±0.03

Table 4.3 Radiochemical Balances of the Reactions Between Activated CsF and WF_5 ^{18}F Under Heterogeneous Conditions.

Exp. No.	Uptake of WF_6 from Mass Balance (mmol)	Count rate of Reactants After Reaction (count min^{-1})		Sp.ct.rate of WF_6 (count min^{-1} $mmol^{-1}$)		Radiochem. Balance (%)
		CsF	WF_6	Initial	Final	
1	1.46 ±0.01	10415 ±102	9830 ±99	6996 ±51	6687 ±82	87
2	1.51 ±0.01	10092 ±100	9924 ±100	6996 ±51	6892 ±84	81
3	0.20 ±0.01	4878 ±70	115770 ±340	43219 ±191	42878 ±203	95
4	0.18 ±0.01	4816 ±66	78603 ±280	43219 ±191	45967 ±316	100
5	0.27 ±0.01	1898 ±44	22581 ±150	11395 ±86	11462 ±96	93
6	0.21 ±0.01	1158 ±34	50833 ±225	11395 ±86	11527 ±58	98
7	1.09 ±0.01	10169 ±101	19279 ±139	9088 ±60	8925 ±77	100
8	1.29 ±0.01	18515 ±136	18282 ±135	13913 ±87	13059 ±135	96

indicating that [^{18}F]-fluorine exchange had taken place. Experiment No.2 was an exception where a more significant decrease in the specific count rate of $WF_5{}^{18}F$ was expected. This result can be accounted for by the relatively poor radiochemical balance (81%) obtained. The difference in behaviour among the different batches was reflected by the growth of [^{18}F]-fluorine activity in the solid with time. Figures 4.1 and 4.2 represent this relationship for batches No.4 and No.3 respectively. The two relationships were obtained under similar conditions of specific count rate of $WF_5{}^{18}F$ and amount of activated CsF. For batch No.4 where the uptake was found to be equivalent to 0.69±0.03 mmol WF_6(mmol CsF)$^{-1}$ the solid count rate increased rapidly initially then followed a slower process (Figure 4.1). The rapid growth of [^{18}F]-fluorine activity can be accounted for in terms of a rapid uptake of $WF_5{}^{18}F$ by CsF followed by a slower exchange of [^{18}F]-fluorine between the adsorbed species and free $WF_5{}^{18}F$. However, in the case of batch No.3 where the uptake was found to be equivalent to 0.10±0.03 mmol WF_6(mmol CsF)$^{-1}$ the solid count rate increased rapidly initially and levelled off thereafter. The level of [^{18}F]-fluorine activity was much smaller in the latter case as compared with the former. In the same way the initial rapid growth of [^{18}F]-fluorine activity in the solid can be accounted for by the small uptake of WF_6. Whereas the constant level of [^{18}F]-fluorine activity is consistent with the non-observable [^{18}F]-fluorine exchange.

Figure 4.1 Heterogeneous Reaction Between Activated CsF and $WF_5{}^{18}F$ with Time.

Ancillary conditions: CsF = 1.59±0.02mmol; $WF_5{}^{18}F$ = 3.28±0.01mmol

Specific count rate: 9008±60 count min^{-1} $mmol^{-1}$

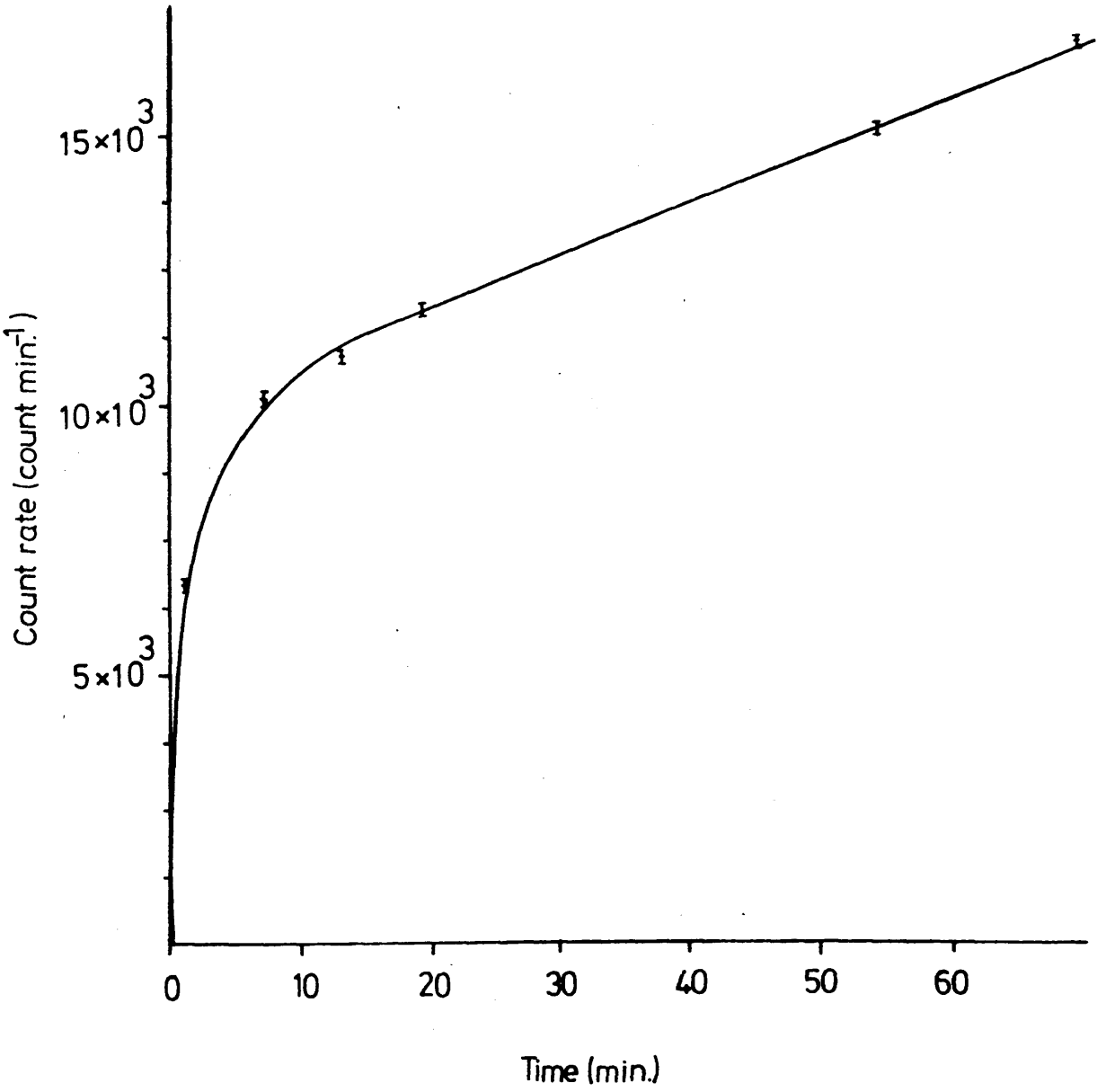

Figure 4.2 Heterogeneous Reaction Between Activated CsF and WF_5 ^{18}F with Time.

Ancillary conditions: CsF = 1.62±0.02mmol; WF_5 ^{18}F = 4.6±0.01mmol

Specific count rate: 11395±86 count min^{-1} $mmol^{-1}$

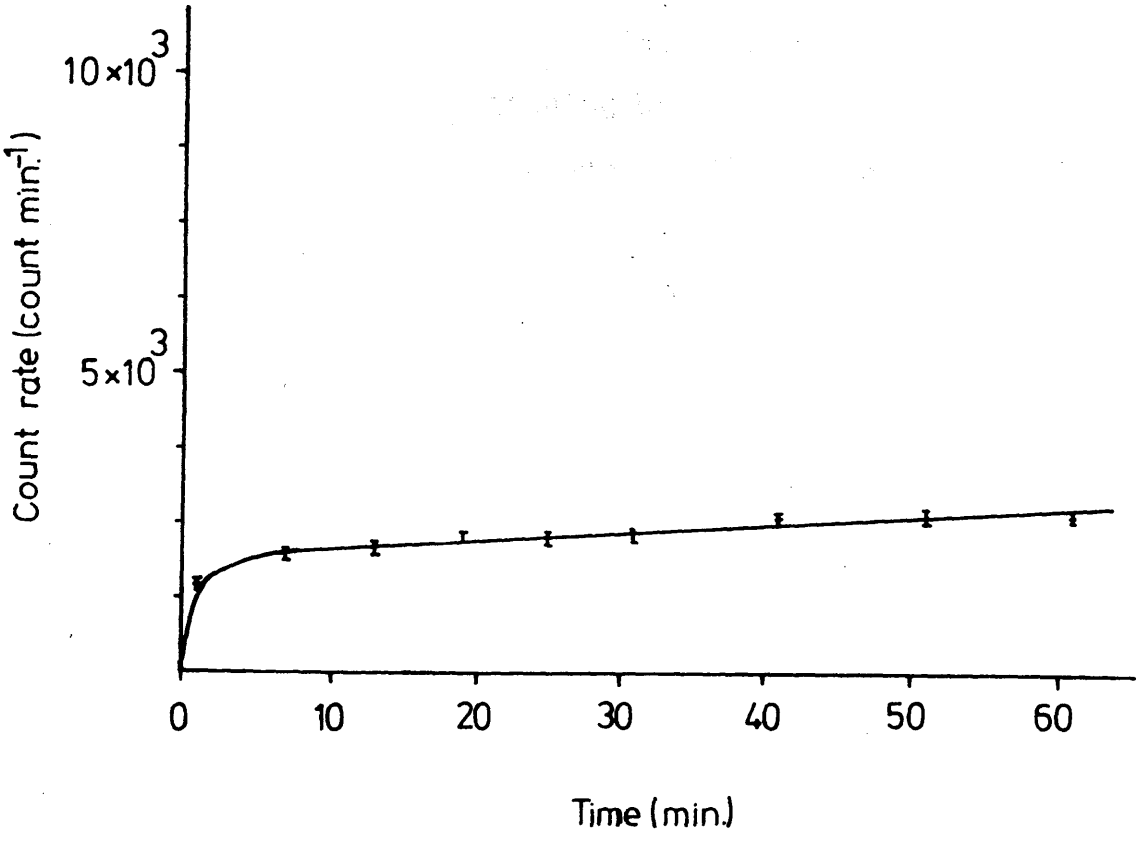

The exchange of [^{18}F]-fluorine between adsorbed $WF_5{}^{18}F$ and free $WF_5{}^{18}F$ was further demonstrated for batch No.4 by reacting inactive WF_6 with CsF which had been treated with $WF_5{}^{18}F$ to produce radioactive solid. [^{18}F]-Fluorine labelled WF_6 (2.77±0.01 mmol) was allowed to react with CsF (2.02±0.02 mmol) for 1h. After removal of excess volatile material an uptake corresponding to 1.29±0.01 mmol $WF_5{}^{18}F$ was observed producing a [^{18}F]-fluorine count rate of 18515±136 count min^{-1}. Inactive WF_6 (1.11±0.01 mmol) was then admitted to the vessel containing $CsF.WF_5{}^{18}F$ and the reaction allowed to proceed for 45 minutes. After separation of reactants both solid and volatile material were assayed for [^{18}F]-fluorine activity. A transfer of [^{18}F]-fluorine activity took place from the solid to the initially inactive WF_6 (1792±42 count min^{-1}) indicating that an exchange of [^{18}F]-fluorine had occurred. Table 4.4 summarises the results of this experiment. A further increase in mass of $CsF.WF_5{}^{18}F$ was observed after reaction. This corresponded to an uptake of 0.17±0.02 mmol WF_6.

Tabel 4.4 Reaction Between WF_6 and Activated CsF Treated With $WF_5{}^{18}F$. Summary of Results.

$CsF.WF_5{}^{18}F$ (g)		$CsF.WF_5{}^{18}F$ count rate.		WF_6 (mmol)		WF_6 count rate (count min^{-1})
Initial	Final	Initial	Final	Initial	Final	
0.6913 ±0.0030	0.7420 ±0.0030	18515 ±136	16853 ±130	1.11 ±0.01	0.81 ±0.01	1792 ±42

Both infrared and Raman spectra of CsF after reaction with WF_6 were recorded. However, in most cases the Raman spectra were more informative than the infrared spectra as the latter were of relatively poor quality. The Raman spectra of the solids after reaction are presented in Table 4.5 together with the literature spectra of $CsWF_7$ and Cs_2WF_8 [28]. Figures 4.3(a) and 4.3(b) represent the Raman spectra of the solid after reaction between CsF and WF_6 for batch No.1 and No.2 respectively. The Raman spectrum of $CsWF_7$ (Figure 4.3(c)) is presented for comparison. Figure 4.4 represents the infrared spectra of the solid after reaction between CsF (Batch No.1) and WF_6 (a), together with the infrared spectrum of $CsWF_7$ (b). Examination of Table 4.5 reveals the presence of WF_7^- species in batches No.1 and No.2 as shown by the bands at ν_{max} 713 (vs), 617 (w) and 442 (m) cm^{-1} which were assigned to ν_1 (A_1'), ν_2(A_1') and ν_8 (E_1'') modes of WF_7^- respectively. The bands at ν_{max} 690 (m) and 688 (w) cm^{-1} suggest that other species may had also been formed. Fluorine bridged species is a possible explanation although these bands were in a region higher than that characteristic of fluorine bridged species, [138]. The band at ν_{max} 656 (m) cm^{-1} in batch No.3 suggests that WF_8^{2-} had been formed as the only species as compared with the Raman spectrum of Cs_2WF_8 [28]. Equally the infrared spectrum of CsF recorded after reaction with WF_6 (Figure 4.4 (a)) suggest that WF_7^- is the species formed as shown by the band at ν_{max} 610 cm^{-1} assigned to ν_3 (A_2''). The band at ν_{max} 505 cm^{-1} suggests the presence of a fluorine bridged species [138].

Table 4.5 Raman Spectra of CsF After Reaction With WF_6 Under Heterogeneous Conditions.

Batch No.	1	2	2	3	$CsWF_7$	Cs_2WF_8
Uptake mmol WF_6 / mmol CsF	1.00	0.20	0.20	0.10	Ref [28]	
						385 w
	442 w		440 m		444 s $\nu_8(E_1)$	
						406 w
			617 w		617 vw $\nu_2(A_1)$	
				656 m		656 vs
	690 m	688 w				
	716 vs	713 vs	711 vs		716 vs $\nu_1(A_1)$	

vs: very strong; s: strong; m: medium; w: weak; vw: very weak

Figure 4.3 Raman Spectra of $CsWF_7$ (a) and CsF After Reaction with WF_6 for Batches No.2 (b) and No.1 (c).

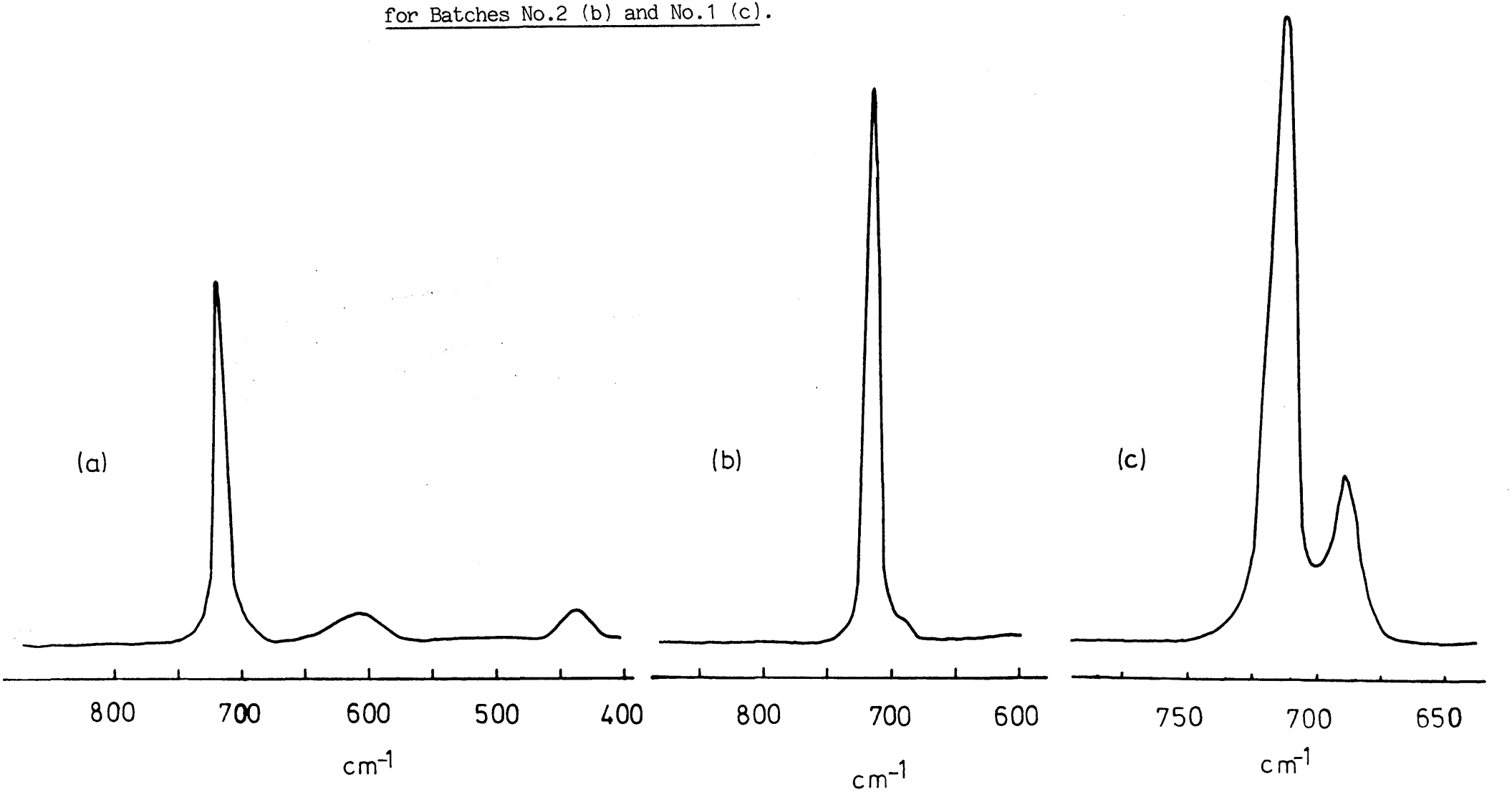

Figure 4.4 Infrared Spectra of CsF After Reaction with WF_6 (a) and $CsWF_7$ (b)

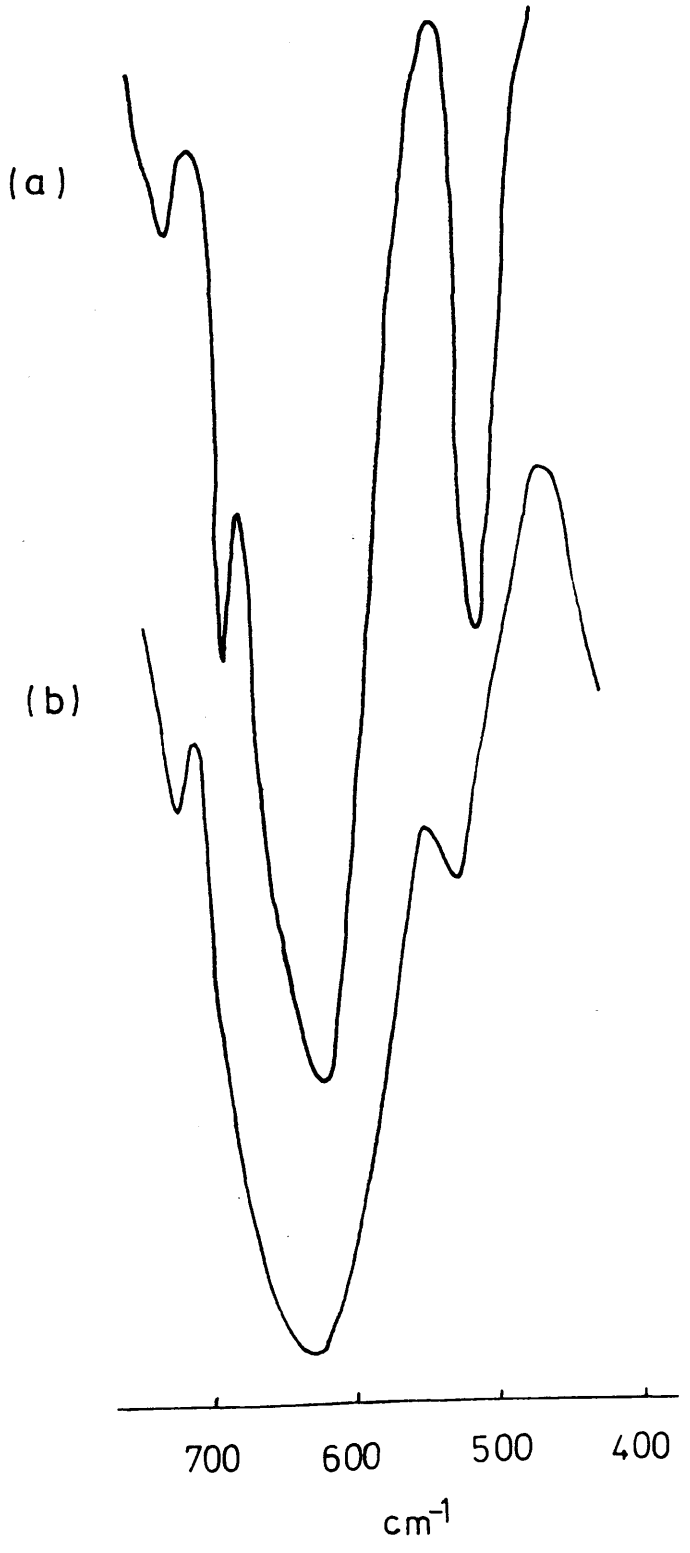

It is noteworthy that the infrared spectra of CsF (Batch No.2 and No.3) recorded after reaction with WF_6 contained bands attributable to $(CF_3)_2CFO^-$ [125] whereas in the case of batch No.1 no such bands were present indicating that $(CF_3)_2CO$, usually present after activation of CsF as $(CF_3)_2CFO^-$ [125], had been totally displaced by WF_6 upon reaction with CsF.

4.4 Reaction Between Activated Caesium Fluoride and [^{18}F]-Fluorine Labelled Molybdenum Hexafluoride Under Heterogeneous Conditions.

A total of five reactions between activated caesium fluoride and [^{18}F]-labelled molybdenum hexafluoride were carried out under heterogeneous conditions at room temperature for 1h. Table 4.6 and 4.7 summarise the results of these reactions. An increase in the mass of the solid together with decrease in the amount of $MoF_5{}^{18}F$ after reactions were observed in all cases. In the same way as with WF_6 (Section 4.3), MoF_6 was taken up to various extents. The mole ratio MoF_6:CsF calculated from the uptake was in the range 0.25:1 to 0.43:1. It is worth noticing at this point the difference in uptake of MoF_6 and WF_6 by the same batches of CsF. While the mole ratio WF_6:CsF calculated from the uptake for batch No.2 was approximately 0.20:1 that for MoF_6 was 0.43:1. For batch No.3 the mole ratio MF_6:CsF (M = Mo,W) calculated from the uptake was 0.11:1 in the case of WF_6 and 0.28:1 in the case of MoF_6. These results suggest the greater affinity of activated

Table 4.6 Mass Balances of the Reactions Between Activated CsF and MoF_5 ^{18}F Under Heterogeneous Conditions.

Exp. No.	Batch. No.	CsF Initial (g) (mmol)	CsF Final (g)	Mass Increase of CsF (g)	Number of mmol. MoF_6 corresponding to Mass Increase (mmol)	MoF_6 (g) (mmol) Initial	MoF_6 (g) (mmol) Final	Decrease of MoF_6 (mmol)	Uptake mmol MoF_6 / mmol CsF
1	1	0.2975 ±0.0030 1.96 ±0.02	0.4082 ±0.0030	0.1107 ±0.0060	0.53 ±0.03	0.1439 ±0.0030 0.69 ±0.02	0.0233 ±0.0030 0.11 ±0.02	0.57 ±0.04	0.27 0.05
2	1	0.2579 ±0.0030 1.70 ±0.02	0.3533 ±0.0030	0.0954 ±0.0060	0.45 ±0.03	0.1342 ±0.0030 0.64 ±0.02	0.0210 ±0.0030 0.10 ±0.02	0.54 ±0.04	0.27 ±0.05
3	2	0.2249 ±0.0030 1.48 ±0.02	0.3600 ±0.0030	0.1351 ±0.0060	0.64 ±0.03	0.5886 ±0.0030 2.80 ±0.02	0.3992 ±0.0030 1.90 ±0.02	0.90 ±0.04	0.43 ±0.05
4	3	0.3106 ±0.0030 2.05 ±0.02	0.4301 ±0.0030	0.1195 ±0.0060	0.57 ±0.03	0.3511 ±0.0030 1.67 ±0.02	0.2325 ±0.0030 1.11 ±0.02	0.56 ±0.04	0.28 ±0.05
5	4	0.4000 ±0.0030 2.63 ±0.02	0.5379 ±0.0030	0.1371 ±0.0060	0.65 ±0.03	0.1653 ±0.0030 0.79 ±0.01	0.0250 ±0.0030 0.12 ±0.01	0.67 ±0.04	0.25 ±0.05

Table 4.7 Radiochemical Balances of the Reactions Between Activated CsF and MoF_5 ^{18}F Under Heterogeneous Conditions.

Exp. No.	Uptake of MoF_6 from Mass Balance (mmol)	Count Rate of Reactants After Reaction (count min^{-1})		Specific Count Rate of MoF_6 (count min^{-1} $mmol^{-1}$)		Radiochemical Balance (%)
		CsF	MoF_6	Initial	Final	
1	0.53 ±0.03	12261 ±111	2343 ±48	23332 ±580	21300 ±2751	92
2	0.45 ±0.03	10753 ±104	2104 ±46	23332 ±580	21040 ±3189	86
3	0.64 ±0.03	35705 ±189	100332 ±317	53707 ±660	52806 ±449	90
4	0.57 ±0.03	7031 ±84	16697 ±192	15138 ±133	15042 ±224	94
5	0.65 ±0.03	19890 ±141	2517 ±50	26359 ±674	20975 ±2699	108

CsF for MoF_6 as compared with WF_6. In this respect uptakes corresponding to 1:1 mole ratio MoF_6:CsF would have been expected for batches No.1 and No.4 as in the case of WF_6. The difference in results was due to the experimental conditions used. Tungsten hexafluoride was used in a proportion exceeding a 1:1 combining ratio with CsF whereas MoF_6 was used in smaller amounts.

With the exception of experiment No.4 a decrease in the specific count rate of $MoF_5{}^{18}F$ after reaction was observed in all cases indicating that an exchange of [^{18}F]-fluorine had occurred between adsorbed $MoF_5{}^{18}F$ and free $MoF_5{}^{18}F$. [^{18}F]-Fluorine exchange was also shown to occur by reacting inactive MoF_6 with $CsF.MoF_5{}^{18}F$. [^{18}F]-Fluorine labelled MoF_6 (0.79±0.02 mmol) was allowed to react with CsF (2.63±0.02 mmol) for 1h. After removal of excess volatile material an uptake corresponding to 0.66±0.02 mmol $MoF_5{}^{18}F$ was observed producing a [^{18}F]-fluorine count rate of 19890±141 count min^{-1}. Inactive MoF_6 (0.63±0.02 mmol) was then admitted to the reaction vessel and allowed to interact with the radioactive solid for 45 minutes. After separation of reactants both solid and volatile material were assayed for [^{18}F]-fluorine activity. The initially inactive MoF_6 was found to be radioactive (1611± 40 count min^{-1}) while the solid count rate decreased consistent with an exchange of [^{18}F]-fluorine. Table 4.8 summarises the results of this reaction. A further increase in mass of $CsF.MoF_5{}^{18}F$ corresponding to an uptake of 0.11±0.03 mmol

Table 4.8 Reaction Between MoF_6 and Activated CsF Treated with $MoF_5{}^{18}F$. Summary of Results.

$CsF.MoF_5{}^{18}F$ (g)		$CsF.MoF_5{}^{18}F$ count rate (count min^{-1})		MoF_6 (mmol)		MoF_6 count rate (count min^{-1})
Initial	Final	Initial	Final	Initial	Final	
0.5379 ±0.0030	0.5609 ±0.0030	19890 ±141	18720 ±137	0.64 ±0.02	0.44 ±0.02	1611 ±40

MoF_6 was observed after reaction.

Figures 4.5 and 4.6 represent the growth of [^{18}F]-fluorine activity in the solid with time during the reaction between $MoF_5{}^{18}F$ and CsF batch No.1 and No.2 respectively. These relationships were obtained for an equal amount of CsF but different specific count rates of $MoF_5{}^{18}F$. However the latter were scaled to the same value to enable comparison between the two batches to be made. In each case the solid activity followed a rapid growth initially and a slower process thereafter. The shape of the curves can be interpreted in terms of a rapid uptake of $MoF_5{}^{18}F$ followed by a slower process of [^{18}F]-fluorine exchange. It is noteworthy that the difference in the level of [^{18}F]-fluorine activity between the two batches was smaller than that found in the case of $WF_5{}^{18}F$ (Section 4.3). This was a reflection of the smaller difference in uptakes of $MoF_5{}^{18}F$ by the different batches of CsF as compared with $WF_5{}^{18}F$.

The Raman spectra of CsF recorded after reaction with $MoF_5{}^{18}F$ are presented in Table 4.9 together with the literature spectra of $CsMoF_7$ and Rb_2MoF_8 [28]. Figure 4.7 represents the Raman spectrum of CsF (Batch No.2) recorded after reaction with $MoF_5{}^{18}F$ together with that of $CsMoF_7$ for comparison. The spectra suggest that more than one species had been formed. The bands at ν_{max} 688 (vs), 683 (m) and 687 (m) cm^{-1} were assigned to $\nu_1(A_1')$ mode of MoF_7^- as compared with $CsMoF_7$ [28]. The bands in the range (593 - 629) cm^{-1}

Table 4.9 Raman Spectra of CsF After Reaction with MoF_6 Under Heterogeneous Conditions.

Batch No	2	2	3	4	$CsMoF_7$	Rb_2MoF_8
Uptake $\frac{\text{mmol } MoF_6}{\text{mmol CsF}}$	0.44	0.43	0.23	0.29	Ref. [28]	
					321 w $\nu_{10}(E'_2)$	
						396 w
					433vw $\nu_8(E''_1)$	
	596 w	593 mw				
	629 w	624 mw	629 s	621 w		
						636 vs
	688 vs	683 m	687 w		687vs $\nu_1(A'_1)$	

vs: very strong; s: strong; m: medium; w: weak;
mw: medium weak; vw: very weak.

Figure 4.5 Heterogeneous Reaction Between Activated CsF and MoF_5 ^{18}F with Time.

Ancillary conditions: CsF = 1.70±0.02mmol; MoF_5 ^{18}F = 0.64±0.02mmol
Specific count rate = 23332±580 count min^{-1} $mmol^{-1}$

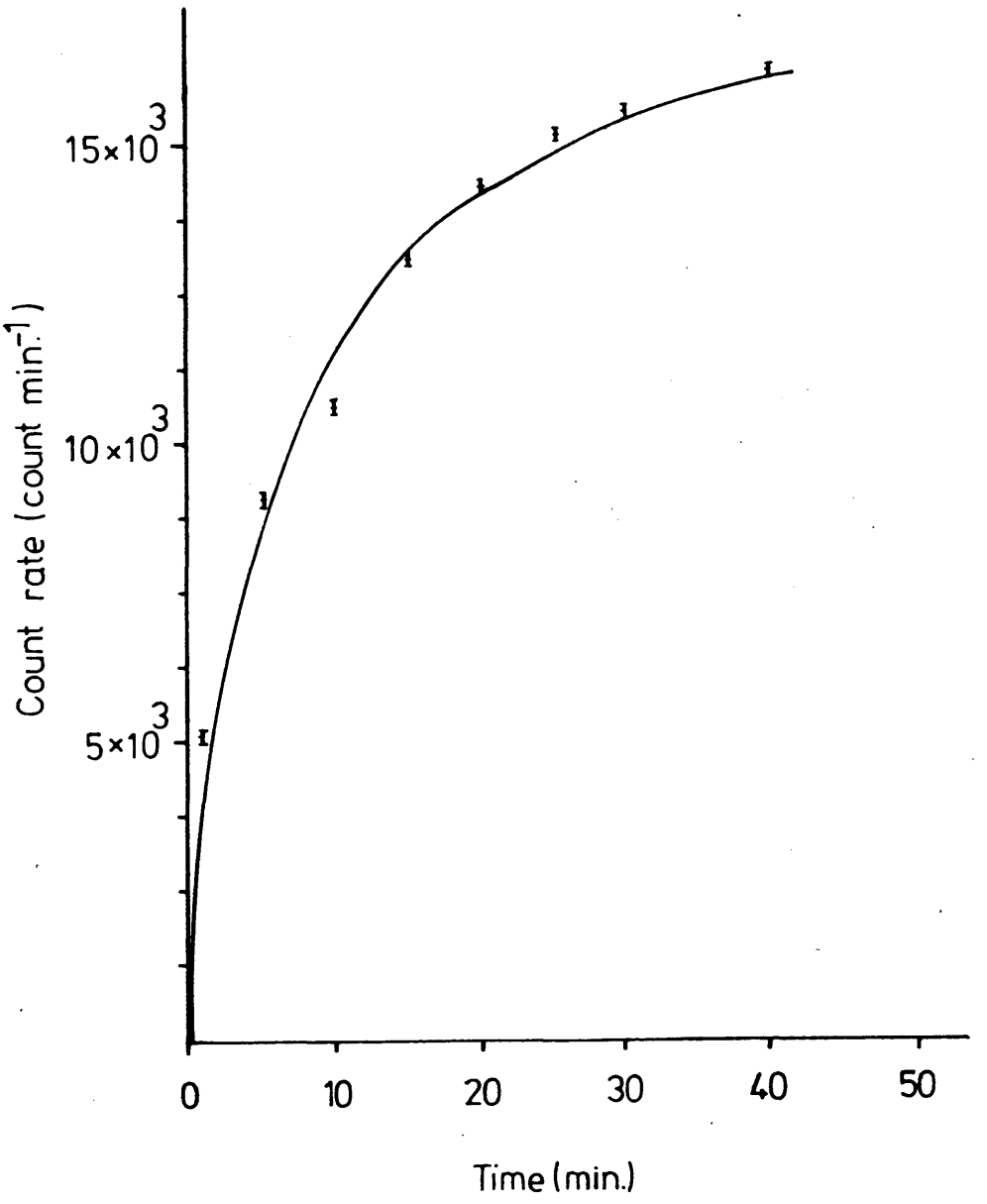

Figure 4.6 Heterogeneous Reaction Between Activated CsF and MoF_5 ^{18}F with Time.

Ancillary conditions: CsF = 1.48±0.02mmol; MoF_5 ^{18}F = 2.80±0.02mmol

Corrected specific count rate = 23332±580 count min^{-1} $mmol^{-1}$

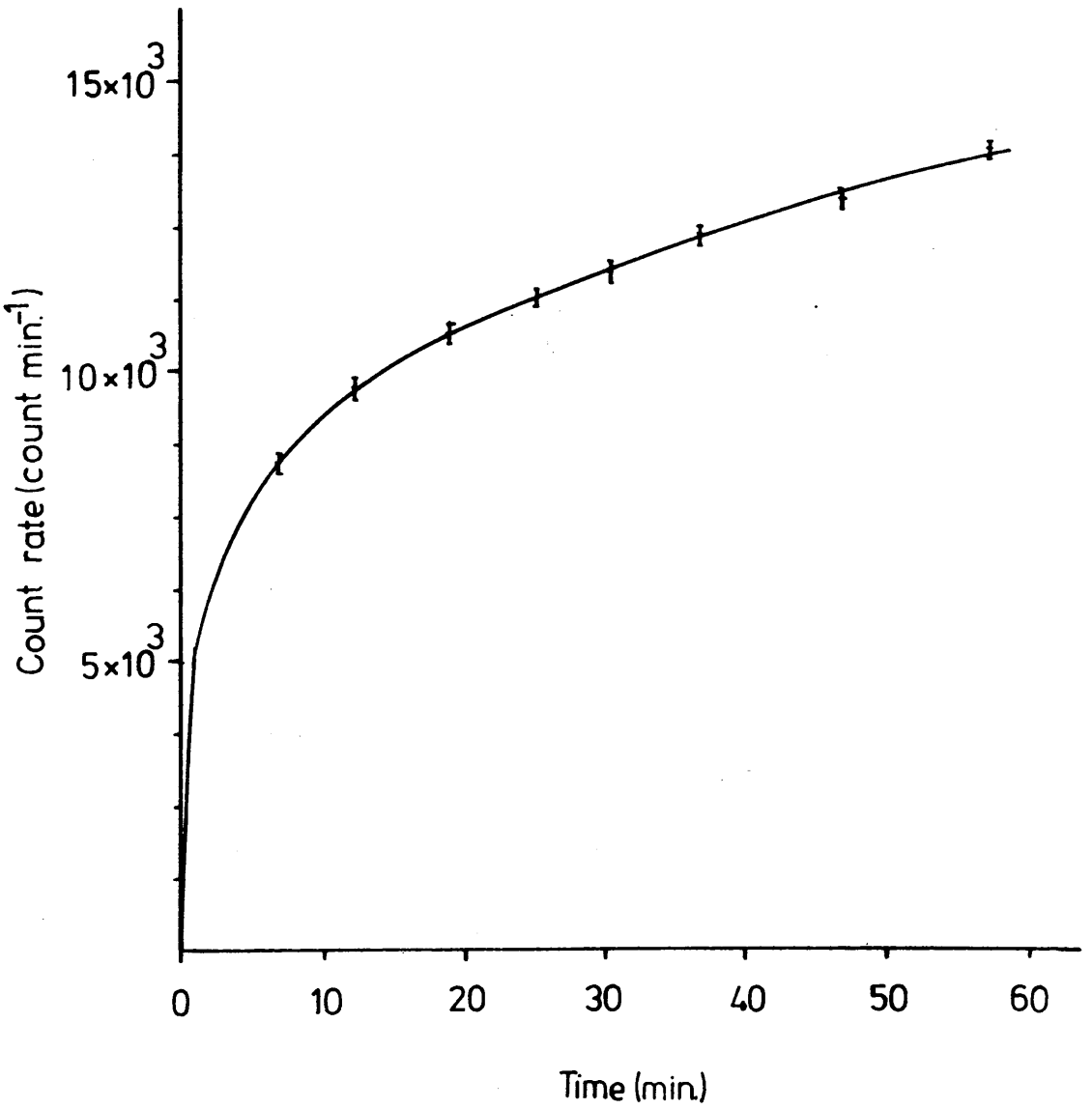

Figure 4.7 Raman Spectra of CsF (Batch 2) After Reaction with MoF_6 (a) and $CsMoF_7$ (b)

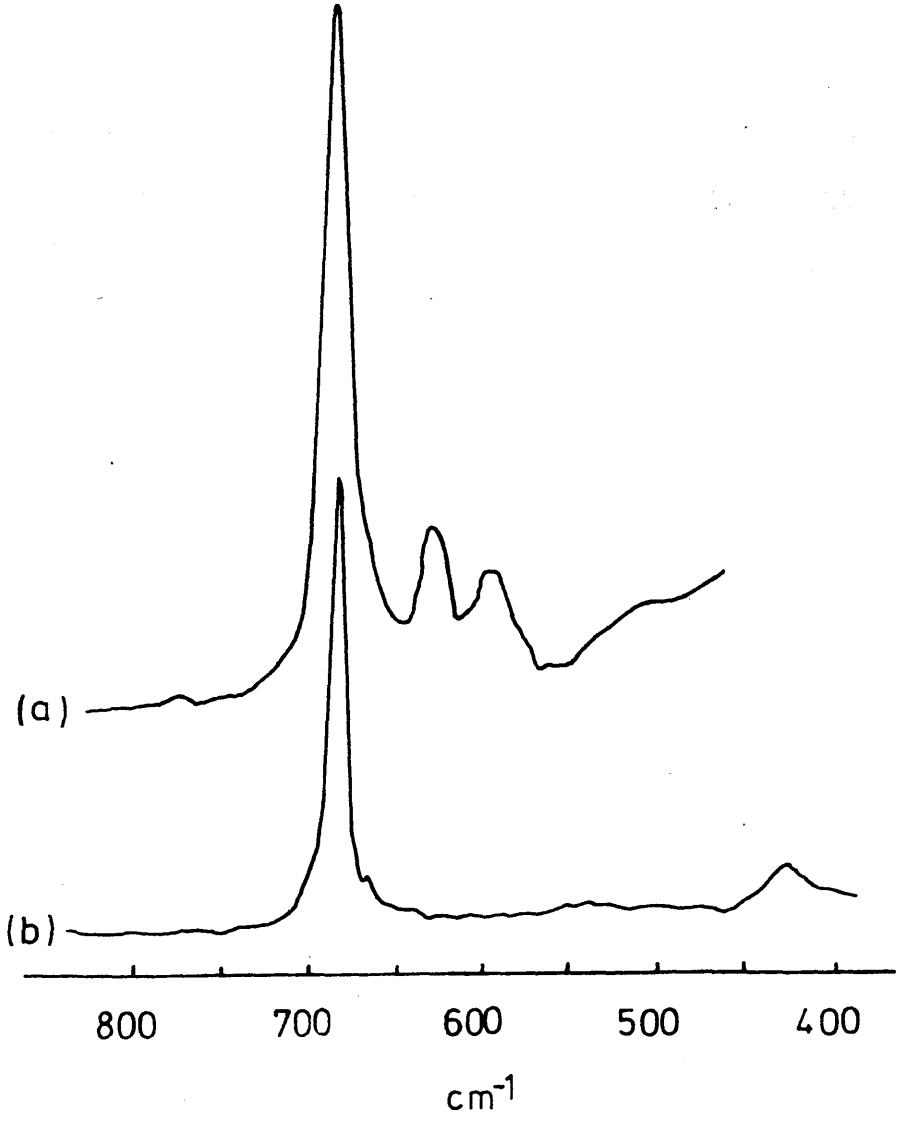

suggest that species other than MoF_7^- were present. Although this range was higher than that characteristic of fluorine bridged species [138] such a possibility cannot be ruled out.

4.5 Reaction Between Activated Caesium Fluoride and [^{18}F]-Fluorine Labelled Uranium Hexafluoride Under Heterogeneous Conditions.

The reaction between activated caesium fluoride and [^{18}F]-labelled uranium hexafluoride under heterogeneous conditions at room temperature was investigated for batches No. 2,3 and 4. A summary of the results of four reactions is presented in Tables 4.10 and 4.11. Interaction between activated CsF and $UF_5{}^{18}F$ for 1h resulted in an increase in the mass of CsF together with a decrease in the amount of $UF_5{}^{18}F$. This was consistent with an uptake of $UF_5{}^{18}F$ by CsF. The mole ratio UF_6:CsF calculated from the uptake was in the range 0.13:1 to 0.26:1. A colour change from off-white to yellow which might be due to traces of hydrolysis of the sample was observed after reaction in all cases. A decrease in the specific count rate of $UF_5{}^{18}F$ after reaction was observed in the case of batches No.2 and No.4 where an exchange of [^{18}F]-fluorine must have taken place. However no significant decrease in the specific count rate of $UF_5{}^{18}F$ after reaction was observed for batch No.3. This was attributed to the relatively small amount of $UF_5{}^{18}F$ taken up by CsF as compared with batches No.2 and No.4. The exchange

Table 4.10 Mass Balances of the Reactions Between Activated CsF and UF_5 ^{18}F Under Heterogeneous Conditions.

Exp. No.	Batch. No.	CsF Initial (g) (mmol)	CsF Final (g)	Mass Increase of CsF (g)	Number of mmol. UF_6 corresponding to Mass Increase (mmol)	UF_6 (g) (mmol) Initial	UF_6 (g) (mmol) Final	Decrease of UF_6 (mmol)	Uptake mmol UF_6 / mmol CsF
1	2	0.2330 ±0.0030 1.53 ±0.02	0.3273 ±0.0030	0.0943 ±0.0060	0.27 ±0.04	0.5569 ±0.0030 1.58 ±0.01	0.4432 ±0.0030 1.26 ±0.01	0.32 ±0.02	0.17 ±0.05
2	3	0.3138 ±0.0030 2.07 ±0.02	0.4110 ±0.0030	0.0972 ±0.0060	0.28 ±0.04	0.4611 ±0.0030 1.31 ±0.01	0.3457 ±0.0030 0.98 ±0.01	0.33 ±0.02	0.14 ±0.05
3	3	0.2800 ±0.0030 1.84 ±0.02	0.3690 ±0.0030	0.0890 ±0.0060	0.25 ±0.04	0.4146 ±0.0030 1.18 ±0.01	0.3129 ±0.0030 0.89 ±0.01	0.29 ±0.02	0.14 ±0.05
4	4	0.2420 ±0.0030 1.59 ±0.02	0.3888 ±0.0030	0.1468 ±0.0060	0.42 ±0.04	0.5600 ±0.0030 1.59 ±0.01	0.3890 ±0.0030 1.11 ±0.01	0.48 ±0.02	0.26 ±0.05

Table 4.11 Radiochemical Balances of the Reactions Between Activated CsF and UF_5 ^{18}F Under Heterogeneous Conditions.

Exp. No.	Uptake of UF_6 from Mass Balance (mmol)	Count Rate of Reactants After Reaction (count min^{-1})		Specific Count Rate of UF_6 (count $min^{-1} mmol^{-1}$)		Radio-chemical Balance (%)
		CsF	UF_6	Initial	Final	
1	0.27 ±0.04	9656 ±98	45312 ±213	40608 ±372	35962 ±941	85
2	0.28 ±0.04	7400 ±86	25967 ±161	26733 ±376	26497 ±436	95
3	0.25 ±0.04	6717 ±82	23953 ±155	26733 ±376	26913 ±487	97
4	0.42 ±0.04	13429 ±116	35112 ±187	35746 ±469	32204 ±464	85

of [^{18}F]-fluorine was also observed during the reaction of inactive UF_6 and CsF which had been treated with $UF_5{}^{18}F$. [^{18}F]-Fluorine labelled UF_6 (1.59±0.01 mmol) was allowed to react with activated CsF (1.59±0.02 mmol) for 1h. After removal of excess volatile material an uptake corresponding to 0.42±0.01 mmol $UF_5{}^{18}F$ was observed producing a [^{18}F]-fluorine count rate of 13429±116 count min^{-1} (Table 4.12). Inactive UF_6 (0.65±0.01 mmol) was then admitted to the vessel containing $CsF.UF_5{}^{18}F$ and the reaction allowed to proceed for 0.5h. After separation of reactants these were assayed for [^{18}F]-fluorine activity. A decrease in the solid count rate was observed while the initially inactive UF_6 contained a [^{18}F]-fluorine activity equivalent to a count rate of 931±81 count min^{-1}. The transfer of [^{18}F]-fluorine activity was accounted for by an exchange between adsorbed $UF_5{}^{18}F$ and gaseous UF_6. A further uptake of UF_6 by $CsF.UF_5{}^{18}F$ was observed as shown by the increase in the mass of the solid after reaction together with a decrease in the amount of UF_6 (Table 4.12). Figures 4.8 and 4.9 represent the growth of [^{18}F]-fluorine activity in CsF with time during the reaction with $UF_5{}^{18}F$ for batches No.2 and No.4 respectively. These were obtained under similar conditions of specific count rate of $UF_5{}^{18}F$ and amount of CsF. The level of [^{18}F]-fluorine activity was significantly higher in the case of batch No.4 as compared with batch No.2 reflecting the difference in behaviour in terms of uptake of $UF_5{}^{18}F$ between the two batches.

Table 4.12 Reaction Between UF_6 and Activated CsF Treated with $UF_5{}^{18}F$. Summary of Results.

$CsF.UF_5{}^{18}F$ (g)		$CsF.UF_5{}^{18}F$ count rate$_{-1}$ (count min^{-1})		UF_6 (mmol)		UF_6 count rate$_{-1}$ (count min^{-1})
Initial	Final	Initial	Final	Initial	Final	
0.3888 ±0.0030	0.4053 ±0.0030	13429 ±116	13391 ±116	0.65 ±0.01	0.57 ±0.01	931 ±31

Figure 4.8 Heterogeneous Reaction Between Activated CsF and $UF_5{}^{18}F$ with Time

Ancillary conditions: CsF = 1.53±0.02mmol; $UF_5{}^{18}F$ = 1.58±0.01mmol

Specific count rate: 40608±372 count min^{-1} $mmol^{-1}$

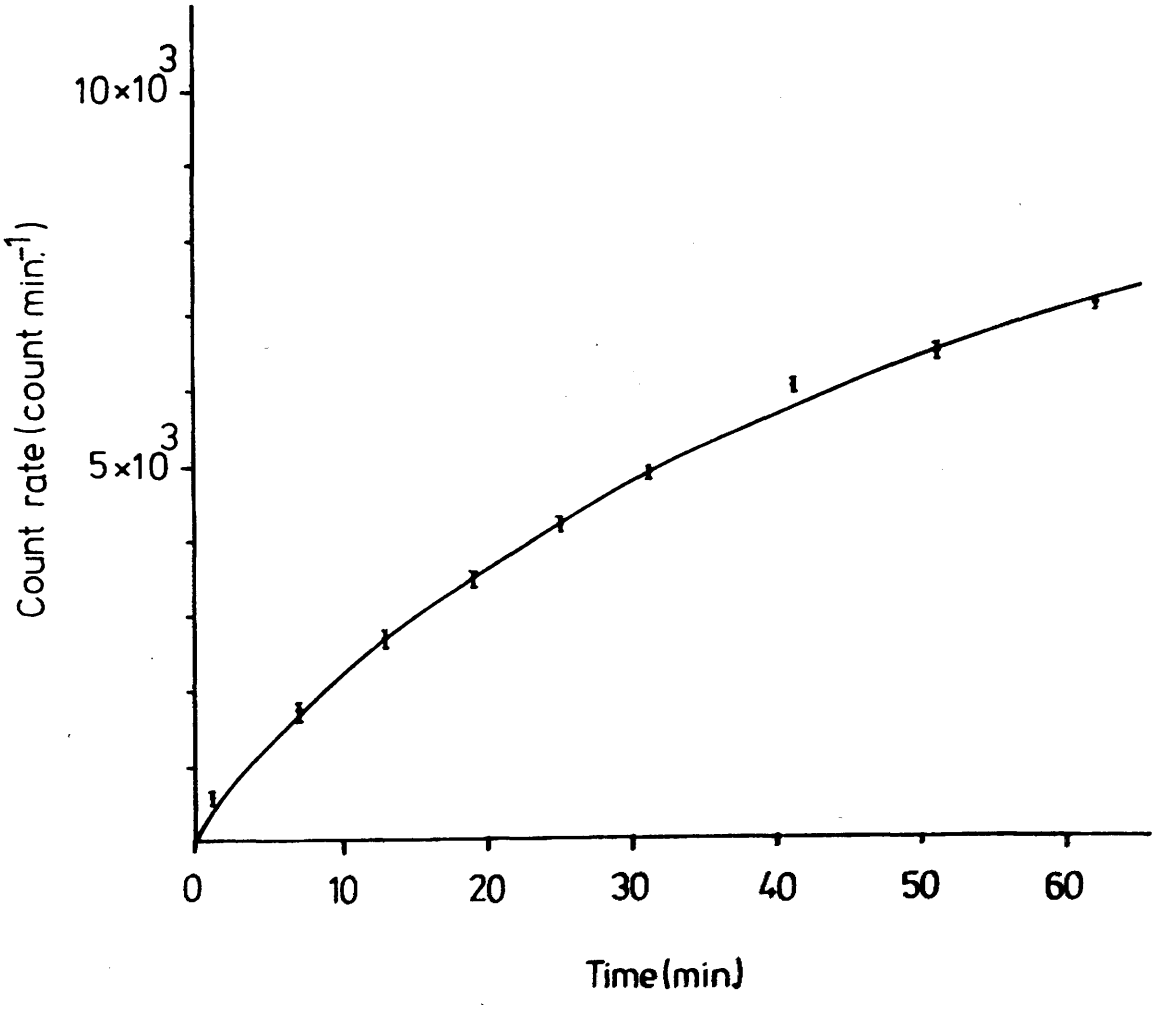

Figure 4.9 Heterogeneous Reaction Between Activated CsF and $UF_5{}^{18}F$ with Time.

Ancillary conditions: CsF = 1.59±0.02mmol; $UF_5{}^{18}F$ = 1.59±0.01mmol

Specific count rate: 35746±469 count min^{-1} $mmol^{-1}$

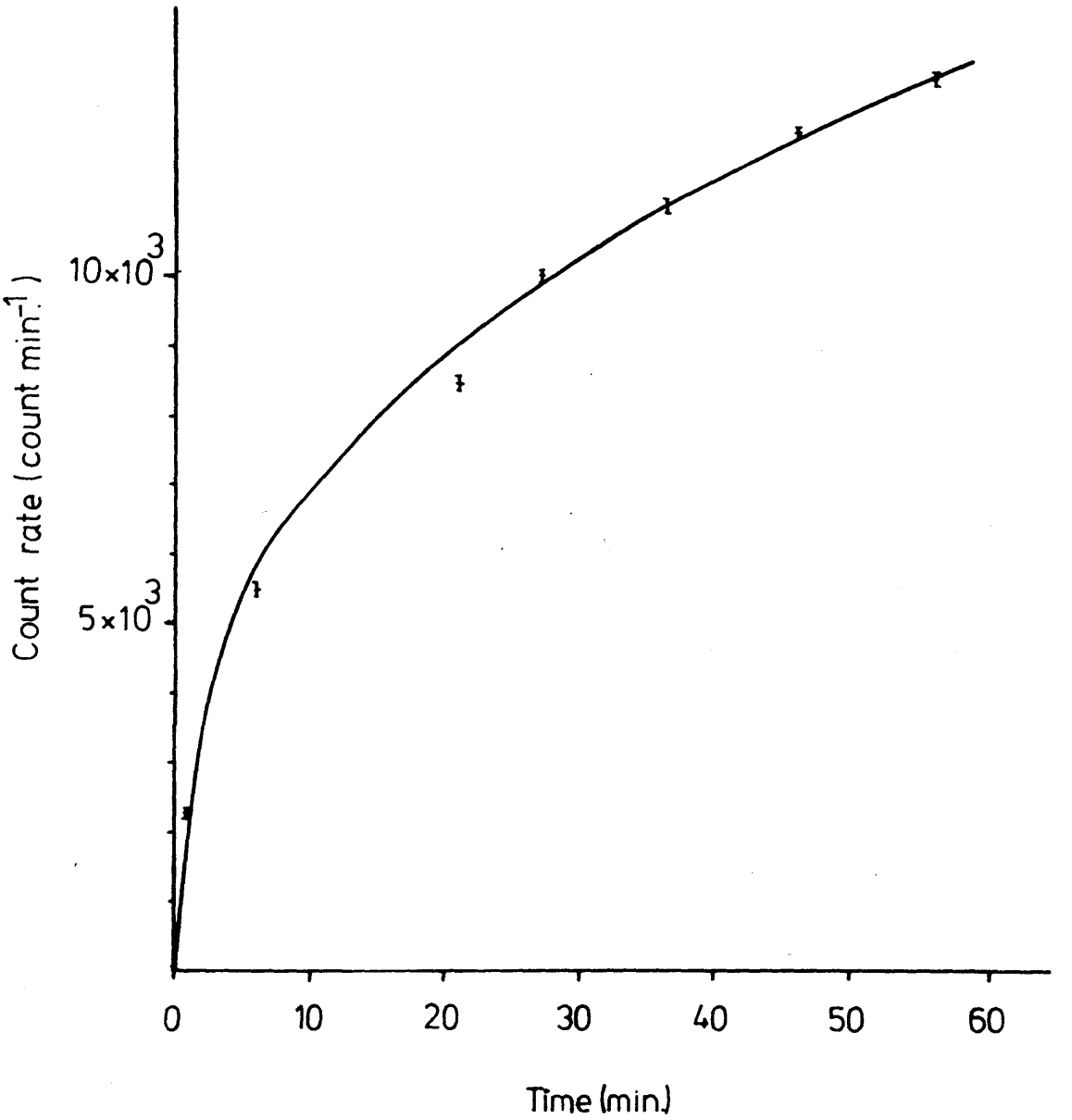

Furthermore the initial growth of [^{18}F]-fluorine activity was faster in the case of the former as compared with the latter indicating the greater and rapid uptake of $UF_5{}^{18}F$ in batch No.4. However in each case a continuous growth of [^{18}F]-fluorine activity was observed throughout the reaction. This was accounted for in terms of a slow exchange of [^{18}F]-fluorine between the adsorbed species and gaseous $UF_5{}^{18}F$.

The Raman spectra of CsF recorded after reaction with $UF_5{}^{18}F$ are presented in Table 4.13 together with the literature spectra of $CsUF_7$ and Cs_2UF_8 [30]. Figure 4.10 shows the Raman spectra of CsF batch No.3 (Figure 4.10(a))and batch No.4 (Figure 4.10 (b)) after reaction with $UF_5{}^{18}F$. Comparison of the spectra obtained in this work with those published suggest that more than one species had been formed. However in all cases bands in the region 582 - 591 cm^{-1} were in good agreement with the $\nu_1(A'_{1g})$ mode of UF_8^{2-} and the bands in the region 623 - 629 cm^{-1} were assigned to the $\nu_1(A'_1)$ mode of UF_7^-. The band at approximately 721 cm^{-1} was due to fluorescence. The weak bands around 540 cm^{-1} were assigned to fluorine bridged species although the region was higher than what was expected for such species [138].

4.6 Reaction Between Copper Difluoride and [^{18}F]-Fluorine Labelled Hexafluorides of Molybdenum, Tungsten and Uranium Under Heterogeneous Conditions.

The reactions between copper difluoride and [^{18}F]-

Table 4.13 Raman Spectra of CsF After Reaction with UF_6 Under Heterogeneous Conditions.

Batch No.	2	3	3	4	$CsUF_7$	Cs_2UF_8
Uptake mmol UF_6 / mmol CsF	0.20	0.14	0.13	0.27	Ref [30]	
					312 $\nu_{10}(E_1')$	321
						395
					444 $\nu_8(E_1')$	
	542 s		573 m	539 w		
	591m,sh	591vs, sh	587 w	582 vs		583
	629 w	631 m		623 w	622 $\nu_1(A_1')$	
	675 vs					
		721 s, br				

vs: very strong; s: strong; m: medium; w: weak;
sh: sharp; br: broad.

Figure 4.10 Raman Spectra of CsF After Reaction with UF_6 for Batch No. 3 (a) and No.4 (b)

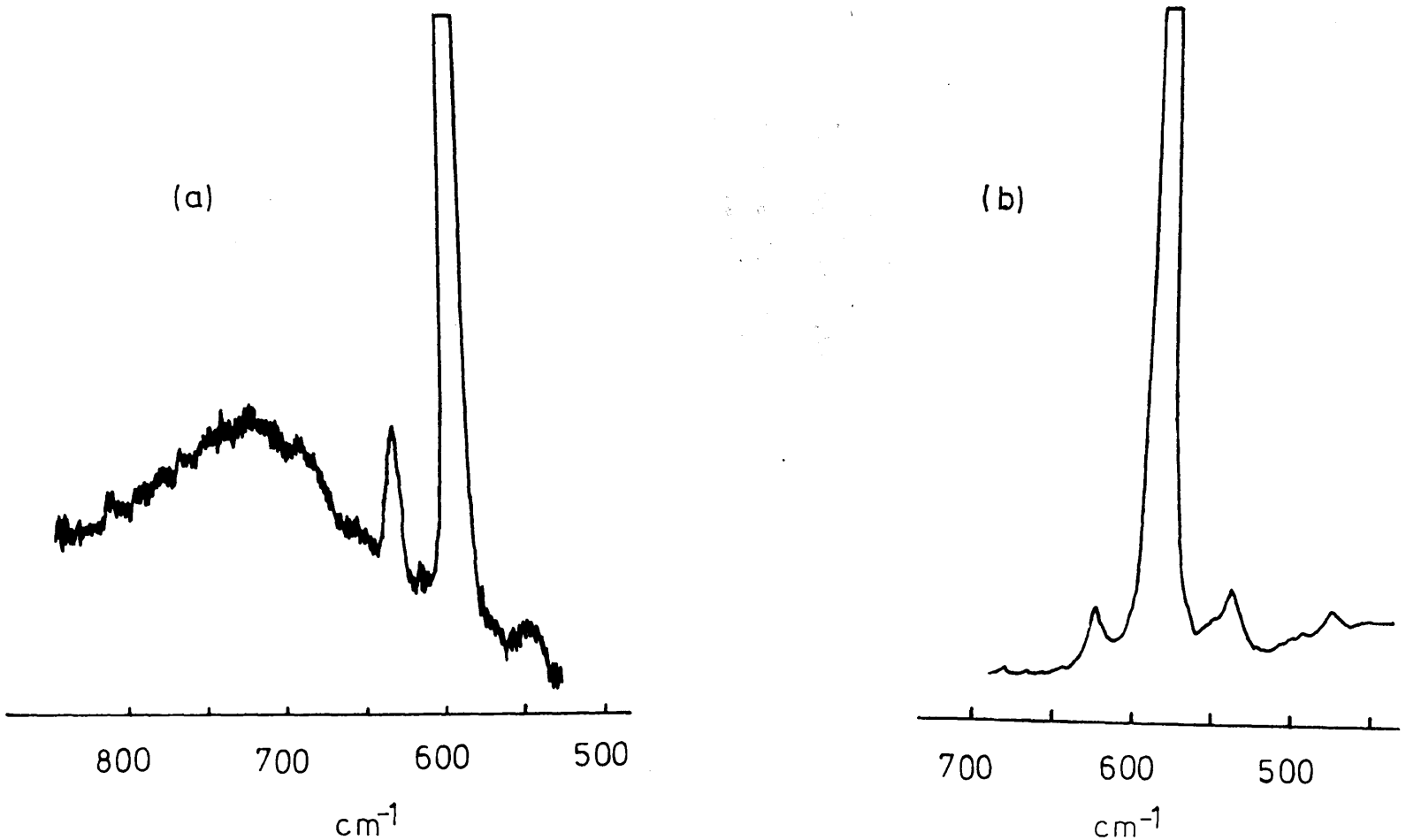

labelled hexafluorides of molybdenum tungsten and uranium under heterogeneous conditions at room temperature resulted in all cases in small uptakes of MF_6 (M = Mo, W or U) by CuF_2 after 1h. Furthermore a slight decrease in the specific count rate of $MF_5{}^{18}F$ (M = Mo or U) was observed indicating that an exchange of [^{18}F]-fluorine had occurred. The results of these reactions are presented in Tables 4.14 and 4.15. The mole ratios MF_6:CuF_2 (M = Mo, W or U) calculated from the uptakes were in the range (0.02-0.06)±0.05:1 for all the systems. The uptakes of MF_6 (M = Mo,W or U) by CuF_2 were also caluclated from the solid count rates. These were in the range (0.01 - 0.02)±0.02:1 for all the systems. These values were within the limits of sensitivity of the methods used. The growth of [^{18}F]-fluorine activity in CuF_2 with time is presented for $MoF_5{}^{18}F$, $WF_5{}^{18}F$ and $UF_5{}^{18}F$ in Figures 4.11, 4.12 and 4.13 respectively. In the case of $MoF_5{}^{18}F$ and $WF_5{}^{18}F$ the growth of [^{18}F]-fluorine activity followed a rapid increase initially then levelled off after approximately 30 minutes. However in the case of $UF_5{}^{18}F$ the [^{18}F]-fluorine activity followed a rapid increase over the first 10 minutes then a slower increase without reaching an equilibrium. This may be an indication of the greater extent of [^{18}F]-fluorine exchange in the latter case as compared with the two former. No satisfactory vibrational spectra of the solids after reaction were obtained although a colour change from blue to green was observed in the reaction between CuF_2 and UF_6.

Table 4.14 Mass Balances of the Reactions Between CuF_2 and $MF_5{}^{18}F$ (M = Mo,W,U) Under Heterogeneous Conditions.

Exp. No.	CuF_2 Initial (g) (mmol)	CuF_2 Final (g)	Mass Increase in CuF_2 (g)	MF_6	Number of mmol MF_6 Corresponding to Mass Increase (mmol)	MF_6 (mmol) Initial	MF_6 (mmol) Final	Decrease in MF_6 (mmol)	Uptake of MF_6 MF_6:CuF_2 mole ratio from mass balance	Uptake of MF_6 MF_6:CuF_2 mole ratio from solid count rate
1	0.4749 ±0.0030 4.68 ±0.030	0.5013 ±0.0030	0.0264 ±0.0060	MoF_6	0.13 ±0.03	0.1993 ±0.0030 0.95 ±0.02	0.1741 ±0.0030 0.83 ±0.02	0.12 ±0.04	0.03 ±0.05	0.02 ±0.02
2	0.3947 ±0.0030 3.89 ±0.030	0.4139 ±0.0030	0.0192 ±0.0060	MoF_6	0.09 ±0.08	0.1040 ±0.0030 0.50 ±0.02	0.0788 ±0.0030 0.38 ±0.02	0.12 ±0.03	0.02 ±0.05	0.02 ±0.02
3	0.0863 ±0.0030 0.85 ±0.03	0.1024 ±0.0030	0.0161 ±0.0060	WF_6	0.05 ±0.02	0.2291 ±0.0030 0.77 ±0.01	0.1918 ±0.0030 0.64 ±0.01	0.13 ±0.02	0.06 ±0.05	0.01 ±0.02
4	0.1092 ±0.0030 1.07 ±0.003	0.1157 ±0.0030	0.0060 ±0.0060	WF_6	0.02 ±0.02	0.4323 ±0.0030 1.45 ±0.01	0.4188 ±0.0030 1.41 ±0.01	0.05 ±0.02	0.03 ±0.05	0.01 ±0.02
5	0.1426 ±0.0030 1.41 ±0.030	0.1529 ±0.0030	0.0103 ±0.0060	UF_6	0.03 ±0.02	0.2334 ±0.0030 0.66 ±0.01	0.2211 ±0.0030 0.63 ±0.01	0.03 ±0.02	0.02 ±0.05	0.01 ±0.02

Table 4.15 Radiochemical Balances of the Reactions Between CuF_2 and $MF_5{}^{18}F$ (M = Mo, W or U) Under Heterogeneous Conditions.

Exp. No.	Uptake of MF_6 from mass Balance (mmol)	Count rate of Reactants After Reaction (count min^{-1})		Specific count Rate of MF_6 (count min^{-1} $mmol^{-1}$)		Radio-chemical Balance (%)
		CuF_2	MF_6	Initial	Final	
1	0.13 ±0.03	4871 ±70	39151 ±198	50846 ±884	47227 ±882	91
2	0.09 ±0.03	6587 ±81	27283 ±165	76025 ±1053	72755 ±2943	90
3	0.05 ±0.02	494 ±22	55648 ±286	84014 ±1402	86410 ±2282	103
4	0.02 ±0.02	183 ±14	51986 ±228	36531 ±303	36979 ±309	98
5	0.03 ±0.02	637 ±25	38650 ±197	63718 ±810	61544 ±752	94

Figure 4.11 Heterogeneous Reaction Between CuF_2 and MoF_5 ^{18}F with Time.

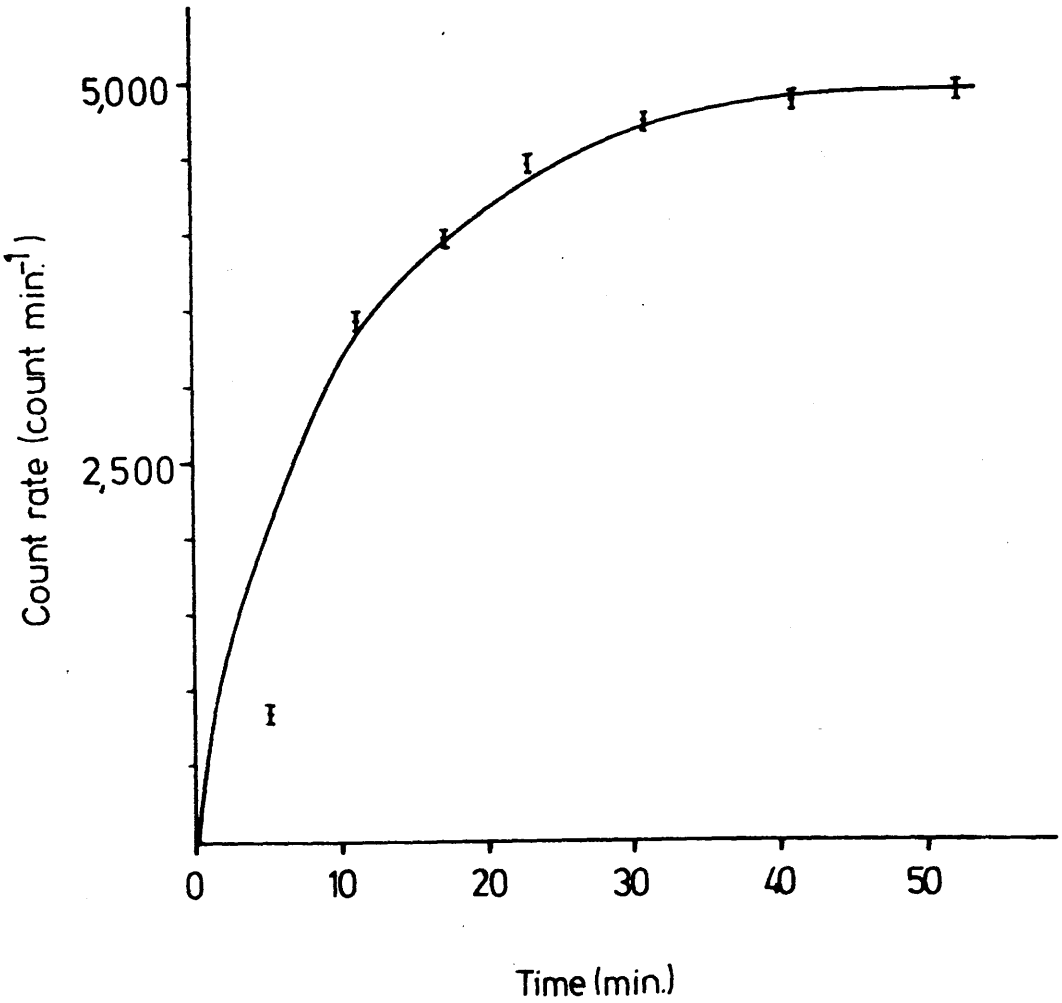

Figure 4.12 Heterogeneous Reaction Between CuF_2 and WF_5 ^{18}F with Time

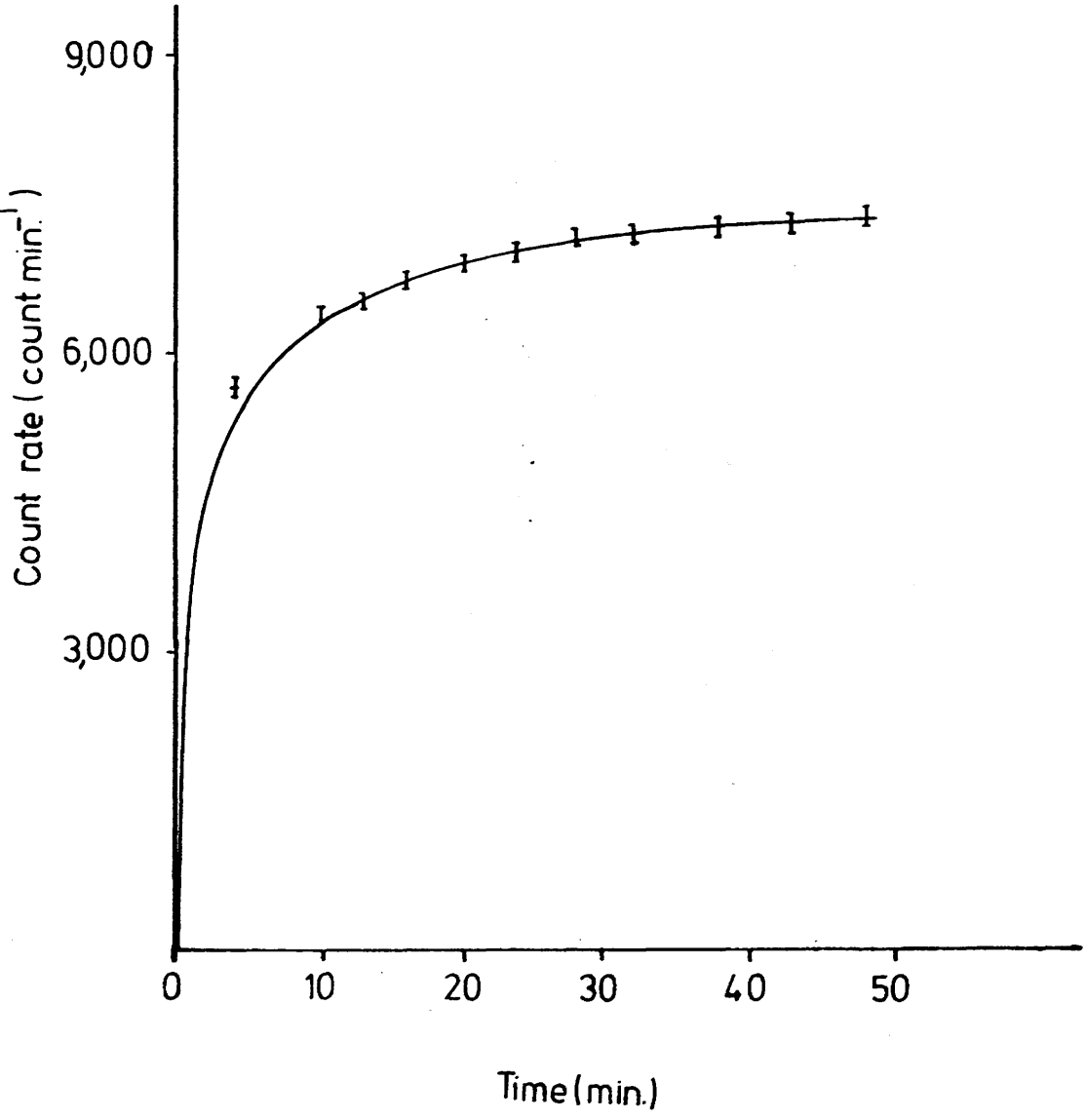

Figure 4.13 Heterogeneous Reaction Between CuF_2 and $UF_5{}^{18}F$ with Time.

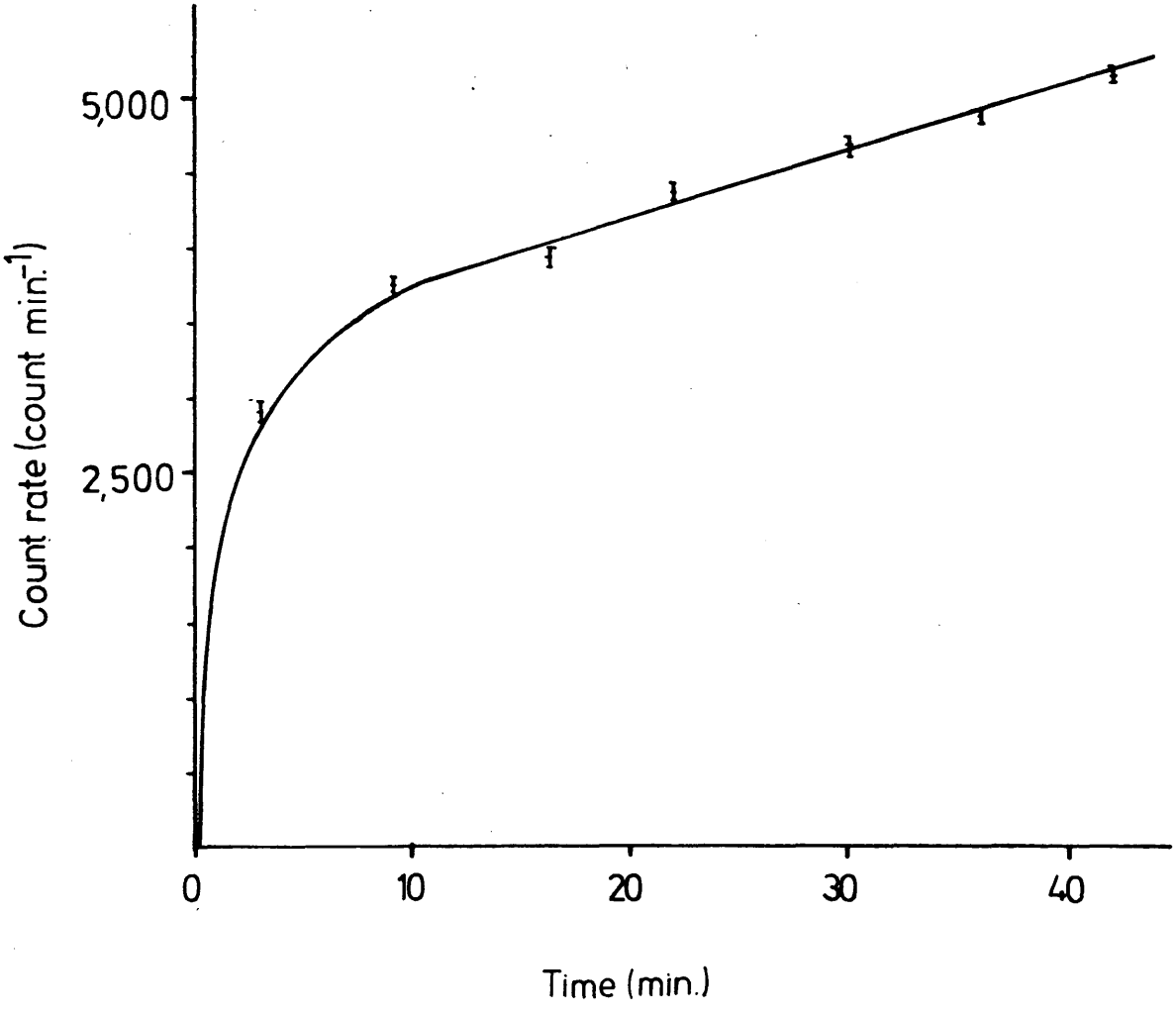

However this might be due to traces of hydrolysis in CuF_2.

4.7 Reaction Between Thallium Fluoride and [^{18}F]-Fluorine Labelled Hexafluorides of Molybdenum, Tungsten and Uranium Under Heterogeneous Conditions.

Admission of [^{18}F]-labelled hexafluorides of molybdenum, tungsten and uranium to thallium fluoride under heterogeneous conditions at room temperature resulted in all cases in an increase in the mass of TlF after 1h indicating that some of the hexafluorides had been adsorbed by the solid. Furthermore a decrease in the specific count rate of $MF_5{}^{18}F$ (M = Mo or U) was observed indicating that an exchange of [^{18}F]-fluorine had occurred between the solid and gaseous $MF_5{}^{18}F$ (M = Mo or U). The results of these reactions are presented in Tables 4.16 and 4.17. The mole ratio MF_6:TlF (M = W or U) calculated from the uptakes were in the range (0.02 - 0.05)±0.05:1. That for MoF_6 was in the range (0.07 - 0.22)±0.05:1. The difference in uptakes among the hexafluorides suggested that the affinity of TlF is greater for MoF_6 as compared with WF_6 or UF_6. Figures 4.14, 4.15 and 4.16 represent the growth of [^{18}F]-fluorine activity in TlF with time during the reaction with $MoF_5{}^{18}F$, $WF_5{}^{18}F$ and $UF_5{}^{18}F$ respectviely. Although these relationships were obtained under different conditions of specific count rates of $MF_5{}^{18}F$ (M = Mo, W or U) and amount of TlF qualitative information can be drawn from their shapes. The greater uptake of MoF_6

Table 4.16 Mass Balances of the Reactions Between TlF and MF_5 ^{18}F (M = Mo,W,U) Under Heterogeneous Conditions.

Exp. No.	TlF		Mass Increase in TlF (g)	MF_6	Number of mmol MF_6 Corresponding to Mass Increase (mmol)	MF_6 (mmol)		Decrease in MF_6 (mmol)	Uptake of MF_6 MF_6:TlF mole ratio	
	Initial (g) (mmol)	Final (g)				Initial	Final		from mass balance	from solid count rate
1	1.3698 ±0.0030 6.13 ±0.01	1.4565 ±0.0030	0.0867 ±0.0060	MoF_6	0.41 ±0.03	0.1390 ±0.0030 0.66 ±0.02	0.0491 ±0.0030 0.23 ±0.02	0.43 ±0.04	0.07 ±0.05	0.07 ±0.02
2	1.2415 ±0.0030 5.56 ±0.01	1.3764 ±0.0030	0.1349 ±0.0060	MoF_6	0.64 ±0.03	0.3165 ±0.0030 1.51 ±0.02	0.1697 ±0.0030 0.81 ±0.02	0.70 ±0.04	0.12 ±0.05	0.10 ±0.02
3	0.5461 ±0.0030 2.44 ±0.01	0.6582 ±0.0030	0.1121 ±0.0060	MoF_6	0.53 ±0.03	0.2358 ±0.0030 1.12 ±0.02	0.1109 ±0.0030 0.53 ±0.02	0.59 ±0.04	0.22 ±0.05	0.15 ±0.02
4	0.3969 ±0.0030 1.78 ±0.01	0.4200 ±0.0030	0.0231 ±0.0060	WF_6	0.08 ±0.02	1.0230 ±0.0030 3.43 ±0.01	0.9977 ±0.0030 3.35 ±0.01	0.08 ±0.02	0.04 ±0.05	0.05 ±0.02
5	0.5595 ±0.0030 2.50 ±0.01	0.5737 ±0.0030	0.0142 ±0.0060	WF_6	0.05 ±0.02	0.1129 ±0.0030 0.38 ±0.01	0.0885 ±0.0030 0.30 ±0.01	0.08 ±0.02	0.02 ±0.05	0.02 ±0.02
6	0.9348 ±0.0030 4.18 ±0.01	1.0016 ±0.0030	0.0668 ±0.0060	UF_6	0.19 ±0.02	0.1668 ±0.0030 0.47 ±0.01	0.0933 ±0.0030 0.27 ±0.01	0.20 ±0.02	0.05 ±0.05	0.05 ±0.02
7	0.7225 ±0.0030 3.23 ±0.01	0.7615 ±0.0030	0.0390 ±0.006	UF_6	0.11 ±0.02	0.2355 ±0.0030 0.67 ±0.01	0.1936 ±0.0030 0.55 ±0.01	0.12 ±0.02	0.03 ±0.05	0.04 ±0.02

Table 4.17 Radiochemical Balances of the Reactions Between TlF and $MF_5{}^{18}F$ (M = Mo,W, or U) Under Heterogeneous Conditions.

Exp. No.	Uptake of MF_6 from mass Balance (mmol)	Count rate of Reactants After Reaction (count min^{-1})		Specific count Rate of MF_6 (count min^{-1} $mmol^{-1}$)		Radio-chemical Balance (%)
		TlF	MF_6	Initial	Final	
1	0.41 ±0.03	15409 ±124	8011 ±90	34445 ±438	34830 ±2228	104
2	0.64 ±0.03	44640 ±211	53383 ±231	76566 ±2655	65905 ±1259	85
3	0.53 ±0.03	48438 ±220	68538 ±262	133744 ±1898	129317 ±3721	81
4	0.08 ±0.02	410 ±20	17790 ±133	5020 ±123	5310 ±43	106
5	0.05 ±0.02	15311 ±124	83370 ±289	262367 ±8884	277900 ±9501	99
6	0.19 ±0.02	15217 ±123	19652 ±140	76939 ±949	72785 ±2955	96
7	0.11 ±0.02	7764 ±88	34234 ±185	63718 ±1107	62244 ±1181	99

Figure 4.14 Heterogeneous Reaction Between TlF and MoF_5 ^{18}F with Time.

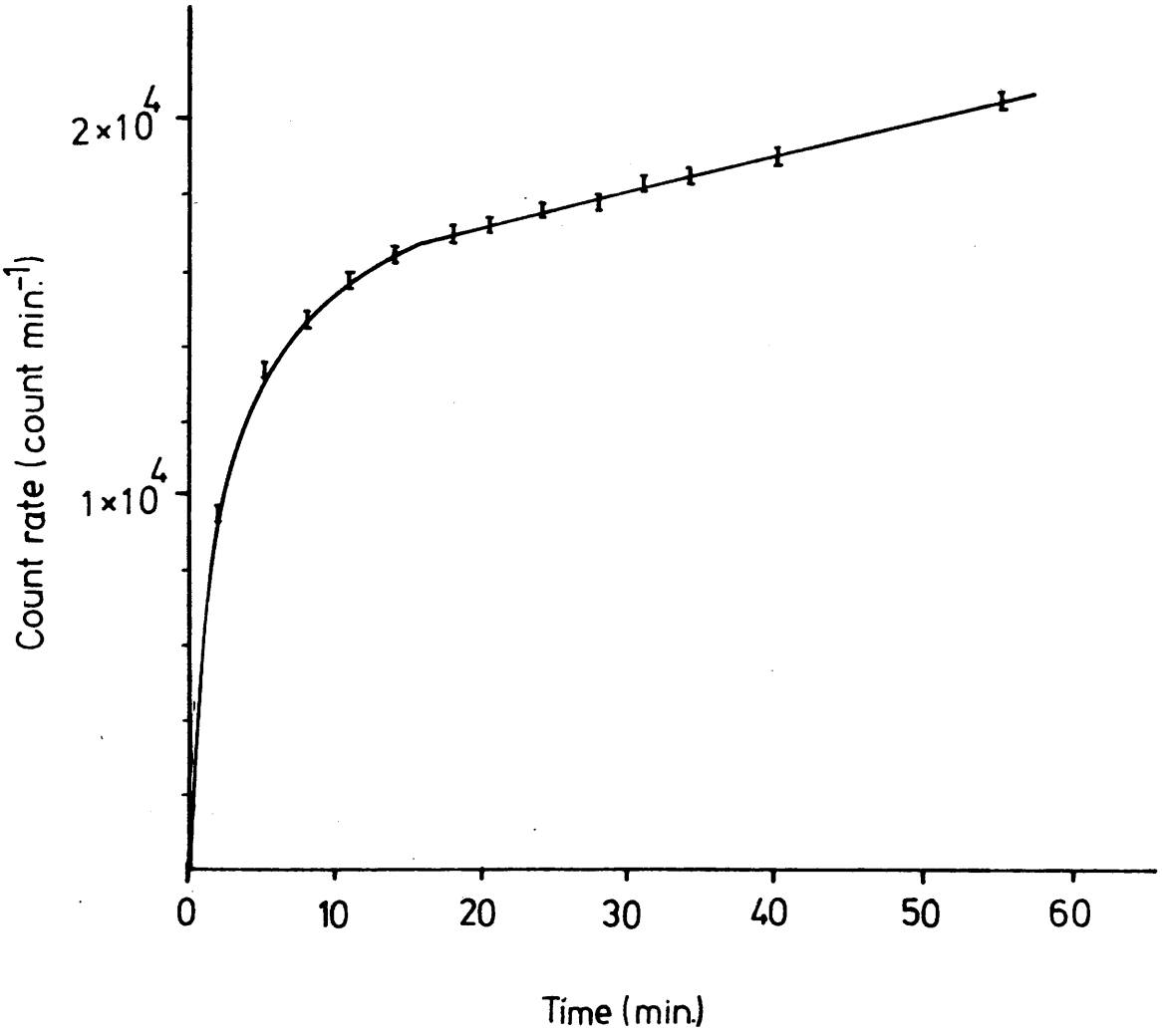

Figure 4.15 Heterogeneous Reaction Between TlF and WF_5 ^{18}F with Time.

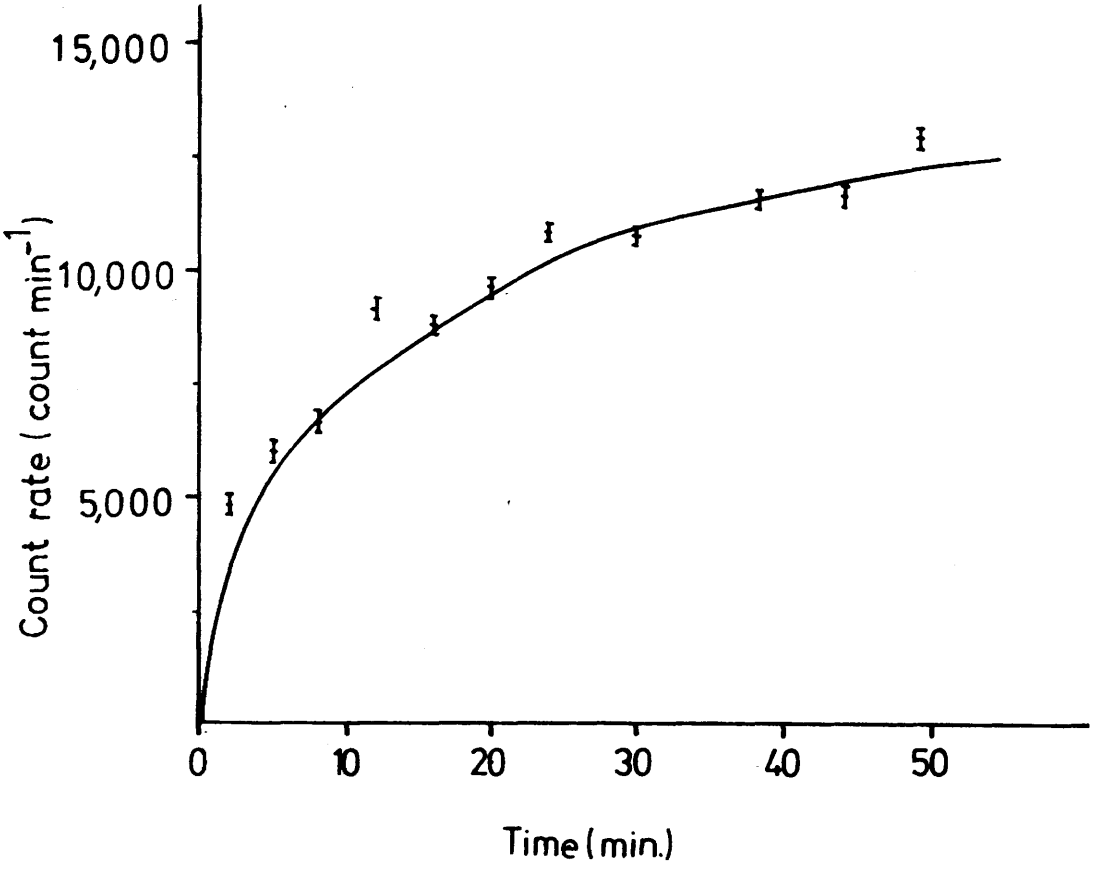

Figure 4.16 Heterogeneous Reaction Between TlF and UF_5 ^{18}F with Time.

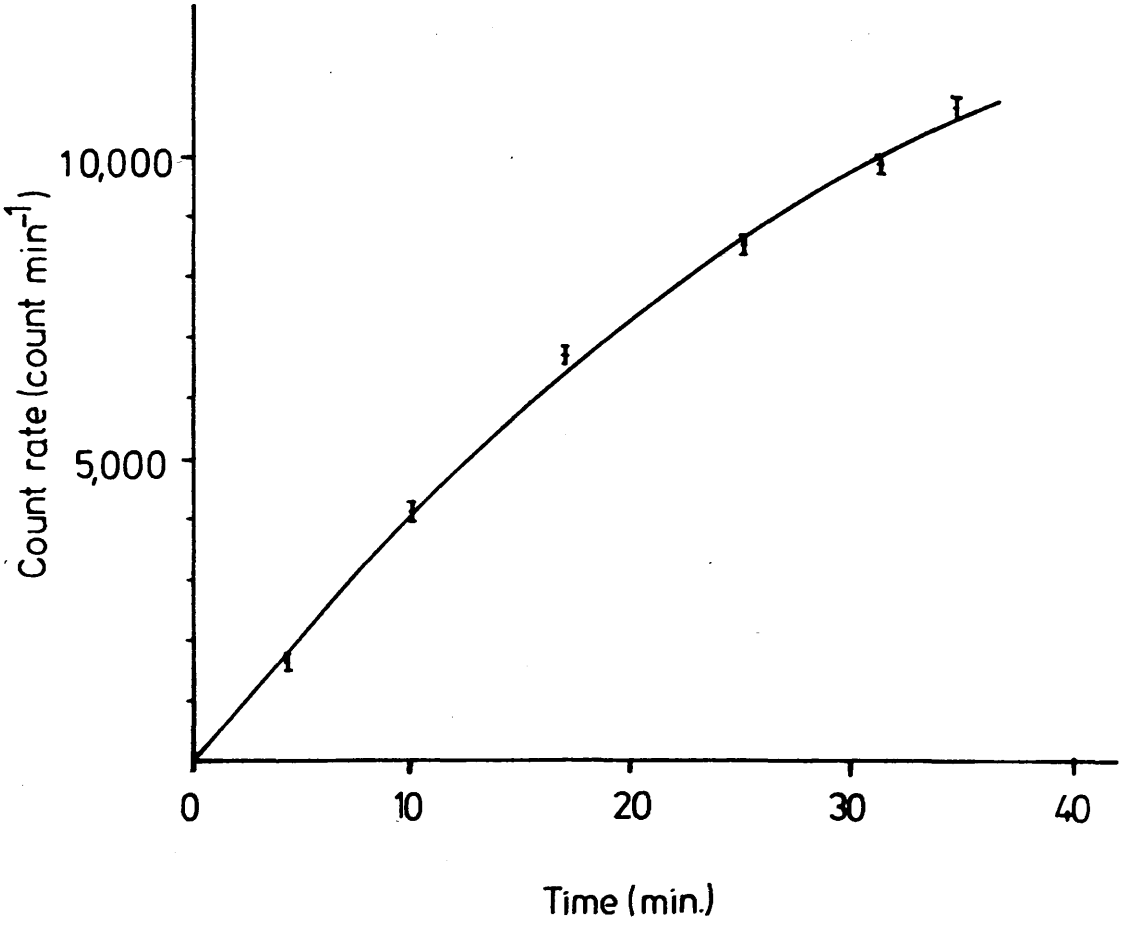

by TlF was reflected by the growth of [^{18}F]-fluorine activity which was rapid as compared with WF_6 or UF_6. Furthermore in the later stage of the reactions the growth of [^{18}F]-fluorine activity tended towards an equilibrium in the case of WF_6 while in the case of MoF_6 or UF_6 a steady growth was observed. This was an indication of the relatively greater extent of [^{18}F]-fluorine exchange in the case of the two latter as compared with the former. No satisfactory vibrational spectra of the solids after reaction were obtained. However a colour change from white to brown together with a sintering of the solid was observed during the reaction with MoF_6. This might be the result of some chemical reaction between the reactants.

CHAPTER FIVE

REACTIONS BETWEEN THE FLUOROANIONS OF BORON, PHOSPHORUS, ARSENIC, ANTIMONY, NIOBIUM AND TANTALUM AND [^{18}F]-FLUORINE LABELLED HEXAFLUORIDES OF MOLYBDENUM, TUNGSTEN AND URANIUM IN ACETONITRILE.

5. Reactions Between the Fluoroanions of Boron, Phosphorus Arsenic, Antimony, Niobium and Tantalum and [^{18}F]-Fluorine Labelled Hexafluorides of Molybdenum, Tungsten and Uranium in Acetonitrile.

5.1 Introduction

The fluoroanions of the main group elements are widely used as counter-anions in synthetic [142] and electrochemical studies [59]. These fluoroanions are regarded as chemically inert. However there are indications in the literature which suggest that this is not always the case. For example, using ^{19}F and ^{195}Pt n.m.r. spectroscopy, Cole-Hamilton et. al. [143] have demonstrated that the lability of water in aquatris(triethylphosphine) platinum(II) hexafluorophosphate, $[Pt(H_2O)(PEt_3)_3][PF_6]_2$, occurs in acetone by abstraction of a fluoride from the hexafluorophosphate ion to give fluorotris(triethylphosphine) platinum(II) cation, $[PtF(PEt_3)_3]^+$. In another example Wimmer and Snow [144] have shown that reaction between manganese pentacarbonyl halide, $Mn(CO)_5X$, or manganese tricarbonyl halide, $Mn(CO)_3L_2X$, (X = Br, L = PPh_3, $P(OPh)_3$, L_2 = 2,2'-bipyridyl) and hexafluorophosphate ion in dichloromethane results in the hydrolysis of the latter to give difluorophosphate complexes in which $PO_2F_2^-$ behaves as mono- or bi-dentate ligand. Clark and Jones [145] have shown that the B-F, P-F and As-F bond in BF_4^-, PF_6^-

and AsF_6^- respectively is hydrolysed under acidic conditions (pH2) in the presence of some hard acids such as Be(II), Al(III), Zr(IV) and Th(IV). The latter act as catalysts in the reaction. Abstraction of fluoride ion in BF_4^- has been shown to occur by Bassindale and Stout [146]. In their attempt to prepare trimethylsilyltetrafluoroborate, Me_3SiBF_4, by reaction between trimethylsilylchloride, Me_3SiCl, and silver tetrafluoroborate, $AgBF_4$, in acetonitrile or acetone the authors have obtained instead trimethylfluorosilane, Me_3SiF, and weakly coordinated boron trifluoride, equations (5.1) and (5.2).

$$Me_3SiCl + AgBF_4 \xrightarrow{MeCN} Me_3SiF + BF_3.NCMe \qquad (5.1)$$

$$Me_3SiCl + AgBF_4 \xrightarrow{Me_2CO} Me_3SiF + BF_3.OCMe_2 \qquad (5.2)$$

Although these examples can be accounted for on thermodynamic grounds they all involve nevertheless bond breaking in the anion. A more convincing piece of evidence for the fluorine bond lability of the fluoroanions is due to Dixon and Winfield [5]. These authors have used [^{18}F]-fluorine as radiotracer to show that the B-F bond in BF_4^- is labile with respect to exchange in the presence of [^{18}F]-labelled boron trifluoride under homogeneous (MeCN) conditions. Fluorine bridged species $B_2F_7^-$ is thought to be the intermediate in the exchange process.

The oxidising properties of the hexafluorides of molybdenum, tungsten and uranium is the subject of an extensive study in this department. Cyclic voltametry is one of the methods of investigation used. This technique employs the fluoroanions of the main group elements as counter-anions of supporting electrolytes. The aim of the work presented in this chapter was to investigate systematically the fluorine bond lability of some fluoroanions of groups VA and VB in the presence of MF_6 (M = Mo,W and U) under homogeneous (MeCN) conditions. The fluoroanions under investigation were those of B, P, As, Sb, Nb and Ta. Radiotracer technique using [^{18}F]-fluorine as the radiotracer was the main technique of investigation used.

5.2 Experimental.

The reactions between the fluoroanions of boron, phosphorus, arsenic, antimony, niobium, tantalum as well as the acetonitrile adduct of arsenic, antimony and niobium and [^{18}F]-labelled hexafluorides of molybdenum, tungsten and uranium were carried out according to the procedure described in Sections 2.12.1 and 2.12.2 using a single or a double limb vessel. In the latter case the mass balances of the reactants were considered to be 100%. This was a reasonable assumption as the reactants were separated within the close system of the double limb vessel. The fluoroanions under investigation were used as their lithium salts except for NbF_6^- which was used as $[Cu(NCMe)_5][NbF_6]_2$.

These were prepared as described in Sections 2.2.9 to 2.2.12 and Sections 2.2.14 and 2.2.15. [^{18}F]-Fluorine labelled hexafluorides were prepared as described in Section 2.13.2. The lithium salts were extremely soluble in MeCN and their separation required prolonged vacuum distillation of the solvent. However in view of the half life of [^{18}F]-fluorine ($t_{\frac{1}{2}}$ = 110 min. [129]) distillation of the solvent was carried out over shorter periods, consequently good separation was not achieved. This resulted in an increase in the mass of these salts after reaction.

5.3 Reaction Between Lithium Tetrafluoroborate and [^{18}F]-Fluorine Labelled Hexafluorides of Molybdenum, Tungsten and Uranium in Acetonitrile.

The reaction between lithium tetrafluoroborate in the range 0.86 - 1.21 ± 0.02 mmol, and [^{18}F]-labelled hexafluorides of molybdenum, tungsten and uranium, in the range 0.40 - 1.08 ± 0.02 mmol, was carried out in acetonitrile (1 cm^3) for 20 minutes. A summary of the results is presented in Table 5.1. The reaction resulted in all cases in a transfer of [^{18}F]-fluorine activity from $MF_5{}^{18}F$ (M = Mo, W, U) to $LiBF_4$ and a decrease in the specific count rate of the hexafluorides. This was consistent with a [^{18}F]-fluorine exchange taking place between the reactants. Using equation (2.7) the exchange was found to be complete in all cases (f = 1). The radiochemical balances and the

Table 5.1 Reactions Between $LiBF_4$ and $MF_5{}^{18}F$ (M = Mo,W,U) in MeCN. Summary of Results.

$LiBF_4$ (mmol)		MF_6	(mmol)		Specific count rate of $MF_5{}^{18}F$ (count min^{-1} $mmol^{-1}$)		Count rate of Reacts after Reaction (count min^{-1})		Radio-chemical Balance	Fraction Exchanged
Initial	Final		Initial	Final	Initial	Final	MF_6	$LiBF_4$	(%)	
1.02 ±0.03	1.17 ±0.03	MoF_6	0.82 ±0.02	0.80 ±0.02	26170 ±451	15004 ±277	12003 ±137	11218 ±121	106	0.94 ±0.07
1.16 ±0.03	1.33 ±0.03	WF_6	1.08 ±0.01	1.06 ±0.01	29701 ±487	18328 ±307	19428 ±139	16184 ±127	110	0.92 ±0.10
0.86 ±0.03	1.07 ±0.03	WF_6	0.50 ±0.10	0.47 ±0.01	27692 ±974	12611 ±433	5927 ±77	8886 ±94	107	1.02 ±0.06
0.90 ±0.03	1.00 ±0.03	UF_6	0.55 ±0.01	0.53 ±0.01	99478 ±1832	46272 ±935	24524 ±157	31677 ±178	108	1.02 ±0.05
1.21 ±0.03	1.35 ±0.03	UF_6	0.40 ±0.01	0.38 ±0.01	84275 ±2215	26397 ±728	10031 ±100	24560 ±157	103	1.03 ±0.05

mass balances of the hexafluorides were in all cases $\geqslant$ 95%. Furthermore no chemical reaction between $LiBF_4$ and MF_6 (M = Mo, W, U) was observed as the infrared spectra of $LiBF_4$ recorded before and after reactions were identical. In view of these indications the reaction between BF_4^- and $MF_5{}^{18}F$ (M = Mo, W, U) can be represented by equation (5.3)

$$BF_4^- + MF_5{}^{18}F \longrightarrow BF_3{}^{18}F^- + MF_5{}^{18}F \qquad (5.3)$$

In order to elucidate the mechanism of [^{18}F]-fluorine exchange between BF_4^- and $MF_5{}^{18}F$ the reaction between MF_7^- and BF_3 was an obvious one to investigate. A reaction between $CsWF_7$ (0.875 mmol) and BF_3 (0.520 mmol) in MeCN was shown by vibrational spectroscopy to lead to the formation of BF_4^- and WF_6. The Raman solution spectrum of the reaction contained bands at ν_{max} 775 and 712 cm^{-1} which were assigned to ν_1 (A_{1g}) mode of WF_6 and ν_1 (A_1') mode of WF_7^- respectively. This was consistent with the displacement of WF_6 from WF_7^- by BF_3. It was not possible to detect bands due to BF_4^-. However the infrared spectrum of the solid product of the reaction (Table 5.2) contained bands at ν_{max} 1100-1035 vs,br, 773 s, 530 m,sh and 520 m,sh cm^{-1} which were assigned to ν_3 (F_2), ν_1(A_1) and ν_4(F_2) modes of BF_4^- respectively [117]. The band at 630 vs, cm^{-1} was assigned to ν_3 (A_2'') mode of WF_7^- [28]. On the basis of the vibrational spectra the reaction between WF_7^- and BF_3 can be represented by equation (5.4)

$$WF_7^- + BF_3 \longrightarrow WF_6 + BF_4^- \qquad (5.4)$$

Table 5.2 : Infrared Spectrum of the Solid Product of the Reaction Between BF_3 and $CsWF_7$ in MeCN.

ν_{max} (cm^{-1})	Assignment [117, 28]
1100 - 1035 vs, br	$\nu_3(F_2)$ BF_4^-
773 (s)	$\nu_1(A_1)$ BF_4^-
720 (m)	?
705 (m)	?
630 (vs)	$\nu_3(A''_{2u})$ WF_7^-
530 (m, sh)	$\nu_4(F_2)$ BF_4^-
520 (m, sh)	

vs : very strong, s : strong, m : medium,
br : broad, sh : sharp.

5.4 Reaction Between Lithium Hexafluorophosphate and [^{18}F]-Fluorine Labelled Hexafluorides of Molybdenum, Tungsten and Uranium in Acetonitrile.

Admission of [^{18}F]-labelled hexafluorides of molybdenum, tungsten and uranium in the range 0.39 - 1.22 ± 0.02 mmol to lithium hexafluorophosphate $LiPF_6$, in the range 0.41 - 0.62 ± 0.02 mmol dissolved in MeCN (1 cm^3) resulted in all cases in a transfer of [^{18}F]-fluorine activity from $MF_5{}^{18}F$ (M = Mo, W, U) to $LiPF_6$ and a decrease in the specific count rate of the hexafluorides after 20 minutes of contact (Table 5.3) This was consistent with a [^{18}F]-fluorine exchange taking place between the reactants. Using equation (2.8) the exchange was found to be complete in all cases (f = 1). The mass and radiochemical balances were ⩾ 95% in all cases. There was no evidence for chemical reaction taking place between $LiPF_6$ and MF_6 (M = Mo, W, U) as the infrared spectra of the former recorded before and after mixing were identical.

The transfer of [^{18}F]-fluorine activity was also shown qualitatively to take place between WF_6 and [^{18}F]-labelled $LiPF_6$. The latter was prepared following the procedure described in Section 2.13.4 and dissolved in MeCN (1 cm^3). Inactive WF_6 (0.70 mmol) was admitted to $LiPF_5{}^{18}F$. After separation of reactants WF_6 was radioactive with a specific count rate of 68327 ± 1021 count min^{-1} $mmol^{-1}$. In a separate experiment [^{18}F]-fluorine

Table 5.3 Reactions Between $LiPF_6$ and $MF_5{}^{18}F$ (M = Mo,W,U) in MeCN. Summary of Results.

$LiPF_6$ (mmol)		MF_6	(mmol)		Specific count rate of $MF_5{}^{18}F$ (count min^{-1} $mmol^{-1}$)		Count rate of Reacts. After Reaction (count min^{-1})		Radio-chemical Balance	Fraction Exchanged
Inital	Final		Initial	Final	Initial	Final	MF_6	$LiPF_6$	(%)	
0.62 ±0.02	0.62 ±0.02	MoF_6	0.65 ±0.02	0.65 ±0.02	20204 ±760	9425 ±365	6126 ±78	7277 ±85	102	1.04 ±0.10
0.41 ±0.02	0.43 ±0.02	WF_6	0.25 ±0.01	0.23 ±0.01	50714 ±1863	19883 ±140	4573 ±77	8730 ±93	106	0.99 ±0.10
0.41 ±0.02	0.44 ±0.02	WF_6	0.59 ±0.01	0.53 ±0.01	60504 ±2295	35617 ±1176	18877 ±137	15774 ±125	98	0.99 ±0.10
0.42 ±0.02	0.44 ±0.02	UF_6	0.39 ±0.01	0.39 ±0.01	127141 ±4849	71574 ±2744	27914 ±167	24631 ±157	106	0.92 ±0.10
0.42 ±0.02	0.42 ±0.02	UF_6	1.22 ±0.01	1.22 ±0.01	52230 ±578	37639 ±497	45920 ±214	16402 ±128	98	1.09 ±0.10

exchange was found to be complete after 20 minutes contact between MoF_6 and [^{18}F]-labelled nitrosonium hexafluorophosphate, $NOPF_5{}^{18}F$, in MeCN. [^{18}F]-Fluorine labelled $NOPF_6$ was prepared *in situ* by reaction between FNO and $PF_4{}^{18}F$ (Section 2.13.4). A summary of the results of this reaction is presented in Table 5.4. The results described so far allow the reactions between PF_6^- and MF_6 (M = Mo, W, U) to be written as (Equations (5.5) and (5.6).

$$PF_6^- + MF_5{}^{18}F \longrightarrow PF_5{}^{18}F^- + MF_5{}^{18}F \qquad (5.5)$$

$$PF_5{}^{18}F^- + MF_6 \longrightarrow PF_5{}^{18}F^- + MF_5{}^{18}F \qquad (5.6)$$

In view of these results the reaction between WF_7^- and PF_5 was investigated. A mixture of $CsWF_7$ (0.75 mmol) and PF_5 (0.86 mmol) was allowed to react in MeCN. The Raman spectrum of the solution and the infrared spectrum of the solid product were then recorded. These are presented in Figure 5.1 and Table 5.5 respectively. The Raman band at ν_{max} 775 cm^{-1} was assigned to ν_1 (A_{1g}) mode of WF_6 while those at 746 and 708 cm^{-1} were assigned to $\nu_1(A_{1g})$ and ν_1 (A_1') mode of PF_6^- and WF_7^- respectively. The infrared bands at ν_{max} 830 and 560 were assigned to $\nu_3(F_{1u})$ and $\nu_4(F_{1u})$ modes of PF_6^-. No bands due to WF_7^- were observed in the infrared spectrum. This may be due to the excess of PF_5 used in the reaction. Additional bands at ν_{max} 740 and 500 cm^{-1} could not be assigned although the latter is characteristic

Table 5.4 Reaction Between $NOPF_5{}^{18}F$ and MoF_6 in Acetonitrile. Summary of Results.

Reactants				Specific count rate of $NOPF_6$ (count min^{-1} $mmol^{-1}$)		Count rate of MoF_6 After Reaction (count min^{-1})	Radio-chemical Balance (%)	Fraction Exchanged
$NOPF_5{}^{18}F$ (mmol)		MoF_6 (mmol)						
Initial	Final	Initial	Final	Initial	Final			
0.80 ±0.02	0.86 ±0.02	0.98 ±0.02	0.88 ±0.02	39557 ±1404	15984 ±1515	15630 ±125	93	0.97 ±0.08

Figure 5.1 Raman Spectrum of the Reaction Between $CsWF_7$ and PF_5 in MeCN.

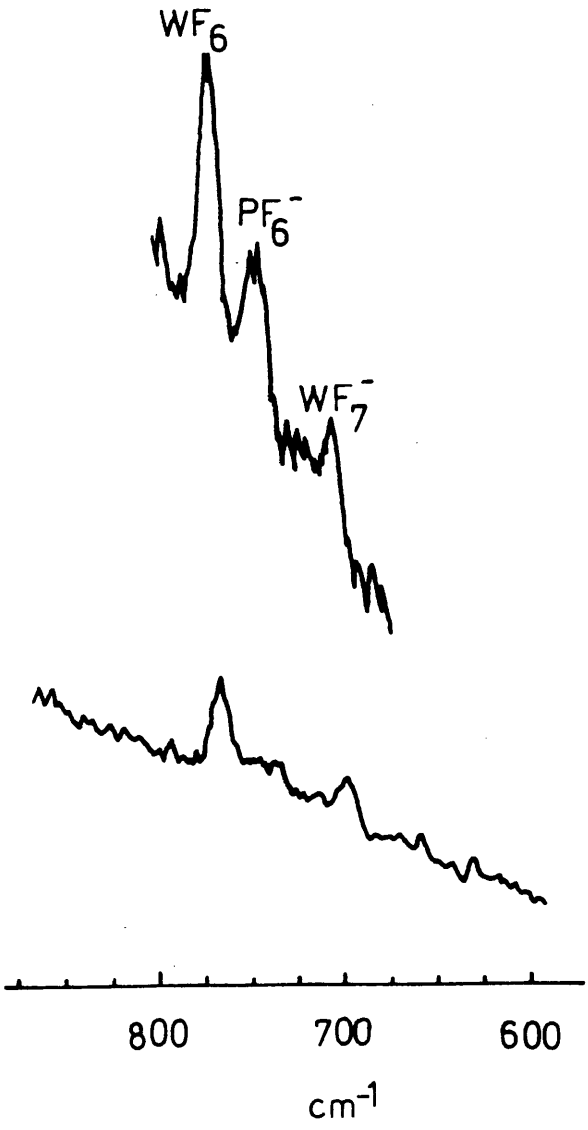

Table 5.5 : Infrared Spectrum of the Solid Product of the Reaction Between PF_5 and $CsWF_7$ in MeCN.

ν_{max} (cm^{-1})	Assignment [74]
830 (vs)	$\nu_3(F_{1u})$ PF_6^-
740 (w)	?
560 (m)	$\nu_4(F_{1u})$ PF_6^-
500 (m)	?

vs : very strong, m : medium, w : weak

of a fluorine bridged species. On the basis of the vibrational spectra the reaction between WF_7^- and PF_5 can be written as (Equation (5.7)).

$$WF_7^- + PF_5 \longrightarrow WF_6 + PF_6^- \qquad (5.7)$$

5.5 Reaction Between Lithium Hexafluoroarsenate and [^{18}F]-Fluorine Labelled Hexafluoride of Molybdenum, Tungsten and Uranium in Acetonitrile.

The interaction between lithium hexafluoroarsenate $LiAsF_6$, and [^{18}F]-labelled hexafluorides of molybdenum, tungsten and uranium in acetonitrile revealed two distinct types of behaviour of the AsF_6^- anion towards the hexafluorides. The amount of $LiAsF_6$ used was in the range 0.39 - 0.62 ± 0.02 mmol dissolved in MeCN (1cm^3). The amount of hexafluorides used was in the range 0.42 - 1.33± 0.02 mmol. The results of this investigation are summarised in Table 5.6. It was found in the case of $MoF_5{}^{18}F$ and $WF_5{}^{18}F$ that a negligible amount of [^{18}F]-fluorine activity was transferred to $LiAsF_6$. Furthermore the specific count rates of $MF_5{}^{18}F$ (M = Mo and W) determined before and after reaction were equal within experimental error indicating that no measurable exchange of [^{18}F]-fluorine was observed. However in the case of $UF_5{}^{18}F$ a transfer of [^{18}F]-fluorine activity to $LiAsF_6$, corresponding to complete exchange, was observed after 20 minutes of interaction. There was no

Table 5.6 Reactions Between $LiAsF_6$ and $MF_5{}^{18}F$ (M = Mo,W,U) in MeCN. Summary of Results.

$LiAsF_6$ (mmol)		MF_6	MF_6 (mmol)		Specific count rate of $MF_5{}^{18}F$ (count min^{-1} $mmol^{-1}$)		Count Rate of Reacts. after Reaction (count min^{-1})		Radio-chemical Balance (%)	Fraction Exchanged
Initial	Final		Initial	Final	Initial	Final	MF_6	$LiAsF_6$		
0.55 ±0.02	0.55 ±0.02	MoF_6	0.75 ±0.02	0.75 ±0.02	20173 ±669	20866 ±692	15566 ±125	480 ±22	106	0
0.62 ±0.02	0.62 ±0.02	MoF_6	1.33 ±0.02	1.33 ±0.02	20317 ±387	20404 ±388	27137 ±165	585 ±24	102	0
0.39 ±0.02	0.40 ±0.02	WF_6	0.47 ±0.01	0.45 ±0.01	266967 ±4433	277816 ±6293	123628 ±352	5305 ±73	103	0
0.51 ±0.02	0.51 ±0.01	WF_6	0.75 ±0.01	0.75 ±0.01	31414 ±787	31585 ±745	23689 ±154	569 ±24	103	0
0.48 ±0.02	0.48 ±0.02	UF_6	0.70 ±0.01	0.70 ±0.01	61250 ±1334	33931 ±753	23752 ±154	20646 ±144	104	1.09 ±0.08
0.41 ±0.02	0.41 ±0.02	UF_6	0.41 ±0.01	0.41 ±0.01	70146 ±2406	34271 ±1188	14051 ±119	15209 ±123	102	1.00 ±0.08

evidence for chemical reaction taking place between $LiAsF_6$ and MF_6 (M = Mo, W and U) as the infrared spectra of the solid recorded before and after reaction were identical.

The inertness of AsF_6^- towards MoF_6 and WF_6 was also demonstrated by the reaction between [^{18}F]-labelled nitrosonium hexafluoroarsenate, $NOAsF_5{}^{18}F$, and MoF_6. Inactive MoF_6 (1.19 ±0.02 mmol) was added by vacuum distillation to a single limb vessel containing $NOAsF_5{}^{18}F$ (0.95 ± 0.02 mmol) which had been prepared <u>in situ</u> by reaction between FNO and $AsF_4{}^{18}F$ and dissolved in MeCN. The starting count rate of $NOAsF_5{}^{18}F$ was 32533 ±180 count min^{-1}. After 20 minutes of contact the reactants were separated and counted for [^{18}F]-fluorine activity. Less than 3% of the original activity of $NOAsF_5{}^{18}F$ was transferred to MoF_6.

In view of these results the reaction WF_7^- and AsF_5 was investigated by Raman spectroscopy and by using [^{18}F]-fluorine radiotracer technique.

Caesium heptafluorotungstate (1.10± 0.01 mmol) was dissolved in acetonitrile (1 cm^3) and AsF_5 (0.75 ±0.02 mmol) was added by vacuum distillation. The mixture was warmed to room temperature and its Raman spectrum recorded. After removal of volatile material the Raman spectrum of the solid product of the reaction was recorded. These spectra are shown in Figure 5.2. The bands in the Raman solution spectrum (Figure 5.2 (a)) at ν_{max} 777, 714 and 684 cm^{-1} were

Figure 5.2 Raman Spectra of $CsWF_7$ in MeCN (a) and Solid Isolated from Reaction (b).

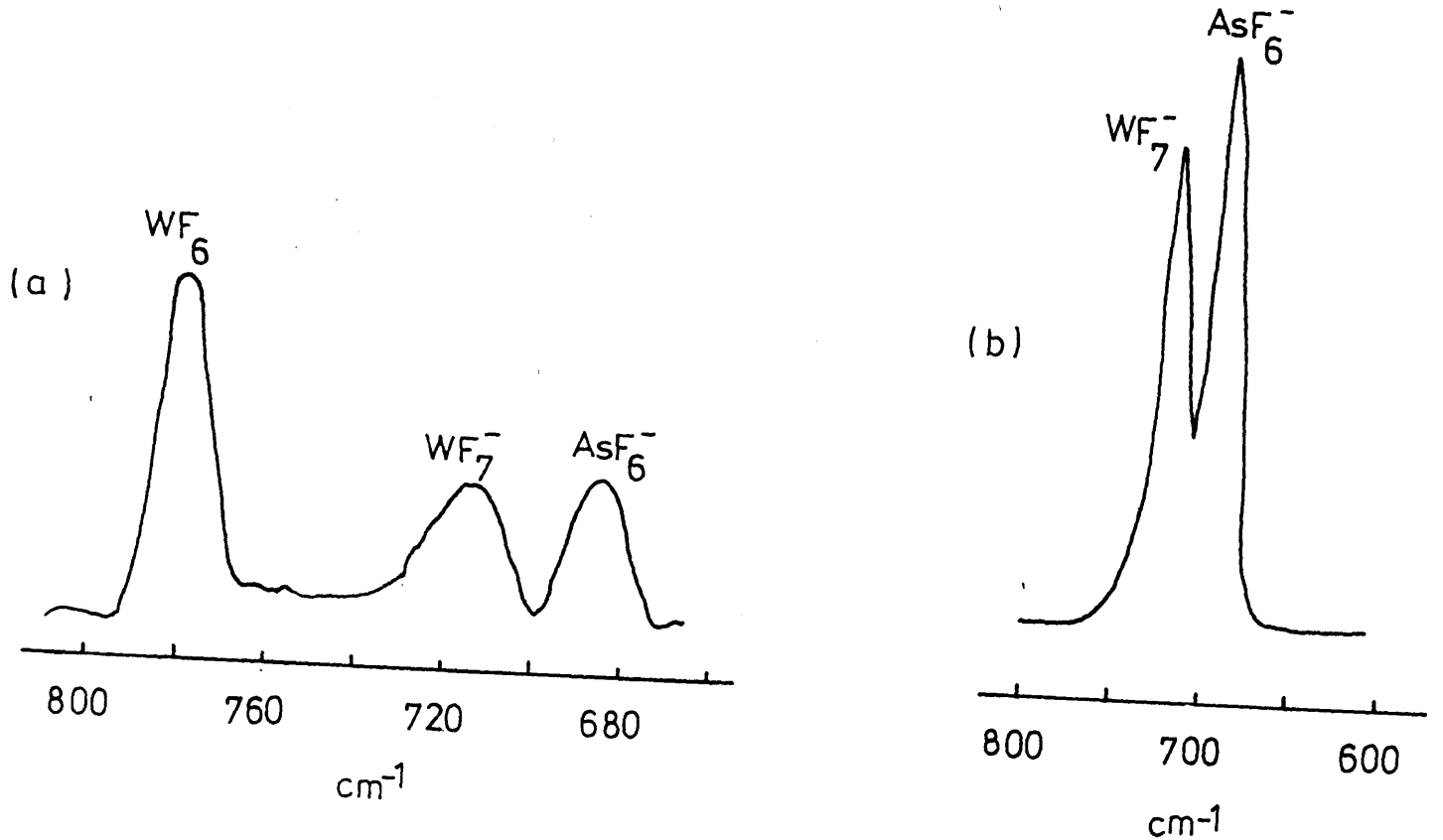

Figure 5.3 Reaction Between $CsWF_7$ and AsF_5 ^{18}F in MeCN with Time.

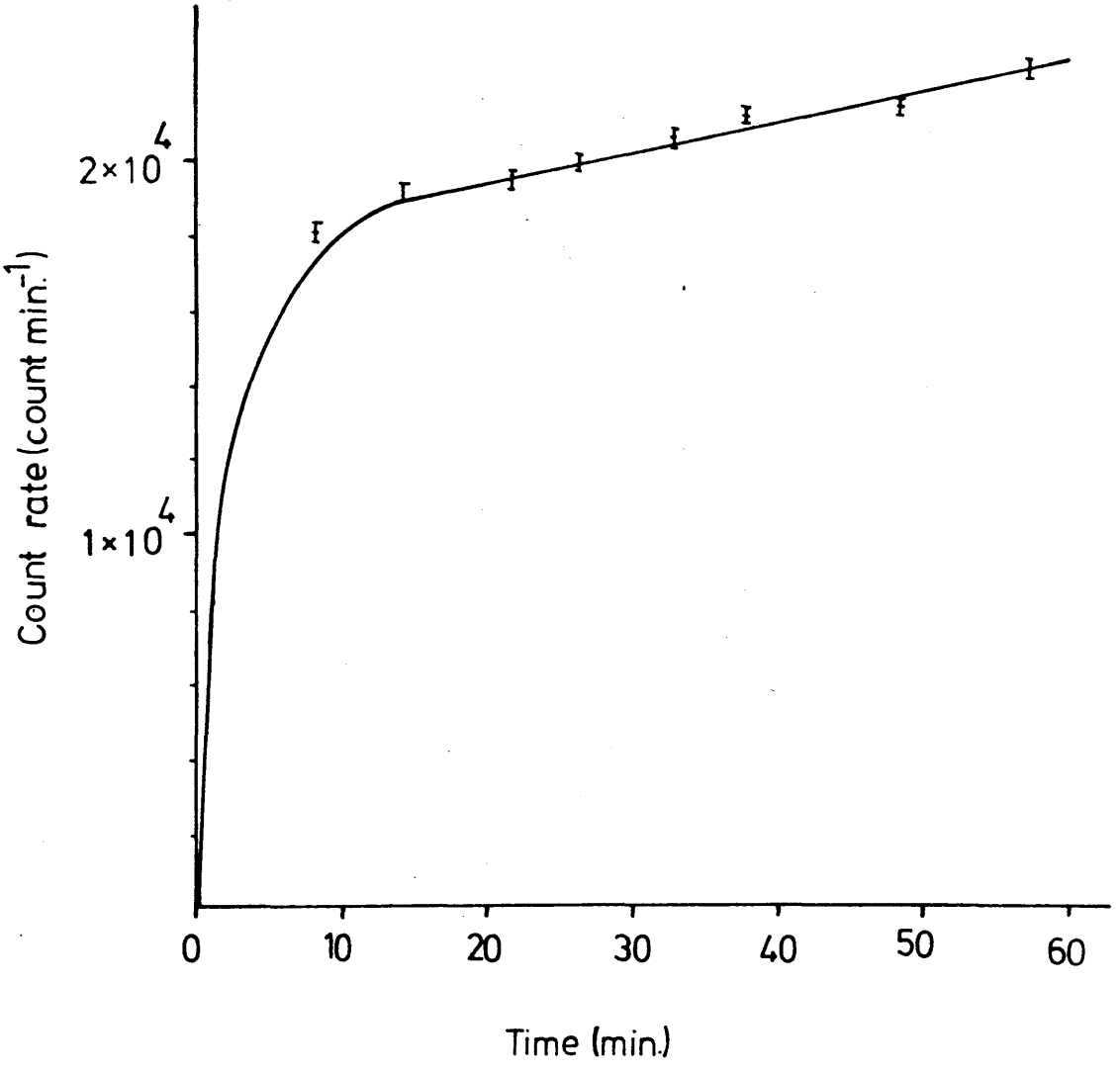

assigned to ν_1 (A_{1g}) mode of WF_6, ν_1 (A_1') mode of WF_7^- and $\nu_1(A_{1g})$ mode of AsF_6^- respectively. The bands in the Raman spectrum of the solid product at ν_{max} 715 and 689 cm^{-1} were assigned to $\nu_1(A_1')$ mode of WF_7^- and $\nu_1(A_{1g})$ mode of AsF_6^- respectively. From the Raman spectra described above the reaction between WF_7^- and AsF_5 can be written as follows (Equation 5.8)

$$WF_7^- + AsF_5 \longrightarrow WF_6 + AsF_6^- \qquad (5.8)$$

where WF_6 is displaced from WF_7^- by AsF_5. This reaction was followed with time by using $AsF_5{}^{18}F$ and $CsWF_7$ in MeCN. The growth of [^{18}F]-fluorine activity in solution with time is presented in Figure 5.3. This was rapid initially then followed a slower process. The continuous growth of [^{18}F]-fluorine activity was attributed to the formation of AsF_5.NCMe and its reaction with WF_7^- following equation (5.8).

5.6 Reaction Between Lithium Hexafluoroantimonate and [^{18}F]-Fluorine Labelled Hexafluoides of Molybdenum, Tungsten and Uranium in Acetonitrile.

Admission of [^{18}F]-labelled hexafluorides of molybdenum, tungsten and uranium in the range 0.68 - 2.16 ± 0.02 mmol to lithium hexafluoroantimonate, $LiSbF_6$, in the range 0.44 - 0.56 ± 0.02 mmol in acetonitrile (1 cm^3) resulted in all cases in a negligible transfer of [^{18}F]-fluorine activity to the latter.

The specific count rates of $MF_5{}^{18}F$ (M = Mo, W, U) before and after reactions were in all cases equal within experimental error. Furthermore the mass and radiochemical balances were in all cases $\geqslant$ 95% (Table 5.7). A change in colour in the solution from clear yellow to brown was observed during the reaction between $LiSbF_6$ and $UF_5{}^{18}F$. This was consistent with polymerisation of MeCN initiated by attack of $UF_5{}^{18}F$ [23]. However when using inactive UF_6 the solution of $LiSbF_6$ in MeCN stayed clear for a longer period. The attack of MeCN by $UF_5{}^{18}F$ may have given rise to the [^{18}F]-fluorine activity left in the solid $LiSbF_6$ after separation.

Taking into consideration these results SbF_6^- anion seemed to be more inert than BF_4^-, PF_6^- or AsF_6^- as far as exchange of [^{18}F]-fluorine activity in the presence of $MF_5{}^{18}F$ (M = Mo, W,U) is concerned.

A reaction between $CsWF_7$ (0.59 ±0.01 mmol) and SbF_5. NCMe (0.95 ±0.01 mmol) in MeCN resulted in the formation WF_6 and SbF_6^- as shown by the Raman spectrum of the solution and the infrared spectrum of the solid product. The Raman spectrum contained bands at ν_{max} 777 and 660 cm^{-1} assigned to $\nu_1(A_{1g})$ modes of WF_6 and SbF_6^- respectively. The infrared spectrum contained one band at ν_{max} 655 which was assigned to $\nu_3(F_{1u})$ mode of SbF_6^-.

On the basis of the vibrational spectra the reaction between WF_7^- and SbF_5 can be presented as (Equation 5.9)

$$WF_7^- + SbF_5 \longrightarrow WF_6 + SbF_6^- \qquad (5.9)$$

Table 5.7 Reaction Between $LiSbF_6$ and $MF_5{}^{18}F$ (M = Mo, W, U) in MeCN. Summary of Results.

$LiSbF_6$ (mmol)		MF_6	(mmol)		Specific count rate of $MF_5{}^{18}F$ (count $min^{-1}mmol^{-1}$)		Count rate of Reacts. after Reaction (count min^{-1})		Radio-chemical Balance	Fraction Exchanged
Initial	Final		Initial	Final	Initial	Final	MF_6	$LiSbF_6$	(%)	
0.51 ±0.02	0.51 ±0.02	MoF_6	0.68 ±0.02	0.68 ±0.02	27786 ±636	28589 ±636	19441 ±139	401 ±20	105	0
0.56 ±0.02	0.59 ±0.02	MoF_6	0.85 ±0.02	0.82 ±0.02	26959 ±491	27706 ±504	22719 ±151	361 ±19	104	0
0.51 ±0.02	0.52 ±0.02	WF_6	1.68 ±0.01	1.68 ±0.01	13930 ±79	13399 ±99	22510 ±150	95 ±10	97	0
0.60 ±0.02	0.61 ±0.02	WF_6	2.16 ±0.01	2.11 ±0.01	8588 ±72	9244 ±96	19504 ±140	72 ±9	100	0
0.51 ±0.02	0.60 ±0.02	UF_6	0.85 ±0.01	0.82 ±0.01	35620 ±666	36263 ±700	29736 ±172	1192 ±35	102	0
0.51 ±0.02	0.68 ±0.02	UF_6	0.93 ±0.01	0.88 ±0.01	30765 ±526	31002 ±674	27282 ±165	1747 ±42	101	0

in which WF_6 is displaced from WF_7^- by SbF_5.

5.7 Reaction Between Lithium Hexafluorotantalate and Copper(II) Hexafluoroniobate Pentakis (Acetonitrile) and [^{18}F]-Fluorine Labelled Tungsten Hexafluoride in Acetonitrile.

The results of two reactions between lithium hexafluorotantalate, $LiTaF_6$, and copper(II) hexafluoroniobate pentakis (acetonitrile), $[Cu(NCMe)_5][NbF_6]_2$, and [^{18}F]-labelled tungsten hexafluoride in acetonitrile are presented in Table 5.8. In each case a transfer of [^{18}F]-fluorine activity from $WF_5{}^{18}F$ to MF_6^- (M = Nb, Ta) was observed. This was accompanied by a decrease in the specific count rate of $WF_5{}^{18}F$ after reaction indicating that an exchange of [^{18}F]-fluorine had occurred between the reactants. The exchange was complete in each case. The infrared spectra of the fluoroanions recorded before and after reaction were identical. Hence from the results presented above the reaction between MF_6^- (M = Nb, Ta) and $WF_5{}^{18}F$ can be written as follows (Equation (5.10)).

$$MF_6^- + WF_5{}^{18}F \longrightarrow MF_5{}^{18}F + WF_5{}^{18}F \qquad (5.10)$$

(M = Nb, Ta)

Table 5.8 : Reactions Between $[Cu(NCMe)_5][NbF_6]_2$ or $LiTaF_6$ and $WF_5{}^{18}F$ in MeCN. Summary of Results.

MF_6^-	(mmol)		WF_6 (mmol)		Specific count rate of $WF_5{}^{18}F$ (count min^{-1} $mmol^{-1}$)		Count rate of Reactants After Reaction (count min^{-1})		Radio-chemical Balance (%)	Fraction Exchanged
	Initial	Final	Initial	Final	Initial	Final	WF_6	MF_6^-		
NbF_6^- *	0.13 ±0.01	0.16 ±0.01	1.14 ±0.01	1.12 ±0.01	34621 ±395	28618 ±169	32052 ±179	8584 ±93	103	0.93 ±0.10
$LiTaF_6$	0.65 ±0.01	0.66 ±0.01	1.98 ±0.01	1.91 ±0.01	13930 ±99	10557 ±120	20164 ±142	6696 ±82	98	0.98 ±0.02

*$[Cu(NCMe)_5][NbF_6]_2$

5.8 Reaction Between Acetonitrile Adducts of Antimony, Arsenic and Niobium Pentafluoride and [^{18}F]-Fluorine Labelled Tungsten Hexafluoride in Acetonitrile.

In view of the results presented in Sections 5.3 to 5.7 it was of interest to examine the behaviour of some of the parent fluorides of the fluoroanions in the presence of tungsten hexafluoride. Table 5.9 summarises the results of the reactions between acetonitrile adducts of antimony, arsenic and niobium pentafluorides and [^{18}F]-labelled tungsten hexafluoride in acetonitrile. The results obtained showed that SbF_5.NCMe was inert as compared with AsF_5.NCMe or NbF_5.NCMe as far as [^{18}F]-fluorine exchange is concerned. This was reflected by the small amount of [^{18}F]-fluorine activity transferred from $WF_5{}^{18}F$ to the former as compared with the two latter. Furthermore the specific count rate of $WF_5{}^{18}F$ after reaction with SbF_5 was within experimental error equal to that before reaction. However in the case of AsF_5 or NbF_5 the specific count rate showed a decrease after reaction indicating that a [^{18}F]-fluorine exchange had taken place between the reactants. The fraction exchanged was close to unity in both cases. The radiochemical and mass balances were $\geq$ 95% in all cases and there was no evidence for chemical reaction taking place as the infrared spectra of the adducts recorded before and after reactions were identical.

Table 5.9 Reactions Between MF_5.NCMe (M = Sb, As, Nb) and WF_5 ^{18}F in MeCN. Summary of Results.

MF_5.NCMe (mmol)		WF_6 (mmol)		Specific count rate of WF_5 ^{18}F (count min^{-1} $mmol^{-1}$)		Count rate of Reactants After Reaction (count min^{-1})		Radiochemical Balance (%)	Fraction exchanged
	Initial	Final	Initial	Final	Initial	Final	WF_6	MF_5.NCMe		
SbF_5NCMe	0.88 ±0.01	0.92 ±0.01	2.11 ±0.01	2.07 ±0.01	13181 ±151	13350 ±136	27635 ±166	134 ±16	100	0
SbF_5.NCMe	1.06 ±0.01	1.07 ±0.01	1.52 ±0.01	1.48 ±0.01	13181 ±151	13191 ±130	19522 ±140	530 ±23	100	0
AsF_5.NCMe	1.10 ±0.02	1.12 ±0.02	1.21 ±0.01	1.18 ±0.01	34621 ±395	21504 ±226	25375 ±159	18897 ±137	106	0.89 ±0.04
AsF_5.NCMe	0.73 ±0.02	0.75 ±0.02	0.24 ±0.01	0.23 ±0.01	34621 ±395	14487 ±678	3332 ±58	5933 ±77	109	0.81 ±0.06
NbF_5NCMe	0.35 ±0.01	0.37 ±0.01	1.49 ±0.01	1.48 ±0.01	12347 ±147	10288 ±108	15226 ±123	3467 ±59	102	1.01 ±0.04
NbF_5.NCMe	0.23 ±0.01	0.23 ±0.01	1.61 ±0.01	1.61 ±0.01	12347 ±147	11135 ±106	17927 ±134	2342 ±48	102	0.92 ±0.05

CHAPTER SIX

REACTIONS BETWEEN TRIS(DIMETHYLAMINO)SULPHONIUM DIFLUOROTRIMETHYLSILICATE AND HEXAFLUORIDES OF MOLYBDENUM, TUNGSTEN, BORON TRIFLUORIDE PHOSPHORUS PENTAFLUORIDE AND [^{18}F]-FLUORINE LABELLED TRIMETHYLFLUOROSILANE IN ACETONITRILE.

6. Reactions Between Tris(dimethylamino)sulphonium Difluorotrimethylsilicate and the Hexafluorides of Molybdenum and Tungsten, Boron Trifluoride, Phosphorus Pentafluoride and [^{18}F]-Fluorine Labelled Trimethylfluorosilane in Acetonitrile.

In this chapter Tris(dimethylamino)sulphonium difluorotrimethylsilicate will be referred to by TAS^+F^-.

6.1 Introduction.

TAS^+F^- [113] is a potential source of soluble fluoride of high anionic reactivity. For example TAS^+F^- has been reacted with carbonyl fluoride to give tris(dimethylamino) sulphonium trifluoromethoxide, $TAS^+CF_3O^-$, the crystal structure of which has been determined [7]. TAS^+F^- has also been used for a variety of other purposes. Fluoride ion from this salt and other tris(dialkylamino) sulphonium difluorotrimethylsilicate has been used to cleave Si-O [147,148] and Si-C=O [148,149] bonds and to prepare other sulphonium salts with high nucleophilic reactivity, including $(R_2N)_3\ S^+$ enolates [150] and phenoxides [151].

In this short investigation an attempt was made to prepare the heptafluoroanions of molybdenum and tungsten, the hexafluoroanion of phosphorus and the tetrafluoroanion of boron with a soluble organic cation as an alternative to the nitrosonium and lithium cations. The lability

with respect to exchange of the Si-F bond in TAS^+F^- was also examined in acetonitrile in the presence of [^{18}F]-labelled trimethylfluorosilane, $Me_3Si^{18}F$.

6.2 Experimental.

TAS^+F^- and Me_3SiF were prepared by literature methods (Sections 2.2.6 and 2.2.7 respectively). The reactions between TAS^+F^- and MoF_6, WF_6, BF_3 and PF_5 were examined by infrared spectroscopy whereas the reaction between TAS^+F^- and $Me_3Si^{18}F$ was examined according to the procedure described in Section 2.12.1. Due to the high solubility of TAS^+F^- in MeCN prolonged vacuum distillation of the solvent was necessary for the separation of the salt. However in view of the half life of [^{18}F]-fluorine ($t_{\frac{1}{2}}$ = 110 min [129]) distillation of the solvent was carried out over shorter periods, consequently good separation was not achieved. This resulted in an increase in the mass of the salt after reaction.

6.3 Reaction Between Tris(dimethylamino)sulphonium Difluorotrimethylsilicate and the Hexafluorides of Molybdenum and Tungsten in Acetonitrile.

The reaction between TAS^+F^- and the hexafluorides of molybdenum or tungsten was carried out in a double-limb vessel in acetonitrile. TAS^+F^- (0.5 mmol) was loaded in the previously evacuated and flamed-out reaction vessel in

the glove-box, transferred to the vacuum line and re-evacuated. Acetonitrile (3 cm^3) and MoF_6 (0.7 mmol) or WF_6 (0.7 mmol) were added successively by vacuum distillation. The reaction vessel was warmed to room temperature and the reaction allowed to proceed for 0.5 h. After removal of the volatile material a brown viscous liquid was isolated in each case. The infrared spectra (thin film) of the reaction products were complicated by the organic fragment of TAS^+F^-. However in each case an additional strong band at approximately 620 cm^{-1} was observed. This was consistent with the ν_3 (A_2'') of MoF_7^- and WF_7^-. No further characterisation of the reaction product was attempted.

6.4 Reaction Between Tris(dimethylamino)sulphonium Difluorotrimethylsilicate and Boron Trifluoride and Phosphorus Pentafluoride in Acetonitrile.

The reaction between TAS^+F^- and boron trifluoride or phosphorus pentafluoride was carried out in a double-limb vessel in acetonitrile. TAS^+F^- (0.6 mmol) was loaded in the previously evacuated and flamed-out reaction vessel in the glove box, transferred to the vacuum line and re-evacuated. Acetonitrile (3 cm^3) and BF_3 (0.6 mmol) or PF_5 (0.6 mmol) were added successively by vacuum distillation. The reaction vessel was warmed slowly to room temperature and the reaction allowed to proceed for 0.5 h. After removal of the volatile material a colourless solid was

isolated in each case. The infrared of the solid obtained from the reaction between TAS^+F^- and BF_3 contained bands in particular at ν_{max} 1090 (vs, br), 770 (m), 530 (s,sh) and 525 (s,sh) cm^{-1} assigned to ν_3 (F_2), ν_1(A_1) and ν_4 (F_2) modes of BF_4^- respectively. The infrared spectrum of the gas phase after reaction contained bands characteristic of Me_3SiF. According to the infrared spectra obtained the reaction between TAS^+F^- and BF_3 can be written as follows (Equation 6.1)

$$(Me_2N)_3S^+Me_3SiF_2^- + BF_3 \longrightarrow (Me_2N)_3S^+BF_4^- + Me_3SiF \qquad (6.1)$$

The infrared spectrum of the solid obtained from the reaction between TAS^+F^- and PF_5 contained bands in particular at ν_{max} 840 (vs) and 560 (m) cm^{-1} assigned to ν_3 (F_{1u}) and ν_4 (F_{1u}) modes of PF_6^- respectively. The infrared spectrum of the gas phase after reaction contained bands characteristic of Me_3SiF. In view of the infrared spectra obtained the reaction between TAS^+F^- and PF_5 can be written as follows (Equation 6.2)

$$(Me_2N)_3S^+Me_3SiF_2^- + PF_5 \longrightarrow (Me_2N)_3S^+PF_6^- + Me_3SiF \qquad (6.2)$$

6.5 Reaction Between Tris(dimethylamino)sulphonium Difluorotrimethylsilicate and [^{18}F]-Fluorine Labelled Trimethylfluorosilane in Acetonitrile.

A reaction between TAS^+F^- (0.25 ± 0.01 mmol) and [^{18}F]-labelled trimethylfluorosilane, $Me_3Si^{18}F$, (0.35 ± 0.03 mmol) resulted in a transfer of [^{18}F]-fluorine activity to TAS^+F^- and decrease in the specific count rate of $Me_3Si^{18}F$. This was consistent with an exchange of [^{18}F]-fluorine between TAS^+F^- and $Me_3Si^{18}F$. Using equation (2.8) the fraction exchanged was found to be 1 corresponding to complete exchange. A summary of the results of this reaction is presented in Table 6.1. In view of this result the reaction between TAS^+F^- and $Me_3Si^{18}F$ can be written as follows (Equation 6.3)

$$(Me_2N)_3S^+Me_3SiF_2^- + Me_3Si^{18}F \longrightarrow (Me_2N)_3S^+Me_3SiF^{18}F + Me_3Si^{18}F \qquad (6.3)$$

Table 6.1 Reaction Between TAS^+F^- and $Me_3Si^{18}F$ in Acetonitrile. Summary of Results.

Reactants				Specific count rate of Me_3SiF (count min^{-1} $mmol^{-1}$)		Final count rate of Reactants (count min^{-1})		Radio-chemical Balance (%)	Fraction Exchanged
TAS^+F^- (mmol)		$Me_3Si^{18}F$ (mmol)							
Initial	Final	Initial	Final	Initial	Final	TAS^+F^-	Me_3SiF		
0.25 ±0.01	0.29 ±0.01	0.35 ±0.03	0.35 ±0.03	58906 ±5441	25049 ±2349	11221 ±106	8767 ±94	96	0.98 ±0.20

CHAPTER SEVEN

DISCUSSION

7. DISCUSSION.

7.1 Fluorine Bond Lability of the Fluoroanions of Boron, Phosphorus, Arsenic, Antimony, Niobium and Tantalum.

Two distinct types of fluorine exchange behaviour have been shown to exist among the fluoroanions of boron, phosphorus, arsenic, antimony, niobium and tantalum. The results presented in Chapter 5 indicate that complete [^{18}F]-fluorine exchange occurs between tetrafluoroborate or hexafluorophosphate anions and [^{18}F]-labelled hexafluorides of molybdenum, tungsten and uranium in acetonitrile (Sections 5.3 and 5.4). Complete [^{18}F]-fluorine exchange also occurs between hexafluoroniobate or hexafluorotantalate anions and $WF_5{}^{18}F$ under the same conditions (Section 5.7). In contrast hexafluoroarsenate and hexafluoroantimonate anions show complete inertness under the same conditions (Sections 5.5 and 5.6) although complete [^{18}F]-fluorine exchange occurs between AsF_6^- and $UF_5{}^{18}F$.

Two mechanisms can be used to account for the exchange between BF_4^-, PF_6^- and $MF_5{}^{18}F$ (M = Mo, W and U) or between NbF_6^-, TaF_6^- and $WF_5{}^{18}F$.

The first (Mechanism 1) involves a reversible dissociation of the fluoroanion into its parent fluoride and F^- (Step (i)). This is followed by transfer of F^- to MF_6

Mechanism (1).

$$\text{(i)}\quad AF_n^- \rightleftharpoons AF_{n-1}.MeCN + F^-$$

$$\text{(ii)}\quad MF_6 + F^- \rightleftharpoons MF_7^-$$

(A = B, n = 4; A = P,Nb or Ta, n = 6; M = Mo,W or U

giving MF_7^- through an equilibrium (Step (ii)) in which the rate constant (k_1) of the forward reaction is smaller than that of the reverse reaction ($k_1 << k_{-1}$).

Step(i) is similar to that proposed by Gillespie et.al. [152] to explain the fluorine exchange of silver tetrafluoroborate in MeCN. During their investigation the authors observed that at high temperature the separate peaks arising from the coupling of fluorine on [^{11}B]-boron and [^{10}B]-boron collapsed to yield a single sharp peak which they took as evidence for rapid fluorine exchange among boron atoms. Furthermore the much faster fluorine exchange observed when BF_3 was added to BF_4^- led the authors to suggest a mechanism involving a slight dissociation of BF_4^- into BF_3 and F^-. In the present study the exchange reactions were carried out at room temperature and it is therefore likely that the rate constant of the dissociation of BF_4^- is much smaller. However this possibility can not be ruled out.

An alternative mechanism (Mechanism 2) involves a fluorine bridged species formed between the fluoroanion and the hexafluoride (step (i)) followed by transfer of the

Mechanism 2.

$$AF_n^- + MF_6 \overset{(i)}{\rightleftharpoons} \left[F_{n-1}A\text{--}F\text{--}MF_6\right]^- \overset{(ii)}{\rightleftharpoons} AF_{n-1}.NCMe + MF_7^-$$

(A = B, n = 4; A = P,Nb or Ta, n = 6; M = Mo,W or U)

bridging fluorine to MF_6 leading to the short lived species MF_7^- (Step (ii)) through an equilibrium which is shifted

towards the thermodynamically more stable AF_n^- species.

Fluorine bridging species involving group VA and VB fluoroanions are well documented. For example Brownstein [86] has provided strong evidence for the formation of fluorine bridging complexes between NbF_6^- or TaF_6^- and AsF_5 or SbF_5 in solution. These consist of two octahedra joined by a fluorine bridge through the corners. Fluorine bridging species have also been determined in the solid state for $SF_3^+BF_4^-$ and $SF_3^+AsF_6^-$ [57] and for $Nb_2F_{11}^-$ and $Ta_2F_{11}^-$ [87]. It is therefore reasonable to assume that such species are likely to form between the fluoroanions under investigation and MF_6 (M = Mo, W and U). Evidence for step (ii) is given by the reaction between BF_3 or PF_5 and $CsWF_7$ in MeCN (Equations (5.4) and (5.7) respectively) where the formation of BF_4^- and

$$WF_7^- + BF_3 \longrightarrow WF_6 + BF_4^- \qquad (5.4)$$

$$WF_7^- + PF_5 \longrightarrow WF_6 + PF_6^- \qquad (5.7)$$

PF_6^- has been shown by infrared and Raman spectroscopy to occur in MeCN.

No direct evidence has been obtained in the present study to enable identification of the mechanism responsible for the fluorine exchange behaviour of the fluoroanions under the conditions used.

It is not easy to rationalise the difference in behaviour between UF_6 and MoF_6 or WF_6 in the presence of AsF_6^-

however, this is consistent with the higher fluoride ion affinity of UF_6 (-2586 $kJmol^{-1}$[153]) as compared with that of WF_6 (-2271±29 $kJmol^{-1}$[19]) or MoF_6. The fluoride ion affinity of MoF_6 is not known but the results presented later in this chapter are consistent with it being smaller than that of WF_6.

A difference in fluorine bond lability with respect to exchange has also been shown to exist among AsF_5.NCMe, NbF_5.NCMe and SbF_5.NCMe in the presence of $WF_5{}^{18}F$ in MeCN. While the two former show complete [^{18}F]-fluorine exchange SbF_5.NCMe is completely inert under the same conditions (Section 5.8). The lability of As-F bond in AsF_5 is unexpected in view of the inertness of AsF_6^- under similar conditions. The exchange of [^{18}F]-fluorine between AsF_5 or NbF_5 and $WF_5{}^{18}F$ can be accounted for in terms of a mechanism (Equation 7.1) involving a fluorine bridged species

$$AF_5 + WF_6 \overset{(i)}{\rightleftharpoons} \left[F_4A\text{--}F\text{--}WF_6\right] \overset{(ii)}{\rightleftharpoons} \left[AF_4(NCMe)_2\right]^+ + WF_7^- \quad (7.1)$$

(step (i)) followed by reversible dissociation of AsF_5, step (ii) in which the equilibrium is thermodynamically favoured to the left. Kolditz and Beierlein [154] claimed to have shown that AsF_5.NCMe dissociates in MeCN into $[AsF_4(NCMe)_2]^+$ and AsF_6^-. However this result was later challenged by Tebbe and Muetterties [50] who found no evidence for ionisation of AsF_5.NCMe or SbF_5.NCMe and argued that Kolditz's result was due to hydrolysis of AsF_5.NCMe. Because of the inertness of SbF_5.NCMe it is

unlikely, although not to be ruled out, that hydrolysis is the major cause of the [^{18}F]-fluorine exchange found in the present work. Ionisation of NbF_5.NCMe in MeCN into $[NbF_4(NCMe)_2]^+$ and NbF_6^- has been reported by Moss [84] and is therefore a possible intermediate in the mechanism of fluorine exchange proposed above.

There is a close similarity between the exchange behaviour of the fluoroanions investigated and the Lewis acidity in terms of fluoride ion affinity of their parent fluorides. A survey of the literature (Table 1.1 and references therein) reveals a Lewis acidity in terms of fluoride ion affinity of the parent fluorides in the order

$$SbF_5 > AsF_5 > PF_5 > BF_3 > NbF_5 \sim TaF_5$$

The inertness of SbF_6^- as compared with the fluoroanions of As, P, B, Nb and Ta can be argued as being due in part to the stronger Lewis acid centre, Sb^V.

It has not been possible, using [^{18}F]-fluorine as radiotracer, to differentiate the exchange behaviour among the fluoroanions of P, B, Nb and Ta.

In a radiotracer study Dixon and Winfield [5] have reported the lack of [^{18}F]-fluorine exchange between AsF_6^- and $AsF_4{}^{18}F$ or between BF_4^- and $BF_2{}^{18}F$ under heterogeneous conditions at room temperature. However [^{18}F]-fluorine exchange has been found to occur between F_3CO^- and $^{18}FFCO$ under the same conditions. All fluoroanions were prepared <u>in situ</u> by reaction between activated CsF and the corresponding Lewis

fluoride. In this case anion-cation interaction rather than the Lewis acidity of the parent fluoride must be taken into consideration to account for the results obtained by the authors. Electrostatic effects between the relatively large Cs^+ cation and the anions are likely to result in stronger fluorine bonds in the anion as result of which their lability with respect to exchange is inhibited. In this respect F_3CO^- is expected to be inert. However an x-ray crystal determination of $[(Me_2N)_3S][OCF_3]$ [7] indicates that all fluorine atoms are equivalent but that the C-F bonds are weaker than expected. This has been rationalised on the basis of negative fluorine hyperconjugation. As a result, $[^{18}F]$-fluorine exchange between F_3CO^- and $^{18}FFCO$ is likely to occur more readily as compared with the two other systems.

7.2 Fluorine Bond Lability of the Heptafluoroanions of Molybdenum and Tungsten.

The heptafluoroanions of molybdenum and tungsten are well characterised in the solid state [28,29] and the existence of WF_7^- in solution is well established [31]. However no evidence for the existence of MoF_7^- in solution is available in the literature. The results presented in Section 3.8 have shown for the first time that reaction between caesium fluoride and molybdenum hexafluoride in acetonitrile leads to the formation of MoF_7^- the symmetry of which is assigned as D_{5h}. Similar experiments have also confirmed

the existence of WF_7^- in MeCN by reaction between CsF and tungsten hexafluoride, the symmetry of WF_7^- being similar to that of MoF_7^-.

The results obtained in Chaper 3 have shown that rapid and complete exchange of $[^{18}F]$-fluorine occurs between heptafluorotungstate ion, WF_7^-, with Cu^{2+}, Tl^+ or NO^+ as counter cation and $[^{18}F]$-labelled hexafluorides of molybdenum or tungsten (Sections 3.3 to 3.5) in acetonitrile at 293 and 253 K. The nature of the cation appears to have no effect on the exchange. Complete exchange of $[^{18}F]$-fluorine also occurs between caesium heptafluoromolybdate(VI) and $WF_5{}^{18}F$ in MeCN (Section 3.9).

Two mechanisms can be considered to explain the $[^{18}F]$-fluorine exchange between MF_7^- (M = Mo and W) and $MF_5{}^{18}F$ (M = Mo and W) in MeCN.

The first (Dissociative mechanism 1) involves a reversible dissociation of MF_7^- (Step (i)) into MF_6 and F^- followed by transfer of F^- to $M'F_6$ (Step (ii)) resulting in

Dissociative mechanism

(i) $MF_7^- \rightleftharpoons MF_6 + F^-$

(ii) $M'F_6 + F^- \rightleftharpoons M'F_7$

(M' = M = Mo or W)

the formation of $M'F_7$. Reversible decomposition of WF_7^- into WF_6 and F^- (Step (i)) has been reported to occur in

MeCN by Bougon et.al. [36]. Using ^{19}F and ^{183}W n.m.r. techniques the authors have used the absence of the ^{19}F-^{183}W satellite together with the narrow resonance, δ-142 ppm with respect to $CFCl_3$, as arguments to support their conclusion. However it is not unlikely that this evidence no longer apply to the present case as WF_6 is added to WF_7^- in MeCN where exchange between the two reactants is taking place. Prescott et.al. [31] have shown that addition of WF_6 to $TlWF_7$ in MeCN results in a shift of the n.m.r signal to a lower applied field. The authors have observed only one signal indicating rapid exchange between WF_7^- and WF_6. Further evidence for the decomposition of WF_7^- is given by the observation (Section 3.3) that, when dissolved in MeCN, $TlWF_7$ decomposes giving a small precipitate presumed to be TlF which redissolves when WF_6 is added.

Evidence for step (ii) can be inferred from the reaction between $CsWF_7$ and MoF_6 or between $CsMoF_7$ and WF_6 in MeCN (Sections 3.7 and 3.9 respectively). In each case the Raman spectrum of the solid after reaction shows bands attributable to MoF_7^- (Figure 3.3) and WF_7^- (Figure 3.4) consistent with the displacement of complexed WF_6 and MoF_6 by free MoF_6 and WF_6 respectively. It is interesting to note that the extent of displacement of complexed MoF_6 by free WF_6 in $CsMoF_7$ is much greater than the displacement of complexed WF_6 by free MoF_6 in $CsWF_7$. This result is consistent with the greater fluoride ion affinity of WF_6 as compared with that of MoF_6. The fluoride ion affinity of MoF_6 is not known.

However the result obtained in the present study suggests that it is smaller than -2271±29 $kJmol^{-1}$ which is the value determined for the fluoride ion affinity of WF_6 [19].

The exchange of [^{18}F]-fluorine between MF_7^- (M = Mo and W) and $MF_5{}^{18}F$ (M = Mo and W) can equally be interpreted in terms of an associative mechanism (2) which involves the formation of a bridged fluorine species as an

Associative mechanism (2)

$$MF_7^- + M'F_6 \overset{(i)}{\rightleftharpoons} \left[F_6M\text{--}F\text{--}M'F_6\right]^- \overset{(ii)}{\rightleftharpoons} MF_6 + M'F_7^-$$

(M′ = M = Mo or W)

intermediate (Step (i)). This step is followed by the transfer of F^- to $M'F_6$ giving $M'F_7^-$ and free MF_6 (Step(ii)). Fluorine bridged species between WF_7^- and WF_6 is believed to form in the solid state after heterogeneous reaction (Section 3.10) and it is likely that such species exist under homogeneous conditions (Step (i)). Evidence for step (ii) is as presented above.

Although the dissociative mechanism (1) fits better the experimental observations made in this work these can not be considered as direct evidence. Because of the lack of such evidence no definite conclusion can be drawn as to which mechanism is the more likely to operate under the conditions used.

Partial exchange of [^{18}F]-fluorine has been found to occur between AWF_7 (A = Cu^{2+}, Tl^+ and NO^+) and $MF_5{}^{18}F$

(M = Mo, W and U) or between $CsMoF_7$ and $WF_5{}^{18}F$ under heterogeneous conditions after 1h of interaction (Sections 3.10 to 3.12 and 3.15 respectively). The partial exchange is also reflected by the slow growth of [^{18}F]-fluorine activity in the solid with time (Figures 3.6 to 3.12).

The partial exchange of [^{18}F]-fluorine between AWF_7 ($A = Cu^{2+}$, Tl^+ and NO^+) and $MF_5{}^{18}F$ (M = Mo, W or U) or between $CsMoF_7$ and $WF_5{}^{18}F$ is best accounted for in terms of an associative mechanism (3) involving a fluorine bridged species as intermediate (Step (i))

Associative mechanism (3)

$$MF_7^- + M'F_6 \underset{}{\overset{(i)}{\rightleftharpoons}} [F_6M\text{--}F\text{--}M'F_6]^- \overset{(ii)}{\rightleftharpoons} MF_6 + M'F_7^-$$

followed by transfer of F^- to $M'F_6$ resulting in a displacement of MF_6 from MF_7^- (Step (ii)). Evidence for step (i) is given by the reaction between $[Cu(NCMe)_5][WF_7]_2$ or $TlWF_7$ and WF_6 under heterogeneous conditions (Section 3.10). In each case additional bands consistent with a fluorine bridged species [138] were observed in the infrared spectra (Figure 3.5) of the solids after reaction. This is further supported by the slight increase in the mass of the solids after reaction corresponding to an uptake of WF_6 by AWF_7 ($A = Cu^{2+}$ or Tl^+) was observed (Table 3.7). The displacement of complexed MF_6 by free MF_6 in step (ii) is supported by the results of the reaction between [^{18}F]-labelled nitrosonium heptafluorotungstate and inactive WF_6 under heterogeneous conditions (Section 3.13).

After reaction some [^{18}F]-fluorine activity was found in WF_6 indicating that complexed $WF_5{}^{18}F$ must have been displaced to a small extent by free WF_6. In view of this result it was hoped to show, using Raman spectroscopy the displacement of complexed MoF_6 in $CsMoF_7$ by WF_6 under heterogeneous conditions. However the Raman spectra of the solid recorded before and after reaction were identical. This is not surprising in view of the partial exchange of [^{18}F]-fluorine reflecting the small amount of MoF_6 displaced which is probably below the sensitivity of the spectroscopic method.

It can be argued that the partial exchange of [^{18}F]-fluorine between MF_7^- (M = Mo or W) and $MF_5{}^{18}F$ (M = Mo, W or U) under heterogeneous conditions is in part due to the electrostatic forces existing between the cations and anions. These forces are restricting the mobility of MF_7^- ion hence rendering the process of exchange slow and incomplete. Such forces are very small or non-existent in solution where the mobility of MF_7^- is easier resulting in more chances of [^{18}F]-fluorine exchange with $MF_5{}^{18}F$.

The results of the reactions between $[Cu(NCMe)_5]$-$[WF_7]_2$, $TlWF_7$ or $NOWF_7$ and $WF_5{}^{18}F$ under heterogeneous conditions show a difference in behaviour among the complexes in terms of [^{18}F]-fluorine exchange and uptake of WF_6. Although the uptake of WF_6 by WF_7^- is greater in the case of $[Cu(NCMe)_5]$-$[WF_7]_2$ (0.26, 0.41±0.05 WF_6:WF_7^- mole ratio) as compared with $TlWF_7$ or $NOWF_7$ (0-0.13±0.05 WF_6:WF_7^- mole ratio) the fraction of [^{18}F]-fluorine exchanged per fluorine atom is

smaller in the former case (f = 0.20,0.12±0.03) as compared with that of $TlWF_7$ (f = 0.24,0.20±0.03) or $NOWF_7$ (f = 0.23± 0.03) (Table 3.7). The difference in behaviour among these complexes is also observed in the growth of [^{18}F]-fluorine activity in the solid with time (Figures 3.6 to 3.8). The rapid growth of [^{18}F]-fluorine activity during the first five minutes in the case of $[Cu(NCMe)_5][WF_7]_2$ is consistent with the greater uptake of WF_6 while in the two other systems this process is less pronounced.

The difference in exchange behaviour among these systems can be accounted for in terms of the relatively larger $Cu(NCMe)_5^{2+}$ cation size as compared with that of Tl^+ or NO^+. The anion-cation interaction together with the steric effects are likely to affect more the exchange between $[Cu(NCMe)_5]$-$[WF_7]_2$ and WF_6.

7.3 Reaction of Activated Caesium Fluoride, Thallium Fluoride and Copper Difluoride with [^{18}F]-Fluorine Labelled Hexafluorides of Molybdenum, Tungsten and Uranium.

The reactions between activated caesium fluoride and [^{18}F]-labelled hexafluorides of molybdenum, tungsten and uranium under heterogeneous conditions at room temperature have resulted in an uptake of the hexafluorides by activated CsF to various extents as shown by the increase in the mass of the solids after reaction (Table 4.2, 4.6 and 4.10). The

uptake of MF_6 by CsF is related to the activation process. When CsF was activated using excess hexafluoroacetone (Batch No.1) the uptake was significant in all cases reaching a 1:1 mole ratio in the case of WF_6 (Table 4.2). However when less $(CF_3)_2CO$ was used, the uptake of MF_6 decreased substantially (Batch No.2). The uptake of MF_6 decreased further when no $(CF_3)_2CO$ was used (Batch No.3).

Activation of CsF by formation followed by thermal decomposition of its 1:1 adduct with $(CF_3)_2CO$ is known to increase its surface area [122(a), 123] and its reactivity [122(b)]. It has been argued [5] that the increase in the surface area of CsF is due to a reduction in its particle size and to the meso- or macro-porous structure produced after thermal decomposition of the adduct. The results obtained in the present study show that the reactivity of CsF in terms of uptake of MF_6 (M = Mo,W and U) and most probably its surface area are closely related to the amount of $(CF_3)_2CO$ used. The same results emphasise the importance of the formation of the $Cs^+OCF(CF_3)_2^-$ adduct in the activation process.

The decrease in the specific count rate of $MF_5{}^{18}F$ (M = Mo, W and U) observed after reaction with CsF indicates that a [^{18}F]-fluorine exchange had occurred between $MF_5{}^{18}F$ and the solid. The [^{18}F]-fluorine exchange can be considered to take place according to different models.

Model 1 : In which [^{18}F]-fluorine exchange can be considered as a result of complete exchange between $MF_5{}^{18}F$

(M = Mo, w and U) and all the fluorine atoms available on the solid. In this case S_∞, in equation (2.7), corresponding to total exchange is determined as follows

$$S_\infty = \frac{n_2 A_o}{n_1 m_1 + n_2 m_2}$$

where A_o (count min^{-1}) is the initial count rate of $MF_5{}^{18}F$; n_2 the number of exchangeable fluorine atoms in MF_6 ($n_2 = 6$); m_1 (mmol) quantity of CsF with n_1 exchangeable fluorine atoms ($n_1 = 1$); m_2 (mmol) quantity of $MF_5{}^{18}F$.

On the basis of these assumptions the fractions exchanged (f_1) of the systems investigated are presented in Tables 7.1 - 7.3 (First column) for MoF_6, WF_6 and UF_6 respectively. However it is unlikely that this model describes the process of exchange for the following reason. Assuming all fluorine atoms on the solid are exchangeable, decrease in the specific count rate of $MF_5{}^{18}F$ would be observed in all cases. However decrease in the specific count rate was observed only in cases where uptakes of MF_6 were significant. This is contrasted with the situation of no measurable decrease in the specific count rates of $MF_5{}^{18}F$ where small uptakes were observed. This leads to consider a model (Model 2) in which [^{18}F]-fluorine exchange is taking place only between the adsorbed species and free hexafluorides.

Model 2 : If it is to exchange, the adsorbed species must have its fluorine atoms equivalent both to that of CsF and among themselves. The MF_7^- or MF_8^{2-} species

Table 7.1 Fractions Exchanged (f) of the Reaction Between Activated CsF and MoF_5 ^{18}F.

Expt No.	Batch	f1	f2	f3
1	1	0.27±0.03	0.76±0.03	0.92±0.03
2	1	0.32±0.03	0.94±0.03	1.02±0.03
3	2	0.21±0.03	0.47±0.03	0.52±0.03
4	3	0	0	0
5	4	0.57±0.03	1.69±0.03	n/d

n/d not determined

Table 7.2 Fractions Exchanged (f) of the Reaction Between Activated CsF and WF_5 ^{18}F.

Expt.No.	Batch	f1	f2	f3
1	1	0.63±0.03	0.61±0.03	0.67±0.03
2	1	0.23±0.03	0.27±0.03	0.27±0.03
3	2	0.13±0.03	0.76±0.03	0.76±0.03
4	2	0	0	0
5	3	0	0	0
6	3	0	0	0
7	4	0.24±0.03	0.31±0.03	0.35±0.03
8	4	0.57±0.03	0.82±0.03	0.91±0.03

Table 7.3 Fractions Exchanged (f) of the Reaction Between Activated CsF and UF_5 ^{18}F.

Expt.No	Batch	f1	f2
1	2	0.82±0.03	4.14±0.03
2	3	0	0
3	3	0	0
4	4	0.69±0.03	2.35±0.03

resulting from a 1:1 or 2:1 combinations between CsF and MF_6 (M = Mo, W or U) are a possibility.

Examination of the Raman spectra of the solids after reaction between activated CsF and MoF_6 or WF_6 reveals bands attributable to MoF_7^- and WF_7^- respectively (Table 4.5 and 4.9 and Figures 4.7 and 4.6). In the case of UF_6 the bands are consistent with UF_8^{2-} being formed (Table 4.13 and Figure 4.10). Under these restrictions the extent of [^{18}F]-fluorine exchange can be determined by using equation (2.7) in which S_∞ is the specific count rate of $MF_5{}^{18}F$ resulting from complete exchange between the species formed and excess $MF_5{}^{18}F$. S_∞ is defined as follows

$$S_\infty = \frac{n_2 A_o}{n_1 b + n_2 a}$$

where A_o (count min^{-1}) is the initial count rate of $MF_5{}^{18}F$ with n_2 exchangeable fluorine atoms (n_2 = 6); b(mmol) quantity of species formed with n_1 exchangeable fluorine atoms (n_1 = 7 or 8); b is determined from the increase in the mass of the solid after reaction; a(mmol) quantity of $MF_5{}^{18}F$ recovered after reaction, a is determined from mass balance measurements.

Using equation (2.7) and S_∞ as defined above the fractions exchanged (f_2) of the systems under investigation are presented in Tables 7.1, 7.2 and 7.3 second column for MoF_6, WF_6 and UF_6 respectively. An increase in the f values is observed in the case of MoF_6 and WF_6 as compared with those

found in the previous model, although in the case of MoF_6, experiment 5, f is >1. The origin of the latter result is unclear. The increase in the f values is a consequence of the restriction of the pool of exchangeable fluorine atoms on the solid.

The exchange between $CsMF_7$ (M = Mo or W) and $MF_5{}^{18}F$ (M = Mo or W) can be explained in terms of a mechanism (1) involving the formation of MF_7^- species (Step (i)).

Mechanism (1)

(i) $CsF + MF_6 \xrightarrow{\text{fast}} CsMF_7$

(ii) $MF_7^- + M^*F_6 \rightleftharpoons \left[F_6M\text{--}{}^*F\text{--}MF_6\right]^- \rightleftharpoons MF_6 + M^*F_7^-$

(M = Mo or W)

This is followed by step (ii) which involves the interaction of free $MF_5{}^{18}F$ with MF_7^- through a fluorine bridged species in which the bridging fluorine is transferred to MF_6 giving MF_7^- and free MF_6 with a specific count rate less than the initial. The decrease in the specific count rate of MF_6 can be accounted for by the fact that the inactive fluorine atom originating from CsF and the [^{18}F]-fluorine atoms originating from $MF_5{}^{18}F$ are exchanged between them in MF_7^- through an intramolecular exchange. This process is likely to lead to the incorporation of the inactive fluorine atom in $MF_5{}^{18}F$ after its displacement. Evidence for the displacement

of MF_6 in MF_7^- by free MF_6 has been obtained by the reaction between [^{18}F]-labelled caesium heptafluoromolybdate(VI) or heptafluorotungstate(VI) and inactive MoF_6 or WF_6 respectively, (Sections 4.3 and 4.4) Transfer of [^{18}F]-fluorine activity from $CsMF_6{}^{18}F$ (M = Mo or W) to inactive MF_6 (M = Mo or W) is an indication of some displacement of complexed MF_6 by free MF_6.

Assuming [^{18}F]-fluorine exchange taking place between UF_8^{2-} and $UF_5{}^{18}F$ through an associative mechanism similar to that proposed for MoF_7^- and WF_7^- the fractions exchanged f were >>1 in all cases (Table 7.3, second column). Although only two experiments were carried out this result is surprising if it is considered that the spectroscopic evidence is consistent with the formation of UF_8^{2-} as the major species. However other bands are consistent with the formation of UF_7^- (Table 4.13).

Sheft et.al. [140] have used [^{18}F]-fluorine as radiotracer to show that interaction between NaF and UF_6 at high temperature leads to the formation of Na_2UF_8. In the present study the reaction between activated CsF and UF_6 at room temperature yields UF_8^{2-} as the major species. The formation of more than one species may be assumed as being due to the lack of uniformity of the surface reaction together with the difference in the surface areas of the solid fluorides. Sheft et.al. [140] have reported a surface area of $7 m^2 g^{-1}$ for NaF activated by HF whereas CsF activated by the $(CF_3)_2CO$ route has a typical surface area in the range 3.01-2.09 $m^2 g^{-1}$ [122(a)].

Of the three hexafluorides UF_6 has proved to be the most difficult to handle under the conditions used in the present work and hydrolysis as origin of the [^{18}F]-fluorine exchange results can not be ruled out. However assuming that hydrolysis is not the direct cause the f values are not consistent with the model proposed. The possibility of the formation of UF_9^{3-} species is unlikely in view of the results of Sheft et.al. [140] which was confirmed in subsequent synthetic work [141,155]. Lower f values would result from the incorporation of more inactive fluorine atoms in UF_8^{2-}. This leads to postulate an exchange between CsF and UF_8^{2-} through a mechanism involving the dissociation of UF_8^{2-}.

Model 3 : The pool of exchangeable fluorine atoms on the solid can be restricted further if it is considered that not all the MF_6 (M = Mo or W) adsorbed give rise to the MF_7^- species. This assumption is based on the finding (Section 3.10) that an increase in the mass of AMF_7 (A = Cu^{2+}, Tl^+, Cs^+ ; M = Mo or W) has been observed after reaction with MF_5 ^{18}F (M = Mo or W) under heterogeneous conditions (Table 3.7). The increase in the mass of the solid was explained in terms of an uptake of MF_6 by AMF_7 corresponding to an average value of 0.1:1 MF_6: MF_7^- mole ratio. It is therefore reasonable to assume that 90% of the quantity of MF_6 taken up result in the formation of the MF_7^- species onto which the remaining 10% of MF_6 are adsorbed.

Under these new restrictions the specific count

rate S_∞ corresponding to complete exchange is determined as follows

$$S_\infty = \frac{n_2 A_o}{0.9 n_1 b + 1.1 n_2 a}$$

where n_2, A_o, n_1, b and a are defined as before.

Using equation (2.7) and S_∞ as defined above the fractions exchanged (f_3) of the systems under investigation are presented in Tables 7.1 and 7.2 third column for MoF_6 and WF_6 respectively. In the case of MoF_6 the fraction exchanged (f_3) ranges from 0.52 to 1.02±0.03 whereas in the case of WF_6 f is <1. Two possible explanations can be used to account for the spread of the results:

1. The partial exchange observed in most cases may be due to the slowness of step (ii) in the mechanism envisaged above (Mechanism 1). Similar argument has been used to account for the partial exchange of [^{18}F]-fluorine between MF_7^- and $MF_5{}^{18}F$ (M = Mo or W) under heterogeneous conditions (Section 7.2).

2. It is possible that more than one species in which not all the fluorine atoms are equivalent among themselves are formed giving rise to different fractions of [^{18}F]-fluorine exchanged. This possibility is supported by the Raman spectra of the solids after reaction (Table 3.4) where additional bands were present (Table 4.5 and 4.9 and Figures 4.7 and 4.6).

In this case the assumption made above may not take into account fully the processes occurring on the surface. The existence of more than one species may be due to the lack of uniformity of the surface reaction.

No evidence for chemical reaction between copper difluoride and [^{18}F]-labelled hexafluorides of molybdenum, tungsten or uranium has been obtained. The colour change observed during the reaction between CuF_2 and UF_6 (Section 4.6) is probably due to an uranyl species resulting from the hydrolysis of CuF_2. Marginal uptake of MF_6 (M = Mo, W and U) by CuF_2 has been found as determined from mass balance, and [^{18}F]-fluorine count rate left on the solid after reactions. In view of the small uptakes of the hexafluorides by CuF_2 it is difficult to determine the fraction exchanged between $MF_5{}^{18}F$ (M = Mo, W andU) and the adsorbed species. The fraction exchanged (f) determined from a random distribution of [^{18}F]-fluorine between $MF_5{}^{18}F$ (M = Mo,W and U) and all the fluorine atoms available on the surface is small in all cases (Table 7.4).

Slightly greater uptakes of $MF_5{}^{18}F$ (M = Mo,W and U) by thallium fluoride have been obtained as compared with CuF_2. The difference is markedly noticeable in the case of MoF_6 (Table 4.16). A colour change from white to brown and sintering of the solid have also been observed after interaction between TlF and $MoF_5{}^{18}F$ (Section 4.7). The increase in mass of the solid together with the colour change and sintering provide an evidence for chemical reaction between TlF and MoF_6 but the

Table 7.4 Fractions Exchanged (f) of the Reactions Between CuF_2 or TlF and $MF_5{}^{18}F$ (M = Mo, W and U) Under Heterogeneous Conditions.

CuF_2 or TlF \ MF_6	Expt.No	MoF_6	Expt.No	WF_6	Expt.No	UF_6
CuF_2	1	0.11 ±0.03	3	0	5	0.08 ±0.03
	2	0.06 ±0.03	4	0		
TlF	1	0	4	0	6	0.09 ±0.03
	2	0.37 ±0.03	5	0		
					7	0.05 ±0.03
	3	0.12 ±0.03				

extent of any reaction that occurs, for example formation of the heptafluoroanion is too small for product identification.

In a radiotracer study involving the reaction between [^{18}F]-labelled-sulphur tetrafluoride $SF_3{}^{18}F$, or -carbonyl fluoride, $^{18}FFCO$, and CuF_2 or TlF, Fraser et.al. [156] have found that while CuF_2 shows a small exchange of [^{18}F]-fluorine with $SF_3{}^{18}F$ and $^{18}FFCO$ (f = 0.05 in each case), TlF shows a greater f value (f = 1.4 and 0.5 for SF_4 and F_2CO respectively). Although the gaseous fluorides are different from the ones used in the present study a similarity in behaviour of CuF_2 and TlF can be drawn as far as uptake of MF_6 (M = Mo, W and U) and [^{18}F]-fluorine exchange are concerned. There is no straightforward explanation to this result. However it is worth mentioning that Tl^+ is a softer Lewis acid. Furthermore the two solid fluorides adopt different structures. Copper difluoride adopts a rutile structure [157] while TlF adopts a distorted sodium chloride structure [158].

7.4 The Chemical Reactivity of Tris(dimethylamino)sulphonium Difluorotrimethylsilicate.

Tris(dimethylamino)sulphonium difluorotrimethylsilicate, TAS^+F^-, has been found to be very reactive towards the hexafluorides of molybdenum and tungsten in acetonitrile. In each case a brown viscous liquid has been obtained (Section 6.3). An intense yellow liquid has been reported by Poole and Winfield [40] as the reaction product between trimethyl-

fluorosilane and MoF_6. The colour of the liquid has been ascribed to contact charge-transfer interactions. In the present case the brown liquid may originate either from abstraction of F^- from the trimethyldifluorosilane ion to give MF_7^- (M = Mo or W) or from the formation of $MF_5.NMe_2$ (M = Mo or W).

The reaction between TAS^+F^- and boron trifluoride or phosphorus pentafluoride in MeCN has resulted in the formation of $TAS^+BF_4^-$ and $TAS^+PF_6^-$ respectively (Section 6.4). Similar reaction has been reported to occur between TAS^+F^- and sulphur tetrafluoride [159] yielding, as a result of F^- transfer, $TAS^+SF_5^-$.

Complete [^{18}F]-fluorine exchange occurs between TAS^+F^- and [^{18}F]-labelled trimethylfluorosilane in acetonitrile (Section 6.5). Fluorine bond lability of pentacoordinated silicon with respect to exchange is well documented. For example Klanberg and Muetterties [160] have shown, using ^{19}F n.m.r. techniques, that rapid exchange occurs between $C_6H_5SiF_4^-$ and excess fluoride ion in alcohol. Marat and Janzen [161] have proposed a fluorine bridged intermediate (Figure 7.1) to account for the rapid exchange between $MeSiF_4^-$ and $MeSiF_3$. A similar mechanism (1) involving a fluorine bridged species between TAS^+F^- and Me_3SiF can be used to explain the complete [^{18}F]-fluorine exchange, the equilibrium being favoured to the more thermodynamically stable species (i.e. TAS^+F^- and Me_3SiF)

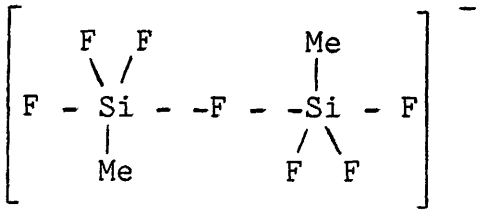

Figure 7.1 The fluorine bridged intermediate between $MeSiF_4^-$ and $MeSiF_3$ [161]

Mechanism (1)

$$(Me_2N)_3SMeSiF_2 + Me_3SiF \underset{k_{-1}}{\overset{k_1}{\rightleftharpoons}} \left[(Me_2N)_3S\ Me_3Si{-}F{-}SiMe_3\right]$$

7.5 Concluding Remarks.

The aim of the present project was to investigate the fluorine bond lability with respect to exchange of some binary fluorides both under homogeneous (acetonitrile) and heterogeneous (gas plus solid) conditions.

A marked difference in behaviour among the fluoro-anions of boron, phosphorus, arsenic, antimony, niobium and tantalum is observed in the presence of MF_5 ^{18}F (M = Mo, W or U) under homogeneous conditions. The inertness of AsF_6^- and SbF_6^- is contrasted by the lability of the fluorine bond with respect to exchange of BF_4^-, PF_6^-, NbF_6^- and TaF_6^- although AsF_6^- exchanges with UF_6^- under the same conditions. A difference in exchange behaviour also exists among AsF_5.NCMe, NbF_5.NCMe

and SbF_5.NCMe in the presence of $WF_5{}^{18}F$ under homogeneous conditions, the latter being completely inert. The inertness of SbF_6^- may be due to the relatively stronger Lewis acidity of Sb^V centre. In this respect SbF_6^- could prove to be a superior inert counter anion of supporting electrolytes in electrochemical studies. A close similarity exists between the lability of M-F bond (M = B,P,As,Sb,Nb and Ta) of the fluoro-anions and the Lewis acidity order in terms of fluoride ion affinity of the parent fluorides, the latter being in the order

$$SbF_5 > AsF_5 > PF_5 > BF_3 > NbF_5 \sim TaF_5$$

The MoF_7^- ion has been shown to exist in MeCN by reacting CsF and $MoF_5{}^{18}F$. Equally the existence of WF_7^- ion in MeCN has been confirmed by reaction between CsF and $WF_5{}^{18}F$. Both heptafluoroanions are assigned in the D_{5h} symmetry. Complete exchange of [^{18}F]-fluorine is found to occur between AWF_7 (A = Cu^{2+}, Tl^+ or NO^+) and $MF_5{}^{18}F$ (M = Mo or W) or between $CsMoF_7$ and $WF_5{}^{18}F$ in MeCN. Two possible mechanisms have been used to account for the complete exchange. A dissociative mechanism which involves a reversible dissociation of MF_7^- into MF_6 and F^- and an associative mechanism which involves a fluorine bridging species between MF_7^- and MF_6. Although the experimental observations are consistent with the former mechanism there is no direct evidence for a definitive conclusion to be drawn.

Under heterogeneous conditions the same systems are found to undergo partial exchange of [^{18}F]-fluorine. The exchange is best accounted for in terms of an associative mechanism involving a fluorine bridged species between MF_7^- and MF_6 followed by displacement of MF_6 in MF_7^- by free MF_6. The partial exchange is thought to be due partially to the electrostatic forces existing between cations and anions. Due to these forces the mobility of the heptafluoroanions is likely to be restricted as a result of which the process of [^{18}F]-fluorine exchange is slowed.

The reaction between activated caesium fluoride and $MF_5{}^{18}F$ (M = Mo,W and U) under heterogeneous conditions results in an uptake of the hexafluorides. The uptake of MF_6 by activated CsF is related to the amount of hexafluoroacetone used during the activation process. This result emphasises the importance of the formation of the $Cs^+OFC(CF_3)_2^-$ adduct during the process of activation. [^{18}F]-Fluorine exchange is found to take place between the adsorbed species and free $MF_5{}^{18}F$. More than one species have been identified during the reaction between activated CsF and $MF_5{}^{18}F$ (M = Mo,W and U), MoF_7^-, WF_7^- and UF_8^{2-} being the major ones formed. The formation of more than one species is explained in terms of the lack of uniformity of the surface reactions.

Difference in behaviour between CuF_2 and TlF is observed during their heterogeneous reaction with $MF_5{}^{18}F$ (M = Mo, W and U). The greater affinity of TlF towards MF_6

as compared with CuF_2 is consistent with the difference of the Lewis acidity of Tl^+ and Cu^{2+} ions, the former being the softer.

Tris(dimethylamine)sulphonium difluorotrimethylsilicate, TAS^+F^-, is found to be very reactive towards MF_6 (M = Mo or W) yielding in each case a brown viscous liquid the composition of which has not been determined. With BF_3 or PF_5, TAS^+F^- yields $TAS^+BF_4^-$ and $TAS^+PF_6^-$ as colourless crystalline solids respectively. Complete [^{18}F]-fluorine exchange is observed between TAS^+F^- and $Me_3Si^{18}F$ in MeCN. The exchange is best accounted for by an associative mechanism involving a fluorine bridged species between TAS^+F^- and Me_3SiF.

REFERENCES

1. N. Bartlett, Angew. Chem., Int. Ed. Engl., 7 (1968) 433

2. R.C. Burns and T.A. O'Donnell, J. Inorg. Nucl. Chem., 42 (1980) 1285; ibid, 43 (1981) 1231.

3. J.R. Geichman, E.A. Smith, S.S. Trond and R.R. Ogle, Inorg. Chem., 1 (1962) 661.

4. e.g. G.B. Hargreaves and R.D. Peacock, J. Chem. Soc., (1958) 2170, 4390

5. K.W. Dixon and J.M. Winfield, paper submitted to J. Chem. Soc. Dalton trans. (1988); J. Fluorine Chem, 29 (1985) 228.

6. (a) J.W. Larson and T.B. McMahon, J. Am. Chem.Soc. 107 (1985) 766 (b) J.C. Haartz and D.H. McDaniel, J. Am. Chem. Soc., 95 (1973) 8532

7. W.B. Farnham, B.E. Smart, W.J. Middleton, J.C. Calabrese and D.A. Dixon, J. Am. Chem. Soc., 107 (1985) 4565

8. e.g. B. Glavincevski and S. Brownstein, J. Inorg. Nucl. Chem., 43 (1981) 1827

9. "Halide of the Transition Metals", J.H. Canterford and R. Colton eds, Wiley Interscience, London 1968.

10. "Halogen Chemistry", V. Gutmann ed, vol.3, Academic Press, London 1967.

11. "Chemistry of the Actinide Elements", J.J. Katz, G.J. Seaborg and L.R. Morss eds., Chapman and Hall London, 1986.

12. J.H. Levy, J.C. Taylor and A.B. Waugh, J. Fluorine Chem., 23 (1983) 29

13. N. Bartlett, S.P. Beaton and N.K. Jha, J. Chem. Soc. Chem. Commun., (1966) 168.

14. J. Shamir and J.G. Malm, J. Inorg. Nucl. Chem., Suppl. (1976) 107

15. T.A. O'Donnell and D.F. Stewart, Inorg.Chem. , 5 (1966) 1434; T.A. O'Donnell, D.F. Stewart and P. Wilson, ibid, 5 (1966) 1438.

16. N. Bartlett and B.W. McQuillan in M.S. Whittingham and A.J. Jacobson (eds), Intercalation Chemistry Academic Press, New York, 1981, p.19.

17. e.g. D. Vaknik, D. Davidov and H. Selig, J. Fluorine Chem., 32, (1986), 345.

18. N. Bartlett, E.M. McCarron and B.W. McQuillan, Synth. Met., 1(1980) 221

19. P.M. George and J.L. Beauchamp, Chem. Phys., 36 (1979) 345

20. A. Prescott, D.W.A. Sharp and J.M. Winfield, J. Chem. Soc. Dalton Trans., (1975) 936.

21. J.A. Berry, R.T. Poole, A. Prescott, D.W.A. Sharp and J.M. Winfield, J. Chem. Soc. Dalton Trans., (1976) 272.

22. G.M. Anderson, I.F. Fraser and J.M. Winfield, J. Fluorine Chem, 23 (1983) 403.

23. J.A. Berry, R.T. Poole, A. Prescott, D.W.A. Sharp and J.M. Winfield, J. Fluorine Chem., 10 (1977) 247

24. G.B. Hargreaves and R.D. Peacock, J. Chem. Soc., (1958) 4212; ibid (1958) 3776

25. S. Brownstein, G.A. Heath, A. Sengupta and D.W.A. Sharp, J. Chem.Soc.Chem.Commun.,(1983)669

26. A.M.Bond, I. Irvine and T.A. O'Donnell, Inorg. Chem., 14(1975) 2408; ibid, 16 (1977) 841

27. G.B. Hargreaves and R.D. Peacock, J.Chem.Soc., (1958) 2170, 4390

28. A. Beuter, W. Kuhlmann and W. Sawodny, J. Fluorine Chem., 6 (1975) 367.

29 W.A. Sunder, A.L. Wayda, D. Distefano, W.E. Falconer and J.E. Griffiths, J. Fluorine Chem., 14 (1979) 299.

30. R. Bougon, R.M. Costes, J.P. Desmoulin, J. Michel and J.L. Person, J. Inorg. Nucl. Chem., Suppl. (1976) 99.

31. A. Prescott, D.W.A. Sharp and J.M. Winfield J. Chem. Soc. Dalton Trans., (1975) 934

32. J.L. Hoard, J. Am. Chem. Soc., 61 (1939) 1252.

33. G.B. Brown and L.A. Walker, Acta. Crystallog, 20 (1966) 220

34. L.B. Bernstein and K.S. Pitzer, J. Chem. Phys., 62 (1975) 2530.

35. R.B. English, A.M. Heyns and E.C. Bevhhardt, J. Phys.C, 16 (1983) 829.

36. R. Bougon, P. Charpin, J.P. Desmoulin and J.G. Malm, Inorg. Chem., 15 (1976) 2532.

37. P. Charpin, J. Michel and P. Rigny, J. Inorg. Nucl. Chem., Suppl. (1976) 131.

38. J.L. Hoard and J.V. Silverton, Inorg. Chem., 7 (1968) 1686.

39. C.J.W. Fraser, A. Majid, G. Oates and J.M. Winfield, J. Inorg. Nucl. Chem., 37 (1975) 1535.

40. R.T. Poole and J.M. Winfield, J.Chem.Soc.Dalton Trans., (1976) 1557.

41. L.H. Sommer, J.D. Citron and G.A. Parker, J. Am. Chem. Soc., 91 (1969) 4729.

42. B. Glavincevski and S. Brownstein, Inorg. Chem., 20 (1981) 3580.

43. D.K. Sanyal and J.M. Winfield, J. Fluorine Chem., 24 (1984) 75.

44. H.S. Booth in J.H. Simson (eds), Fluorine Chemistry, Academic Press, New York 1968, Vol.1 p. 201

45. K.F. Purcell and R. Drago, J. Am. Chem. Soc., 88 (1966) 919.

46. J.L. Hoard, S. Geller and T.B. Owen, Acta. Cryst., 4 (1951) 405.

47. E.L. Muetterties, T.A. Bither, M.W. Farlow and D.D. Coffman, J. Inorg. Nucl. Chem., 16 (1960) 52.

48. D.M. Byler and D.F. Shriver, Inorg. Chem., 13 (1974) 2697.

49. A.C. Baxter, J.H. Cameron. A. McAuley, F.M. McLaren and J.M. Winfield, J.Fluorine Chem., 10 (1977) 289.

50. F.N. Tebbe and E.L. Muetterties, Inorg. Chem., 6, (1967) 129.

51. W. Wieker, A.R. Grimmer and L. Kolditz, Z. Chemie, 7 (1967) 434

52. L. Lunazzi and S. Brownstein. J. Magn. Res., 1 (1969) 119 ; W.S. Sheldrick, J. Chem. Soc., (1974) 1402.

53. W. Storzer, D. Schomburg, G.V. Röschenthaler and R. Schmutzler, Chem. Ber., 116 (1983) 367.

54. R.J. Gillespie and A. Whitla, Can. J. Chem., 48 (1970) 657.

55. N. Bartlett and P.L. Robinson, J. Chem. Soc., (1961) 3417.

56. M. Azeem, M. Brownstein and R.J. Gillespie, Can. J. Chem., 47 (1969) 4159.

57. D.D. Gibler, C.J. Adams, M. Fisher. A. Zalkin and N. Bartlett, Inorg. Chem., 11 (1972) 2325.

58. S. Brownstein, Can.J.Chem., 47(1969) 605.

59. e.g. J.K. Foley, C. Korzenievski and S. Pons, Can.J.Chem.,66 (1988) 201; G.M. Anderson, J. Iqbal D.W.A. Sharp, J.M.Winfield, J.H. Cameron and A.G.McLeod, J. Fluorine Chem., 24 (1984) 303.

60. T. Osaka, K. Naoi, H. Sakai and S. Ogano, J. Electrochem., 134 (1987) 285.

61. D.M. Morrison and R.C. Thompson, Can.J.Chem., 56 (1978) 985.

62. R.D.W. Kemitt, M. Murray, V.M.McRae, R.D. Peacock, M.C.R. Symons and T.A. O'Donnell J. Chem. Soc (A), (1968) 862.

63. E.M. McCarron and N. Bartlett, J.Chem.Soc.Chem Commun., (1980) 404.

64. T.E. Thompson, E.M.McCarron and N. Bartlett, Synth. Met, 3 (1981) 255

65. (a) J. Bacon, P.A.W. Dean and R.J. Gillespie Can. J. Chem., 48 (1970) 314; (b) R.J. Gillespie and K.C. Moss, J.Chem.Soc (A), (1966) 1170; (c) C.F. Hoffman, B.E. Holder and W.L. Jolly, J. Phys. Chem., 62 (1958) 364.

66. J. Fawcett, A.J. Hewitt, J.H. Holloway and M.A. Stephen, J. Chem.Soc Dalton Trans., (1976) 2422.

67. E.W. Lawless, Inorg. Chem., 10(1971) 2084; M.J. Vasile, G.R. Jones and W.E. Falconer, J. Chem. Soc. Chem. Commun., (1971) 1355 ; A. Müller, H.W. Roesky and D. Böhler, Z. Chemie, 7 (1967) 469.

68. e.g. G.A. Olah, W.S. Tolgysei, S.J. Kuhn, M.E. Moffatt, I.J. Bastien and E.B. Baker, J. Am. Chem. Soc., 85 (1963) 1328.

69. P.A.W. Dean, R.J. Gillespie, R. Hulme and D.A. Humphreys, J. Chem. Soc (A), (1971) 341.

70. A.J. Edwards and G.R. Jones, J. Chem. Soc (A), (1969) 1467.

71. A.J. Edwards and R.J.C. Sills, J. Chem. Soc.,(A), (1970) 2697.

72. A.J. Edwards, J. Chem. Soc.Chem. Commun., (1970) 820, J.Chem. Soc. Dalton Trans., (1972) 2325.

73. V.M. McRae, R.D. Peacock and D.R. Russell, J. Chem. Soc. Chem. Commun., (1969) 62.

74. G. Begun and A.C. Rutenberg, Inorg. Chem., 6 (1967) 2212.

75. D.M. Byler and D.F. Shriver, Inorg. Chem., 12 (1973) 1412.

76. C.D. Davies, R.J. Gillespie, P.R. Ireland and J.M. Sowa, Can.J. Chem., 52 (1974) 2048.

77. (a) H.C. Clark and H.J. Emeléus, J.Chem.Soc., (1958) 190; (b) J.H. Canterford and T.A. O'Donnell Inorg. Chem., 5 (1966) 1442 ; (c) F. Fairbrother and W.C. Frith, J. Chem. Soc., (1951) 3051.

78. O. Ruff and E. Schiller, Z. Anorg. Chem., 72 (1911) 329.

79. A.J. Edwards, J. Chem. Soc., (1964) 3714.

80. I.R. Beattie, K.M.S. Livingston, G.A. Ozin and D.J. Reynolds, J. Chem. Soc., (1969) 958.

81. J. Brunvoll, A.A. Ischenko, I.N. Miakshin, G.W. Romanov, V.B. Sokolov, V.P. Spiridonov and T.G. Strand, Acta. Chem. Scand.Ser.A., 33 (1979) 775; J. Brunvoll, A.A. Ischenko, I.N.Miakshin, G.V. Romanov, V.P.Spiridonov, T.G.Strand and V.F. Sukhoverkhov, Acta.Chem.Scand.Ser.A., 34 (1980) 733; G.V.Girichev, V.N.Petrova, N.M.Petrov and K.S. Krasnov, Koord. Khim, 9 (1983) 799.

82. F. Fairbrother, K.H. Grundy and A. Thompson, J. Chem. Soc., (1965) 765

83. K.C. Moss, J. Chem. Soc (A), (1970) 1224.

84. J.A.S. Howell and K.C. Moss, J. Chem. Soc.(A) (1971) 2483.

85. D.W.A. Sharp and A.G. Sharpe, J.Chem.Soc., (1956) 1855 ; ibid (1956) 1858 ; O.L. Keller, Inorg. Chem., 2 (1963) 783 ; R.D.W. Kemmitt, D.R. Russell and D.W.A. Sharp, J. Chem.Soc., (1963) 4408.

86. S. Brownstein, Inorg. Chem., 12 (1973) 584.

87. A.J. Edwards and G.R. Jones, J.Chem.Soc. A., (1970) 1494

88. S. Arrhenius, Z. Phys. Chem., 1 (1887) 631

89. J.N. Brönsted, Rec. Trav. Chim., 42 (1923) 718.

90. T.M. Lowry, Chem. Ind., 42 (1923) 43.

91. E.C. Franklin, J. Am.Chem.Soc., 27 (1905) 820

92. G.N. Lewis and J. Franklin, Inst., 226 (1938) 293.

93. "Determination of Organic Structures by Physical Methods", vol. I, F.C. Nachod and E.A. Braude eds. Academic Press, New York, 1955.

94. "Survey of Progress in Chemistry", vol. 5, A.F. Scott, ed., Academic Press, New York 1969.

95. V. Gutmann and E. Wychera, Inorg. Nucl; Chem. Lett., 2 (1966) 257.

96. M.K. Kroger and R.S. Drago, J.Am.Chem.Soc., 103 (1981) 3250.

97. D.A. MacCauley and A.P. Lien, J.Am. Chem. Soc., 73 (1951) 2013 ; D.A. MacCauley, W.S. Higley, and A.P. Lien, ibid, 78 (1956) 3009.

98. J.M.S. Henis and C.A. Mabie, J. Chem. Phys., 53 (1970) 2999

99. J.D. McDonald, C.H. Williams, J.C. Thompson and J.L. Margrave, Advan. Chem. Ser., 72 (1968) 265.

100. F.M. Page and G.C. Goode, "Negative Ions and the Magnetron", Wiley Interscience, New York. 1969.

101. T.C. Rhyne and J.G. Dillard; Inorg. Chem., 10 (1971) 730

102. A.P. Alshuller, J.Am. Chem. Soc., 77 (1955) 6187

103. J.L. Bills and F.A. Cotton, J. Phys. Chem., 64 (1966) 1477

104. T.E. Mallouk, G.C.Rosenthal, G.Muller, R.Brusasco and N. Bartlett, Inorg. Chem., 23 (1984) 3167.

105. J.M. Winfield, J. Fluorine Chem, 25 (1984) 91

106. M. Walker and L. Ramaly, Anal. Chem., 45 (1973) 418

107. O. Ruff and E. Ascher, Z. Anorg. Allg. Chem., 196 (1931) 418.

108. "Practical Inorganic Chemistry", G. Pass and H. Sutcliffe eds, Chapman and Hall, London 1974 p. 127.

109. G.E. Moore, J. Opt. Soc. Amer., 43 (1953) 1045.

110. C.T. Ratcliffe and J.M. Shreeve, Inorg. Synth., 11 (1968) 194; C.T. Ratcliffe and J.M. Shreeve, J. Chem. Soc. Chem. Commun., (1966) 674.

111. P.J.H. Woltz, E.A. Jones and A.H. Nielson, J. Chem. Phys., 20 (1952) 378.

112. L.H. Jones, L.B. Asprey and R.R. Ryan, J. Chem. Phys., 47 (1967) 3371.

113. W.J. Middleton, Org. Synth., 64 (1986) 221.

114. H. Kriegsmann, Z. Anorg. All. Chem., 294 (1958) 113.

115. L. Kolditz and W. Rehak, Z. Anorg. Allg. Chem., 342 (1966) 32.

116. J.C. Fuggle, D.W.A. Sharp and J.M. Winfield, J. Fluorine Chem., 1 (1971/72) 427.

117. N.N. Greenwood, J. Chem. Soc., (1959) 3811

118. A.M. Heyns and C.W.F.T. Pistorius, Spectrochimica Acta., 31A (1975) 1293.

119. R.D. Peacock and D.W.A. Sharp, J. Chem. Soc., (1959) 2762.

120. O.L. Keller Jr., Inorg. Chem., 2 (1963) 783.

121. J. Reedi, A.P. Zuur and W.L. Groeneveld, Rec. Trav. Chim., 86 (1967) 1127.

122. (a) K.W. Dixon and J.M. Winfield, J. Fluorine Chem., 29 (1985) 355; (b) M.E. Redwood and C.J. Willis, Can. J. Chem., 45 (1967) 389.

123. G.A. Kolta, G. Webb and J.M. Winfield, J. Fluorine Chem., 14 (1979) 331.

124. C.J. Schack, R.D. Wilson and M.G. Warner, J. Chem. Soc. Chem. Commonun., (1969) 1110.

125. K.W. Dixon, Ph. D. Thesis, University of Glasgow, 1986.

126. F. Joliot and I. Curie, Nature, 133 (1934) 201.

127. G. Hersey, Trans. Faraday Soc., 34 (1938) 841.

128. H.A.C. McKay, Nature, 142 (1940) 199.

129. J.D. Marhoney and S.S. Markowitz, J. Inorg. Nucl. Chem., 26 (1964) 907.

130. A.H. Snell, Phys. Rev., 51 (1937) 143.

131. "Advances in Inorganic Chemistry", A.F. Cotton and G. Wilkinson eds, 5th edition, Wiley Interscience, New York, 1988, p. 546. ; J.M. Winfield, J. Fluorine Chem., 16 (1980) 17.

132. J.P. De Kleijn, J. Fluorine Chem., 10 (1977) 341.

133. J. Nazoki, M. Iwamato and T. Ido, Int. J. Appl. Radiot. Isot., 25 (1974) 393.

134. R.J. Nickles, R.D. Hichwa, M.E. Doube, G.D. Hutchins and D.D. Congdon, Int. J. Appl. Radiot. Isot., 34 (1983) 625.

135. R.M. Lambrecht, R. Neirinckx and A.P. Wolf, Int. J. Appl. Radiot. Isot., 29 (1978) 175.

136. "Nuclear and Radiochemistry", G. Friedlander, J.W. Kennedy, E.S. Macias and J.M. Miller eds, 3rd edition, Wiley Interscience, New York, 1981.

137. J.E. Whitley, Scottish Research Reactor Centre Report No. S.R.R.C. 26/68; Nucl. Sci. Abs., 22 (1968) 30592

138. J.H. Holloway, G.M. Stauton, K. Rediess, R. Bougon and D. Brown, J. Chem. Soc. Dalton Trans., (1984) 2163.

139. B. Cox, D.W.A. Sharp and A.G. Sharpe, J. Chem. Soc., (1956) 1242.

140. I. Sheft, H.H. Hyman, R.M. Adams and J.J. Katz, J. Am. Chem. Soc., 83 (1961) 291.

141. S. Katz, Inorg. Chem., 3 (1964) 1598 ; ibid, 5 (1966) 666.

142. e.g. B. Frlec, D. Gantar and J.H. Holloway, J. Fluorine Chem., 20 (1982) 385.

143. D.W. Bruce, R.F. Jones and D.J. Cole-Hamilton, J.Chem.Soc. Dalton Trans., (1984) 2249.

144. E.L. Wimmer and M.R. Snow, Aust.J.Chem., 31 (1978) 267.

145. H.R. Clark and M.M. Jones, J.Am.Chem.Soc., 92 (1970) 816.

146. A.R. Bassindale and T. Stout, Tetrahedron Lett. 25 (1984) 1631.

147. R. Noyori, I. Nishida and J. Sakata, J.Am. Chem. Soc., 103 (1981) 2106.

148. K.C. Brinkman and J.A. Gladysz, J. Chem. Soc. Chem. Commun., (1980) 1260.

149. A.J. Blakeney, D.J. Johson, P.W. Donovan and J.A. Gladysz, Inorg. Chem., 20 (1981) 4415.

150. R. Noyori, I. Nishida, J. Sakata and M. Nishizawa, J.Am. Chem.Soc., 102 (1980) 1223.

151. R. Noyori, J. Nishida and J. Sakata, Tetrahedron Lett., 22 (1981) 3993.

152. R.J. Gillespie, J.S. Hartman and M. Parekh, Can. J. Chem., 46(1968) 1601.

153. J.L. Beauchamp, J. Chem. Phys., 64(1976) 929.

154. L. Kolditz and I. Beierlein, Z. Chem., 7(1967) 468.

155. A.J. Malm, H. Selig and S. Siegel, Inorg. Chem., 5(1966) 30.

156. C.J.W. Fraser, D.W.A. Sharp, R.A. Sule, G. Webb and J.M. Winfield, J. Chem. Res., M(1978) 311.

157. A.J. Edwards, Adv. Inorg. Chem. Radiochem., 27 (1983) 83.

158. N.W. Alcock and H.D.B. Jenkins, J.Chem.Soc. Dalton. Trans., (1974) 1907.

159. W. Heilemann, T. Meier and R. Mews, J. Fluorine Chem., 35(1987) 143.

160. F. Klanberg and E.L. Muetterties, Inorg. Chem., 7(1968) 155.

161. R.K. Marat and A.F. Janzen, Can. J. Chem., 55 (1977) 3845.